DETECTOR PHOTON RESPONSE AND ABSORBED DOSE AND THEIR APPLICATIONS TO RAPID TRIAGE TECHNIQUES

A Dissertation

by

SHANNON PRENTICE VOSS

Submitted to the Office of Graduate Studies of
Texas A&M University
in partial fulfillment of the requirements for the degree of

DOCTOR OF PHILOSOPHY

August 2008

Major Subject: Nuclear Engineering

DETECTOR PHOTON RESPONSE AND ABSORBED DOSE AND THEIR APPLICATIONS TO RAPID TRIAGE TECHNIQUES

A Dissertation

by

SHANNON PRENTICE VOSS

Submitted to the Office of Graduate Studies of
Texas A&M University
in partial fulfillment of the requirements for the degree of

DOCTOR OF PHILOSOPHY

Approved by:

Chair of Committee,	John W. Poston, Sr.
Committee Members,	John R. Ford
	Leslie A. Braby
	John S. Moore
Head of Department,	Raymond Juzaitis

August 2008

Major Subject: Nuclear Engineering

ABSTRACT

Detector Photon Response and Absorbed Dose and Their Applications to Rapid Triage Techniques.

(August 2008)

Shannon Prentice Voss, B.S., Oregon State University;

M.S., San Diego State University

Chair of Advisory Committee: Dr. John W. Poston, Sr.

As radiation specialists, one of our primary objectives in the Navy is protecting people and the environment from the effects of ionizing and non-ionizing radiation. Focusing on radiological dispersal devices (RDD) will provide increased personnel protection as well as optimize emergency response assets for the general public. An attack involving an RDD has been of particular concern because it is intended to spread contamination over a wide area and cause massive panic within the general population. A rapid method of triage will be necessary to segregate the unexposed and slightly exposed from those needing immediate medical treatment. Because of the aerosol dispersal of the radioactive material, inhalation of the radioactive material may be the primary exposure route. The primary radionuclides likely to be used in a RDD attack are Co-60, Cs-137, Ir-192, Sr-90 and Am-241. Through the use of a MAX phantom along with a few Simulink MATLAB programs, a good anthropomorphic phantom was created for use in MCNPX simulations that would provide organ doses from internally deposited radionuclides. Ludlum model 44-9 and 44-2 detectors were used to verify the simulated dose from the MCNPX code. Based on the results, acute dose rate limits were developed for emergency response personnel that would assist in patient triage.

ACKNOWLEDGEMENTS

I would like to thank my graduate advisor, Dr. John Poston, for his invaluable guidance and encouragement throughout the duration of this project. Without his continuous support, this research could never have been completed. I would also like to thank Dr. John Ford for his invaluable knowledge and guidance on issues relating to internal dosimetry and radiation biology. My thanks and respect go out to the Texas A&M Nuclear Engineering faculty for their help including, but not limited to: Dr. L. A. Braby. Additional thanks and support go out to Dr. Steven Moore who has graciously accepted a critical role in evaluating this project.

A special note of recognition goes out to Mrs. Debra A. Voss whose moral support and encouragement have lifted me up through the years and given me strength and encouragement to challenge and break limits that on my own, I would not have overcome or even attempted.

Funding for this research was provided in total by the United States Navy under the Duty Under Instruction program for Outservice Training.

TABLE OF CONTENTS

Page

ABSTRACT iii

ACKNOWLEDGEMENTS iv

TABLE OF CONTENTS v

LIST OF FIGURES xi

LIST OF TABLES xvii

CHAPTER

I INTRODUCTION: RADIOLOGICAL DISPERSAL DEVICES 1

II RADIOLOGICAL DISPERSAL DEVICE BACKGROUND 2

III METHODS FOR SIMULATING MCNP PHANTOM 4

IV METHODS FOR MCNP ORGAN DOSE CALCULATIONS 8

Introduction 8
Description 8
Method comparisons 9
The Monte Carlo method 10

V METHODS FOR BUILDING AND TRANSFORMING THE INTERNAL DOSE MODEL INTO A READABLE LANGUAGE USABLE BY MCNPX 11

Introduction 11
Method description 11

VI METHODS FOR BUILDING AN MCNPX INPUT CODE 18

Introduction 18
Cell card 18
Surface card 19
Data card 19
Material definition card 22
Output file 25

VII METHODS FOR BUILDING VOLUME DETECTORS INTO THE MODEL 28

Introduction 28

CHAPTER		Page
	Method description	28
VIII	METHODS FOR EVALUATING ACTIVITY AND DOSE OVER TIME BASED ON LIKELY SOURCES FROM AN RDD EVENT	35
	Introduction	35
	Method description	36
IX	METHODS FOR IMPROVING EFFICIENCY BY TESTING THE NUMBER OF HISTORIES AND NUMBER OF SOURCES IN A VOLUME	48
	Introduction	48
	Method description	48
	Volume source results	49
X	STATISTICAL ANALYSIS BY MCNP	54
	Introduction	54
	Method description for Monte Carlo means, variances and standard deviations	54
XI	ESTIMATING ORGAN DOSE BASED ON VOLUME SOURCE IN THE LUNG	60
	Organ data verification	60
	Dose to organ conversion	60
	Statistical analysis of output file	62
	Co-60 organ dose profile	63
	Cs-137 organ dose profile	63
	Ir-192 organ dose profile	66
	Sr-90 organ dose profile	68
	Y-90 organ dose profile	72
	Results from lung volume source	74
XII	ESTIMATING ORGAN DOSE BASED ON VOLUME SOURCE IN THE LUNG FOR THE FEMALE PHANTOM ALONG WITH MALE LUNG COMPARISON	77
	Organ data verification	77
	Dose to organ conversion	77
	Statistical analysis of output file	79
	Co-60 organ dose profile	80
	Cs-137 organ dose profile	80
	Ir-192 organ dose profile	83
	Sr-90 organ dose profile	88
	Y-90 organ dose profile	89

CHAPTER Page

Results from female lung volume source 91

XIII ESTIMATING ORGAN DOSE BASED ON VOLUME SOURCE IN THE STOMACH 96

Organ data verification 96
Co-60 organ dose profile 96
Statistical analysis of output file 97
Cs-137 organ dose profile 100
Ir-192 organ dose profile 101
Sr-90 organ dose profile 104
Y-90 organ dose profile 107
Results from stomach volume source 111

XIV ESTIMATING ORGAN DOSE BASED ON VOLUME SOURCE IN THE COLON 113

Organ data verification 113
Co-60 organ dose profile 113
Statistical analysis of output file 114
Cs-137 organ dose profile 117
Ir-192 organ dose profile 118
Sr-90 organ dose profile 121
Y-90 organ dose profile 124
Results from colon volume source 128

XV ESTIMATING ORGAN DOSE BASED ON VOLUME SOURCE IN THE SMALL INTESTINES 130

Organ data verification 130
Co-60 organ dose profile 130
Statistical analysis of output file 131
Cs-137 organ dose profile 134
Ir-192 organ dose profile 135
Sr-90 organ dose profile 138
Y-90 organ dose profile 141
Results from small intestine volume source 145

XVI ESTIMATING ORGAN DOSE BASED ON VOLUME SOURCE IN THE SKIN 147

Organ data verification 147
Co-60 organ dose profile 147
Statistical analysis of output file 148
Cs-137 organ dose profile 149
Ir-192 organ dose profile 152

CHAPTER Page

Sr-90 organ dose profile 157
Y-90 organ dose profile 158
Results from skin volume source 160

XVII ESTIMATING ORGAN DOSE BASED ON VOLUME SOURCES IN THE LUNG, STOMACH, SMALL INTESTINE AND COLON ONE HOUR AFTER A LUNG INHALATION 163

Dose to multiple organ verification 163
Statistical analysis of output file 165
Co-60 organ dose profile 166
Cs-137 organ dose profile 166
Ir-192 organ dose profile 169
Sr-90 organ dose profile 172
Y-90 organ dose profile 176
Results from multi-organ lung, stomach, liver, small intestine and colon volume sources after one hour 180

XVIII ESTIMATING ORGAN DOSE BASED ON VOLUME SOURCES IN THE LUNG, STOMACH, SMALL INTESTINE AND COLON SIX HOURS AFTER A LUNG INHALATION 182

Co-60 organ dose profile 182
Statistical analysis of output file 183
Cs-137 organ dose profile 184
Ir-192 organ dose profile 187
Sr-90 organ dose profile 192
Y-90 organ dose profile 193
Results from multi-organ lung, stomach, liver, small intestine and colon volume source after six hours 197

XIX ESTIMATING ORGAN DOSE BASED ON VOLUME SOURCES IN THE LUNG, STOMACH, SMALL INTESTINE AND COLON TWELVE HOURS AFTER A LUNG INHALATION 199

Co-60 organ dose profile 199
Statistical analysis of output file 200
Cs-137 organ dose profile 201
Ir-192 organ dose profile 205
Sr-90 organ dose profile 209
Y-90 organ dose profile 210
Results from multi-organ lung, stomach, liver, small intestine and colon volume sources after twelve hours 214

CHAPTER Page

XX ESTIMATING ORGAN DOSE BASED ON VOLUME SOURCES IN THE LUNG, STOMACH, SMALL INTESTINE AND COLON 18 HOURS AFTER A LUNG INHALATION 216

Co-60 organ dose profile 216
Statistical analysis of output file 217
Cs-137 organ dose profile 218
Ir-192 organ dose profile 222
Sr-90 organ dose profile 226
Y-90 organ dose profile 227
Results from multi-organ lung, stomach, liver, small intestine and colon volume sources after 18 hours 231

XXI ESTIMATING ORGAN DOSE BASED ON VOLUME SOURCES IN THE LUNG, STOMACH, SMALL INTESTINE AND COLON 24 HOURS AFTER A LUNG INHALATION 233

Co-60 organ dose profile 233
Statistical analysis of output file 234
Cs-137 organ dose profile 235
Ir-192 organ dose profile 239
Sr-90 organ dose profile 243
Y-90 organ dose profile 244
Results from multi-organ lung, stomach, liver, small intestine and colon volume sources after 24 hours 248

XXII DOSE TO MODEL CONFIRMATION USING EXPERIMENTAL TESTING OF SCANDIUM-46 IN A RANDO MALE TORSO PHANTOM 250

Description of the RANDO phantom 250
Experimental source and phantom arrangement 250
44-9 Alpha, beta and gamma probe measurements 252
44-2 NaI probe measurements 253
Lithium Fluoride TLD dose confirmation 254

XXIII EVALUATION OF EMERGENCY RESPONSE GUIDELINES APPLICABLE TO A RADIOLOGICAL DISPERSAL DEVICE 256

Particle dispersal in air 256
Dose comparison 256

XXIV CONCLUSIONS AND FUTURE WORK 262

Page

REFERENCES 264

APPENDIX A 266

VITA 268

LIST OF FIGURES

FIGURE		Page
5.1	A color representation of MAX phantom slice 121 showing various body tissues	13
5.2	A portion of the Matrix number representation of MAX phantom slice 121	13
5.3	Front view Scion MAX phantom	14
5.4	Rear view Scion MAX phantom	14
5.5	Sample input of MCNPX geometry card	17
6.1	Sample of MCNPX input deck cell card	20
6.2	Sample of an MCNPX input deck surface card	21
6.3	Sample of an MCNPX input deck data card	21
6.4	Sample of an MCNPX input deck material definition card	23
7.1	MATLAB three-dimensional representation of the voxmap using the voxplot program	29
7.2	Anterior view of MAX phantom with 5cm diameter detector located at the upper left chest wall	31
7.3	Lateral view of MAX phantom with 5cm diameter detector located at upper chest wall without entering the phantom	32
7.4	Anterior view of MAX phantom with five 5cm diameter detectors placed around the chest wall	33
7.5	Lateral view of MAX phantom with ten 5cm diameter detectors located around the anterior and posterior portions of the lung	34
8.1	Outer shell wire diagram of MATLAB Simulink internal dose program	38
8.2	Simulink second shell wire diagram of internal dose program	40
8.3	Simulink third shell wire diagram of internal dose lung model	42
8.4	Simulink fourth shell wire diagram of compartment A lung model	43
8.5	Simulink fourth shell wire diagram of stomach from GI tract model	45
8.6	Simulink fourth shell wire diagram of small intestine from GI tract model	45

FIGURE Page

8.7 Simulink third-shell wire diagram of transfer compartment 46

8.8 Simulink third-shell diagram of Co-60 subsystem compartment..... 46

9.1 Average gonad dose per history from four independent simulations vs. number of source positions located within the lung..... 52

9.2 Average gonad dose per history from four independent simulations vs. number of histories with 15,000 source voxels located within the lung.... 52

9.3 Percent error in gonad dose vs. number of histories with lung sources..... 53

11.1 Three-dimensional human dose profile from a 1.33 MeV photon source located within the lung 64

11.2 Three-dimensional human dose profile from a Cs-137 source located within the lung 67

11.3 Three-dimensional human dose profile from the 0.47 MeV Ir-192 photon source located within the lung 70

11.4 Three-dimensional human dose profile from the 0.66 MeV Ir-192 electron source located within the lung 71

11.5 Three-dimensional human dose profile from a Sr-90 volume source located within the lung 73

11.6 Three-dimensional human dose profile from a Y-90 beta source located within the lung 75

11.7 Comprehensive graph of organ doses for the five potential lung sources..... 76

12.1 Three-dimensional human dose profile from a 1.33 MeV photon source located within the female lung 81

12.2 Three-dimensional human dose profile from a Cs-137 photon source located within the female lung 84

12.3 Three-dimensional human dose profile from a 0.47 MeV Ir-192 photon source located within the female lung 86

12.4 Three-dimensional human dose profile from a 0.66 MeV Ir-192 electron source located within the female lung 87

12.5 Three-dimensional human dose profile from a Sr-90 beta source located within the female lung 90

FIGURE Page

12.6 Three-dimensional human dose profile from a Y-90 beta source located within the female lung 92

12.7 Summary graph of organ doses for the five potential female lung sources 93

12.8 Summary comparison of male and female organ doses for Co-60 and Sr-90 94

13.1 Three-dimensional human dose profile from a 1.33 MeV photon source located within the stomach 99

13.2 Three-dimensional human dose profile from a Cs-137 photon source located within the stomach 102

13.3 Three-dimensional human dose profile from the 0.47 MeV Ir-192 photon source located within the stomach 105

13.4 Three-dimensional human dose profile from the 0.66 MeV Ir-192 electron source located within the stomach 106

13.5 Three-dimensional human dose profile from a Sr-90 beta source located within the stomach 108

13.6 Three-dimensional human dose profile from a Y-90 beta source located within the stomach 110

13.7 Summary graph of organ doses for the five potential stomach sources 112

14.1 Three-dimensional human dose profile from a 1.33 MeV photon source located within the colon 116

14.2 Three-dimensional human dose profile from a Cs-137 photon source located within the colon 119

14.3 Three-dimensional human dose profile from the 0.47 MeV Ir-192 photon source located within the colon 122

14.4 Three-dimensional human dose profile from the 0.66 MeV Ir-192 beta source located within the colon 123

14.5 Three-dimensional human dose profile from a Sr-90 beta source located within the colon 125

14.6 Three-dimensional human dose profile from a 2.28 MeV Y-90 beta source located within the colon 127

14.7 Comprehensive graph of organ doses for the five potential colon sources 129

FIGURE Page

15.1 Three-dimensional human dose profile from a 1.33 MeV photon source located within the small intestine 133

15.2 Three-dimensional human dose profile from a Cs-137 photon source located within the small intestine 136

15.3 Three-dimensional human dose profile from the 0.47 MeV Ir-192 photon source located within the small intestine 139

15.4 Three-dimensional human dose profile from the 0.66 MeV Ir-192 electron source located within the small intestine 140

15.5 Three-dimensional human dose profile from a Sr-90 beta source located within the small intestine 142

15.6 Three-dimensional human dose profile from a Y-90 beta source located within the small intestine 144

15.7 Summary graph of organ doses for the five potential small intestine sources 146

16.1 Three-dimensional human dose profile from a 1.33 MeV photon source located within the skin 150

16.2 Three-dimensional human dose profile from a Cs-137 photon source located within the skin 153

16.3 Three-dimensional human dose profile from a 0.47 MeV Ir-192 photon source located within the skin 155

16.4 Three-dimensional human dose profile from a 0.66 MeV Ir-192 electron source located within the skin 156

16.5 Three-dimensional human dose profile from a Sr-90 beta source located within the skin 159

16.6 Three-dimensional human dose profile from a Y-90 electron source located within the skin 161

16.7 Comprehensive graph of organ doses for the five potential skin sources 162

17.1 Three-dimensional human dose profile from a 1.33 MeV photon source located within multiple organs after time T plus one hour 167

17.2 Three-dimensional human dose profile from a Cs-137 photon source located within multiple organs after time T plus one hour 170

17.3 Three-dimensional human dose profile from a 0.47 MeV Ir-192 photon source located within multiple organs after T plus one hour 173

FIGURE Page

17.4 Three-dimensional human dose profile from a 0.66 MeV Ir-192 electron source located within multiple organs after T plus one hour 174

17.5 Three-dimensional human dose profile from a Sr-90 beta source located within multiple organs after T plus one hour 177

17.6 Three-dimensional human dose profile from a Y-90 beta source located within multiple organs after T plus one hour 179

17.7 Summary graph of organ doses for the five potential multi-organ sources located in multiple organs after time T plus one hour 181

18.1 Three-dimensional human dose profile from a 1.33 MeV photon source located within multiple organs after T plus six hours 185

18.2 Three-dimensional human dose profile from a Cs-137 photon source located within multiple organs after T plus six hours 188

18.3 Three-dimensional human dose profile from a 0.47 MeV Ir-192 photon source located within multiple organs after T plus six hours 190

18.4 Three-dimensional human dose profile from a 0.66 MeV Ir-192 beta source located within multiple organs after T plus six hours 191

18.5 Three-dimensional human dose profile from a Sr-90 beta source located within multiple organs after T plus six hours 194

18.6 Three-dimensional human dose profile from a Y-90 beta source located within multiple organs after T plus six hours 196

18.7 Summary graph of organ doses for the five potential multi-organ sources located in multiple organs after time T plus six hours 198

19.1 Three-dimensional human dose profile from a 1.33 MeV photon source located within multiple organs after T plus 12 hours 202

19.2 Three-dimensional human dose profile from a Cs-137 photon source located within multiple organs after T plus 12 hours 204

19.3 Three-dimensional human dose profile from a 0.47 MeV Ir-192 photon source located within multiple organs after T plus 12 hours 207

19.4 Three-dimensional human dose profile from a 0.66 MeV Ir-192 electron source located within multiple organs after T plus 12 hours 208

19.5 Three-dimensional human dose profile from a Sr-90 beta source located within multiple organs after T plus 12 hours 211

FIGURE Page

19.6 Three-dimensional human dose profile from a Y-90 beta source located within multiple organs after T plus 12 hours 213

19.7 Summary graph of organ doses for the five potential multi-organ sources after T plus 12 hours 215

20.1 Three-dimensional human dose profile from a 1.33 MeV photon source located within multiple organs after T plus 18 hours 219

20.2 Three-dimensional human dose profile from a Cs-137 photon source located within multiple organs after T plus 18 hours 221

20.3 Three-dimensional human dose profile from a 0.47 MeV Ir-192 photon source located within multiple organs after T plus 18 hours 224

20.4 Three-dimensional human dose profile from a 0.66 MeV Ir-192 beta source located within multiple organs after T plus 18 hours 225

20.5 Three-dimensional human dose profile from a Sr-90 beta source located within multiple organs after T plus 18 hours 228

20.6 Three-dimensional human dose profile from a Y-90 beta source located within multiple organs after T plus 18 hours 230

20.7 Summary graph of organ doses for the five potential multi-organ sources after time T plus 18 hours 232

21.1 Three-dimensional human dose profile from a 1.33 MeV photon source located within multiple organs at time T plus 24 hours 236

21.2 Three-dimensional human dose profile from a Cs-137 photon source located within multiple organs at time T plus 24 hours 238

21.3 Three-dimensional human dose profile from a 0.47 MeV Ir-192 photon source located within multiple organs at T plus 24 hours 241

21.4 Three-dimensional human dose profile from a 0.66 MeV Ir-192 electron source located within multiple organs at T plus 24 hours 242

21.5 Three-dimensional human dose profile from a Sr-90 beta source located within multiple source organs at T plus 24 hours 245

21.6 Three-dimensional human dose profile from a Y-90 beta source located within multiple source organs at T plus 24 hours 247

21.7 Summary graph of organ doses for the five potential multi-organ sources after T plus 24 hours 249

LIST OF TABLES

TABLE Page

9.1 Energy deposited in selected organs from a 1.17 MeV photon that is randomly emitted from one of the ten source voxels 50

9.2 Number of histories versus simulation time..... 53

11.1 Organ doses from a Co-60 volume source in the lung..... 61

11.2 Organ doses for a Cs-137 volume source in the lung 65

11.3 Organ doses for an Ir-192 volume source in the lung..... 66

11.4 Organ doses from a Sr-90 volume source in the lung..... 69

11.5 Organ doses from a Y-90 volume source in the lung..... 72

12.1 Organ doses from a Co-60 volume source in the female lung..... 78

12.2 Organ doses for a Cs-137 volume source in the female lung 82

12.3 Organ doses for an Ir-192 volume source in the female lung..... 83

12.4 Organ doses from a Sr-90 volume source in the female lung..... 88

12.5 Organ doses from a Y-90 volume source in the female lung..... 89

13.1 Organ doses from a Co-60 volume source in the stomach..... 97

13.2 Organ doses for a Cs-137 volume source in the stomach 100

13.3 Organ doses for an Ir-192 volume source in the stomach..... 103

13.4 Organ doses from a Sr-90 volume source in the stomach..... 104

13.5 Organ doses from a Y-90 volume source in the stomach 109

14.1 Organ doses from a Co-60 volume source in the colon 114

14.2 Organ doses for a Cs-137 volume source in the colon..... 117

14.3 Organ doses for an Ir-192 volume source in the colon 120

14.4 Organ doses from a Sr-90 volume source in the colon 121

14.5 Organ doses from a Y-90 volume source in the colon..... 126

15.1 Organ doses from a Co-60 volume source in the small intestine..... 131

15.2 Organ doses for a Cs-137 volume source in the small intestine 134

15.3 Organ doses for an Ir-192 volume source in the small intestine..... 137

TABLE Page

15.4 Organ doses from a Sr-90 volume source in the small intestine 138
15.5 Organ doses from a Y-90 volume source in the small intestine 143
16.1 Organ doses from a Co-60 volume source in the skin 148
16.2 Organ doses for a Cs-137 volume source in the skin 151
16.3 Organ doses for an Ir-192 volume source in the skin 152
16.4 Organ doses from a Sr-90 volume source in the skin 157
16.5 Organ doses from a Y-90 volume source in the skin 158
17.1 Organ doses from Co-60 volume source in multiple organs at T plus one hour 164
17.2 Organ doses for a Cs-137 volume source in multiple organs at T plus one hour 168
17.3 Organ doses for an Ir-192 volume source in multiple organs at T plus one hour 171
17.4 Organ doses from a Sr-90 volume source in multiple organs at time T plus one hour 175
17.5 Organ doses from a Y-90 volume source in multiple organs at time T plus one hour 176
18.1 Organ doses from Co-60 volume source in multiple organs at time T plus six hours 182
18.2 Organ doses for a Cs-137 volume source in multiple organs at time T plus six hours 184
18.3 Organ doses for an Ir-192 volume source in multiple organs at time T plus six hours 187
18.4 Organ doses from a Sr-90 volume source in multiple organs at time T plus six hours 192
18.5 Organ doses from a Y-90 volume source in multiple organs at time T plus six hours 195
19.1 Organ doses from a Co-60 volume source in multiple organs at time T plus 12 hours 199
19.2 Organ doses for a Cs-137 volume source in multiple organs at time T plus 12 hours 201

TABLE Page

19.3 Organ doses for an Ir-192 volume source in multiple organs at time T plus 12 hours 205

19.4 Organ doses from a Sr-90 volume source in multiple organs at time T plus 12 hours 209

19.5 Organ doses from a Y-90 volume source in multiple organs at time T plus 12 hours 210

20.1 Organ doses from Co-60 volume source in multiple organs at time T plus 18 hours 216

20.2 Organ doses for a Cs-137 volume source in multiple organs at time T plus 18 hours 218

20.3 Organ doses for an Ir-192 volume source in multiple organs at time T plus 18 hours 222

20.4 Organ doses from a Sr-90 volume source in multiple organs at time T plus 18 hours 226

20.5 Organ doses from a Y-90 volume source in multiple organs at time T plus 18 hours 229

21.1 Organ doses from Co-60 volume source in multiple organs at time T plus 24 hours 233

21.2 Organ doses for a Cs-137 volume source in multiple organs at time T plus 24 hours 235

21.3 Organ doses for an Ir-192 volume source in multiple organs at time T plus 24 hours 239

21.4 Organ doses from a Sr-90 volume source in multiple organs at time T plus 24 hours 243

21.5 Organ doses from a Y-90 volume source in multiple organs at time T plus 24 hours 244

22.1 Organs and detector doses from a Sc-46 point source position in lung 251

22.2 Position and dose rate for 18 LiF TLDs inside the RANDO phantom with the Sc-46 source 255

23.1 Activities that correspond to preset organ dose limits for the five radionuclides considered in this problem 258

23.2 Lung activity limits to reach a dose limit of 0.01 Gy for the five radionuclides in this problem 259

TABLE Page

23.3 Dose rate limits for GM pancake and NaI probes based on five radionuclides within the lung using a dose limit of 0.01 Gy. 259

23.4 Dose rate limits for GM pancake and NaI probes based on five radionuclides within the lung using a dose limit of 1 Gy 260

CHAPTER I
INTRODUCTION: RADIOLOGICAL DISPERSAL DEVICES

As radiation specialists, our primary objectives in the Navy is protecting people and the environment from the effects of ionizing and non-ionizing radiation, advancing radiological techniques through research and development and providing radiological expertise and intelligence in the War on Terrorism. Focusing on radiological dispersal devices (RDD) will accomplish the Navy's objectives as well as providing protection and of the general public. RDDs are a potential threat to local, state and federal government agencies. They are the most likely nuclear component that can be accessed by terrorist organizations and formed into a radiological weapon. An attack involving an RDD has been of particular concern because of the widespread use of radioactive materials in the United States and abroad by industry, hospitals, and academic institutions (DOE/NRC 2003). Such a device is intended to spread radioactive contamination over a wide area, and causing a panic within the general population. RDDs typically involve the use of explosives as the mechanism for dispersal, resulting in an aerosol plume of radioactive material with a potential for wide-scale contamination of a population. Because of the aerosol dispersal of the radioactive material, inhalation of the material may be the primary exposure route. It is anticipated that large numbers of the general population could have intakes of radioactive materials. In addition, a large portion of the population, who are unexposed (the "worried well"), will go to hospital emergency rooms and other medical facilities seeking treatment and/or assurance that they have not been exposed. In these cases, a rapid method of triage will be necessary to segregate the unexposed and slightly exposed from those needing immediate medical treatment.

This dissertation follows the style of Health Physics.

CHAPTER II
RADIOLOGICAL DISPERSAL DEVICE BACKGROUND

One of the main goals of the Department of Energy (DOE) is nuclear nonproliferation. They define their job as it relates to Nuclear Nonproliferation by providing technical leadership to limit or prevent the spread of materials, technology, and expertise relating to weapons of mass destruction; advance the technologies to detect the proliferation of weapons of mass destruction worldwide; and eliminate or secure inventories of surplus materials and infrastructure usable for nuclear weapons (Abraham 2003). Over the past seven and one-half years, the DOE has significantly improved its ability to prevent and reverse the proliferation of weapons of mass destruction (WMD) but they admit that nuclear material must be made more physically secure. While border monitoring and export controls help to ensure nuclear material remains outside of our borders, nuclear material can and should be consolidated. Reducing the number of sites storing material coincides with reducing the vulnerability to threat or sabotage. Down-blending and burning excess material is another way to prevent the material from falling into the wrong hands. The DOE is working to enhance the international framework to reduce the threat of a radiological attack against the United States (US) and its interests abroad (Abraham 2003). According to the DOE, September 11th made these concerns more immediate. There are any number of states and non-state actors interested in acquiring nuclear or radiological materials. The International Atomic Energy Agency (IAEA) has reported some 200 attempts at the illicit smuggling of nuclear materials in the past decade alone (Abraham 2003). Dirty bombs are much simpler to make and use than nuclear weapons. While dirty bombs are not comparable to nuclear weapons in destructiveness, they are far easier to assemble and deploy. The materials that might be used in a dirty bomb exist in many everyday forms, including medical nuclides, radiography sources, large sources at scientific research facilities, and sources that provide electric power. Such material can be found in virtually every country. While the physical destruction an RDD would cause is comparable to conventional explosives,

the disruption and panic caused by widespread contamination is far greater. And it is disruption and panic that terrorists seek. All it takes is one small successful smuggling attempt to ignite a catastrophic chain of events that can significantly impact our people and targeted infrastructures. Over the last 20 years, our main concern has been rogue states seeking to acquire illicit radioactive material. Now terrorist networks are seeking such weapons and materials. The greatest threat according to the DOE is under secured radiological sources that would be used in a radiological dispersion attack (Abraham 2003).

Sandia National Laboratories have conducted experiments on the aerosolization on RDDs. They have conducted over 500 explosive experiments with more than 20 materials and 85 device geometries to determine the aerosol physics that are representative of what might occur from the detonation of an actual device. Their experimental chambers are large enough so that almost all of the aerosol generated remains in the air and is not deposited on the walls of the chamber but small enough so that detectable quantities of the aerosol can be collected (Harper 2006). These experiments provide the basic information needed to evaluate exposure to individuals in the vicinity of an RDD event.

CHAPTER III
METHODS FOR SIMULATING MCNP PHANTOM

The basic dosimetric quantity related to the probability of the appearance of stochastic radiation effects, as defined by the International Commission on Radiological Protection (ICRP), is the effective dose, which is 'the sum of the weighted equivalent doses in all tissues and organs of the body'. The ICRP Publication 60 effective dose is given in Equation 3.1 by (ICRP 1991):

$$E = \sum_T w_T H_T \tag{3.1}$$

where H_T is the equivalent dose in tissue or organ T and w_T is the stochastic tissue weighting factor for tissue T (ICRP 1991).

Effective dose is the most important quantity of the protection philosophy of ICRP Publication 60 (ICRP 1991), and as a consequence dose limits for stochastic effects recommended by the Commission are expressed in terms of effective dose for routine occupational exposures. In a radiological attack, the initial focus will be on acute, deterministic effects. Therefore, it becomes the main task of radiation protection dosimetry to determine organ and tissue absorbed dose in units of gray (Gy).

With respect to the execution of this task, the development of mathematical heterogeneous human phantoms was a major achievement, because equivalent doses cannot be measured directly in the human body. In mathematical human phantoms, the size and form of the body and its organs are described by mathematical expressions representing combinations and intersections of planes, circular and elliptical cylinders, spheres, cones, tori, etc. Fisher and Snyder (1967, 1968) introduced this type of phantom for an adult male, which also contains ovaries and a uterus. Since 1979 it has been known as ‘MIRD5 phantom’ (Medical Internal Radiation Dose Committee). Body height and weight as well as the organ masses are in accordance with Reference Man data (ICRP 1975). Most of the recent dosimetric data for adult humans published by the ICRP were the same as for the MIRD5-type phantoms.

Now, tomographic or voxel phantoms represent the latest evolutionary step of exposure models. Tomographic phantoms are based on digital images recorded from scanning of real persons using computed tomography (CT) or magnetic resonance imaging (MRI). Compared to the mathematical phantoms, voxel phantoms are true to nature representations of a human body. But, as hard as we try to justify these voxel phantoms, they only represent a single human. Reference Man represents an average over a large population. Tomographic or voxel phantoms were introduced by (Gibbs 1984) and independently also by (Williams 1986).

A tomographic phantom is a three-dimensional matrix of small voxels (volume pixels), to which, depending on their location, organ volume identification (ID) numbers have been assigned by segmentation. The media ID number, the elemental composition and the density, which define the material to fill a voxel, have still to be defined by the user. Tissue compositions and densities of the materials used for the construction of the MAX phantom are taken from or are based on the ICRU Report No. 44 (ICRU 1989).

Zubal used segmented CT and MRI data of a patient who was scanned from head to mid-thigh (Zubal 1994a), (Zubal 1994b) and Dimbylow introduced the voxel phantom NORMAN based on MRI data of a healthy volunteer (Dimbylow 1995). The voxel dimensions have been scaled to match the body height and weight of the Reference Man (ICRP 1975), that is, a body weight of 70 kg and a body height of 170 cm.

Equivalent doses to organs and tissues of human phantoms are usually calculated with Monte Carlo methods, and the results are normalized to measurable quantities. A ratio between a quantity of interest and a measurable quantity is called a conversion coefficient (CC) which, in general, depends on the energy and directional distribution of the radiation field.

Equivalent dose to air-kerma CCs have been determined by Saito *et al* (2001) for the OTOKO voxel phantom, for the VIPMAN voxel phantom for external exposure to photons by Chao *et al* (2001a), for the same phantom for external exposure to electrons by Chao *et al* (2001b), and by Zankl *et al* (2002a) for external photon exposure of the GOLEM and other voxel phantoms. In most of the cited studies incident particle fluence,

or air-kerma free in air or at the phantom surface were the normalization quantities for the CCs.

For *internal exposures* Petoussi-Henss and Zankl (1998) published photon specific absorbed fractions for the pediatric BABY and CHILD voxel phantoms, as well as for the adult voxel phantoms GOLEM and VOXELMAN. These studies have been continued by Smith *et al* (2000, 2001) and the data have been compared to those of the MIRD5 system. Voxel data from Zubal *et al* (1994a, 1994b, 1995) have been used by Johnson *et al* (2000) to determine CCs for organ equivalent dose normalized to activity and by Yoriyaz *et al* (2000) and by Stabin and Yoriyaz (2002) to calculate specific absorbed fractions to be used in nuclear medicine.

Yale University created three voxel phantoms VOXELMAN, MANTISSUE3-6, and VOXTISS8 with the same data base, namely 78 CT images acquired from neck to mid-thigh with 1 cm slice thickness, 55 CT images of the head and neck region with 0.5 cm slice thickness, and 124 high-resolution transverse MRI images with 0.15 cm slice thickness from a patient, who was scheduled for head, thorax, abdomen and pelvic scans for diagnosis of diffuse melanoma. His height was 175 cm and the weight was 70 kg (Kramer 2003).

VOXELMAN represents the combination of the segmented head and body CT images with a 4-mm cubic voxel size. Later arms and legs, segmented from the Visible Man's red color cross-sections (Spitzer andWhitlock 1998), were added by Stuchly (1996) to the torso phantom, which was called MANTISSUE3-6. This phantom was resampled to achieve a 3.6-mm cubic voxel size (Kramer 2003).

Finally, the arms of the MANTISSUE3-6 phantom have been straightened along the sides of the body by Sjogreen (1998), maintaining the 3.6-mm cubic voxels. This version has been called VOXTISS8, and consisted of 487 segmented body cross-sections, each of which expanded into a 192 × 96 pixel matrix. About 40 organs and tissues were segmented in the trunk, arms and legs and about 56 organs and tissues in the head. The VOXTISS8 phantom had a body height of 175.3 cm, and it was this voxel

model which has been chosen as the database for the construction of the MAX phantom (Kramer 2003).

To represent the skin by a 1.5-mm thick surface layer as established based on data given in ICRP Publication 89 (ICRP 2003); no effort has been made to change the segmentation of the 3.6-mm skin of the VOXTISS8 phantom. Instead a dosimetric method was developed to separate the deposition of energy in the 1.5-mm surface layer from the absorption of energy in the 2.1-mm layer underneath. Depending on the location on the surface of the body, every cubic skin voxel has at least one surface bordering on an air voxel. This criterion already helps to eliminate voxels falsely segmented as skin below the first surface layer. Once an interaction has been identified as having taken place in a skin voxel, the algorithm checks to determine if the point of interaction lies within the first 1.5-mm. In this case, the energy loss will be deposited in skin, otherwise in adipose tissue. The method takes into account the specific location of a skin voxel, the number of bordering air voxels and the direction of radiation incidence. A slightly modified technique was used to determine the mass of the new 1.5 mm skin. This method allows the skin depth to be chosen for any depth below the voxel thickness (Kramer 2003).

CHAPTER IV
METHODS FOR MCNP ORGAN DOSE CALCULATIONS

Introduction

MCNPX is a general purpose Monte Carlo radiation transport code that tracks continuous energy using a coupled neutron, photon and electron transport code. It is the next generation in the series of Monte Carlo transport codes that began at Los Alamos National Laboratory fifty years ago. MCNPX 2.4.0 is a superset of MCNP4C3 and MCNPX 2.3.0, LAHET 2.8 and CEM (RSICC 2002).

The MCNPX program began in 1994 as an extension of MCNP and LAHET in support of the Accelerator Production of Tritium Project (APT). The work involved a formal extension of MCNP to all emissions and all energies, improvement of physics simulation models, extension of neutron, photon and photonuclear libraries to 150 MeV, and the formulation of new variance reduction and data analysis techniques. The program also included cross section measurements, benchmark experiments, deterministic code development, and improvements in transmutation code and library tools through the CINDER ’90 project (RSICC 2002).

Description

MCNP has built-in flexibility and can be used for single transport or coupled transport of photons, neutrons and electrons. The neutron/photon transport code has the capability to track photons produced by neutron interactions. The range of neutron energies is from 10^{-11} MeV to 20 MeV for all nuclides and for a select few, the energy extends to 150 MeV. For photons, the energy range is from 1 keV to 100 GeV. The electron energy range is from 1 keV to 1 GeV (RSICC 2002).

Independent input files are created by the user. The input file should include the following basic subsections: geometry specification, material description with cross-

section evaluations, source specifications and tally or answer specifications. The more detailed each area can be described, the more accurate answers MCNP will deliver. The general rules of thumb are defining and sampling the geometry and source well and always questioning the stability and reliability of results (RSICC 2002).

Method comparisons

There are two basic methods for analyzing a transport code, the Monte Carlo method and deterministic transport methods. The Monte Carlo method and deterministic methods solve problems in very different ways. Deterministic methods provide fairly complete information throughout each step of the problem. Monte Carlo only supplies information specifically requested by the user. The most common deterministic method is the discrete ordinates method that solves the transport equation for the average particle behavior. The Monte Carlo method simulates individual particles and records different aspects of their average behavior and places the answers in defined bins. The central limit theorem is used to deduce the average behavior of simulated particles within the system (RSICC 2002).

Monte Carlo and discrete ordinates methods solve the transport equation in two different ways. The Monte Carlo method solves the integral transport equation while the discrete ordinates methods solve the integro-differential transport equation. Monte Carlo uses simulated particle histories to solve the transport problem without solving the equation. From the solution, an equation can be derived that describes the probability density of particles (RSICC 2002).

The discrete ordinates methods breaks down the phase space into many small boxes. As particles move from one box to another, the boxes become consecutively smaller and the particles take a differential amount of time to cross a differential amount of space. This method has two different derivatives in space and time. On the other hand, the Monte Carlo method tracks particles between interaction events that are

separated by time and distance. In the Monte Carlo method, the integral equation does not contain terms involving time or space derivatives (Center 2002).

The Monte Carlo method is specifically designed for solving complicated, three-dimensional, time-dependent problems. There are no averaging approximations required in space, energy, and time. This allows all aspects of physical data to be represented (RSICC 2002).

The Monte Carlo method

Theoretically, statistical processes that cannot be modeled by computer codes using deterministic methods can be described by using Monte Carlo methods. The Monte Carlo codes use sequential simulation to comprise individual probabilistic events that make up a process. The totality of the event can be described by statistically sampling the probability distributions that control the event. Since it usually takes a large number of events, simulations are usually performed on a digital computer. A selection of random numbers is used to perform the statistical sampling. The basis of this process is tracking individual particles from their source to some predefined stopping point. Probability distributions are randomly sampled to determine the outcome at each step (LANL 2003).

CHAPTER V
METHODS FOR BUILDING AND TRANSFORMING THE INTERNAL DOSE MODEL INTO A READABLE LANGUAGE USABLE BY MCNPX

Introduction

Developing the input for MCNPX requires a specific set of instructions that must follow a logical sequence. The MAX/FAX phantom requires the use of Scion Image software to interpret the electronic image of the phantom (Vieira 2005). The phantom is saved as a tagged image file format (tiff) file. The Scion Image program is used to upload the file by changing the default width, height and slice parameters to match values of the matrix. The matrix values for the MAX phantom are 158, a width or x-axis, 74, a height or y-axis and 487, and a slice or z-axis. Each slice contains an x- and y-component as a two-dimensional matrix that has a value corresponding to a particular material in the body. Each value is unique and defined in a Microsoft Excel spreadsheet (Kramer 2003). The Excel spreadsheet contains 61 unique identifiers ranging from 1 to 160, the corresponding name of the material located in the body along with the number of voxels that contain the unique identifier number. Each voxel represents a volume of 0.36 cm^3.

Method description

Once the image is opened, each slice is loaded into a matrix that is displayed as a 3-dimensional image of the human body. Tools within the Scion program allow manipulation of the image in various ways such as enlarging, cropping or changing the image from black and white to a color format. The image originally appears in grayscale. The image was converted into a color format to differentiate between the various materials within the body. Under the options, color table menu, the system button was selected and the image on the computer screen appears as a color conversion

of the matrix for each slice starting with top of the head. The first slice corresponds to z=1. Each corresponding slice can be toggled by using the < and > keys. Figure 5.1 is an example of slice 121 of the MAX phantom that illustrates the various body tissues using color to correspond to the unique number identifier (Kramer 2003). In this figure, the purple represents the lung and the light blue represents the heart. The entire MAX tiff image is saved in appendix A.

Once the file is uploaded into the Scion Image program, each slice must be saved as an individual two-dimensional matrix. The DAT file contains a matrix of unique number identifiers that correspond to each type of tissue located within the body. Any voxel within the 74 x 158 matrix, that is not part of the body, is designated with the number 0. Figure 5.2 represents a portion of the 74 x 158 matrix delineated in number patterns. Each number represents a voxel with a unique x-, y- and z-position.

Each slice of the MAX phantom must be individually saved as a DAT file and stored in the same folder. For the MAX phantom, 487 DAT files were created and stored in an exported matrix folder.

As part of the MCNPX input deck, the matrix must be in a specific sequence which corresponds to the geometry of the universe that will be created. The program MATLAB was used to read the individual DAT files and convert them into a single DAT file that could be read into the MCNPX input deck. Appendix B provides a copy of the MATLAB code that was used to read the 487 individual DAT files and create a single voxmap that contained the MAX phantom data (MathWorks 2007). Figures 5.3 and 5.4 provide a 55% opaque image of the MAX phantom for both the anterior and posterior views illustrating the z-axis slice grid along with a color chart associated with different body tissues. The color scale to the right of each figure represents the tissue or organ number. Each number is assigned a unique color. The colors range from dark blue to dark red.

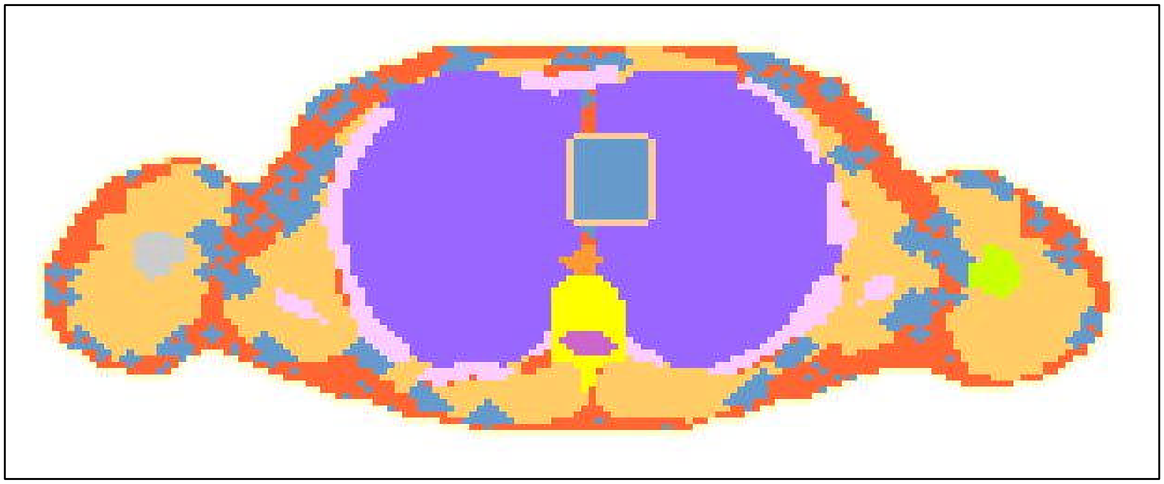

Fig. 5.1. A color representation of MAX phantom slice 121 showing various body tissues (MathWorks 2007).

0	0	0	0	0	0	0	0	0	0	0	0	0	0	0	0	0	0	0	0	0	0	0	0
0	0	0	0	0	0	0	0	0	0	0	0	0	0	0	0	0	0	0	0	0	0	0	0
0	0	0	0	0	0	0	0	0	0	0	0	0	0	0	0	0	0	0	0	0	0	0	0
0	0	0	0	0	0	0	0	0	0	0	0	0	0	0	0	0	0	0	0	0	0	0	0
0	0	0	0	0	0	0	0	0	0	0	0	0	0	0	0	0	0	0	0	0	0	0	0
0	0	0	0	0	0	0	0	0	0	0	0	0	0	0	0	0	0	0	0	0	0	0	0
0	0	0	0	0	0	0	0	0	0	0	0	0	0	0	0	0	0	0	0	0	0	0	0
0	0	0	0	0	0	0	0	0	0	0	0	0	0	0	0	0	0	1	1	1	1	1	0
0	0	0	0	0	0	0	0	0	0	0	0	0	0	0	1	1	1	9	22	22	22	22	1
0	0	0	0	0	0	0	0	0	0	0	0	0	1	1	22	22	22	22	9	9	9	9	121
0	0	0	0	0	0	0	0	0	0	0	1	1	121	121	22	22	22	22	9	9	9	121	121
0	0	0	0	0	0	0	0	0	0	1	22	22	121	22	22	22	9	9	9	9	9	9	121
0	0	0	0	0	0	0	0	0	1	22	22	22	22	22	9	9	9	9	9	9	9	9	9
0	0	0	0	0	0	0	0	1	22	22	22	22	9	9	9	9	9	9	9	9	9	9	9
0	0	0	0	0	0	0	0	1	22	22	22	22	9	9	9	9	9	9	9	9	9	9	9
0	0	0	0	0	0	0	1	22	22	22	22	22	9	9	9	9	9	9	9	9	9	9	9
0	0	0	0	0	0	1	22	22	22	22	22	22	9	9	9	9	9	9	9	9	9	9	9
0	0	0	0	0	1	22	22	22	22	9	9	9	9	9	9	9	9	9	9	9	9	9	9
0	0	0	0	0	1	22	22	22	9	9	9	9	9	9	9	9	9	9	9	9	9	9	121
0	0	0	0	1	22	22	22	22	9	9	9	9	9	9	9	9	9	9	9	9	9	121	121
0	0	0	0	1	22	22	22	22	9	9	9	9	9	9	43	43	43	43	9	9	121	121	121
0	0	0	1	22	22	22	22	22	9	9	9	9	9	43	43	43	43	43	43	43	9	121	121
0	0	0	1	22	22	22	22	22	22	9	9	9	9	43	43	43	43	43	43	43	9	9	121
0	0	1	22	22	22	22	22	9	9	9	9	9	9	43	43	43	43	43	43	43	9	9	121
0	0	1	22	22	22	22	22	9	9	9	9	9	9	43	43	43	43	43	43	43	9	9	9
0	1	22	121	22	22	9	9	9	9	9	9	9	9	43	43	43	43	43	9	9	9	9	121
0	1	121	121	121	121	121	9	9	9	9	9	9	9	9	43	43	43	43	9	9	9	121	121
0	1	22	121	22	121	9	9	9	9	9	9	9	9	9	9	43	9	9	9	9	9	9	121
0	1	121	22	22	9	9	9	9	9	9	9	9	9	9	9	9	9	9	9	9	9	9	9
0	1	121	121	22	121	9	9	9	9	9	9	9	9	9	9	9	9	9	9	9	9	9	9
0	1	121	121	121	121	121	9	9	9	9	9	9	9	9	9	9	9	9	9	9	9	9	22
0	1	22	121	22	121	9	9	9	9	9	9	9	9	9	9	9	9	9	9	9	9	9	22
0	1	22	22	22	9	9	9	9	9	9	9	9	9	9	9	9	9	9	9	9	9	9	22
0	1	22	22	22	9	9	9	9	9	9	9	9	9	9	9	9	9	9	9	9	9	9	22
0	0	1	22	22	9	9	9	9	9	9	9	9	9	9	9	9	9	9	9	9	9	22	22
0	0	1	22	22	9	121	9	9	9	9	9	9	9	9	9	9	9	9	9	121	22	22	22
0	0	1	1	22	22	121	121	9	9	9	9	9	9	9	9	9	9	9	121	121	22	22	121
0	0	0	1	22	22	121	22	121	9	9	9	9	9	9	9	9	9	121	22	121	22	22	22
0	0	0	0	1	121	121	121	121	121	9	9	9	9	9	9	9	121	121	121	121	121	22	22
0	0	0	0	0	1	1	22	22	121	121	9	9	121	9	9	9	121	121	121	121	121	22	1
0	0	0	0	0	0	0	1	22	121	22	9	121	121	121	22	22	22	22	22	121	1	1	0
0	0	0	0	0	0	0	0	1	22	22	22	22	121	22	22	22	22	121	22	1	0	0	0
0	0	0	0	0	0	0	0	0	1	1	1	1	22	22	22	22	121	22	1	0	0	0	0
0	0	0	0	0	0	0	0	0	0	0	0	0	1	1	1	1	1	1	0	0	0	0	0
0	0	0	0	0	0	0	0	0	0	0	0	0	0	0	0	0	0	0	0	0	0	0	0

Fig. 5.2. A portion of the Matrix number representation of MAX phantom slice 121.

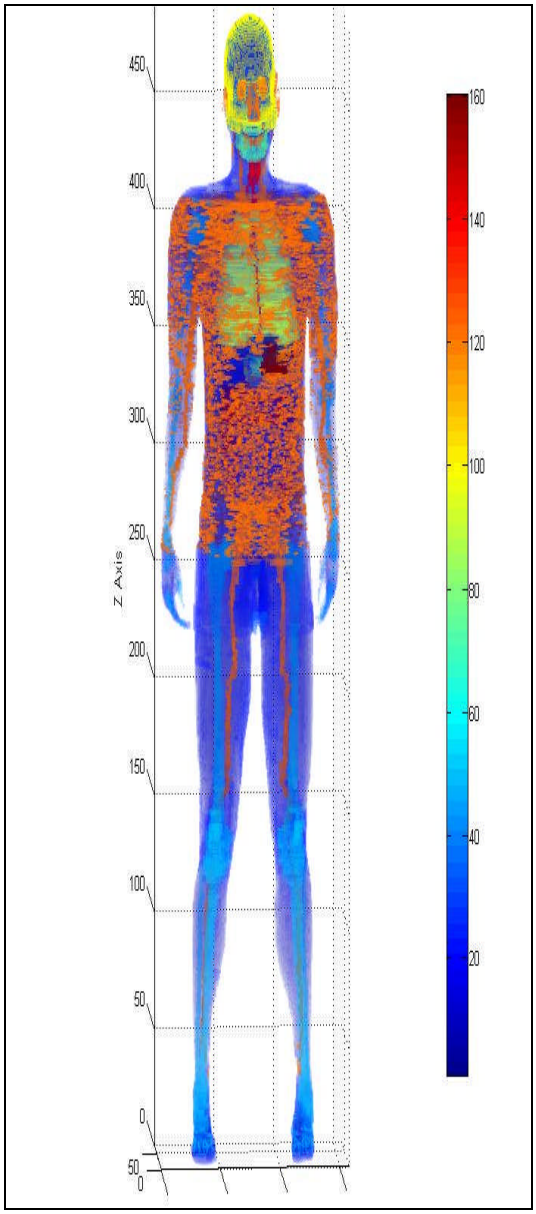

Fig. 5.3. Front view Scion MAX Phantom

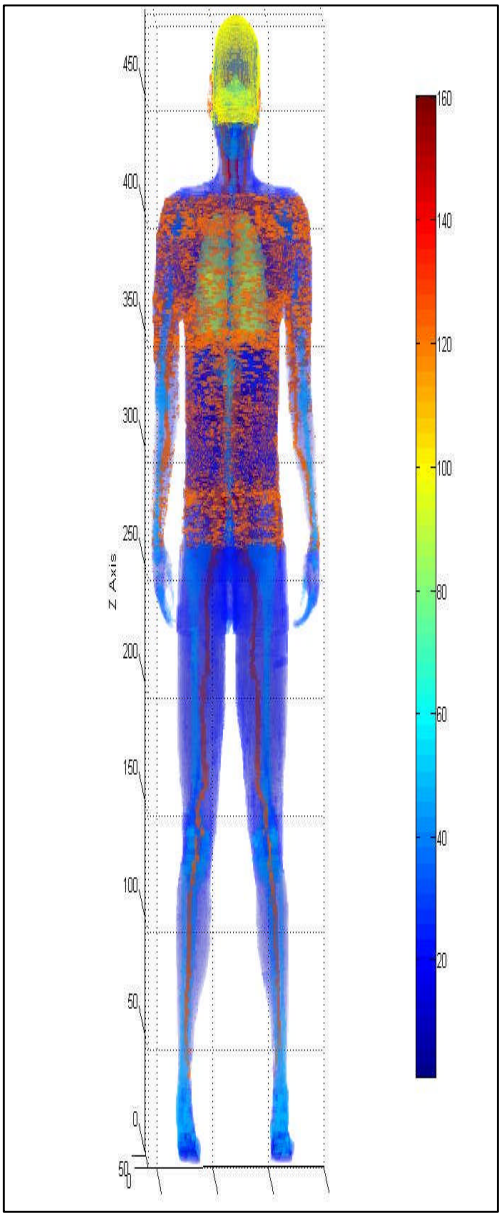

Fig 5.4. Rear view Scion MAX Phantom

The phantom images can be manipulated in any 360-degree orientation. Internal organs can be viewed by adjusting the opacity of the image. An opacity of 55% was chosen as the best representation for the phantom. The dose profile can be viewed in a similar manner.

The program creates a voxel map with a three-dimensional, x-, y- and z-matrix that correctly corresponds to the 74 x 158 x 487 matrix. Each data file is opened and read into the corresponding slice of the voxmap. Once the voxmap is built, another program is used to transform the voxmap into a single file that can be directly copied into the MCNPX input file.

In the MAX phantom, all of the voxels outside of the phantom correspond to air and are given the unique identifier of zero. The MCNPX basic geometry code, that builds the universes to be used, does not allow a universe coded as zero. In MCNPX, zero constitutes a vacuum. Therefore, in the code used in this research all of the values within our voxmap and any value that contains a zero was replaced with the arbitrary number three. The number three was uniquely identified as air. Once this process is complete, the program must transform a three dimensional-matrix into a one-dimensional string.

Three different indices are set up to correspond with each dimension in the voxmap matrix. The indices are given a maximum value equivalent to the largest value in each dimension. Due to the rules associated with the MCNPX input code, the string of values must be printed in a specific format. No line can extend beyond 80 characters in length, including punctuation and spaces; nor should a character be placed within the first 5 spaces of the line. The program initially sets each x-, y- and z-index to 1. Since the z-index, which corresponds to the horizontal slices through the phantom, are the last values to be read, a loop is set up to increment the z-index. Another loop limits the length of the print line to less than 70 characters. To maintain the integrity of the phantom, the voxmap values are read starting in the [1,1,1] position and moving to the [2,1,1] point. Therefore, the program must index the x-position first until x reaches its maximum. The next step is to increment the y-index while simultaneously returning the

x-index to one. The program will proceed in this manner until the y-index reaches its maximum value. Only then will the program increment the z-index while simultaneously returning the x- and y-indices to one. This iterative process will continue until all of the values have been read into a one-dimensional array. Since there are over 5,694,004 values that average 2 characters apiece and have one space between them, this would require 244,028 lines of code just for the phantom. The program was designed to reduce the number of lines of code for the phantom down to 26,318 lines by using a repeat function.

An if-statement is used to compare the current index x, y and z with the next index x, y and z. If the value located at the current position (1, 1, 1) and the value at the adjacent position (2, 1, 1) is the same, the program will count the number of repetitive values while incrementing the next index to the next position and repeating the evaluation until a different value is found. Once this occurs, the repeat variable will be reset to zero and the process will continue through the string of values. This step follows the same order as mentioned above. Finally, the output of this program will begin with five spaces, the value located at the first position, followed by a space and either the number of repeats along with the letter r and a space or a new value and a space. This process will continue until the number of characters on the line reaches 70 and then a new line with 5 spaces is created and the process continues until all of the values are printed in the output file labeled MCNP_INPUT. A small snapshot sample of the MCNP_INPUT file is listed in Figure 5.5.

```
3 2082r 1 28r 3 40r 1 35r 3 36r 1 38r 3 33r 1 41r 3 30r 1 46r 3 26r
1 48r 3 23r 1 52r 3 20r 1 53r 3 19r 1 55r 3 17r 1 55r 3 17r 1 55r
3 17r 1 55r 3 18r 1 54r 3 18r 1 53r 3 21r 1 50r 3 23r 1 43r 3 30r
1 39r 3 34r 1 30r 3 45r 1 6r 3 10r 1 1r 3 55r 1 1r 3 4724r 1 14r
3 56r 1 24r 3 47r 1 47r 3 24r 1 52r 3 21r 1 54r 3 18r 1 55r 3 18r
1 55r 3 18r 1 54r 3 19r 1 53r 3 20r 1 52r 3 20r 1 52r 3 21r 1 50r
3 23r 1 48r 3 24r 1 46r 3 27r 1 44r 3 29r 1 42r 3 31r 1 39r 3 39r
1 26r 3 4184r 1 28r 3 40r 1 3r 22 2r 9 8r 22 16r 1 2r 3 36r 1 22 6r
9 8r 22 12r 9 6r 1 1r 3 33r 1 22 7r 9 8r 22 10r 48 4r 9 22 3r 9 1 1r
3 30r 1 22 8r 9 8r 22 6r 48 8r 22 7r 1 3r 3 25r 1 22 9r 9 8r 22 6r
48 8r 22 8r 9 48 1r 1 1r 3 23r 1 22 9r 9 8r 22 6r 48 8r 22 1r 48 2r
22 2r 9 2r 48 2r 1 2r 3 19r 1 22 10r 9 8r 22 6r 48 13r 22 9 4r 48 3r
9 22 1 3 18r 1 22 10r 9 8r 22 6r 48 8r 9 4r 22 9 4r 48 3r 9 2r 1 1r
3 16r 1 22 10r 9 8r 22 6r 48 8r 9 4r 22 9 4r 48 3r 9 2r 22 1r 1 3 15r
1 22 10r 9 8r 22 12r 9 7r 22 48 8r 9 2r 22 1r 1 3 15r 1 22 10r 9 8r
22 5r 9 22 5r 9 7r 22 48 8r 9 22 3r 1 3 15r 1 22 26r 48 1r 22 2r
9 9r 48 7r 9 1r 22 3r 1 3 16r 1 22 24r 48 2r 22 1r 9 10r 48 4r 9 4r
22 3r 1 3 16r 1 22 24r 48 2r 22 1r 9 10r 48 4r 9 4r 22 2r 1 3 18r
1 1r 22 22r 48 9 14r 48 1r 9 6r 22 2r 1 3 21r 1 22 21r 9 17r 22 1r
9 22 1 5r 3 23r 1 22 2r 9 7r 22 9r 9 11r 22 6r 1 2r 3 30r 1 22 1r
9 7r 22 9r 9 8r 22 1r 1 7r 3 34r 1 2r 22 6r 1 10r 9 1r 1 7r 3 45r
1 1r 22 1r 1 2r 3 10r 1 1r 3 55r 1 1r 3 4576r 1 14r 3 56r 1 1r 22 3r
9 3r 22 1r 9 22 3r 1 7r 3 47r 1 22 5r 9 3r 22 1r 9 1r 22 2r 9 22 6r
1 21r 3 24r 1 22 6r 9 3r 22 1r 9 1r 22 2r 9 22 21r 9 5r 22 1 3r 3 20r
22 7r 9 3r 22 1r 9 3r 22 9 46 22 9 5r 22 13r 9 5r 22 4r 1 2r 3 17r
1 22 6r 9 3r 22 1r 9 46 9 1r 22 1r 46 9 7r 22 12r 9 5r 22 7r 1 3 16r
1 22 6r 9 3r 22 1r 9 46 9 1r 22 1r 46 9 7r 22 12r 9 5r 22 8r 1 3 16r
1 22 5r 9 3r 22 1r 9 46 9 1r 46 22 1r 9 11r 22 8r 9 5r 22 9r 1 3 16r
1 22 4r 9 3r 22 1r 9 22 9 22 46 22 2r 9 10r 22 9 5r 22 1r 9 5r 22 9r
1 3 17r 1 22 3r 9 3r 22 1r 9 22 2r 46 22 1r 46 2r 9 5r 22 2r 9 6r
22 1r 9 10r 22 4r 1 3 18r 1 22 2r 9 3r 22 1r 9 22 1r 46 1r 22 1r
46 2r 9 5r 22 2r 9 6r 22 1r 9 10r 22 4r 1 3 18r 1 22 2r 9 3r 22 8r
46 2r 22 1r 9 4r 22 5r 9 2r 22 6r 9 5r 22 4r 1 3 19r 1 22 1r 9 3r
22 17r 9 22 1r 9 22 4r 9 22 6r 9 5r 22 3r 1 3 21r 1 22 25r 9 6r 22 2r
9 2r 22 9 5r 22 2r 1 3 22r 1 22 12r 9 22 9 6r 22 5r 9 4r 22 2r 9 2r
22 7r 1 1r 3 24r 1 22 11r 9 22 9 6r 22 5r 9 4r 22 2r 9 2r 22 6r 1
3 27r 1 22 11r 9 46 3r 9 3r 22 12r 9 2r 22 5r 1 3 29r 1 22 11r 46 2r
9 3r 46 1r 22 18r 1 1r 3 31r 1 5r 22 7r 9 3r 46 11r 22 2r 1 6r 3 39r
1 26r 3 4109r 1 29r 3 40r 1 2r 22 3r 9 8r 22 16r 1 2r 3 36r 1 22 6r
9 8r 22 12r 9 6r 1 1r 3 33r 1 22 7r 9 8r 22 10r 48 4r 9 22 3r 9 1 2r
3 29r 1 22 8r 9 8r 22 6r 48 8r 22 8r 1 2r 3 25r 1 22 9r 9 8r 22 6r
```

Fig. 5.5. Sample input of MCNPX geometry card.

CHAPTER VI
METHODS FOR BUILDING AN MCNPX INPUT CODE

Introduction

MCNPX requires several elements as part of its input file. The first element usually contains a message block followed by a blank line delimiter. This element is optional but recommended. The second element is a One-line Problem Title Card. This is followed by the third element which contains the Cell Card. A blank line delimiter is next followed by the fourth element which contains a Surface Card. Another Blank Line Delimiter follows and than the fifth element contains the Data Card. Finally, a Blank Line terminator is optional (RSICC 2002).

Cell card

Knowing that multiple input files would be used, the most generic form of code was chosen. The title of the input file was simply One Plane Code followed by a blank line delimiter. A comment line was used to notify the user that the following lines would begin the MCNP input deck. The Cell card consists of 73 cells, the first is defined by cell 998 that does not initially contain any material but is bounded by 6 surfaces defined as -2, 1, -4, 3, -6 and 5. The second cell is defined by cell 999 that initially contains a void and is bounded by 6 surfaces defined as -7, 1, -8, 3, -9, 5 and contains universe 999. A lattice command is inserted with a fill instruction of 0 to 73 elements in the x-direction, 0 to 157 elements in the y-direction and 0 to 486 elements in the z-direction. The following lines from 6 through 26318 hold the MAX phantom that has been redefined by the MATLAB program mentioned in Chapter V. The third is defined as Cell 1, filled with material one, has a density of 1.09 g/cm^3, bounded by surfaces -7, 1, -8, 3, -9, 5, and contains universe one. A comment notes that this material is defined as skin. Cells 2 through 189 are bounded by surfaces like one but contain a different material, have a defined density and a unique universe. A comment has been

added to the end of each cell that defines the specific material represented in the phantom. Cells 180 through 189 are defined as air within a detector located outside of the MAX phantom but within the phantom matrix. Cell 74 is a void that contains no materials or cells and is bounded by opposite surfaces 2, -1, 4, -3, 6 and -5 as those bounding Cell 998. Figure 6.1 provides an example of part of the Cell card.

Surface card

As per the MCNPX manual, a blank line delineator has been added to separate the cell card from the surface card. Since the phantom consists of a cubed matrix, planer surfaces were the natural choice for the surface card. Figure 6.2 provides an example of the surface card. Each surface that is used in the cell card must contain a surface number. Following the surface number is the surface type. The letters px, py and pz indicate planes normal to the x-, y- and z-axis. The following entry on the command line is the numerical position in centimeters where the surface starts. Therefore, Cell 998 is bound by two planes normal to the x axis from 0 cm to 26.64 cm, two planes normal to the y-axis from 0 cm to 56.88 cm and two planes normal to the z-axis from 0 cm to 175.32 cm. A blank line delineator separates the cell card from the surface card.

Data card

Figure 6.3 represents the important commands within the data card. The data card is broken down into five distinct subsections. The first section is the mode. Since neutrons or protons are not a concern for this experiment, the mode that was chosen for the program was “p e” which directs the MCNPX program to perform photon and electron transport only. For proton or neutron sources, the program can easily be modified to accommodate those types of radiations. A line of code was added after the mode section. The line of code specifies the number of particles or number of histories

that will be followed by the program. The larger the number of histories, the better the statistics but it will also mean the longer the time it will require to complete the simulation. One million histories provided good statistics without the prolonged expenditure of time.

```
    4-        998    0   -2  1  -4  3  -6  5  fill=999 (0.0  0.0  0.0)
    5-        999    0   -7  1  -8  3  -9  5  u=999  lat=1  fill=0:73 0:157 0:486


26319-          1    1  -1.09  -7  1  -8  3  -9  5   u=1    $ Skin
26320-          2    like 1 but mat=2   rho=-1.007   u=2    $ Cer Sp Fl
26321-          3    like 1 but mat=3   rho=-0.0013  u=3    $ air
26322-          5    like 1 but mat=5   rho=-1.038   u=5    $ Spine
26323-          6    like 1 but mat=6   rho=-1.41    u=6    $ Rib Clav
26324-          7    like 1 but mat=7   rho=-1.29    u=7    $ Pelvis
26325-          8    like 1 but mat=8   rho=-1.05    u=8    $ Heart
26326-          9    like 1 but mat=9   rho=-1.06    u=9    $ Muscle
26327-         11    like 1 but mat=11  rho=-1.05    u=11   $ Brain
26328-         12    like 1 but mat=12  rho=-1.06    u=12   $ Liver
26329-         14    like 1 but mat=14  rho=-1.05    u=14   $ Kidneys
26330-         15    like 1 but mat=15  rho=-1.05    u=15   $ Pharynx
```

Fig. 6.1. Sample of MCNPX input deck Cell card.

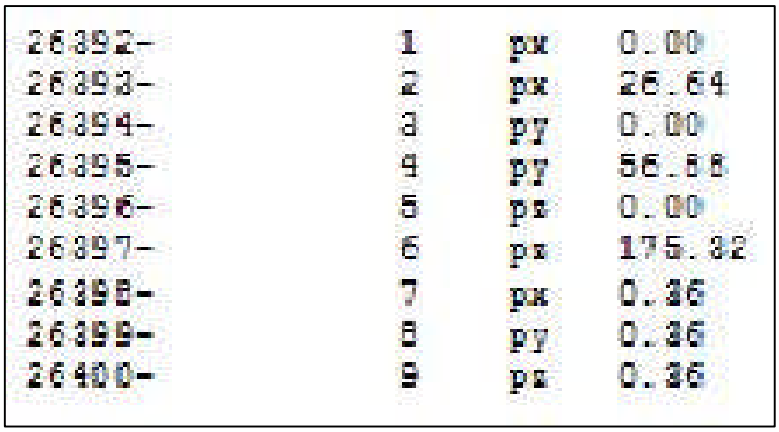

Fig. 6.2. Sample of an MCNPX input deck surface card.

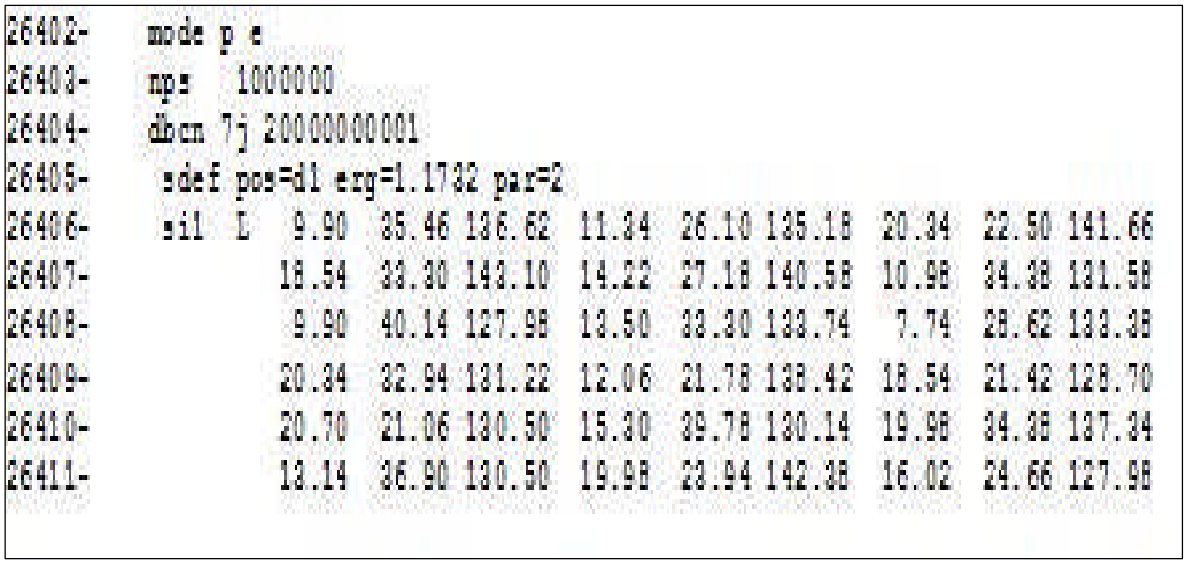

Fig. 6.3. Sample of an MCNPX input deck data card.

Material definition card

An example of the material definition card can be seen in Figure 6.4. The material definition card refers to the cell and surface parameters defined by their appropriate cards. The importance of each cell must be entered in the order that they appear. An importance must be given to each mode and for each cell. For photons and electrons, an importance of one was selected for cells 1 through 73. For cell 74 an importance of zero was chosen. The program would than be directed to consider all electron and photon interactions within cells 1 through 73 but would ignore any interactions within cell 74. The importance command was placed at the end of the data card. This provided easier access to the line command when small errors were encountered while writing the code. To save time and memory, a repeat command was used since all of the cells were given equal importance with the exception of the last cell.

The third section refers to the source specification card. In Figure 6.3, line 26405 is the SDEF command line. This will define the starting history. The first part of the command is the position of the starting history. In the code listed above, "pos=d1" refers to a subset command listed in line 26406. The abbreviation "si1" refers to the first source information card. The "L" refers to a lattice that will follow with a matrix of x-, y- and z-positions. A volume source was desired and for that another MATLAB computer program was created that would search for all of the voxels associated with a given material. To improve efficiency, a fraction of the total voxels was used that would represent the entire organ without losing statistical significance. This program would than select the positions of the identified voxels, reformat and print them in accordance with the strict MCNPX code and create a probability of having a starting history occur in each of the selected voxels.

The program to create the source file was added as a subsection to the original read file that creates the MAX phantom "voxmap". The source program creates a minimum z-variable and sets it to one and a maximum z-variable and sets it to the maximum z-value of 487. Selecting a source is an option available to the user.

```
31406-          sp1  0.0000667 14999r
31407-          m1   1000.04p     -.100
31408-               6000.04p     -.204
31409-               7000.04p     -.042
31410-               8000.04p     -.645
31411-               11000.04p    -.002
31412-               15000.04p    -.001
31413-               16000.04p    -.002
31414-               17000.04p    -.003
31415-               19000.04p    -.001   $ Skin, Adult [ICRU Report 46, 1992]
31416-          m2   1000.04p     -.111
31417-               8000.04p     -.880
31418-               11000.04p    -.005
31419-               17000.04p    -.004   $ Cerebrospinal fluid [Duck FA, 1990]
```

Fig. 6.4. Sample of an MCNPX input deck material definition card.

The user may choose any material to become a volume source or the user may read in just the phantom into the "voxmap". By placing the value one in the variable "makingasource", the command will initiate the source code. If the user does not wish to create a source, a zero is assigned to the variable. The next line asks the user to select the organ or material into which a source is to be placed. By entering the unique material identifier within the brackets separated by a space, the user can enter as many sources as there are materials. The fraction of activity from zero to one can than be entered for each source organ specified in the organ variable. This allows the user to create a spectrum of activities throughout the body by normalizing all activity to unity. As the activity changes over time, the user can create a source output file that will match the change by adjusting the fraction of activity in accordance with each source organ. The source density is defined by the user. The optimum source density was based on several statistical simulations for the lung. A density fraction of 15,000 source voxels per 87,506 total lung voxels was sufficient to provide a volume source for each material

within the body. The user would specify the name of a new source file. The voxmap is created and the values from the MAX phantom are read into the voxmap. The source file is opened and five blank spaces, “si1”, a space and the letter “L” are printed in the first line. An if-statement is used to determine if a source will be created. A variable is set to zero and used to count the number of sources that have been entered by the user. A loop is used starting from one up to the number of values entered in the organ string. Based on the number of source organs, the program counts the number of voxels associated with each organ in the voxmap and assigns that to a new variable. Another variable will be assigned the value based on the size of the entire voxmap. The “sourcesfound” variable will be set to zero. The source density is calculated based on the lung fraction multiplied by the number of voxels for the organ in the phantom. The result is rounded to the nearest whole number. This value is assigned to another variable. A loop is set up to measure the number of sources found with the number of sources calculated. Three random number generators are used to select a random position along each of the three axes and retrieve the unique number value located at that location. The material located at a random position is compared to the source organ value. If the two values are equal, the "sourcesfound" and "totalsourcesfound" variables are incremented by one. The x, y and z position indicators are than converted to centimeters. Another limitation of the MCNP code is that a source cannot be located on any surface. Therefore, each x-, y- and z-position is altered by 0.18 cm ensuring that the source is placed in the middle of the voxel. The new source position is printed with a blank space between the x-, y- and z-values. Another if-statement was inserted to print the three source position values on one code line before creating another code line with 10 blank spaces at the beginning of the line. This keeps all of the source values in three even columns. This loop will continue until the number of source positions is equal to the calculated value for each source organ. The program will print a new line, four blank spaces, "sp1" and two more blank spaces. It will assign a new variable based on normalizing the activity. The variable is equal to the activity in each source organ provided by the user divided by the total activity of all source organs. A loop is set up

to print the source probability for each source organ followed by a space. The source probability is the normalized activity for each source organ divided by the number of source organ voxels. This result is followed by a space until all source organs have a corresponding probability associated with each source organ voxel. All of the data are printed to the source organ file. This information is cut and pasted into the data card.

The fourth section is the material specification card. Each cell card must have a material number and each material number must be identified on the material card. Each material within the human body is made up of a number of elements. Each element has a different interaction cross-section for different radiations at different energies. The elemental compositions and densities of all the selected body tissues were provided by ICRU Report 46 (ICRP 1990). Material numbers one through 160 were chosen for this code. Each material number is followed by an identification number corresponding to the constituent element or nuclide followed by the atomic fraction of that element or nuclide. This process continues until all of the elements needed to define the material have been listed. The atomic number is followed by the mass number. The ".04p" refers to the photon interaction library that is used to determine the interaction cross section. A negative sign followed by a three digit number behind a decimal refers to the weight fraction of element in the material. A comment has been included to identify the organ associated with the material.

The final section of the data card is the tally card. The tally cards are used to specify what values the program should return. The return information is requested with specific codes. The "f6:p" code was used to track the estimate of energy deposition and the "f4:p" code was used to track the estimate of fluence rate through a cell.

Output file

MCNP automatically prints out a listing of the input file, a problem summary of particle creation and loss, KCODE cycle summaries, tallies, tally fluctuation charts along with basic and default tables. There are many different print variations that the user can activate but are not included in the input file (RSICC 2002).

The output file is the return that MCNP provides the user based on the input file and tallies that the user has requested. The first section of the output card is a simple copy and paste of the input card. The program that was created had 31,990 lines of code. This is followed by a list of warnings that notify the user of potential problems within the code. The input code created 10 warnings. The first six warnings notify the user that surfaces 1, 3, 5, 7, 8, 9 appear more than once in a chain. This is not a concern because the input code does not ask for any tallies based on individual surfaces within the code. The seventh warning is that one material contains an unnormalized fraction. The materials that were used in the input code were derived from ICRU Report 46 and some contain fractions of less than 0.03 percent (ICRU 1990). This does not produce any significant problems with the cross-section data libraries. The final two warnings represent the volume or area for repeated structure tally 4 and 6 may be wrong. This is based on the duplication of more than one surface. The volume and area used within the tally have been verified to be correct.

MCNPX creates a table that lists the basic properties of the cell. The table consists of the cell and material numbers, calculated atomic and mass density values, volume and mass of a cell along with photon and electron importance. The next section contains the random number control along with the starting random number. Following the random number is a print table that provides material cross sections. The cross section information comes from a MCNP library. ENDF/B-VI Release 8 Photoatomic Data provides the cross sections for all of the elements contained in the phantom and listed in the material section. The table is accessed by the designator ".04p" which follows the element and atomic number of the material. The next section provides a table with the maximum photon and electron energies as well as the minimum or cutoff energy for the history. The energies can be adjusted to better optimize the time requirements of the program but some information may be lost at lower energies. Following the energy table is the table that provides the dynamic memory allocation. The program tracks the number of histories and the time that the first history begins as well as the time the last history ends.

The next section is the problem summary section. Two tables tracking information on photons and electrons are provided. For photons, one table provides information on the creation of photons while the other table provides information on the loss of photons. The same two tables apply for electrons. The photon creation table provides the number and energy of source particles, the number and energy of bremsstrahlung, positron annihilation, electron and first fluorescence x rays created. A total for each category is provided at the end. The photon loss table provides the same track, weight per source particle and energy for photons that escape, are captured, interact via Compton scatter or are involved in pair production. The electron creation table measures pair production, Compton recoil, photoelectric, photon-auger, electron-auger and knock-on collisions that are produced. The electron loss table provides the number of electrons that are lost and the number that achieve energy cutoff. It also provides the energy lost from scattering and bremsstrahlung.

Following the creation and loss table is the bin tally analysis. The tally is listed in two tables for photons and electrons. The table provides a summation of activity in each cell. It provides the number of particles entering the cell, population and number of collisions within the cell. It also provides the average track weight and distance.

The last section is the estimate of particle fluence for photons across user defined cells. The user has created 10 defined cells representing the location of detectors outside of the predefined phantom but inside the air boundary. The detectors are air but can contain any predefined user material. The detectors are placed in user defined positions around the anterior and posterior of the lung. The top of the table provides the volumes within each cell followed by the fluence in units of $1/cm^2$. The middle portion contains the tabulated fluence along with their associated error. The bottom portion provides an analysis of the tallies which includes 10 statistical checks. The test file passed all 10 statistical analyses for the fluence tally.

CHAPTER VII
METHODS FOR BUILDING VOLUME DETECTORS INTO THE MODEL

Introduction

Part of the MCNPX output tallies allow the user to request a fluence rate (particles per unit area per second) or a dose (energy per gram). It would be convenient to derive a volume detector that allows the user to predefine the volume and material outside of the human phantom but within the universe. With this information, the user can match up various commercial detectors for calibration and use in the field.

Method description

Figure 7.1 is a three-dimensional representation of the basic voxmap created by the Scion program. The voxmap is simulation through a MATLAB voxplot program to create the image (MathWorks 2007). A 55 percent opacity was used to allow the viewer to see internal organs. The color bar to the right provides each organ with a specific color. Each organ has a unique number identifier that is given a color code from 160 (Dark Red) to 0 (Dark Blue). The universe outside of the phantom is made up of air. The user defines air based on the chemical make-up and density in the material section of the MCNPX input program. Since the entire model is made up of small voxels, a program has been created to allow the user to define a point in space where the center of a detector would be.

The user would define a material number that does not coincide with any of the predefined materials within the phantom. Ten arbitrary detectors were chosen and placed in a pattern around the front and back of the phantom. Since the lung was chosen as the primary organ of interest, the detectors where positioned at the top, bottom, left, right and center. The positions where chosen based on the accessibility and ease of

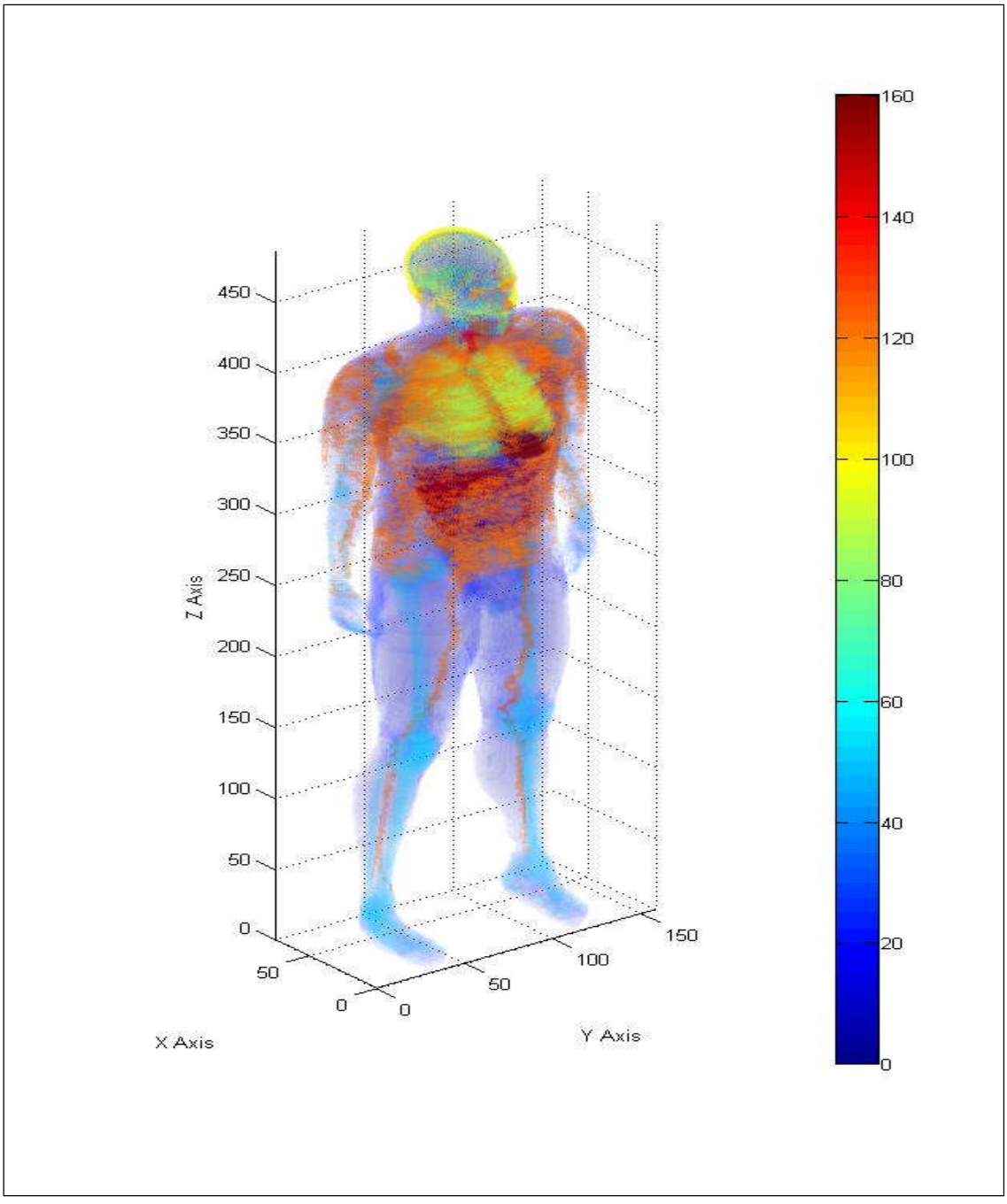

Fig. 7.1. MATLAB three-dimensional representation of the voxmap using the voxplot program.

identifying locations by emergency responders. The flexibility of the program allows the user to define the size, volume, density and location of a single detector or multiple detectors.

For ease of this test, a detector made of air with a circular radius of 5 cm and a thickness of one voxel was selected. This configuration represents a standard Geiger-Mueller pancake probe that represents a common detector issued to emergency responders. The detector number selected was 180 and the geometry selected was a circle with a radius of 5 cm. As an example, the center of detector 180 was located at [20 90 401]. The position of the detector is located in the x-, y-, and z-direction by taking each number and multiplying it by 0.36 cm. The program starts two loops that run from minus the radius to plus the radius based on the center of the detector. Three separate if-statements are built into the program to determine which plane the user wants to define as running parallel to the detector. This allows the user to determine the detector orientation. Once the user selects the orientation, the program finds the material located at the center of the detector position. Based on the radius of the detector, the program determines if any of the voxels are inside the human phantom and if so, it will end and notify the user that the detector is hitting the body. If all of the detector voxels are outside of the body, the program replaces the old air number with the new detector number. Figure 7.2 provides an example of a detector being placed at the upper, left, front of the lung. Figure 7.3 provides a side view to show that the detector is not located within the body. Figure 7.4 provides the anterior view of the test phantom that was used in this problem. Figure 7.5 provides the lateral view of the test phantom. The color scale to the right of each figure represents the tissue or organ number. Each number is assigned a unique color. The colors range from dark blue to dark red. It is based on the 10 detector design of a simple one voxel thick 5 cm diameter cylinder with 5 detectors placed around the front and five around the back of the lung.

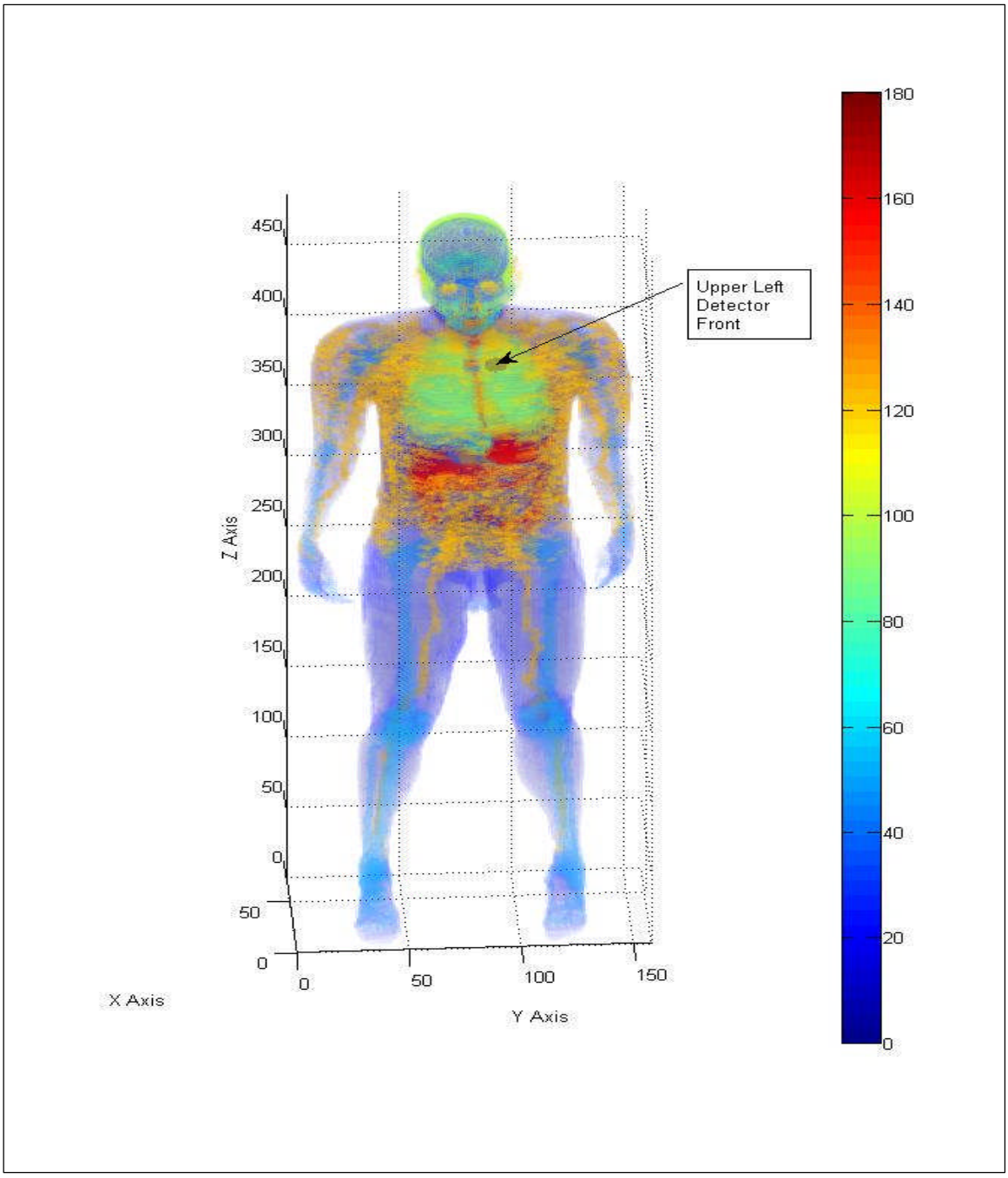

Fig. 7.2. Anterior View of MAX phantom with 5 cm diameter detector located at the upper left chest wall.

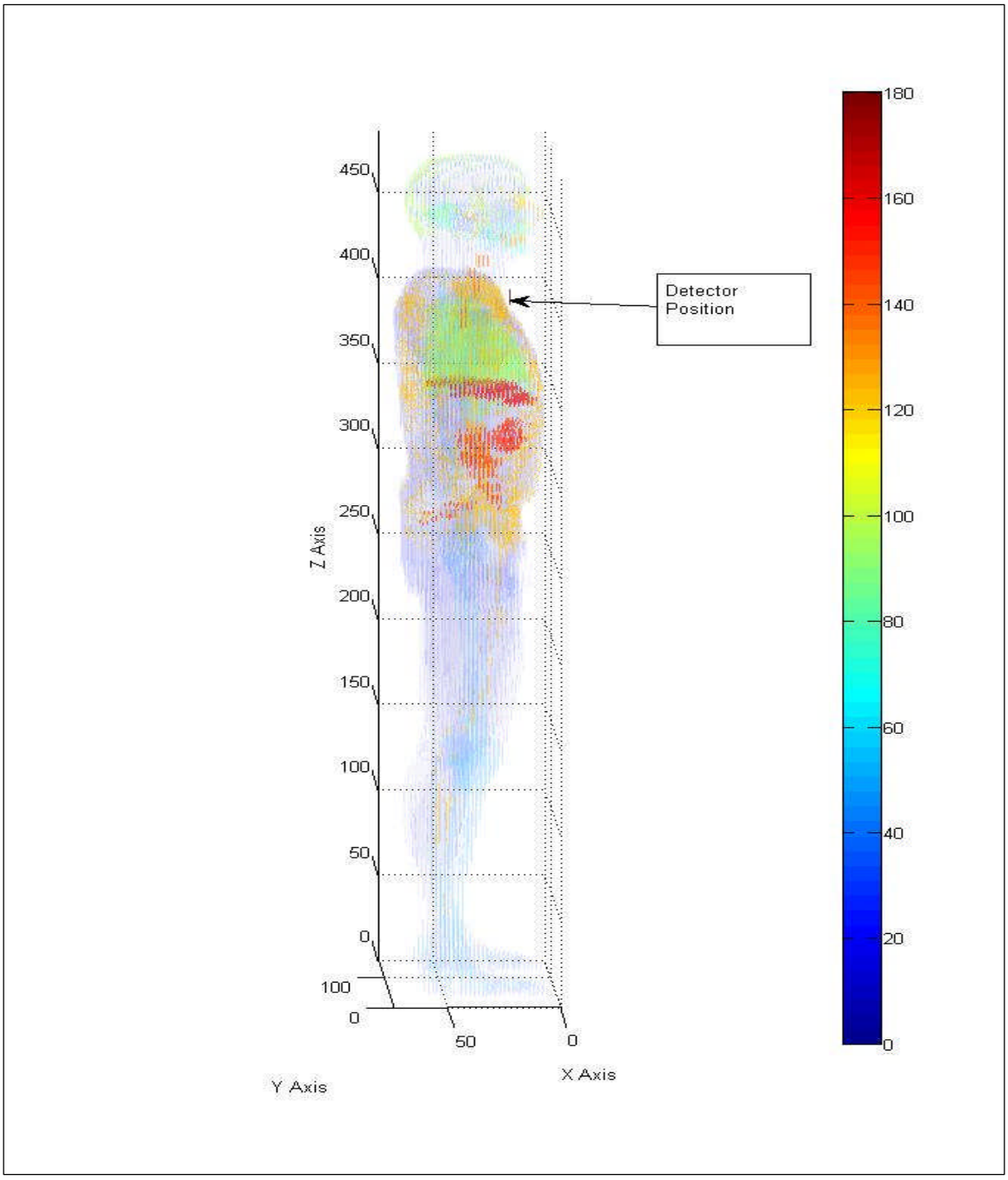

Fig. 7.3. Lateral view of MAX phantom with 5 cm diameter detector located at upper chest wall without entering the phantom.

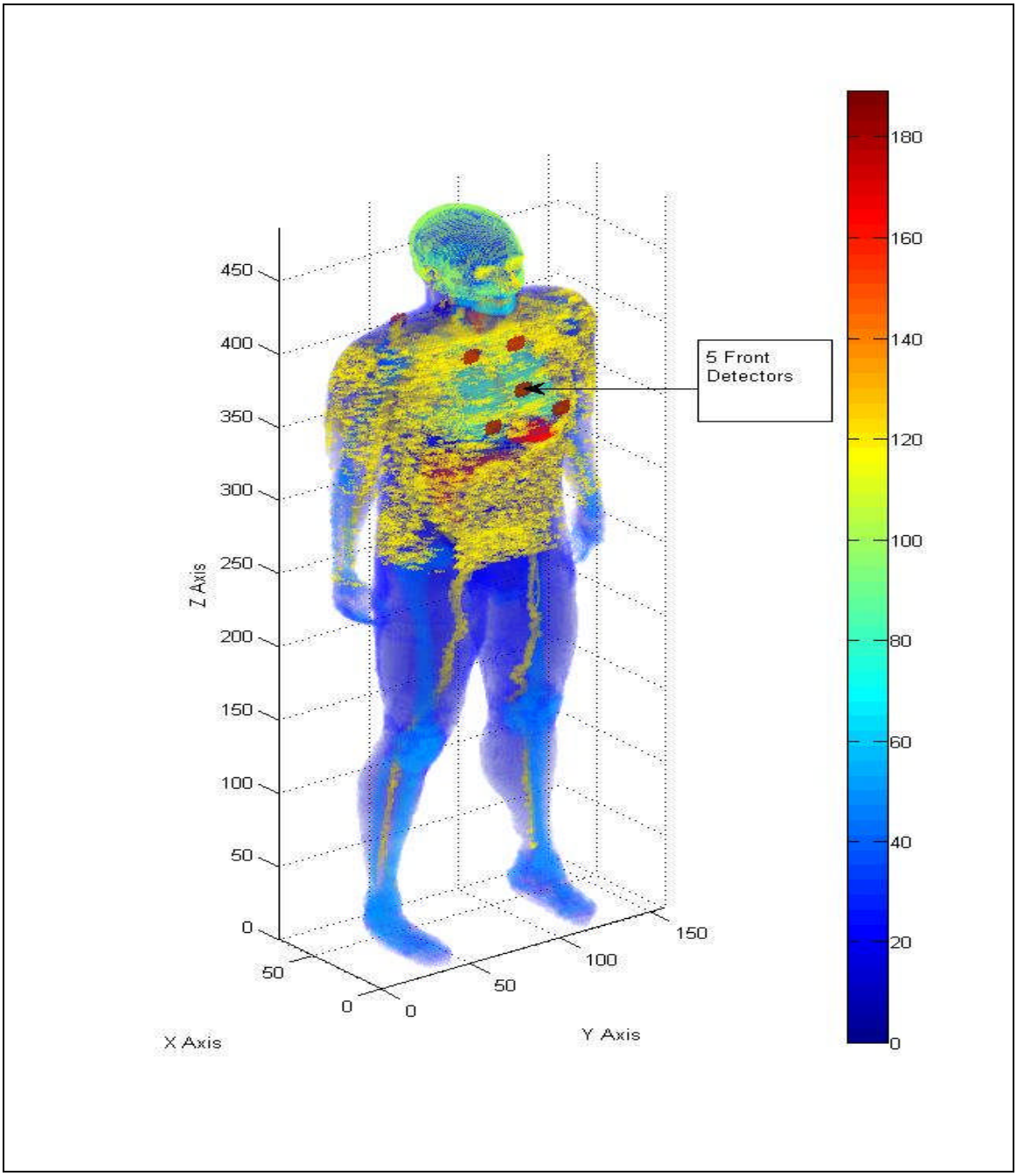

Fig. 7.4. Anterior view of MAX phantom with five 5 cm diameter detectors placed around the chest wall.

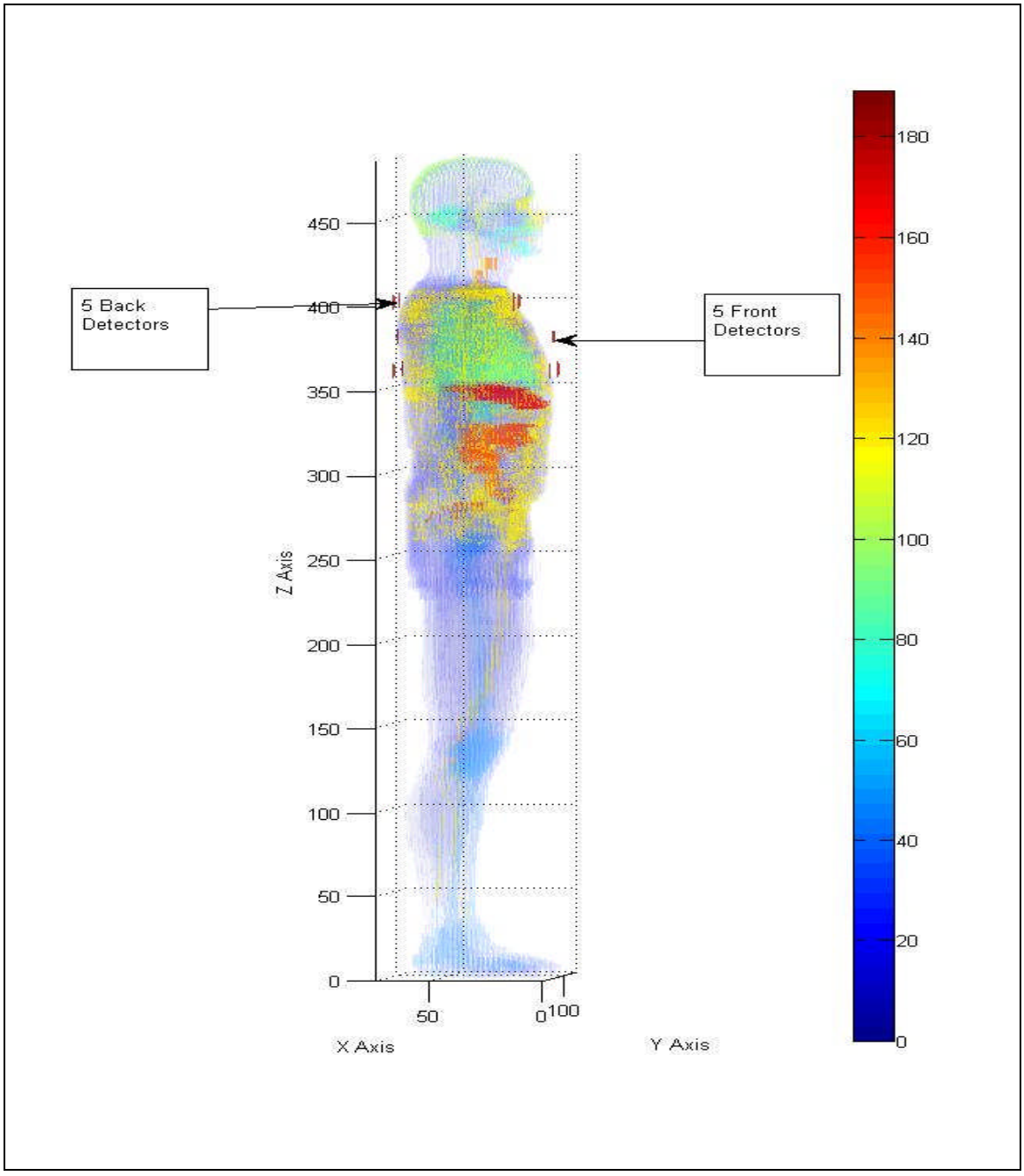

Fig. 7.5. Lateral view of MAX phantom with ten 5 cm diameter detectors located around the anterior and posterior portions of the lung.

CHAPTER VIII

METHODS FOR EVALUATING ACTIVITY AND DOSE OVER TIME BASED ON LIKELY SOURCES FROM AN RDD EVENT

Introduction

MCNPX is an extremely good program for calculating dose to a defined material located within a defined universe. The program requires a known source at a specified location. Inhalation of radioactive materials within the human body delivers a dose to known organs that change over time. The activity changes with time, either increasing or decreasing following a set of simple 2^{nd} order differential equations. Internal dosimetry tries to model the change in activity and hence the change in dose to selected organs.

In 1978, the International Committee on Radiation Protection (ICRP) issued ICRP Publication 30 which describes Limits for Intakes of Radionuclides by Workers (ICRP 1978). The report focuses on how an internal limit is reached over a 50 year time period. It is recognized that radioactive material is transported throughout the body at different rates. Depending upon how the radionuclide emissions, energy can be transported and deposited to various organs throughout the body. The commission decided that the selected organ limit should not be exceeded over an integrated exposure time frame of 50 years (ICRP 1978). The committee decided that in any year of practice, the values of the committed dose equivalent (H_{50}) in all the organs of the body must be limited so that the resulting total risk of cancer and hereditary disease is less than or equal to the risk from irradiating the whole body uniformly to the appropriate annual dose equivalent limit of 50 mSv (5rem) as recommended by ICRP Publication 26.

In order to derive an activity that will result in any one organ receiving a committed dose equivalent, the radionuclide, chemical form, particle size and the

method of intake, either inhalation or ingestion must be considered. For the most common radionuclides, the Annual Limits on Intake (ALI) have been derived for ingestion or by inhalation using a Reference Man listed in ICRP Publication 23 (ICRP 1975). A second quantity, called the Derived Air Concentration (DAC) can be calculated, which would provide the minimum activity present in air that would result in a selected organ reaching the ALI. Based upon the methodology provided in ICRP Publication 30, a program was created to measure the number of transformations that would occur in the body over the 50-year time period. This program could be used to calculate the time integrated activity and dose to various organs.

Method description

The MATLAB program is set up using a program called Simulink (MathWorks 2007). The program was designed in shells that interact with one inside the other. All functional data are calculated and displayed in the outer shell. Figure 8.1 shows a wire diagram of the outer shell of the Radionuclide Dose Calculator. This program will automatically assume a time period of 50 years or the user can select a different time period.

The user inputs three pieces of information into the outer shell. The first is an inhalation function in the form of activity in units of becquerel (Bq). A box that displays a final tally for activity in the whole body over time from inhalation is attached. The second is an ingestion function also in the form of activity in units of becquerel (Bq). The third input is the activity median aerodynamic diameter (AMAD) of the inhaled particles. This input allows the program to adjust for different particle sizes. Particle size ranges from 0.2 to 10 μm. A program code safety feature will convert any other particle size to the nearest allowable size. Particle size affects the amount and location of radioactive deposition in the respiratory system. The three inputs flow into the second shell that is tailored for a specific radionuclide.

Three separate final tally boxes provide the user with activity over time. The first tracks activity for the four main organs of the gastrointestinal tract: stomach, small intestine, upper and lower large intestines. The second tracks activity originating from inhalation: the lung, body transfer compartment, and activity excreted from the transfer compartment. A final tally box displays the activity in the entire body as a function of time. There are seven separate adders that show the total number of transformations that occur in each of the pertinent compartments over the pre-selected time. There are 10 adders that sum the committed dose equivalent (CDE) for each of the selected organs listed in ICRP-30 (ICRP 1978). A final adder is attached to show the committed effective dose equivalent (CEDE). Finally, three tally boxes are added to show the CDE as a function of time for each of the selected organs. Figure 8.2 provides a picture of the Simulink wire diagram for the second shell.

The second shell requires four separate user inputs that are specific to the radionuclide that will be used: 1. The "F1" transfer value from the GI tract to the transfer compartment. This information can be found in the ICRP-30 metabolic data (ICRP 1978). 2. The half life of the radionuclide in days. This information can be found in the chart of the nuclides (KAPL 2002). 3. The half-life of the transfer compartment in days. This information can be found in the ICRP-30 metabolic data (ICRP 1978). 4. An inhalation class, the user will enter either 1, 2 or 3 which corresponds to days (D), weeks (W) and years (Y). This information is also found in the ICRP-30 metabolic data (ICRP 1978). These inputs, combined with the outer shell inputs for inhalation and the AMAD size, are fed into a third-shell comprised of the lung model. The lung model provides ten activity outputs that are sent to an adder and on to a vector integrator. There is an output flow to the GI tract as well as an output flow to the transfer compartment. The "F1" input is sent directly into a third-shell GI tract compartment. The half life is converted into a decay constant which is used in all third-shell compartments. The ingestion intake activity from the outer shell is converted into decays per second and than input into an adder before going into the third-shell GI tract compartment. The same adder receives an input from the third-shell lung compartment.

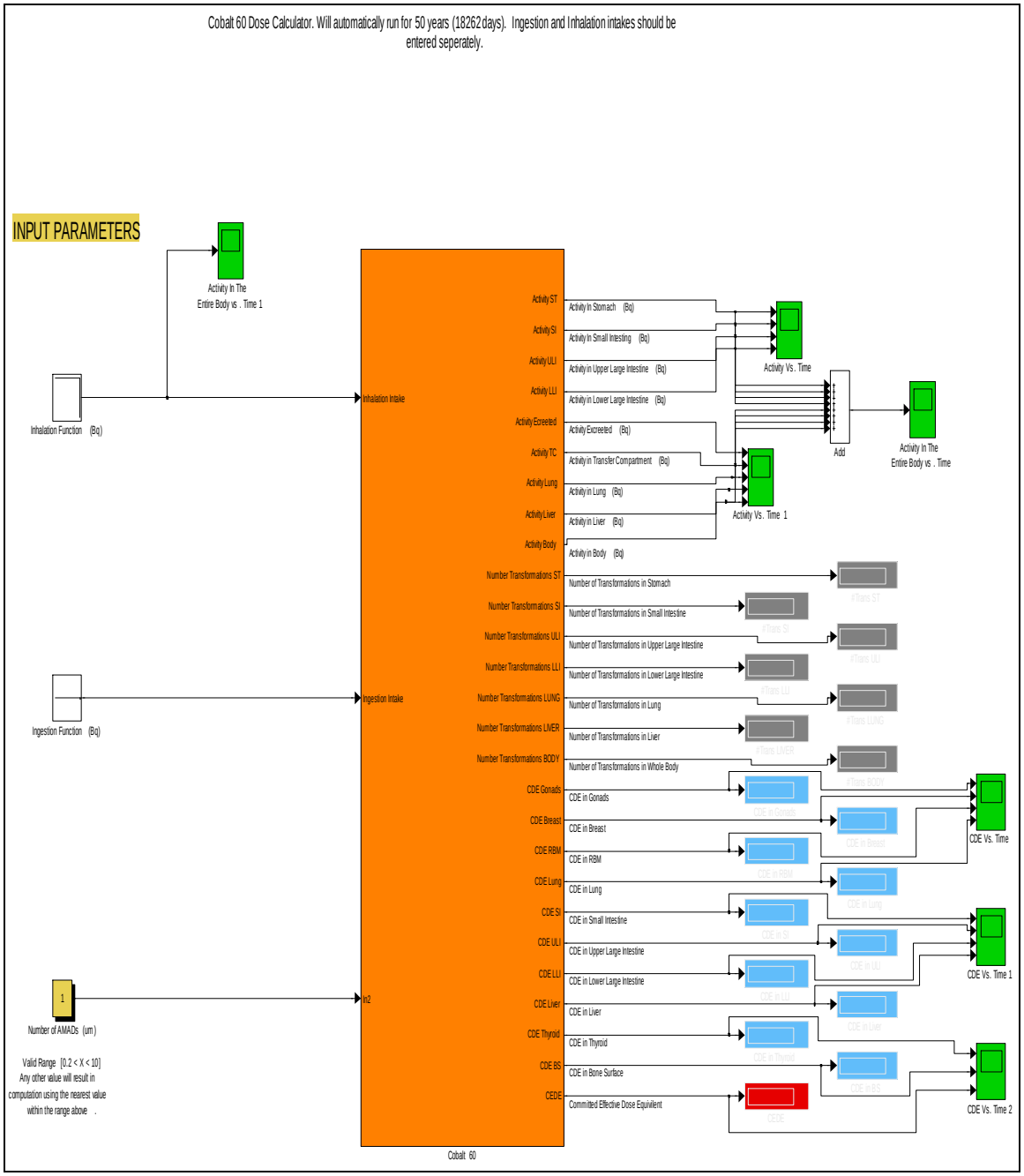

Fig. 8.1. Outer shell wire diagram of MATLAB Simulink internal dose program.

The output from the GI tract model provides four activity outputs for the various digestive organs that are sent to the first shell readers as well as to a vector integrator.

The activity integrator takes the activity input, multiplies it by a gain of 86,400 which corresponds to the number of seconds in one day. It adds the activity on a second by second basis. It outputs the integrated sum as the number of transformations (U) for each of the appropriate organs into a dose calculator as well as to the first stage readers. The dose calculator is a function that includes an embedded MATLAB editor. The editor sets up a matrix for each of the selected organs listed in the ICRP-30 supplement and provides the specific effective energy that a target organ would absorb from a radionuclide located in a source organ (ICRP 1978). It calculates a dose to each organ by multiplying the specific effective energy by the number of transformations along with a conversion factor to change energy into dose. It also calculates a committed effective dose equivalent (CEDE) by multiplying the dose from each organ by its weighting factor and summing the products. The final step is to calculate an Annual Limit on Intake (ALI) by dividing 0.05 by the CEDE as long as the ALI is controlled by the stochastic limit. The dose calculator outputs the CDE for each organ to the first shell readers.

There are two other third-shell compartments that play a part in this program. The third-shell transfer compartment receives three inputs and provides two outputs. There is an inflow of activity summed from the lung compartment and the GI tract compartment. The decay constant comes from the radiological half-life converted into a decay constant. The removal coefficient comes from the biological half life converted into a removal coefficient. The transfer compartment provides two outputs. The first output is the current activity from the transfer compartment sent to the first shell and the second output is total activity from the transfer compartment sent to the third-shell subsystem compartment. The third-shell subsystem compartment requires input from the transfer compartment as well as the decay constant used in the other third-shell compartments. This third-shell subsystem calculates excreted activity and outputs the activity to an adder and to the first shell. The excreted activity receives additional inputs

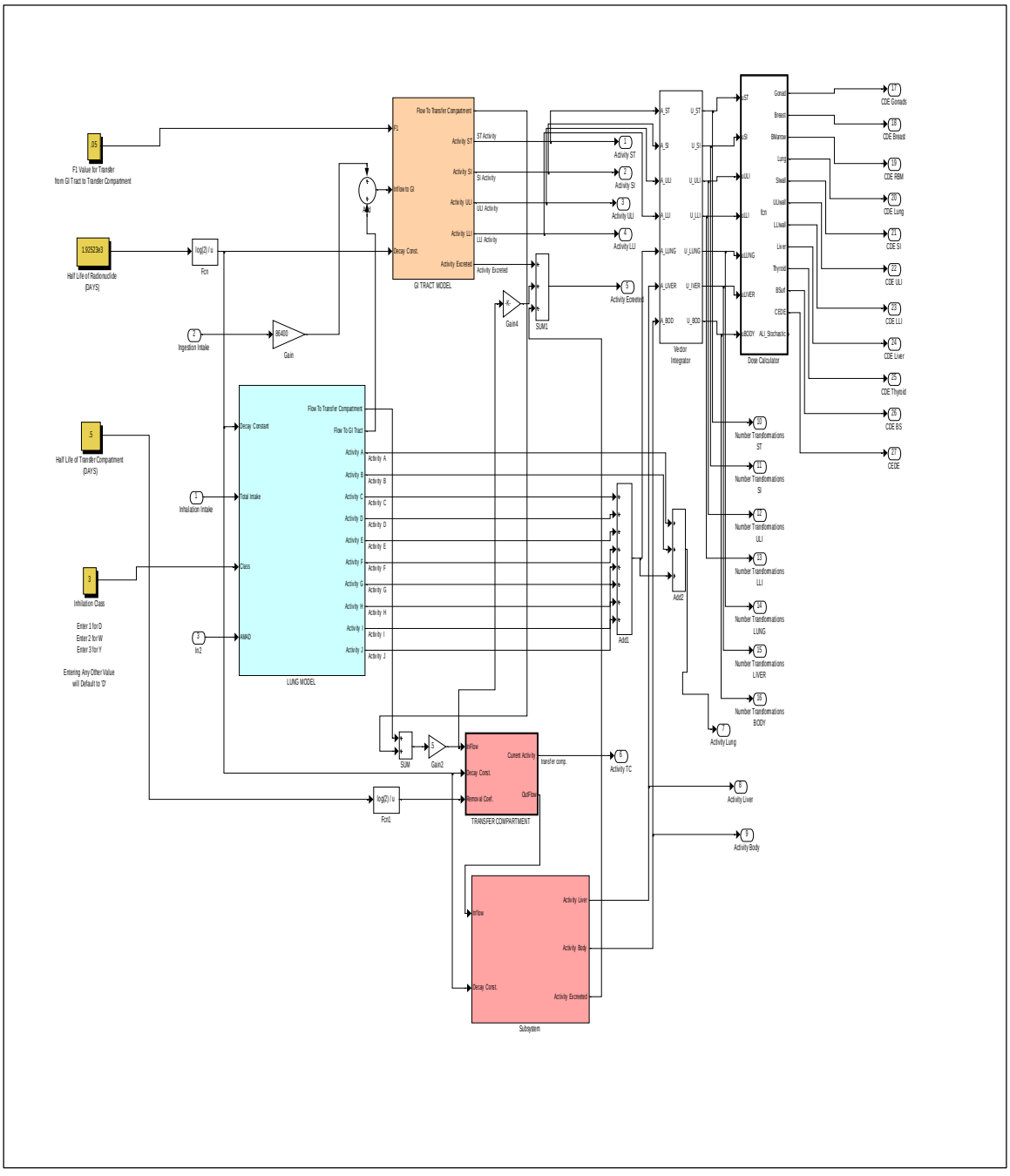

Fig. 8.2. Simulink second shell wire diagram of internal dose program.

from the GI tract compartment along with a negative input calculated by the radiological decay constant before it enters the transfer compartment. The activity from the body and liver are sent to a vector integrator and to the first shell. Figure 8.3 provides an overview of the third stage lung model. The lung model follows the model discussed in ICRP-30 (ICRP 1978). The inhalation class input goes into an embedded MATLAB function that is used to calculate the biological decay constants and absorption fractions for each compartment and sub-compartment within the three lung regions. The absorption fraction and biological removal constant is sent to the appropriate compartment.

The decay constant from the initial first stage input is sent to the ten compartments that comprise the lung model. The compartments are broken down into three regions consisting of the Nasal Pharyngeal (NP), Trachea Bronchial (TB) and Pulmonary regions (P). The NP region consists of two compartments, A and B where A represents the activity cleared to the transfer compartment and B represents the activity cleared to the GI tract model. The TB region consists of two compartments C and D where C is cleared to the transfer compartment and D is cleared to the GI tract model. The P region consists of four compartments and two sub-compartments labeled E through I. Compartment E is cleared to the transfer compartment and F and G are cleared to the GI tract model. Compartment H clears to the pulmonary lymph nodes with some portion of this activity moving through compartment I to the transfer compartment. Compartment J represents the possibility that some activity may be retained in the lymph nodes. Each region consists of a split function contained in an embedded MATLAB editor. There are four inputs and two outputs. The total intake comes from the total activity converted into disintegrations per second. The second input comes from the fraction that is deposited in the NP region. The third and fourth inputs come from the fraction that is absorbed in compartments A and B based on the inhalation class of the compound. The two outputs are the intakes for compartments A and B. Figure 8.4 show an example of the input, calculations and output from compartment A. The intake from each compartment is fed into an adder and than

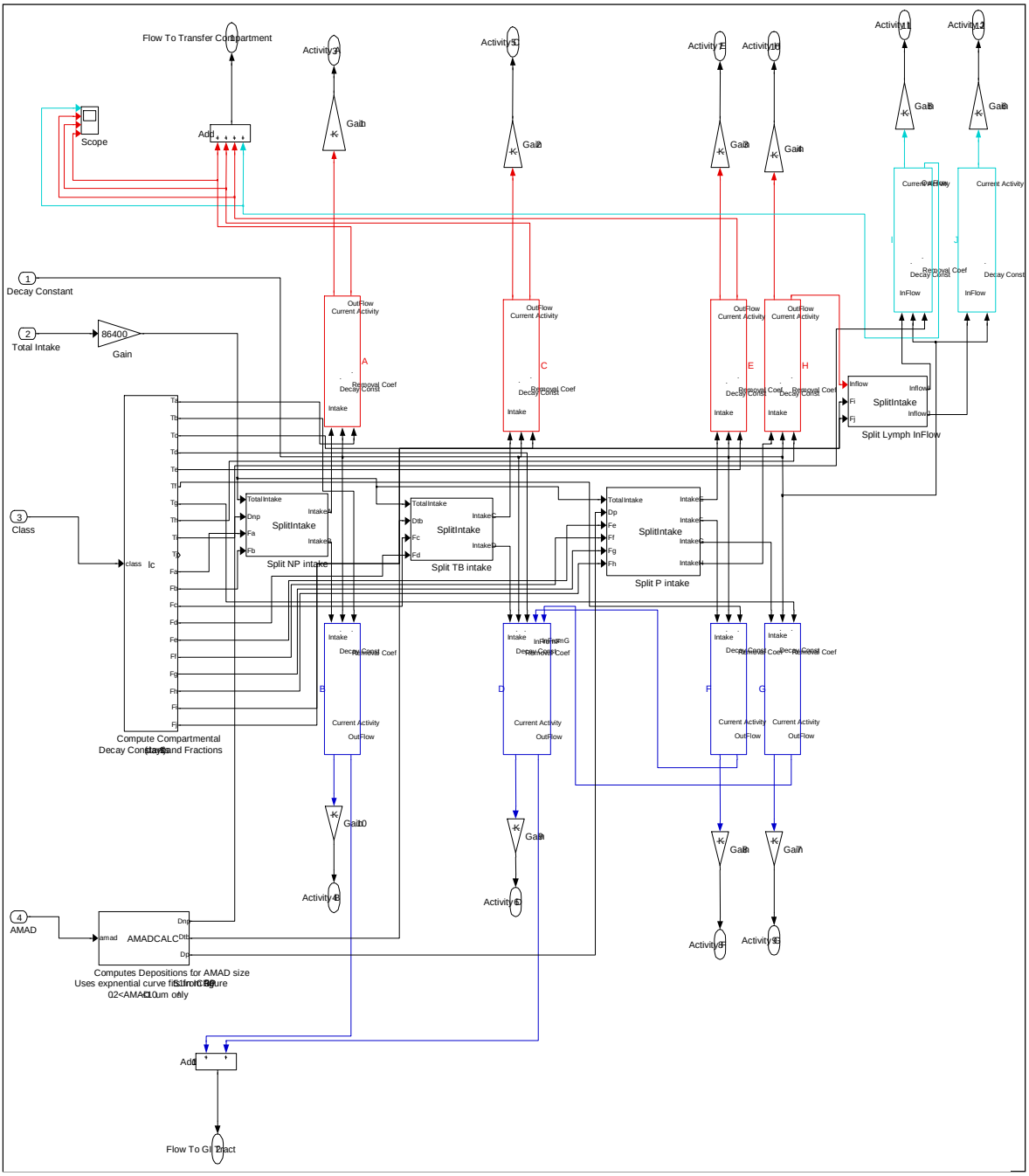

Fig. 8.3. Simulink third-shell wire diagram of internal dose lung model.

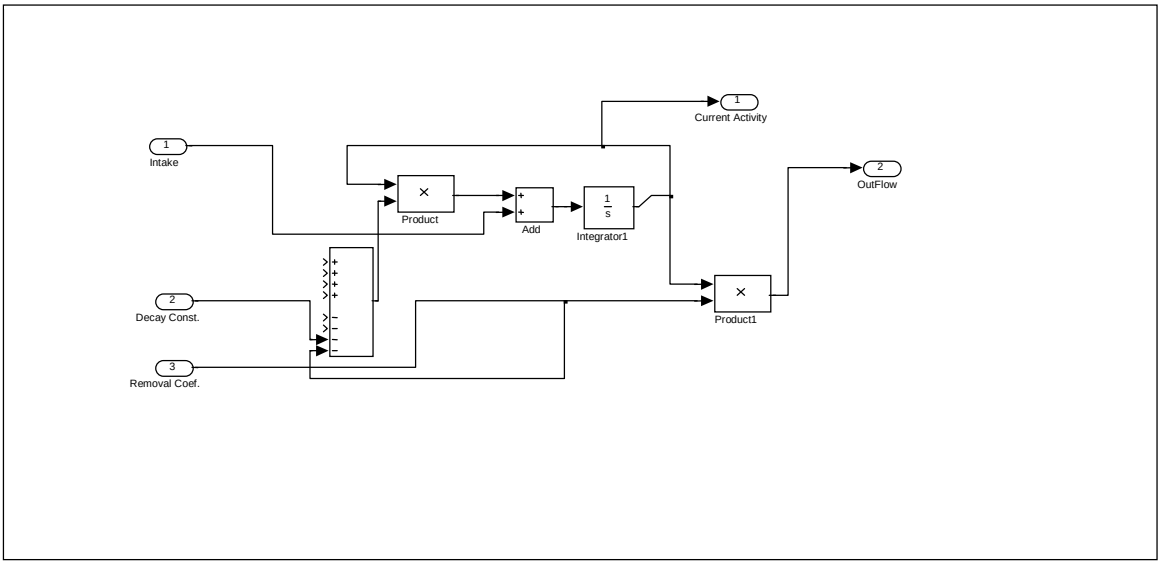

Fig. 8.4. Simulink fourth shell wire diagram of compartment A lung model.

compiled over time. The compiler removes a portion of the activity based on the decay and removal constants. There are two outputs from the compartment. The first output is the current activity and the second is the activity that goes to the transfer compartment. Compartments B, C, E and G are similar in nature. Compartment D has an additional input from Compartments F and G. Compartments I and J are similar to the other compartments but J does not have any output flow.

The GI tract model contains four sections that represent the four major sections of the digestive system. Two inputs flow into the stomach. The first is the radiological decay constant and the second is the inflow to the GI tract compartment either from ingestion or inhalation transport. Figure 8.5 represents the stomach compartment. The intake activity is integrated over time. The radiological decay and the biological removal constants reduce the activity over time. The reduced activity based on the biological removal constant is sent to the small intestine compartment. An output from this compartment allows the user to see the real time activity. A second output sends the reduced activity based on the radiological decay constant into the upper large intestine compartment. Figure 8.6 shows the small intestine compartment. The only difference between this compartment and the stomach compartment is that there is one additional input and output. That additional input is based on the reduction of activity in the compartment from the fractional uptake of activity into the blood. The output is the amount of activity removed from the small intestine compartment and to the blood. The upper and lower intestinal compartments are similar to the stomach compartment.

The transfer compartment is represented by a similar model. Figure 8.7 shows the diagram of the transfer compartment. Two activity inputs flow into the transfer compartment. The first is based on the activity removed from the lung system model by the biological removal constant and the second is based on the small intestine compartment in the GI tract model based on the biological removal constant. Two outputs show the current activity in the transfer compartment and the outflow of activity from the transfer compartment into the subsystem compartment. Figure 8.8 shows a diagram of the subsystem compartment.

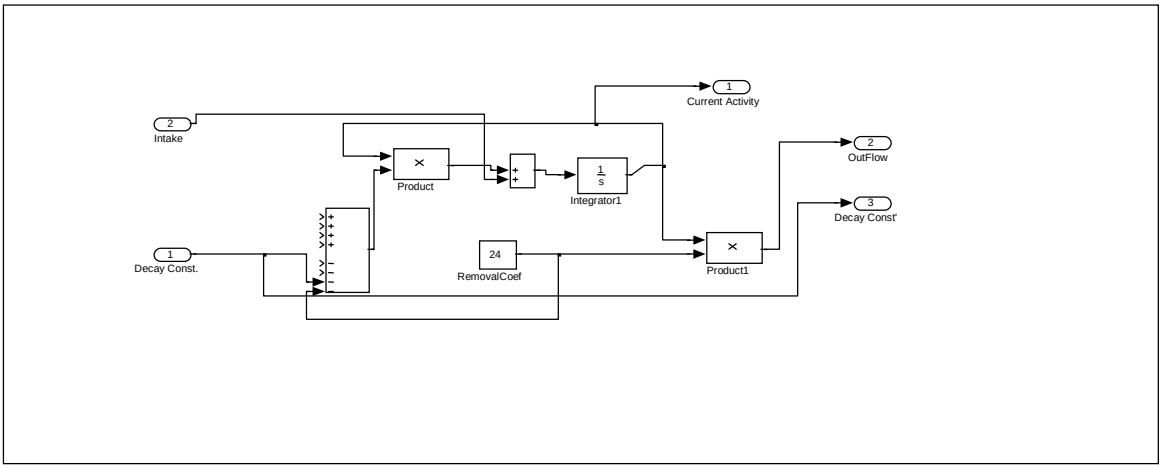

Fig. 8.5. Simulink fourth shell wire diagram of stomach from GI tract model.

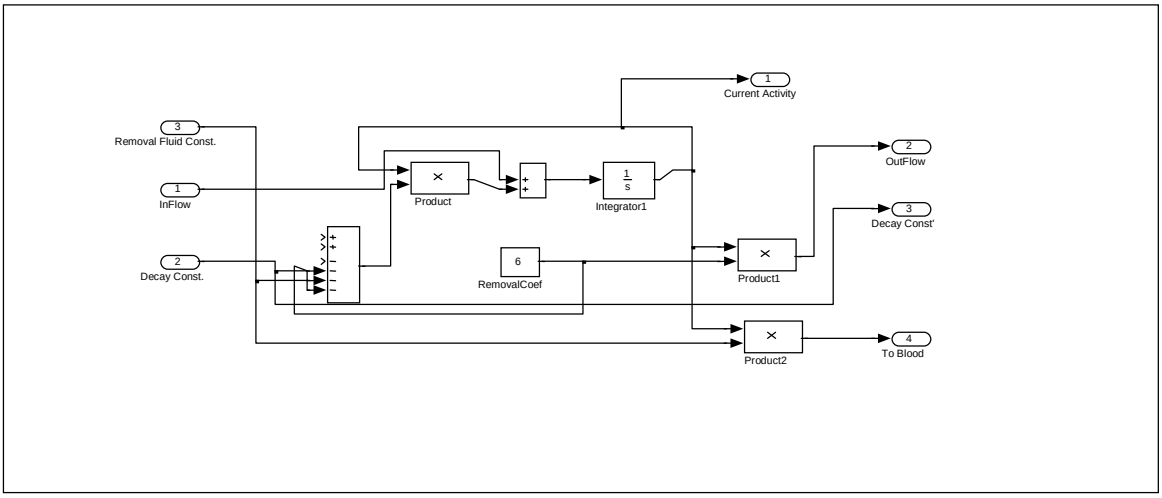

Fig. 8.6. Simulink fourth shell wire diagram of small intestine from GI tract model.

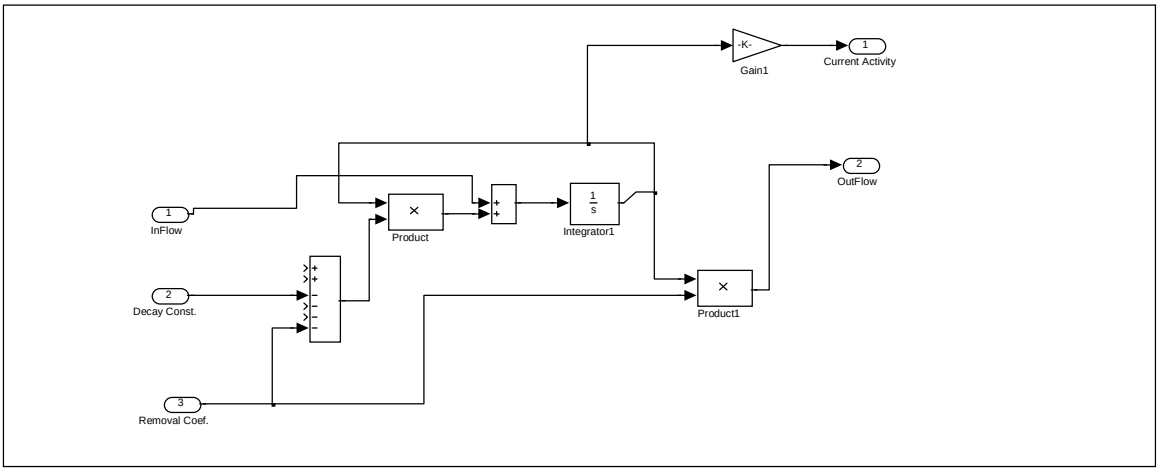

Fig. 8.7. Simulink third-shell wire diagram of transfer compartment.

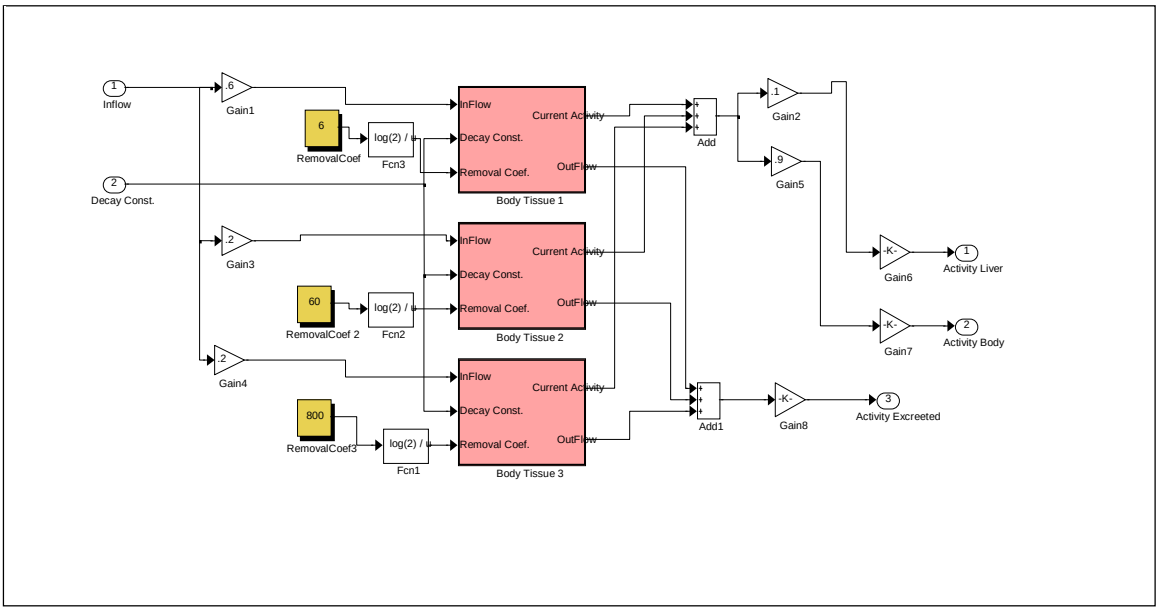

Fig. 8.8. Simulink third-shell diagram of Co-60 subsystem compartment.

The subsystem compartment is unique for each radionuclide. The current example is based on the metabolic data for Co-60. The input activity from the GI tract model undergoes a 3-way split that is governed by three different removal coefficients. Each body region identified in the Co-60 metabolic data from ICRP-30 provides a separate current activity and outflow for excretion, the liver and the whole body (ICRP 1978).

CHAPTER IX
METHODS FOR IMPROVING EFFICIENCY BY TESTING THE NUMBER OF HISTORIES AND NUMBER OF SOURCES IN A VOLUME

Introduction

Using the rules and terminology required by the MCNPX code, a basic input deck was developed. The number of histories and the number of source voxels that would be required to develop a volume source required statistical testing to improve efficiency. Ideally, every voxel within the source organ would contain a source and the user could simulate an infinite number of histories to acquire the best statistics. In an emergency response situation, time is of the essence for emergency responders. At the same time, prompt and accurate data are required. To optimize the two requirements, the program was tested utilizing a 10 percent error mark for important organs (RSICC 2002).

Method description

Based on the most likely RDD scenario, an explosive device would be used to disperse radioactive sources into the environment. This event would create radioactive dust that would most likely be inhaled and potentially ingested by both civilians as well as emergency responders. During this type of an event, the lungs, skin and eyes become selected organs of concern. Once the radionuclide or radionuclides are identified, ICRP-30 provides metabolic and elemental data that can be used to determine internal dose as well the selected organs affected by the radionuclide (ICRP 1978). Cobalt-60 was chosen as the standard radionuclide to which all other radionuclides will be compared. Based on the five main radionuclides of concern, 11 organs were chosen for the male MAX phantom to reflect the organs of most concern. The skin, lungs and eyes were chosen based on the susceptibility to both external and internal exposure. The trachea,

stomach, small intestine, colon (upper and lower large intestine), and rectum were chosen based on their role in biologically removing internal contamination as well as the large potential for ingestion. The ribs, which include the scapulae, sternum and clavicles were chosen as representative examples of the skeletal system that include 16.6 percent of the blood forming regions. The gonads were chosen based on the small risk of passing on genetic defects and the thyroid was chosen based on its regulatory role as well as its affinity for iodine.

Since inhalation is the primary means by which radioactive material would enter the body in the scenario described above, the lung was chosen as the organ to provide the statistical analysis necessary for determining the number of particles and number of voxels necessary to create a volume source. The lung contains 87,506 voxels and is in a shape that is not easily described with a mathematical model. Utilizing a volume source that more closely follows the actual shape of the human lung would provide a more accurate description of dose from sources within the lung. One million histories were chosen to ensure good statistics. A range of 10, 100, 500, 1000, 5000, 10000, and 20000 source voxels where chosen out of a potential of 87,506 lung voxels. Four different simulations, each with a different location of source voxels within the source organ were used. One million histories were selected to test any variability in the program.

Volume source results

The approach was to optimize the simulation by providing good statistics based on a volume source that approaches the shape of the source organ and minimize the number of line codes necessary for the source input card. The dose to each organ was simulated by four independent simulations that used a separate source card. Each source card contained ten random voxels within the source organ. From the four independent simulations, the dose to each organ was averaged and a standard deviation was calculated. This test was repeated by increasing the number of source voxels randomly selected from the source organ. Table 9.1 provides a high- and low-dose comparison,

error range, average of all four simulations and the standard deviation for each organ as a result of a volume source in the lung containing ten source voxels. The dose is based on the average energy deposited in a single voxel from a 1.17 MeV photon emitted from one of the ten source voxels located within the lung per history.

Table 9.1. Energy deposited in selected organs from a 1.17 MeV photon that is randomly emitted from one of the ten source voxels.

Comparison of Radiation Dose for 10 Lung Source Voxels

Organ	Lowest Dose (MeV/g)	Highest Dose (MeV/g)	Avg Dose (MeV/g)	STD
Skin	2.97E-04	3.20E-04	3.09E-04	9.63E-06
Ribs/Sternum/ Clavical/Scapula	6.66E-01	7.17E-01	7.00E-01	2.39E-02
Gonads	1.01E-05	1.12E-04	9.48E-05	1.55E-05
Rectum	5.30E-04	6.55E-04	5.68E-04	5.87E-05
Leg Sup	1.09E-03	1.35E-03	1.23E-03	1.13E-04
Thyroid	8.15E-03	2.43E-02	1.50E-02	7.04E-03
Lung	4.35E+00	4.90E+00	4.59E+00	2.29E-01
Eyes	3.15E-04	3.98E-04	3.58E-04	3.41E-05
Trachea	2.51E-02	8.35E-02	4.88E-02	2.47E-02
Colon	3.34E-02	4.41E-02	4.03E-02	4.72E-03
Stomach	6.03E-02	1.47E-01	1.13E-01	3.84E-02

As expected, the most sensitive organ is the lung based on dose, followed by the rib bone group and the stomach, which was expected based upon the organs in a proximate position with the lungs. The gonads are the least exposed organs based on size and proximal distance from the lungs. If the lung is used as the source organ and the gonads are the smallest organ of the organs selected and located at the greatest distance from the lungs, a condition would exist if the dose to the gonads from four independent simulations with a source located within the lungs are within one standard deviation, than the dose to all of the remaining selected organs should be within one

standard deviation. In order to test this hypothesis, the dose to the gonads was compared to the average of the four independent simulations using the calculated standard deviation in order to determine if the dose to the gonads from each of the four simulations is within one standard deviation as the number of source voxels within the lung was increased. The approximate cut-off for the number of source voxels within the lung was approximately 5,000. Once the minimum number of lung source voxels was determined, the number of source voxels was increased to see if there was any significant difference between the four independent simulations. The 5,000, 10,000 and 20,000 source voxels were compared to see if any significant differences occurred. An example of the different number of source voxels is provided using the gonads. Figure 9.1 provides a dose profile for the gonads from different numbers of sources within the lung. Good source volume statistics appear to stabilize with 5,000 or more sources. The optimal number of sources for the lung is between 10,000 and 20,000. 15,000 sources were selected to ensure good statistics without sacrificing simulation time.

Figure 9.2 shows the average gonad dose per history from four independent simulations versus the number of histories from 15,000 source voxels located within the lung. While there was still a significant difference between 100,000 histories and 1,000,000 histories, there was very little difference between the 1,000,000 histories and 10 million histories. Figure 9.3 provides a better visual of how the error in dose is reduced as the number of histories is increased. The objective was to discover how many histories were required to achieve less than a 10 percent error for each of the selected organs. Using 1,000,000 histories reduced the gonad error to less than 10 percent. As expected, the other organs show a similar error reduction and dose profile versus the number of histories used. Table 9.2 shows the simulation time difference between the different number of histories. No significant time delays occurred between 10 and 100,000 particles. There is a large increase in time when 1,000,000 histories are used and another ten fold increase when 10,000,000 histories are used. The error reduction savings does not appear to be worth the added time cost.

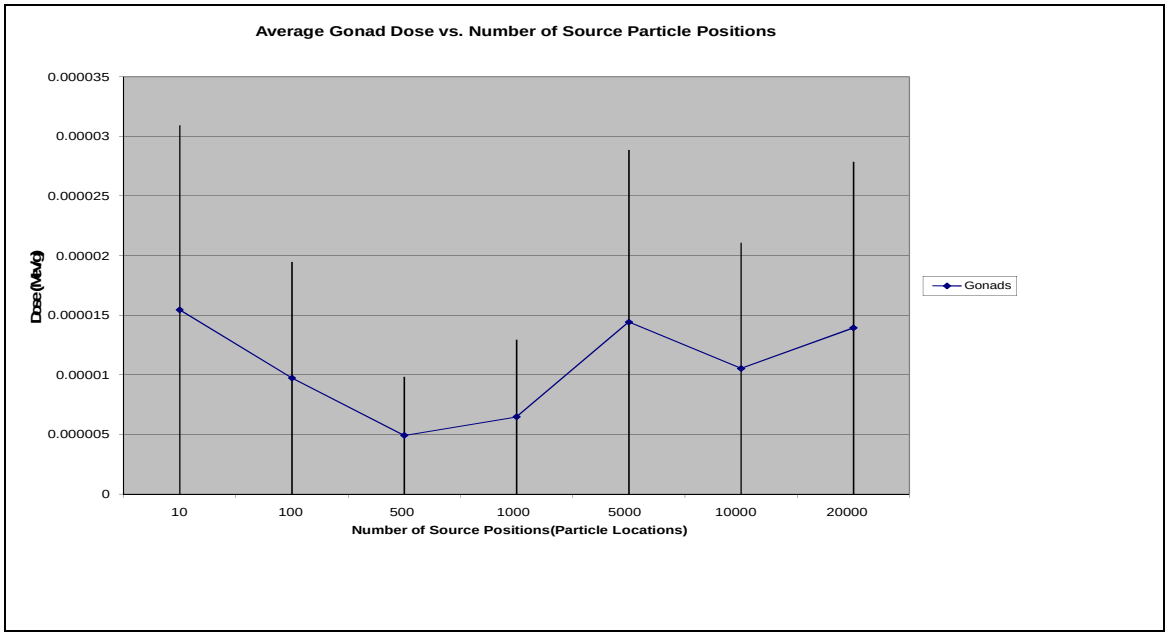

Fig. 9.1. Average gonad dose per history from four independent simulations vs. number of source positions located within the lung.

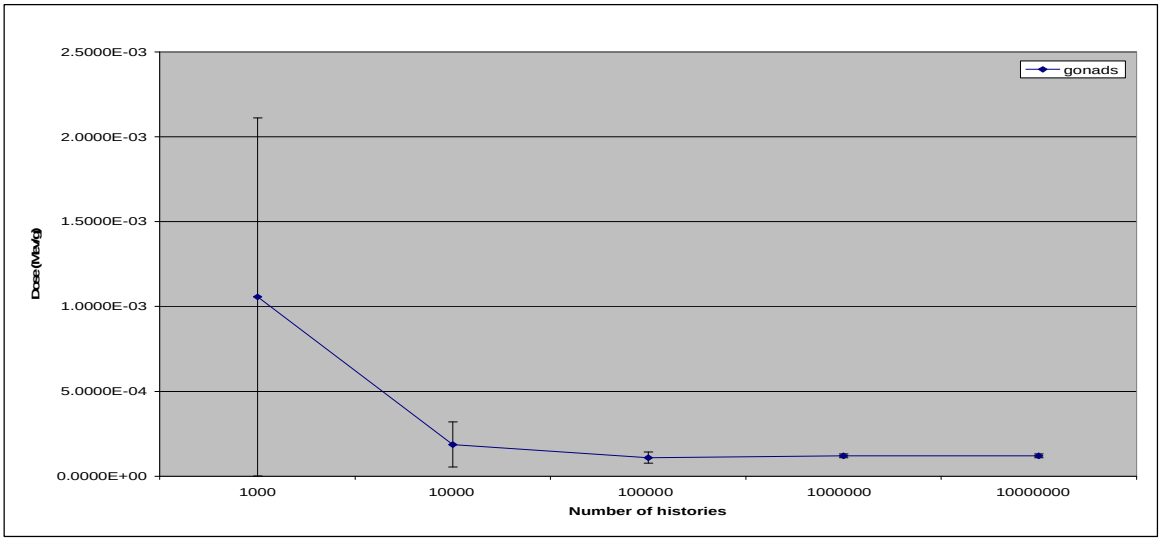

Fig. 9.2. Average gonad dose per history from four independent simulations vs. number of histories with 15,000 source voxels located within the lung.

Table 9.2. Number of histories versus simulation time.

Number of Particles (nps)	Time (m)
10	1.64
100	1.69
1000	1.69
10000	2.05
100000	5.07
1000000	36.39
10000000	334.39

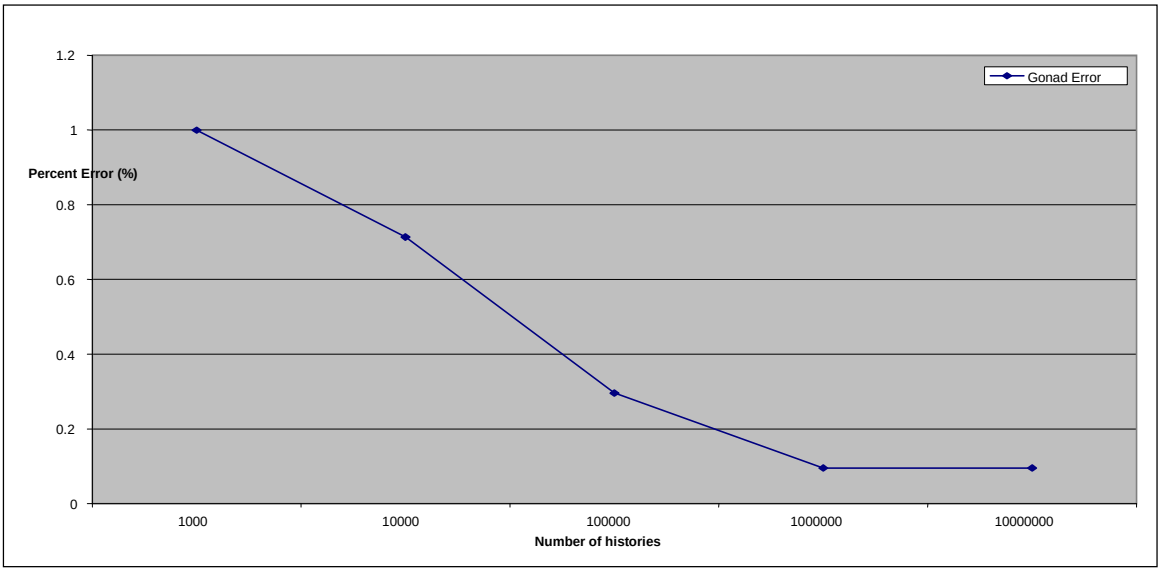

Fig. 9.3. Percent error in gonad dose vs number of histories with lung sources.

CHAPTER X
STATISTICAL ANALYSIS BY MCNP

Introduction

MCNPX provides an in-depth statistical analysis of the program output based upon default and user defined settings. The MCNP manual contains a detailed description, including mathematical models to support the statistical analysis. A brief synopsis will be provided in this section. Monte Carlo results represent an average of the contributions from many histories sampled during the course of the problem. The statistical error associated with the result is as important as the result itself. The error defines the quality of the result. The major tools used to define the error include the estimated mean, relative error, variance of the variance and history score probability density function. The tally should be well behaved and properly converge in accordance with the tally fluctuation charts (RSICC 2002).

Method description for Monte Carlo means, variances and standard deviations

Monte Carlo results are obtained by sampling possible random walks and assigning a score x_i to each random walk. Based on the tally selected, a range of scores will be produced. The true mean is expressed in equation 10.1 as the expected value of x, E(x), where

$$E(x) = \int x f(x) dx = \text{true mean.}$$

The function f(x) is seldom explicitly known and is implicitly sampled by the Monte Carlo random walk process. The true mean can be estimated by the sample mean $\bar{x}$ as in equation 10.2

$$\bar{x} = \frac{1}{N} \sum_{i=1}^{N} x_i \quad ,$$

where x_i is the value of x selected from f(x) for the i^{th} history and N is the number of histories in the problem. The Monte Carlo mean $\bar{x}$ is the average value of the scores x_i for all the histories calculated in the problem. The variance of the population of x values is a measure of the spread in these values and is given by equation 10.3:

$$\sigma^2 = \int (x - E(x))^2 f(x) dx = E(x^2) - (E(x))^2 \quad .$$

The square root of the variance is σ, which is called the standard deviation of the population of scores. As with E(x), σ is seldom known but can be estimated by Monte Carlo as S, given by equations 10.4 and 10.5:

$$S^2 = \frac{\Sigma_{i=1}^{N} (x_i - \bar{x})^2}{N-1} \approx \overline{x^2} - \bar{x}^2$$

and

$$\overline{x^2} = \frac{1}{N} \sum_{i=1}^{N} x_i^2 \quad .$$

The quantity S is the estimated standard deviation of the population of x based on the values of x_i that were actually sampled. The estimated variance of *x* is given by equation 10.6:

$$S_{\bar{x}}^2 = \frac{S^2}{N} \quad .$$

These formulas do not depend on any restriction on the distribution of x or $\bar{x}$.

Precision and accuracy

There is an extremely important difference between precision and accuracy of a Monte Carlo calculation. Precision is defined as the uncertainty in $\bar{x}$ caused by the statistical fluctuations of the x_i's for the

portion of physical phase space sampled by the Monte Carlo process. For various user-defined reasons, portions of the physical phase space might not be sampled. Accuracy is a measure of how close the expected value of $\bar{x}$ is to the true physical quantity being estimated. The results of Monte Carlo calculations refer only to the precision of the result.

There are three main factors that can affect the accuracy of a Monte Carlo result, the code, problem modeling and the user. There are four main user-controlled factors that affect the precision, forward vs. adjoint calculation, tally type, variance reduction techniques and number of histories simulated.

Central limit theorem and Monte Carlo confidence intervals

To define confidence intervals for the precision of a Monte Carlo result, the Central Limit Theorem of probability theory is used. Equation 10.7 states that

$$\lim_{N\to\infty} Pr\left[E(x)+\alpha\frac{\sigma}{\sqrt{N}} < \bar{x} < E(x)+\beta\frac{\sigma}{\sqrt{N}}\right] = \frac{1}{\sqrt{2\pi}}\int_{\alpha}^{\beta} e^{-t^2/2}dt \quad ,$$

where α and β can be any arbitrary values. Therefore, for any distribution of tallies, the distribution of resulting $\bar{x}$'s will be approximately normally distributed. If S is approximately equal to σ, which is valid for a statistically significant sampling of a tally, than equations 10.8 and 10.9 are valid:

$$\bar{x} - S_{\bar{x}} < E(x) < \bar{x} + S_{\bar{x}}, \sim 68\% \text{ of the time and}$$

$$\bar{x} - 2S_{\bar{x}} < E(x) < \bar{x} + 2S_{\bar{x}} \quad , \sim 95\% \text{ of the time}$$

from a standard table for the normal distribution function.

Estimated relative errors in MCNP

All standard MCNP tallies are normalized to per starting particle history and are printed in the output with a second numerical value, which is the estimated relative error defined as equation 10.10:

$$R \equiv S_{\bar{x}} / \bar{x} \quad .$$

The relative error is a convenient number because it represents the statistical precision as a fractional result with respect to the estimated mean. By combining the above equations, R can be written as shown in equation 10.11:

$$R = \left[\frac{1}{N} \left(\frac{\overline{x^2}}{\bar{x}^2} - 1 \right) \right]^{1/2} = \left[\frac{\Sigma_{i=1}^{N} x_i^2}{(\Sigma_{i=1}^{N} x_i)^2} - \frac{1}{N} \right]^{1/2} \quad .$$

If all the x_i's are nonzero and equal, R is zero. Low-variance solutions should strive to reduce the spread in the x_i's. If the x_i's are all zero, R is defined to be zero. If only one nonzero score is made, R approaches unity as N becomes large. For positive and negative x_i's, R can exceed unity. The range of R values for x_i's of the same sign is therefore between zero and unity.

Based on the qualitative analysis and the experience of Monte Carlo practitioners, Table 10.1 presents the recommended interpretation of the estimated 1 σ confidence interval $\bar{x}$ (1 ± R) for various values of R associated with an MCNP tally. These guidelines were determined empirically, based on years of experience using MCNP on a wide variety of problems. Just before the tally fluctuation charts, a “Status of Statistical Checks” table prints how many tally bins of each tally have values of R exceeding these recommended guidelines.

Table 1.1 Guidelines for interpreting the relative error R[a].

Range of *R*	Quality of the Tally
0.5 to 1	Garbage
0.2 to 0.5	Factor of a few
0.1 to 0.2	Questionable
< 0.10	Generally reliable except for point detector
< 0.05	Generally reliable for point detector

[a] $R = S_{\bar{x}}/\bar{x}$ and represents the estimated statistical relative error at the 1σ level. These interpretations of *R* assume that all portions of the problem phase space have been well sampled by the Monte Carlo process. Please use statistical checks for detailed information.

MCNP figure of merit

The estimated relative error squared, R^2, should be proportional to 1/N. The computer time T used in an MCNP problem should be directly proportional to N. The product of R^2T should be approximately a constant within any single Monte Carlo simulation. It is convenient to define a figure of merit (FOM). Equation 10.12 defines a figure of merit as:

$$FOM \equiv \frac{1}{R^2 T} .$$

MCNP prints the FOM for one bin of each numbered tally as a function of N, where the unit of computer time T is in minutes.

The FOM is a very important statistic about a tally bin and should be studied by the user. It is a tally reliability indicator in the sense that if the tally is well behaved, the FOM should be approximately a constant with the possible exception of statistical fluctuations very early in the problem. An order-of-magnitude estimate of the expected fractional statistical fluctuations in the FOM is 2R. This result assumes that both the relative statistical uncertainty in the relative error is of the order of the relative error itself and the relative error is small compared to unity. The

user should always examine the tally fluctuation charts at the end of the problem to check that the FOMs are approximately constant as a function of the number of histories for each tally.

Variance of the variance

Previous sections have discussed the relative error R and figure of merit FOM as measures of the quality of the mean. A quantity called the relative variance of the variance (VOV) is another useful tool that can assist the user in establishing more reliable confidence intervals. The VOV is the estimated relative variance of the estimated R. The VOV involves the estimated third and fourth moments of the empirical history score probability density function (PDF), f(x), and is much more sensitive to large history score fluctuations than is R. The magnitude and behavior of the VOV are indicators of tally fluctuation chart (TFC) bin convergence (RSICC 2002).

CHAPTER XI
ESTIMATING ORGAN DOSE BASED ON VOLUME SOURCE IN THE LUNG

Organ data verification

Based on the statistical simulations provided in Chapter X, a source volume of 15,000 lung voxels was selected and the number of source histories selected was one million. The number of source voxels for additional organs will be based on the ratio of lung source voxels divided by the total number of lung voxels. This fraction will than be multiplied by the total number of organ voxels to determine the number of source voxels in the organ. Of the five sources, Co-60 was chosen as the first test source for our phantom model. To keep things simple, two simulations were set up. The first simulation analyzed the lower energy photon of 1.17 MeV and the second tracked the higher energy 1.33 MeV photon. Volumes and masses were checked against ICRU-46 established values for both simulations (ICRU 1990). Using the values from Table A-2 of Appendix A, the hand calculated lung volume was 4082.68 cm^3, the volume of a single voxel was 4.67×10^{-2} cm^3 (Kramer 2003). According to figure A-1 of appendix A, the MCNPX code calculated a volume of 4.67×10^{-2} cm^3 for a single voxel. The hand calculated mass of the lung was 1060 g and the mass per voxel was 1.21×10^{-2} g. Based on Figure A-1 of appendix A, the code calculated a mass of 1.21×10^{-2} g in a single voxel. Therefore, the phantom lung provided a good simulation that was representative of standard man.

Dose to organ conversion

The MCNP output file provides a dose to all tissues defined within the phantom. The dose is listed in g/cm^3 and applies to a single voxel. The dose is based on the average energy deposited per unit mass for a single history. In this case, a single 1.17 MeV photon would deliver an average dose of $4.75 \pm 7.0 \times 10^{-4}$ MeV/g of tissue

contained in a single voxel. To derive any meaningful information from this value, simple dose conversion calculations were applied to create an absorbed dose in gray (Gy) for each organ. The above value provides an average lung dose of 9.48×10^{-19} Gy from a single 1.17 MeV photon, if the photon originates within a lung volume source. Because of the extremely small dose from a single photon, the organ dose is compared in units of MeV/g for each organ. Co-60 also emits a beta radiation with a yield of 0.23 percent and an average energy of 606 KeV. The dose from the beta decay is only applicable to the lung and the dose from the beta particle to the lung is over 1000 times smaller than the dose to the lung from the photons. Table 11.1 provides calculated dose conversions for each of the selected organs that were considered in this problem.

Table 11.1. Organ doses from a Co-60 volume source in the lung.

Organs	MCNP Dose (MeV/g-his)	Std Deviation	MCNP Wght (g)	En Dep (MeV/his)	Organ Wt (g)	Organ Dose (MeV/g-his)	Organ Dose (Gy/his)
Skin	6.98E-04	3.01E-11	5.09E-02	3.55E-05	2830	1.26E-08	2.01E-18
Rib Bone Group	1.53E+00	1.02E-07	6.58E-02	1.00E-01	2167	4.63E-05	7.42E-15
Small Int	1.51E-01	1.87E-07	4.81E-02	7.26E-03	640	1.13E-05	1.82E-15
Gonads	2.38E-04	6.69E-08	4.85E-02	1.16E-05	37.1	3.11E-07	4.99E-17
Rectum	1.30E-03	9.69E-08	4.90E-02	6.36E-05	63	1.01E-06	1.62E-16
Thyroid	2.10E-02	1.20E-06	4.90E-02	1.03E-03	19.6	5.26E-05	8.42E-15
Lung	9.98E+00	1.70E-07	1.21E-02	1.21E-01	999	1.21E-04	1.94E-14
Eyes	8.33E-04	3.05E-07	4.90E-02	4.08E-05	15	2.72E-06	4.36E-16
Trachea	5.19E-02	4.04E-06	4.90E-02	2.54E-03	10	2.54E-04	4.07E-14
Colon	9.43E-02	2.05E-07	4.90E-02	4.62E-03	369	1.25E-05	2.01E-15
Stomach	3.13E-01	8.78E-07	4.90E-02	1.53E-02	150	1.02E-04	1.64E-14

As expected, the largest dose concentrations are to the organs in the immediate vicinity of the lung which includes the trachea, stomach and thyroid. The dose to the skin is smaller than the dose to the lung by a factor of 1,000. This reflects the average dose over the entire volume of skin. This is a large assumption. In reality, the dose to the skin is a gradient based on the distance each skin voxel is from each source voxel.

Statistical analysis of output file

The tally-four fluence analysis for each detector, setup as described in chapter VII provided a random behavior for the mean. The desired relative error should be less than 0.10 and the observed relative error was 0.02. The desired and observed relative errors decreased in relation to the inverse of the square root of the number of histories. The desired variance of the variance should be less than 0.10 and the observed VoV was 0.02. The figure of merit value was constant and the behavior was random. The probability density function (pdf) desired should be greater than three, the observed pdf value was 10. The tally-four fluence passed all 10 statistical checks. Out of 10 tally-four bins, only one had a zero value and no bins contained relative errors greater than 0.10. This occurred because the tenth lung detector was not created and located at the center back position. This error was not discovered until after a significant number of simulation files were created. While this can easily be rectified for future phantoms, it is not significant to the current MCNPX problem. The second 1.33 MeV photon simulation provided similar statistical results with the exception of the VoV. The observed VoV value was 0.00.

The tally-six dose analysis for each tissue showed a random behavior for the mean. The desired relative error should be less than 0.10 and the observed relative error was 0.02 for the 1.17 MeV photon and 0.00 for the 1.33 MeV photon. The desired and observed relative errors decreased in relation to the inverse of the square root of the number of histories. The desired variance of the variance should be less than 0.10 and the observed VoV was 0.00. The figure of merit value was constant and the behavior was random. The desired probability density function (pdf) should be greater than 3.00 and the observed value was 10.00 for the 1.17 MeV photon and 5.87 for the 1.33 MeV photon. The tally-six dose passed all 10 statistical checks. Out of 61 tally-six bins, no bin had a zero value and only 7 bins contained relative errors greater than 0.10.

Co-60 organ dose profile

A Co-60 source located within the lung would deliver a dose to the selected organs that ranges from a high of 2.54 x 10^{-4} MeV/g to the trachea and a low of 1.26 x 10^{-8} MeV/g to the skin. This organ dose contribution is the sum of two photons emitted from Co-60 that occur with a yield of about 100 percent. Figure 11.1 provides a simulated 3-dimensional view of the human body with a color profile that equates to the MCNP dose for the high-energy photon of Co-60 absorbed by each organ. The color bar units to the right of the phantom are in MeV/organ weight in grams. The current MATLAB program that was created to provide a simulated 3-dimensional view of dose to the human body can only read and convert one MCNPX output file at a time. Each axis is represented in the figure along with a color bar that indicates the organ dose in MeV/g provided by the MCNPX output file. In the MCNPX output file, the trachea receives a slightly lesser dose than the lung based upon the number of voxels versus the measured mass of the trachea. The phantom includes the airway as part of the trachea. The dose difference is not significant.

Cs-137 organ dose profile

A Cs-137 source located within the lung would deliver a dose to the selected organs that ranges from a high of 7.54 x 10^{-5} MeV/g for the trachea and a low of 3.41 x 10^{-9} MeV/g for the skin. This organ dose contribution is from a 0.66 MeV photon emitted from Cs-137 that occur with a yield of about 86 percent. Cs-137 also emits a beta particle with a yield of approximately 5.3 percent and an average energy of 416 KeV. The dose from the beta decay is only applicable to the lung and the dose delivered to the lung by the beta particle is over 1000 times smaller than the dose to the lung from the photons. Table 11.2 provides the dose output to the selected organs from the 0.66 MeV photon.

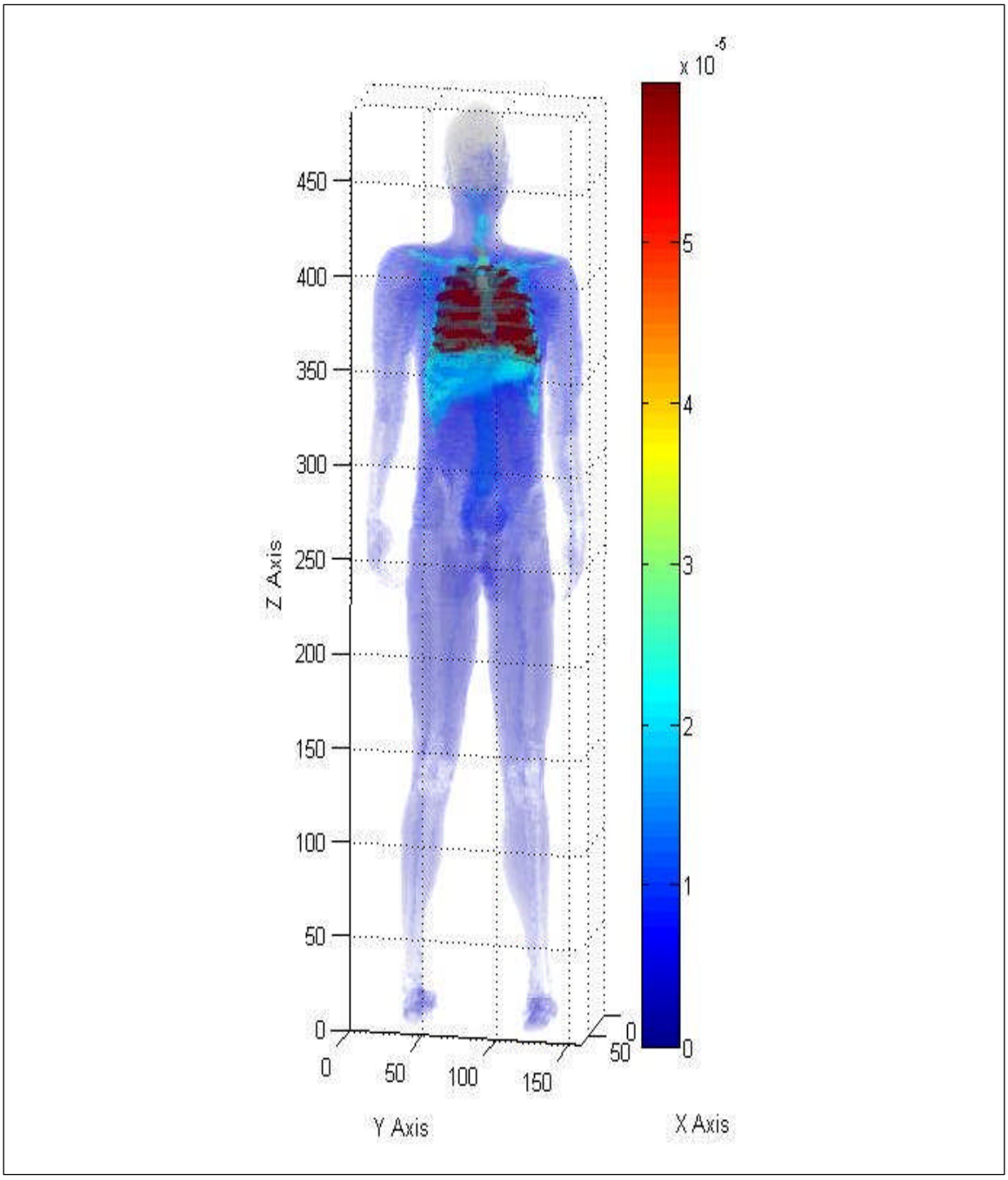

Fig. 11.1. Three-dimensional human dose profile from a 1.33 MeV photon source located within the lung.

Table 11.2. Organ doses for a Cs-137 volume source in the lung.

Organs	MCNP Dose (MeV/g-his)	Std Deviation	MCNP Wght (g)	En Dep (MeV/his)	Organ Wt (g)	Organ Dose (MeV/g-his)	Organ Dose (Gy/his)
Skin	1.90E-04	4.10E-12	5.09E-02	9.66E-06	2830	3.41E-09	5.47E-19
Rib Bone Group	4.61E-01	1.40E-08	6.58E-02	3.03E-02	2167	1.40E-05	2.24E-15
Small Int	4.17E-02	2.54E-08	4.81E-02	2.00E-03	640	3.13E-06	5.01E-16
Gonads	3.77E-05	6.85E-09	4.85E-02	1.83E-06	37.1	4.94E-08	7.91E-18
Rectum	2.75E-04	1.15E-08	4.90E-02	1.35E-05	63	2.14E-07	3.43E-17
Thyroid	6.30E-03	1.75E-07	4.90E-02	3.09E-04	19.6	1.58E-05	2.52E-15
Lung	2.96E+00	2.52E-08	1.21E-02	3.59E-02	999	3.60E-05	5.76E-15
Eyes	1.87E-04	3.66E-08	4.90E-02	9.17E-06	15	6.11E-07	9.79E-17
Trachea	1.54E-02	5.81E-07	4.90E-02	7.54E-04	10	7.54E-05	1.21E-14
Colon	2.61E-02	2.81E-08	4.90E-02	1.28E-03	369	3.47E-06	5.56E-16
Stomach	9.21E-02	1.26E-07	4.90E-02	4.51E-03	150	3.01E-05	4.82E-15

As expected, the dose to the selected organs is similar to the dose produced by the Co-60 photons. The largest dose concentration remains with organs in the immediate vicinity of the lung. The lung dose is reduced by approximately a factor of two. This reduction is expected based on the energy reduction between the 1.17 MeV Co-60 photon and the 0.66 MeV photon of Cs-137.

Statistical checks were performed on the Cs-137 Dose output file. The same warnings present with Co-60 were observed. The 10 statistical checks for tally-four fluence analysis passed and produced similar results. The 10 statistical checks for tally-six dose passed and produced similar results as with Co-60. Of the 61 tally bins, 9 bins had relative errors exceeding 0.10. Figure 11.2 provides a simulated 3-dimensional view of the human body with a color profile that shows the MCNP dose for the single photon of Cs-137 absorbed by each organ. The color bar units to the right of the phantom are in MeV/organ weight in grams.

The Co-60 lung dose was 5.77×10^{-5} MeV/g for the 1.17 MeV photon compared with the Cs-137 lung dose of 3.60×10^{-5} MeV/g for the 0.66 MeV photon. As expected, the dose profile is similar to that of the photons emitted by Co-60. The dose to each individual organ is proportionally reduced based on the lower-energy of the source photon and the energy dependent stopping power of the material within the phantom.

Ir-192 organ dose profile

An Ir-192 source located within the lung would deliver a dose to the selected organs that ranges from a high of 9.45 x 10^{-05} MeV/g for the trachea and a low of 3.96 x 10^{-9} MeV/g for the skin. This organ dose is sum of two photons with energies of 0.47 MeV and 0.32 MeV along with two electrons that have maximum energies of 0.66 MeV and 0.54 MeV. All four emissions are produced with a yield of about 26.2%, 22.4%, 10.1% and 6.7%, respectively. Table 11.3 provides the calculated dose conversions for each of the selected organs.

Table 11.3. Organ doses for an Ir-192 volume source in the lung.

Organs	MCNP Dose (MeV/g-his)	Std Deviation	MCNP Wght (g)	En Dep (MeV/his)	Organ Wt (g)	Organ Dose (MeV/g-his)	Organ Dose (Gy/his)
Skin	2.20E-04	1.65E-10	5.09E-02	1.12E-05	2830	3.96E-09	6.35E-19
Rib Bone Group	6.02E-01	4.91E-07	6.58E-02	3.96E-02	2167	1.83E-05	2.93E-15
Gonads	3.11E-05	1.27E-08	4.85E-02	1.51E-06	37.1	4.06E-08	6.51E-18
Small Int	3.91E-04	9.54E-09	4.81E-02	1.88E-05	640	2.94E-08	4.70E-18
Rectum	2.52E-04	2.20E-07	4.90E-02	1.24E-05	63	1.96E-07	3.14E-17
Thyroid	7.92E-03	4.74E-06	4.90E-02	3.88E-04	19.6	1.98E-05	3.17E-15
Lung	3.69E+00	6.68E-07	1.21E-02	4.48E-02	999	4.48E-05	7.18E-15
Eyes	1.84E-04	1.03E-06	4.90E-02	9.03E-06	15	6.02E-07	9.65E-17
Trachea	1.93E-02	1.50E-05	4.90E-02	9.45E-04	10	9.45E-05	1.51E-14
Colon	3.11E-02	1.00E-06	4.90E-02	1.52E-03	369	4.13E-06	6.62E-16
Stomach	1.15E-01	1.92E-06	4.90E-02	5.64E-03	150	3.76E-05	6.02E-15

As expected, the organ dose was driven by the two photons over the two electrons by a factor of 100 or greater. This confirms the ICRP assumption for beta sources where the absorbed fraction is equal to one when the source organ is equal to the target organ. Compared to the Co-60 and Cs-137 organ dose, the most sensitive organs for Ir-192 were the lung, trachea and thyroid. The total lung dose in Gy/his from Ir-192 located in the lung is slightly greater than the total lung dose from Cs-137 located in the lung. The sum of the two Ir-192 photons is comparable to the energy of the single Cs-137 photon.

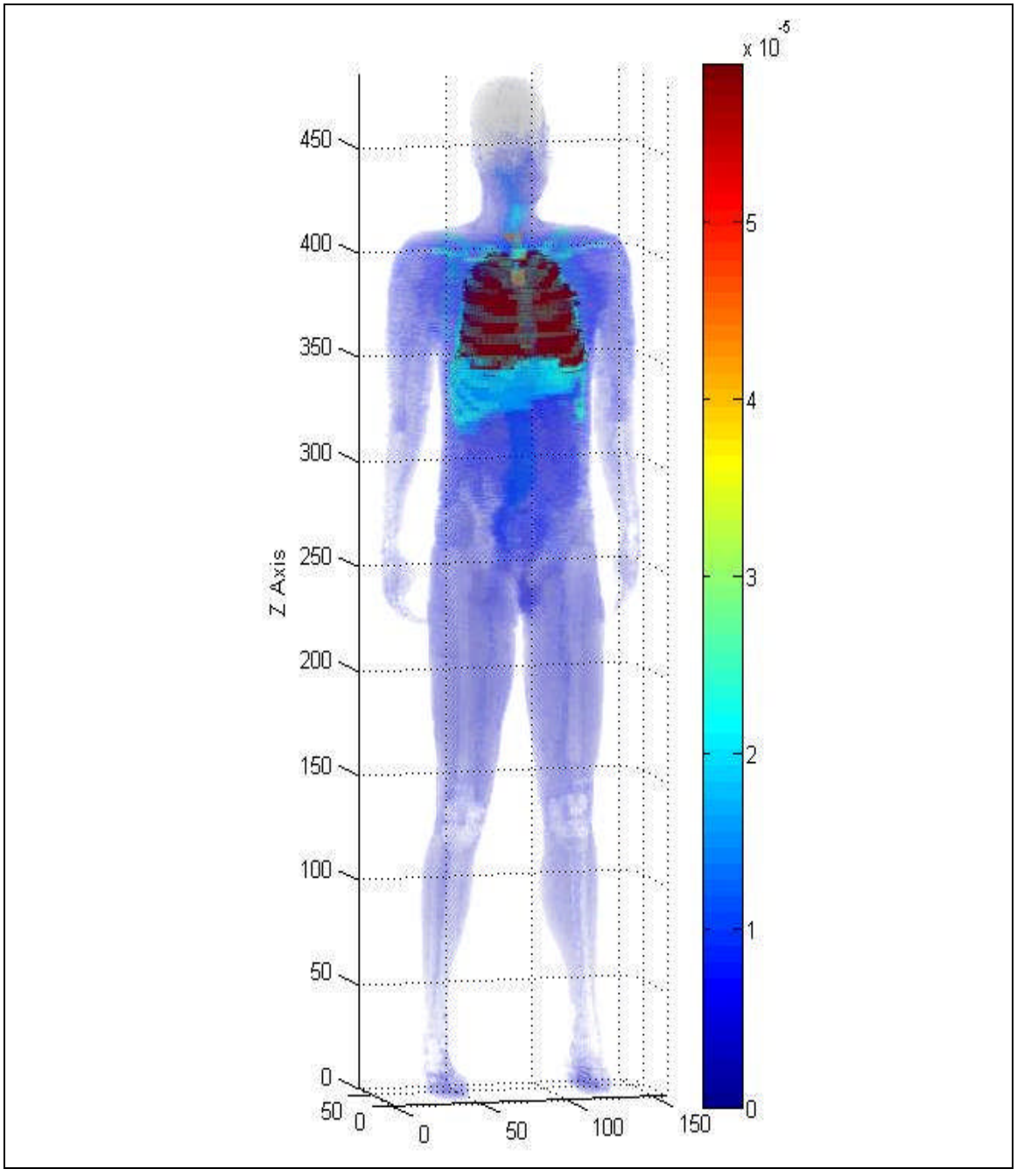

Fig. 11.2. Three-dimensional human dose profile from a Cs-137 source located within the lung.

Statistical checks on the Ir-192 Dose output file were performed. The same warnings present with Co-60 were observed. The 10 statistical checks for tally-four fluence passed and produced similar results. The 10 statistical checks for tally-six dose passed and produced similar results as with Co-60. Of the 61 tally bins, 9 bins had relative errors exceeding 0.10 for the 0.47 MeV photon.

The tallies for the electron sources in the lung had to be evaluated in a slightly different manner based on their inability to penetrate uniformly throughout the phantom. Secondary emissions, such as bremsstrahlung, characteristics x rays and electrons were the primary radiation source for organs outside of the lung. Three of the 10 statistical checks did not pass. The relative error for tally-four fluence was 0.26, the VoV was 0.35 and the pdf was 0. This reflects a large number of zero doses and slightly greater than zero doses based on the volume electron source in the lung. For the electron source, only the selected organs were reviewed for their relative error.

Figures 11.3 and 11.4 provide a simulated 3-dimensional view of the human body with a color profile that equates to the MCNP dose for the 0.47 MeV photon of Ir-192 and the 0.66 MeV electron of Ir-192 absorbed by each organ, respectively. The color bar units to the right of the phantom are in MeV/organ weight in grams.

Sr-90 organ dose profile

A Sr-90 source located within the lung would deliver a dose to the selected organs that ranges from a high of 2.94×10^{-7} MeV/g for the trachea and a low of 4.60×10^{-12} MeV/g for the skin. This organ dose contribution is from a single beta particle with a maximum energy of 0.55 MeV. The beta particle is produced with a yield of about 100%. Table 11.4 provides the calculated dose conversions for each of the selected organs that will be considered in this problem.

Table 11.4. Organ doses from a Sr-90 volume source in the lung.

Organs	MCNP Dose (MeV/g-his)	Std Deviation	MCNP Wght (g)	En Dep (MeV/his)	Organ Wt (g)	Organ Dose (MeV/g-his)	Organ Dose (Gy/his)
Skin	2.56E-07	9.85E-14	5.09E-02	1.30E-08	2830	4.60E-12	7.37E-22
Rib Bone Group	2.66E-03	1.07E-09	6.58E-02	1.75E-04	2167	8.08E-08	1.29E-17
Gonads	1.87E-07	2.44E-10	4.85E-02	9.06E-09	37.1	2.44E-10	3.91E-20
Small Int	5.15E-05	4.18E-10	4.81E-02	2.47E-06	640	3.86E-09	6.19E-19
Rectum	6.74E-07	5.24E-10	4.90E-02	3.30E-08	63	5.24E-10	8.40E-20
Thyroid	1.60E-05	4.69E-09	4.90E-02	7.85E-07	19.6	4.01E-08	6.42E-18
Lung	2.30E-02	1.98E-09	1.21E-02	2.79E-04	999	2.79E-07	4.47E-17
Eyes	0.00E+00	0.00E+00	4.90E-02	0.00E+00	15	0.00E+00	0.00E+00
Trachea	6.00E-05	2.09E-08	4.90E-02	2.94E-06	10	2.94E-07	4.71E-17
Colon	3.46E-05	4.91E-10	4.90E-02	1.69E-06	369	4.59E-09	7.36E-19
Stomach	2.07E-04	3.09E-09	4.90E-02	1.01E-05	150	6.76E-08	1.08E-17

As expected, the lung and trachea receive the greatest dose from a moderately energetic beta particle source located within the lung. The stomach and thyroid due to their close proximity to the source organ receive less than half the dose of the lung. Statistical checks on the Sr-90 Dose output file were performed. The same warnings present with Co-60 were observed. The 10 statistical checks for tally-four fluence missed four of the 10 checks. The relative error was 0.22, VoV did not decrease with a rate of inverse the number of histories, the FOM was not constant and increased and the pdf was 0. The 10 statistical checks for tally-six dose passed. Of the 61 tally bins, 9 bins had no dose and 31 bins had relative errors exceeding 0.10 for the 0.55 MeV beta radiation. Figure 11.5 provides a simulated 3-dimensional view of the human body with a color profile that equates to the MCNP dose for the beta radiation of Sr-90 absorbed by each organ. The color bar units to the right of the phantom are in MeV/organ weight in grams.

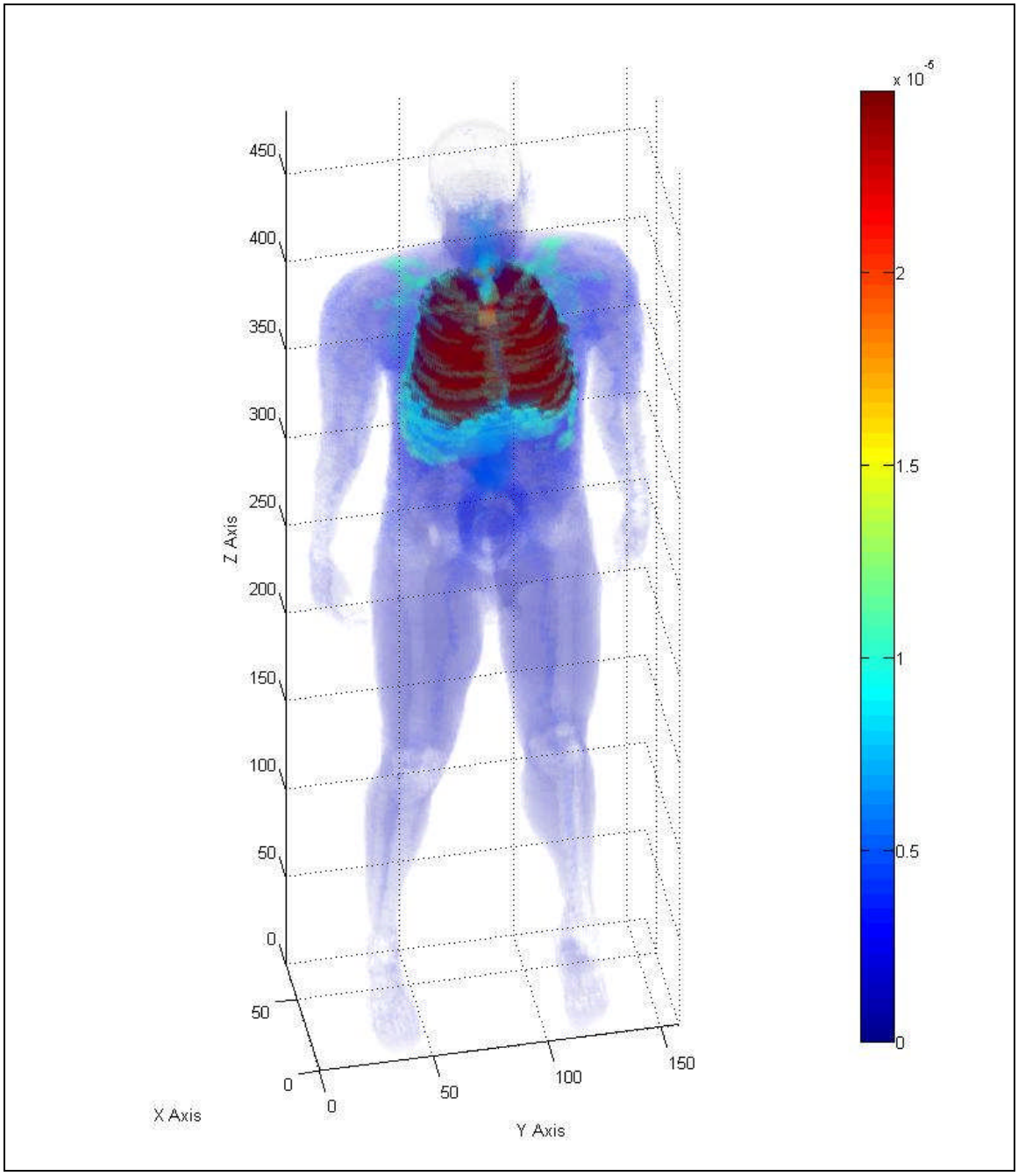

Fig. 11.3. Three-dimensional human dose profile from the 0.47 MeV Ir-192 photon source located within the lung.

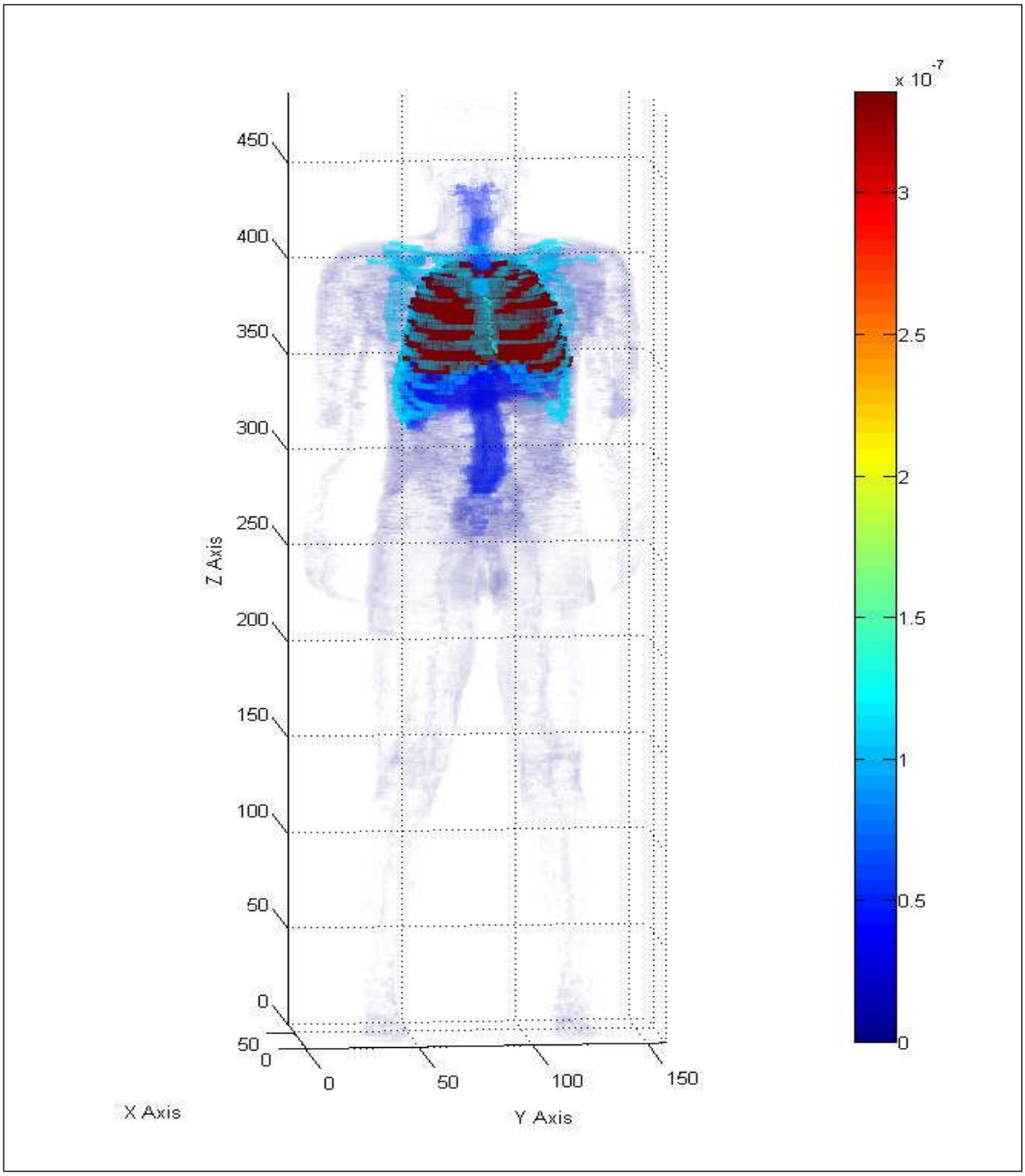

Fig. 11.4. Three-dimensional human dose profile from the 0.66 MeV Ir-192 electron source located within the lung.

Y-90 organ dose profile

A Y-90 source located within the lung would deliver a dose to the selected organs that ranges from a high of 3.42 x 10^{-6} MeV/g for the trachea and a low of 9.11 x 10^{-11} MeV/g for the skin. This organ dose contribution is from a single beta particle with a maximum energy of 2.281 MeV. The beta radiation is produced with a yield of about 100%. The energy dose and relative errors are provided in Table 11.5.

Table 11.5. Organ doses from a Y-90 volume source in the lung.

Organs	MCNP Dose (MeV/g-his)	Std Deviation	MCNP Wght (g)	En Dep (MeV/his)	Organ Wt (g)	Organ Dose (MeV/g-his)	Organ Dose (Gy/his)
Skin	5.07E-06	7.66E-13	5.09E-02	2.58E-07	2830	9.11E-11	1.46E-20
Rib Bone Group	2.77E-02	3.87E-09	6.58E-02	1.82E-03	2167	8.40E-07	1.35E-16
Gonads	3.14E-07	3.98E-10	4.85E-02	1.52E-08	37.1	4.11E-10	6.58E-20
Small Int	1.12E-03	3.61E-09	4.81E-02	5.36E-05	640	8.38E-08	1.34E-17
Rectum	7.12E-06	1.57E-09	4.90E-02	3.49E-07	63	5.53E-09	8.87E-19
Thyroid	2.48E-04	2.87E-08	4.90E-02	1.21E-05	19.6	6.19E-07	9.92E-17
Lung	1.44E-01	6.82E-09	1.21E-02	1.75E-03	999	1.75E-06	2.80E-16
Eyes	6.15E-06	6.41E-09	4.90E-02	3.01E-07	15	2.01E-08	3.22E-18
Trachea	6.99E-04	9.93E-08	4.90E-02	3.42E-05	10	3.42E-06	5.49E-16
Colon	7.12E-04	4.06E-09	4.90E-02	3.49E-05	369	9.45E-08	1.51E-17
Stomach	3.03E-03	1.90E-08	4.90E-02	1.48E-04	150	9.90E-07	1.59E-16

As with Sr-90, the lung and trachea received the highest dose from a highly-energetic beta particle source located within the lung. The stomach and thyroid, due to their close proximity to the source organ, received approximately 80% of the dose to the lung. The Y-90 lung dose was approximately 10 times greater than the dose delivered by the Sr-90 beta particle even though the energy of the Y-90 beta particle was approximately 4 times greater than the Sr-90. The difference in dose is attributed to the difference in energy dependent stopping power as well as the energy and type of secondary radiations.

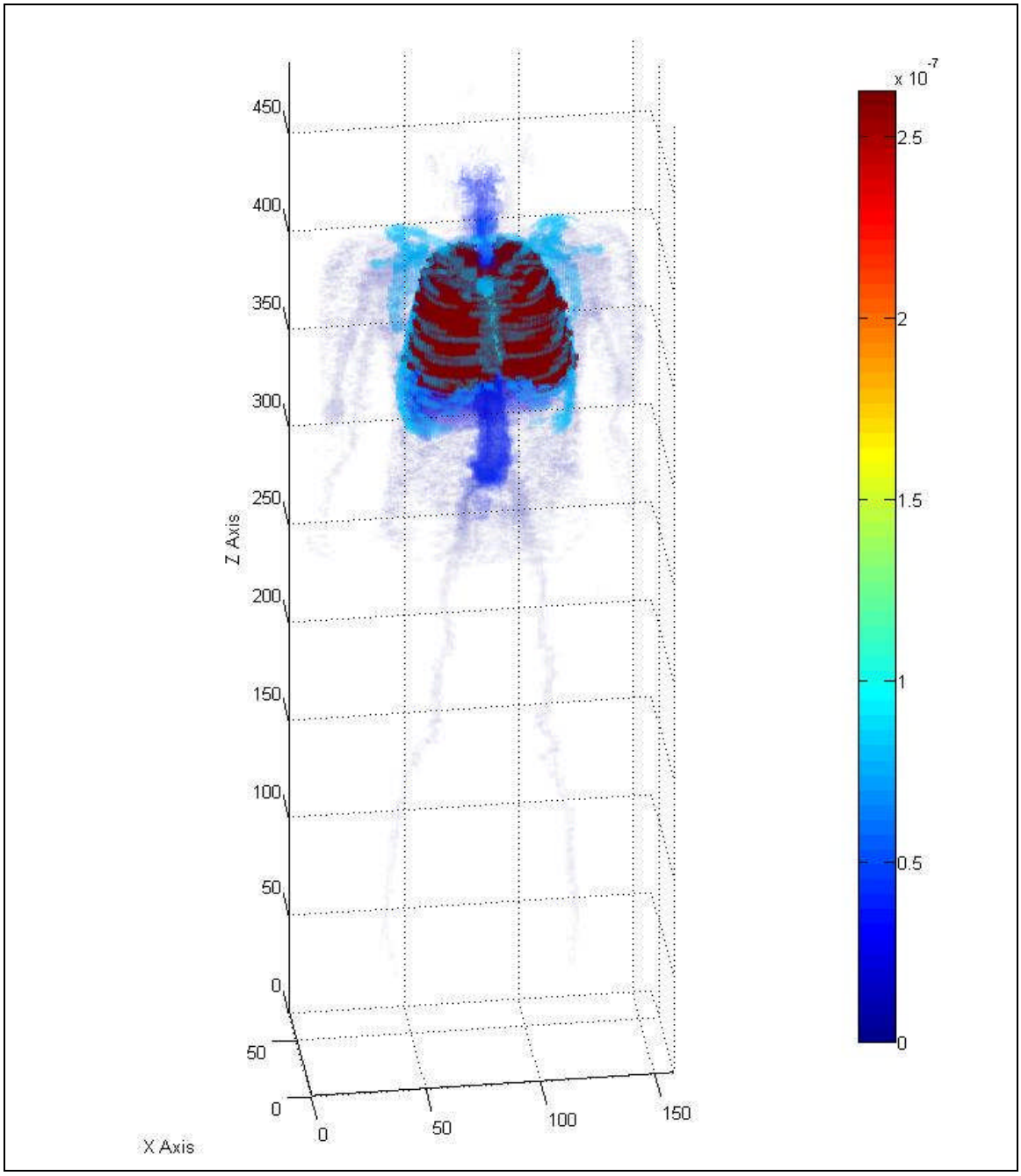

Fig. 11.5. Three-dimensional human dose profile from a Sr-90 volume source located within the lung.

Statistical checks on the Y-90 Dose output file were performed. The same warnings present with Co-60 were observed. The 10 statistical checks for tally-four fluence passed all checks except for the pdf which was 0. The 10 statistical checks for tally-six dose passed. Of the 61 tally bins, 2 bins had a zero dose and 25 bins had relative errors exceeding 0.10 for the 2.28 MeV beta particle. Figure 11.6 provides a simulated 3-dimensional view of the human body with a color profile that equates the MCNP organ dose for an Y-90 source in the lung. The color bar units to the right of the phantom are in MeV/organ weight in grams.

Results from lung volume source

Figure 11.7 provides an graph of all of the potential sources distributed in the lung. Based upon the results of the observed programs, Co-60 is the most limiting radionuclide. The trachea and lungs appear to be the most sensitive organs based upon a single decay from a source located within the lung. Even though the trachea shows the highest sensitivity, the dose is a little deceiving. The observed dose for the trachea is based on the number of voxels which include the air encircled by the trachea. The actual dose based on the weight of the organ is less than that for the lung. The dose to all of the selected organs from Sr-90 and Y-90 appears to be almost 100 times lower than the other three radionuclides. Ir-192 and Cs-137 appear to deliver almost identical doses to the selected organs.

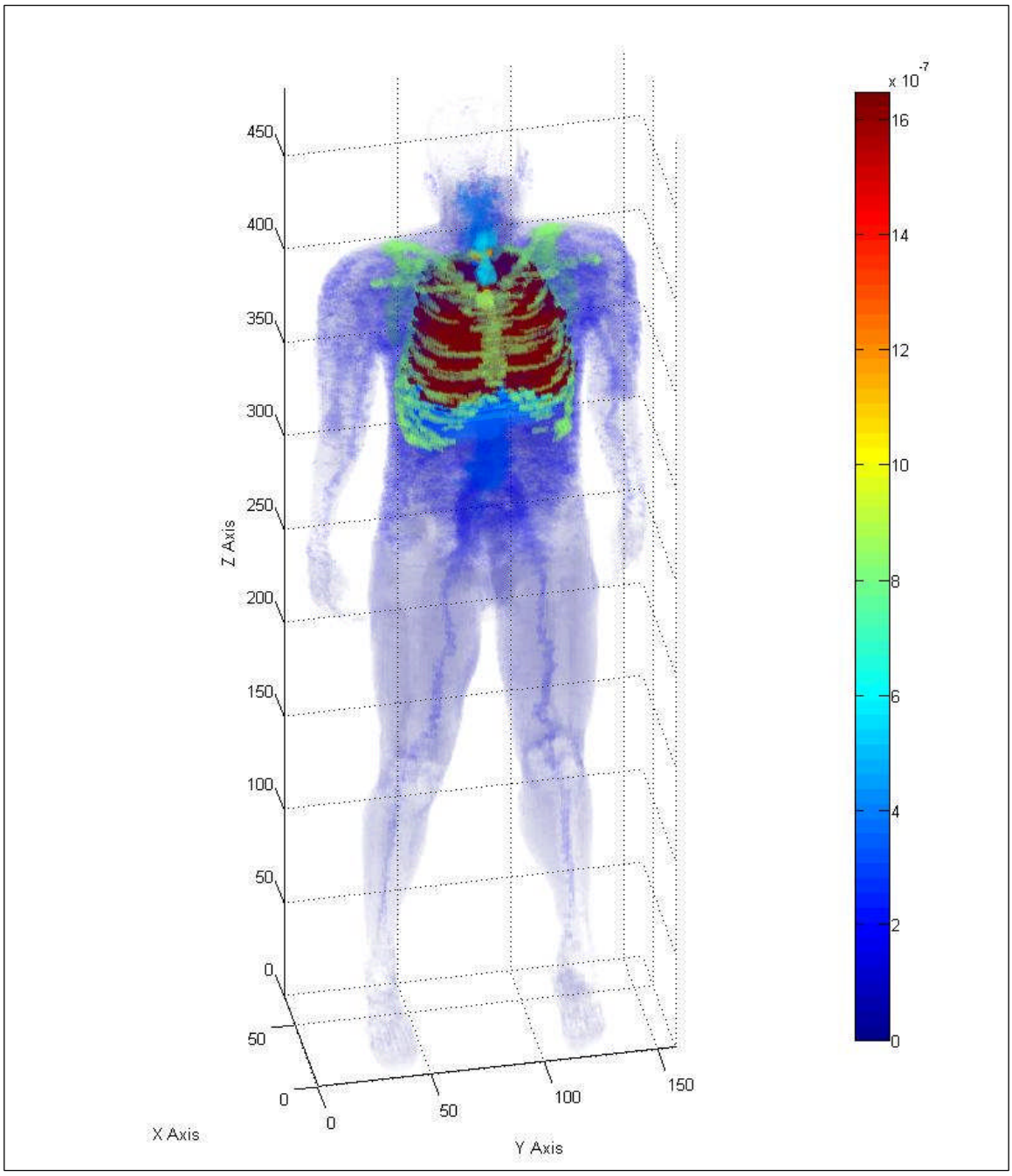

Fig. 11.6. Three-dimensional human dose profile from a Y-90 beta source located within the lung.

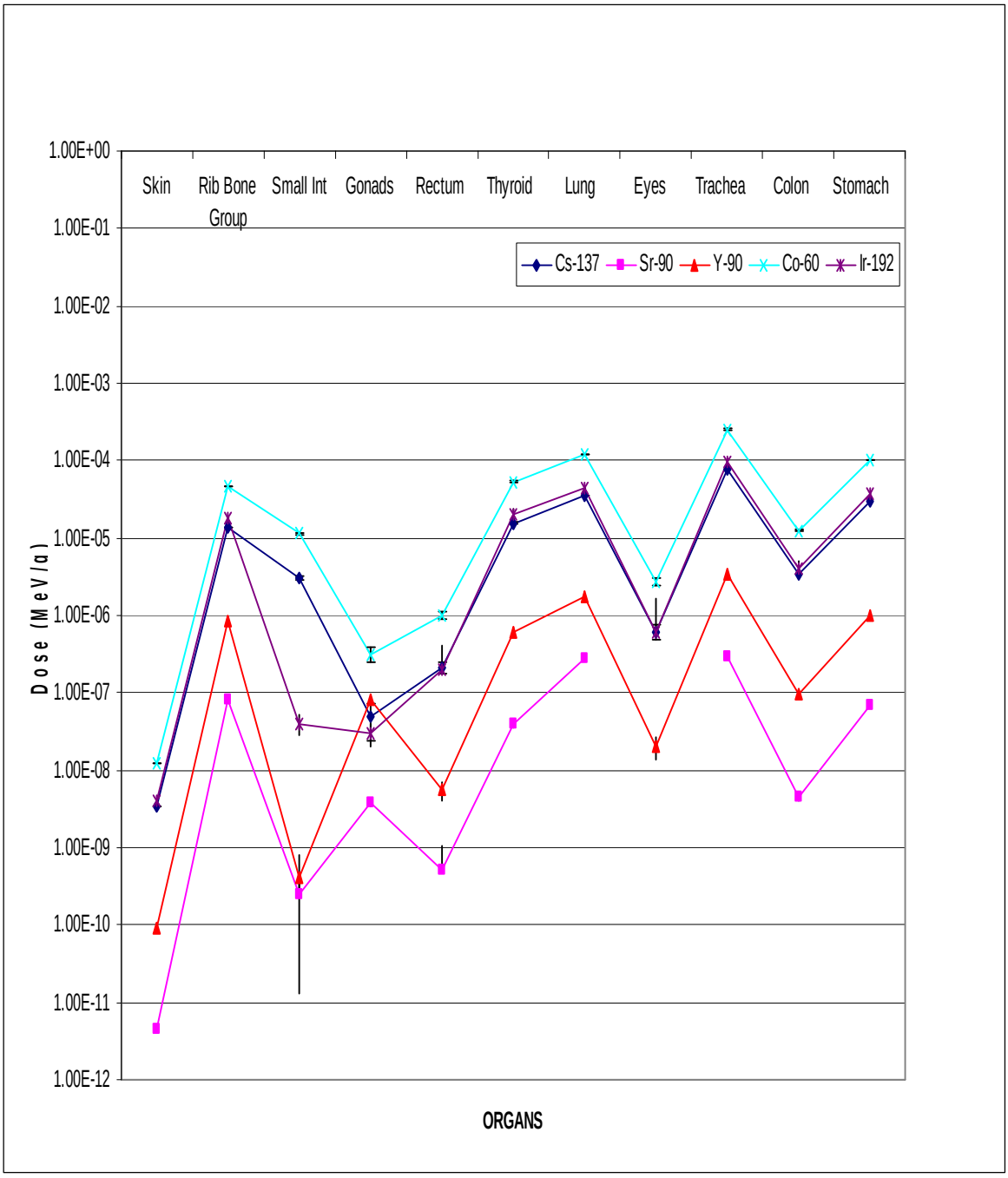

Fig. 11.7. Comprehensive graph of organ doses for the five potential lung sources.

CHAPTER XII
ESTIMATING ORGAN DOSE BASED ON VOLUME SOURCE IN THE LUNG FOR THE FEMALE PHANTOM ALONG WITH MALE LUNG COMPARISON

Organ data verification

The number of source voxels for additional organs will be based on the ratio of MAX lung source voxels divided by the total number of MAX lung voxels. This fraction will than be multiplied by the total number of organ voxels to determine the number of source voxels in the organ. The female phantom contained 78,315 lung voxels, therefore using the same ratio, 13,425 voxels were selected as the source volume and one million histories were selected. Co-60 was chosen for a comparison test between the two phantom models. The same two simulations were established. The first simulation analyzed the 1.17 MeV photon and the second tracked the 1.33 MeV photon. Volumes and masses were checked against ICRU-46 established values for both simulations (ICRU 1990). Using the provided values from Table A-2 of Appendix A, the hand calculated lung volume was 3,653.86 cm^3, the volume of a single voxel was 4.67×10^{-2} cm^3 (Kramer 2003). According to figure A-1 of Appendix A, the MCNPX code calculated a volume of 4.67×10^{-2} cm^3 for a single voxel. The hand calculated mass of the lung was 1,000 g and the mass per voxel was 1.27×10^{-2} g. Based on Figure A-1 of Appendix A, the code calculated a mass of 1.21×10^{-2} g in a single voxel. Therefore, the phantom lung provided a good simulation that was representative of standard woman based on standard man.

Dose to organ conversion

The MCNP output file provides a dose to all tissues defined within the phantom. The dose is listed in MeV/g and applies to a single voxel. The dose is based on the average energy deposited per unit mass for a single history. For the female phantom, a

single 1.17 MeV photon would deliver an average dose of $4.00 \pm 7.0 \times 10^{-4}$ MeV/g of tissue contained in a single voxel. To derive any meaningful information from this value, simple dose conversion calculations were applied to obtain a dose in gray (Gy) for each organ. The above value provided an average lung dose of 7.79×10^{-15} Gy from a single 1.17 MeV photon, if the photon originates within a lung volume source. Because of the extremely small dose from a single photon, the organ dose is compared in units of MeV/g for each organ. Co-60 also emits a beta radiation with a yield of 0.23 percent and an average energy of 606 KeV. The dose from the beta decay is only applicable to the lung and the dose from the beta radiation to the lung is over 1000 times smaller than the dose to the lung from the photons. Table 12.1 provides the calculated dose conversions for each of the selected organs that were considered in this problem.

Table 12.1. Organ doses from a Co-60 volume source in the female lung.

Organs	MCNP Dose (MeV/g)	Std Deviation	MCNP Wght (g)	En Dep (MeV/his)	Organ Wt (g)	Organ Dose (MeV/g)	Organ Dose (Gy)
Skin	7.52E-04	3.24E-11	5.09E-02	3.83E-05	2830	1.35E-08	2.17E-18
Rib Bone Group	5.90E-01	5.01E-08	6.58E-02	3.88E-02	2167	1.79E-05	2.87E-15
Small Int	9.08E-02	1.35E-07	4.81E-02	4.36E-03	640	6.82E-06	1.09E-15
Breasts	8.13E-03	3.40E-07	4.85E-02	3.94E-04	26	1.52E-05	2.43E-15
Thyroid	7.85E-03	6.37E-07	4.90E-02	3.84E-04	19.6	1.96E-05	3.14E-15
Ovaries	4.07E-04	1.51E-07	4.90E-02	1.99E-05	16	1.24E-06	1.99E-16
Lung	8.41E+00	1.43E-07	1.21E-02	1.02E-01	999	1.02E-04	1.64E-14
Eyes	7.80E-04	2.70E-07	4.90E-02	3.82E-05	15	2.55E-06	4.08E-16
Trachea	2.85E-02	2.58E-06	4.90E-02	1.39E-03	10	1.39E-04	2.23E-14
Colon	8.31E-02	1.68E-07	4.90E-02	4.07E-03	369	1.10E-05	1.77E-15
Stomach	1.78E-01	7.86E-07	4.90E-02	8.73E-03	150	5.82E-05	9.32E-15

As expected, like the male phantom, the largest dose concentrations are to the organs in the immediate vicinity of the lung which includes the trachea, breasts, colon, stomach and thyroid. The dose to the skin is smaller by a factor of 10,000. The assumption applied to the skin dose is that the dose is uniform across the entire volume of skin. The actual skin dose is delivered on a gradient depending upon the distance

from the source as well as the amount and type of material between the source and the skin.

Statistical analysis of output file

Similar to the male MAX lung phantom, the tally-four fluence analysis for each simulated detector, setup in accordance with chapter VII provided a random behavior for the mean. The desired relative error should be less than 0.10 and the observed relative error was 0.02. The desired and observed relative errors decreased according to the inverse of the square root of the number of histories. The desired variance of the variance should be less than 0.10 and the observed VoV was 0.00. The figure of merit value was constant and the behavior was random. The probability density function (pdf) desired should be greater than three, the observed pdf was 6.63. The tally-four fluence passed all 10 statistical checks. Out of 10 tally-four bins, no bins had a zero value and no bins contained relative errors greater than 0.10. The second 1.33 MeV photon simulation provided similar results with the exception of the pdf where the observed value was 10.00.

The tally-six dose analysis for each tissue showed a random behavior for the mean. The desired relative error was less than 0.10 and the observed relative error was 0.00 for both the 1.17 MeV and 1.33 MeV photons. The desired and observed relative errors decreased according to the inverse of the square root of the number of histories. The desired variance of the variance was less than 0.10 and the observed VoV was 0.00. The figure of merit value was constant and the behavior was random. The desired probability density function (pdf) should be greater than 3.00 and the observed value was 8.67 for the lower-photon and 6.71 for the higher-photon. The tally-six dose passed all 10 statistical checks. Out of 61 tally-six bins, no bin had a zero value and only 5 bins contained relative errors greater than 0.10.

Co-60 organ dose profile

A Co-60 source located within the lung would deliver a dose to the selected organs that ranges from a high of 1.39 x 10^{-4} MeV/g for the trachea and a low of 1.35 x 10^{-8} MeV/g for the skin. This organ dose contribution is the sum of two photons emitted from Co-60 that occur with a yield of about 100 percent. Figure 12.1 provides a simulated 3-dimensional view of the human body with a color profile that shows the organ dose for the 1.33 MeV photon of Co-60. The color bar units to the right of the phantom are in MeV/organ weight in grams. Each axis is represented in the figure along with a color bar that indicates the organ dose in MeV/g provided by the MCNPX output file. In the MCNPX output file, the trachea receives a slightly lesser dose than the lung based upon the number of voxels versus the measured gram weight of the trachea. The phantom includes the airway as part of the trachea. The dose difference is not significant.

Cs-137 organ dose profile

A Cs-137 source located within the lung would deliver a dose to the selected organs that ranges from a high of 4.14 x 10^{-5} MeV/g for the trachea and a low of 3.73 x 10^{-9} MeV/g for the skin. This organ dose contribution is from a 0.66 MeV photon emitted from Cs-137 that occurs with a yield of about 86 percent. Table 12.2 provides the dose output to the selected organs from 0.66 MeV photon.

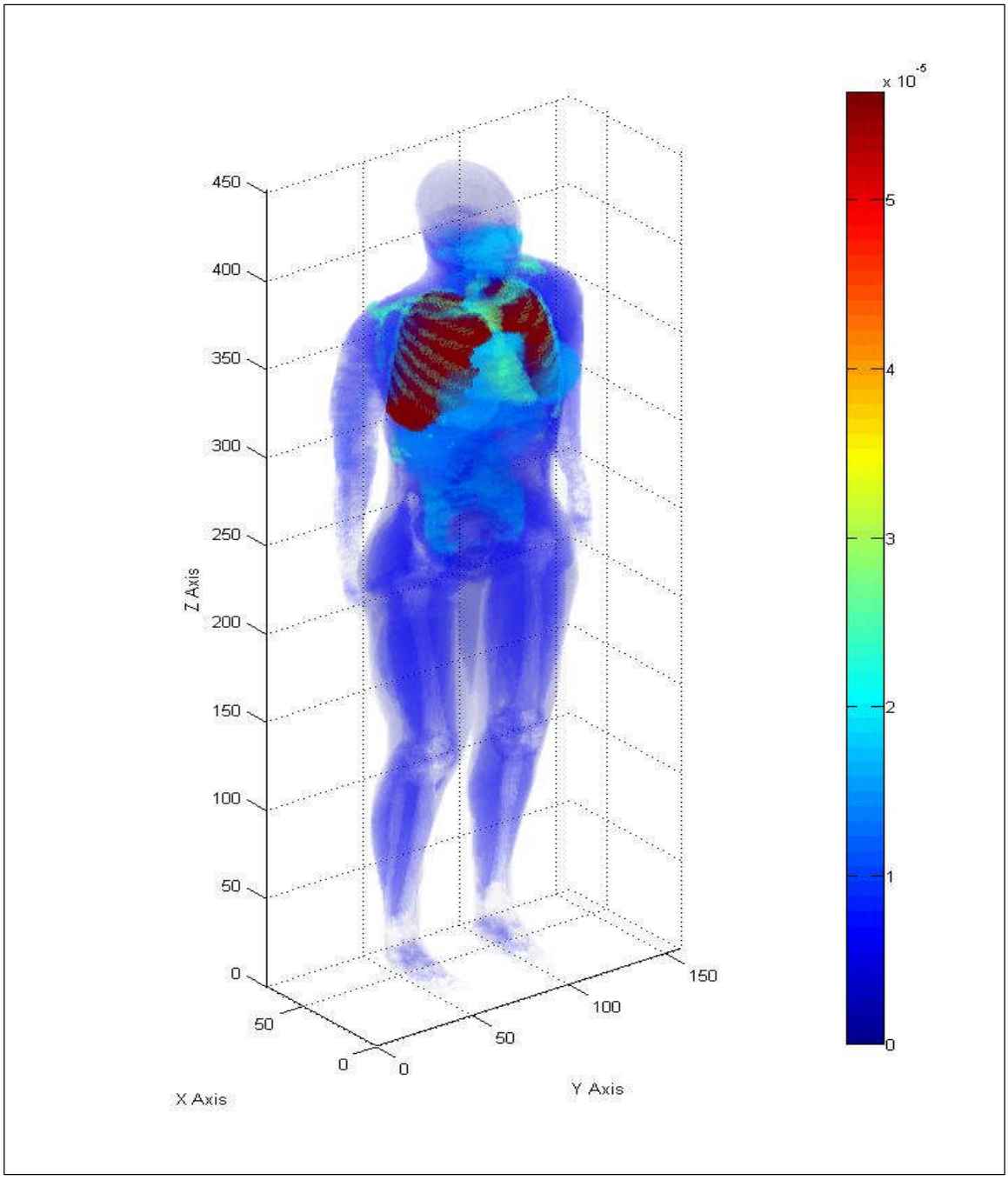

Fig. 12.1. Three-dimensional human dose profile from a 1.33 MeV photon source located within the female lung.

Table 12.2. Organ doses for a Cs-137 volume source in the female lung.

Organs	MCNP Dose (MeV/g)	Std Deviation	MCNP Wght (g)	En Dep (MeV/his)	Organ Wt (g)	Organ Dose (MeV/g)	Organ Dose (Gy)
Skin	2.07E-04	4.47E-12	5.09E-02	1.05E-05	2830	3.73E-09	5.97E-19
Rib Bone Group	1.77E-01	7.51E-09	6.58E-02	1.16E-02	2167	5.36E-06	8.59E-16
Small Int	2.38E-02	1.78E-08	4.81E-02	1.14E-03	640	1.78E-06	2.86E-16
Breasts	2.18E-03	4.64E-08	4.85E-02	1.06E-04	26	4.07E-06	6.52E-16
Thyroid	2.37E-03	9.37E-08	4.90E-02	1.16E-04	19.6	5.93E-06	9.50E-16
Ovaries	9.45E-05	1.86E-08	4.90E-02	4.63E-06	16	2.89E-07	4.63E-17
Lung	2.49E+00	2.11E-08	1.21E-02	3.02E-02	999	3.02E-05	4.84E-15
Eyes	1.76E-04	3.29E-08	4.90E-02	8.63E-06	15	5.75E-07	9.22E-17
Trachea	8.46E-03	3.73E-07	4.90E-02	4.14E-04	10	4.14E-05	6.64E-15
Colon	2.24E-02	2.29E-08	4.90E-02	1.10E-03	369	2.97E-06	4.76E-16
Stomach	5.18E-02	1.12E-07	4.90E-02	2.54E-03	150	1.69E-05	2.71E-15

As expected, the dose to the selected organs is similar to the dose produced by the Co-60 photons. The largest dose concentration remains in the immediate vicinity of the lung. The lung dose is reduced by approximately 25%. All organs reflect a similar reduction in dose. Compared with the male Cs-137 lung source, the female dose is slightly lower in all organs with the exception of the skin. This difference is attributed to the reduction in the number of skin voxels without reducing the organ mass of the skin. Statistical checks on the Cs-137 Dose output file were performed. The same warnings present with Co-60 were observed. The 10 statistical checks for tally-four passed and produced similar results. The 10 statistical checks for tally-six passed and produced similar results as with Co-60. Of the 61 tally bins, 5 bins had relative errors exceeding 0.10. Figure 12.2 provides a simulated 3-dimensional view of the human body with a color profile that shows the MCNP dose for the single photon of Cs-137. The color bar units to the right of the phantom are in MeV/organ weight in grams.

The Co-60 lung dose was 1.02×10^{-4} MeV/g for the 1.17 MeV photon compared with the Cs-137 lung dose of 3.02×10^{-5} MeV/g for the 0.66 MeV photon. As expected, the dose profile is similar to that of the photons emitted by Co-60. As expected, the dose to each individual organ is proportionally reduced based on the lower-energy of the

source photon and the energy dependent stopping power of the material within the phantom.

Ir-192 organ dose profile

An Ir-192 source located within the lung would deliver a dose to the 11 selected organs that ranges from a high of 5.10 x 10^{-5} MeV/g for the trachea and a low of 4.37 x 10^{-9} MeV/g for the skin. This organ dose is the sum of two photons with energies of 0.47 MeV and 0.32 MeV along with two electrons that have maximum energies of 0.66 MeV and 0.54 MeV. All four emissions are produced with a yield of 26.2%, 22.4%, 10.1% and 6.7%, respectively. Table 12.3 provides the calculated dose conversions for each of the selected organs.

Table 12.3. Organ doses for an Ir-192 volume source in the female lung.

Organs	MCNP Dose (MeV/g)	Std Deviation	MCNP Wght (g)	En Dep (MeV/his)	Organ Wt (g)	Organ Dose (MeV/g)	Organ Dose (Gy)
Skin	2.43E-04	1.67E-10	5.09E-02	1.24E-05	2830	4.37E-09	7.00E-19
Rib Bone Group	2.26E-01	2.37E-07	6.58E-02	1.49E-02	2167	6.85E-06	1.10E-15
Small Int	2.75E-02	5.48E-07	4.81E-02	1.32E-03	640	2.07E-06	3.31E-16
Breasts	2.63E-03	1.54E-06	4.85E-02	1.28E-04	26	4.91E-06	7.86E-16
Thyroid	2.71E-03	2.91E-06	4.90E-02	1.33E-04	19.6	6.78E-06	1.09E-15
Ovaries	1.06E-04	6.95E-07	4.90E-02	5.21E-06	16	3.26E-07	5.22E-17
Lung	3.07E+00	5.56E-07	1.21E-02	3.73E-02	999	3.73E-05	5.97E-15
Eyes	1.82E-04	1.10E-06	4.90E-02	8.94E-06	15	5.96E-07	9.55E-17
Trachea	1.04E-02	1.07E-05	4.90E-02	5.09E-04	10	5.09E-05	8.16E-15
Colon	2.57E-02	6.42E-07	4.90E-02	1.26E-03	369	3.41E-06	5.47E-16
Stomach	6.35E-02	3.01E-06	4.90E-02	3.11E-03	150	2.07E-05	3.32E-15

As expected with the male phantom, the organ dose was driven by the two photons over the two electrons by a factor of 100 or greater. Compared to the Co-60 and Cs-137 organ dose, the most sensitive organs for Ir-192 were the lung, trachea and stomach. The dose to the lung is slightly greater than the Cs-137 lung dose. The sum of the two Ir-192 photons is comparable to the energy of the single Cs-137 photon.

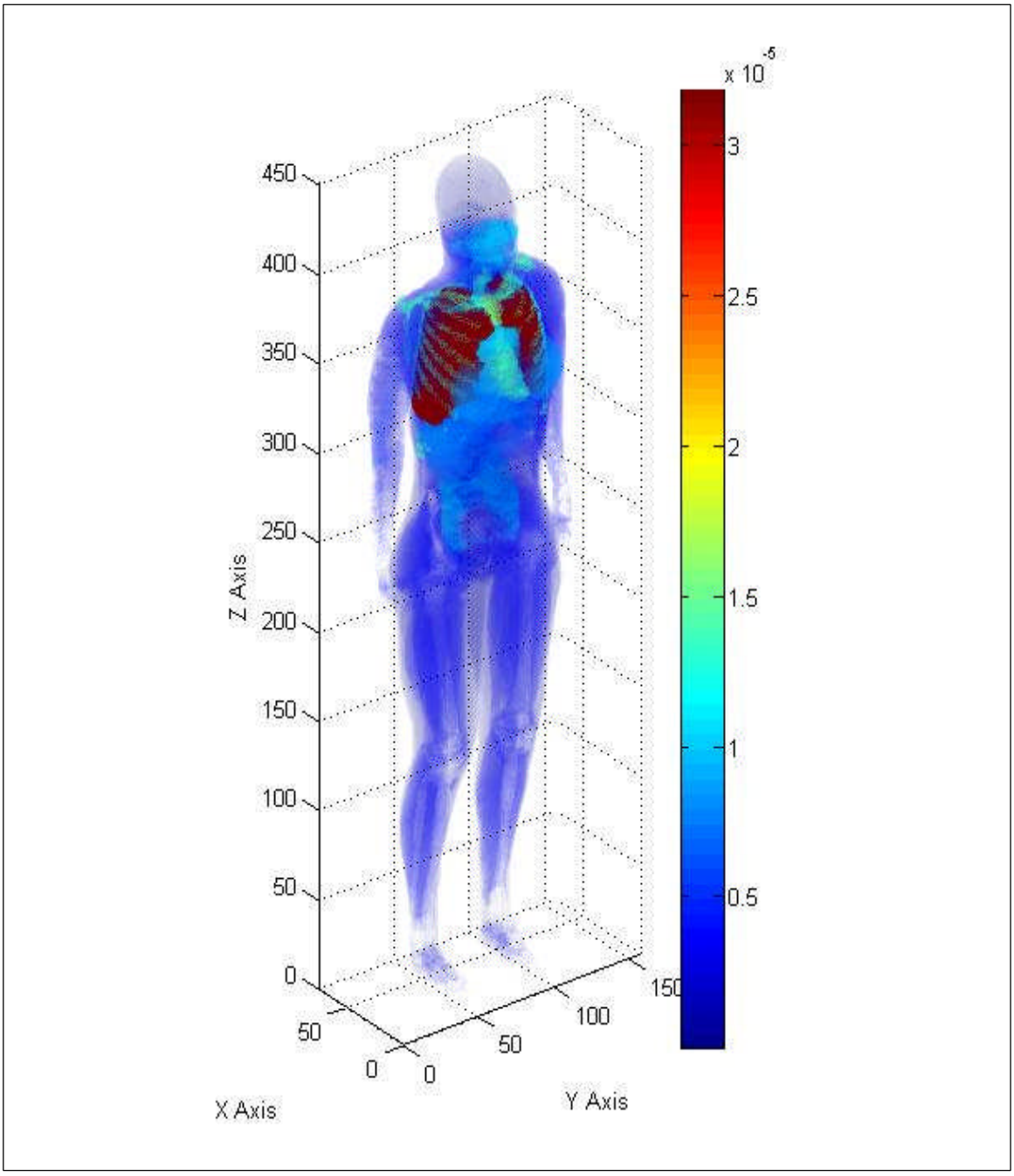

Fig. 12.2. Three-dimensional human dose profile from a Cs-137 photon source located within the lung.

Statistical checks on the Ir-192 Dose output file were performed. The same warnings present with Co-60 were observed. The 10 statistical checks for tally-four fluence passed and produced similar results. The 10 statistical checks for tally-six dose passed and produced similar results as with Co-60. Of the 61 tally bins, 5 bins had relative errors exceeding 0.10 for the 0.47 MeV photon. The 0.32 MeV photon produced similar results.

The tallies for the electron sources in the lung had to be evaluated in a slightly different manner based on their inability to penetrate uniformly throughout the phantom. Secondary emissions, such as bremsstrahlung and characteristics x rays and electrons were the primary radiation source for organs outside of the lung. Two of the 10 statistical checks did not pass. The relative error for electron simulation was 0.17 and the pdf was 0. This reflects a large number of zero doses and slightly greater than zero doses based on the volume electron source in the lung. For the electron source, only the selected organs were reviewed for their relative error.

Figures 12.3 and 12.4 provide a simulated 3-dimensional view of the human body with a color profile that equates to the MCNP dose for the 0.47 MeV photon of Ir-192 and the 0.66 MeV electron of Ir-192 absorbed by each organ, respectively. The color bar units to the right of the phantom are in MeV/organ weight in grams.

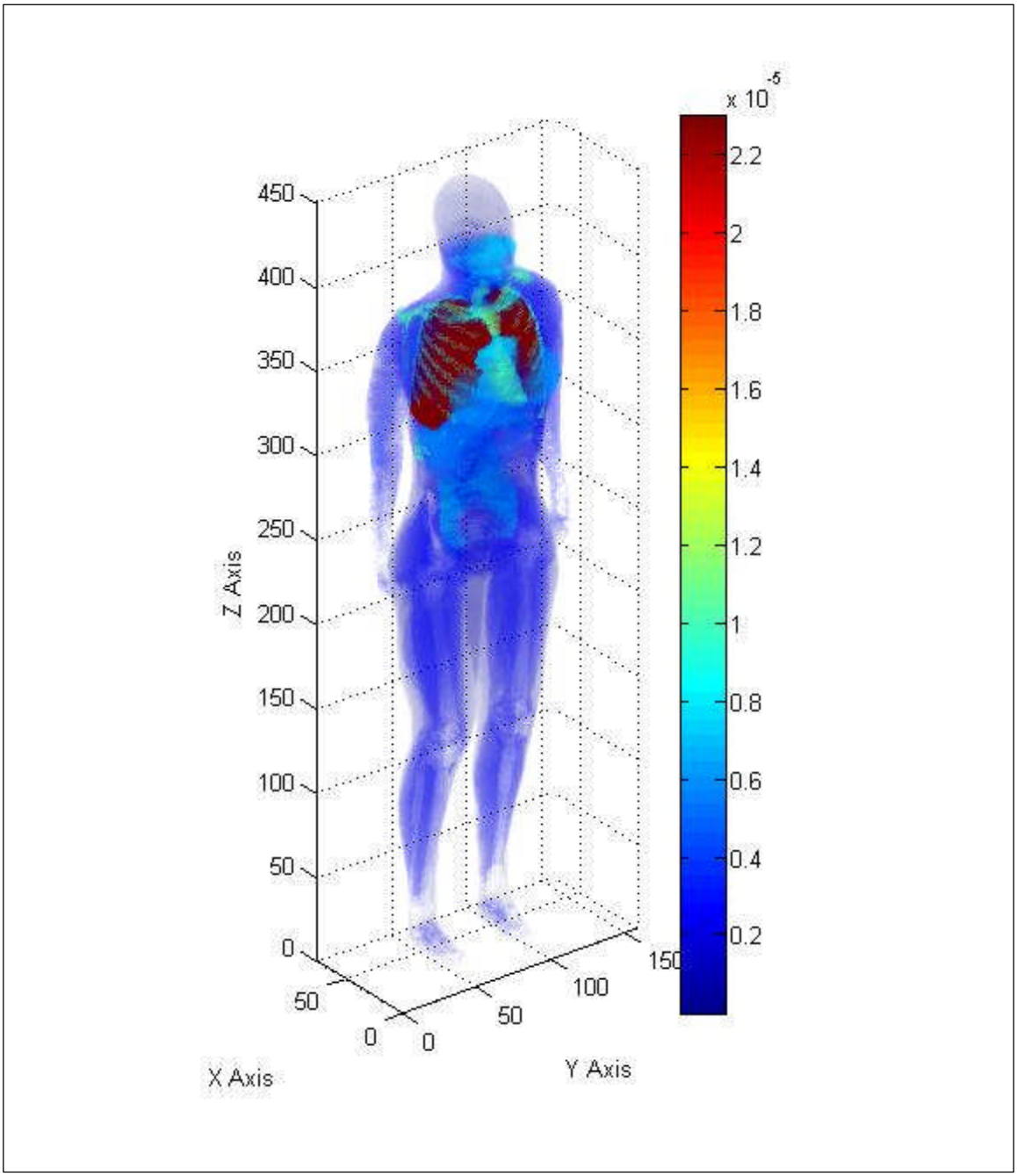

Fig. 12.3. Three-dimensional human dose profile from a 0.47 MeV Ir-192 photon source located within the lung.

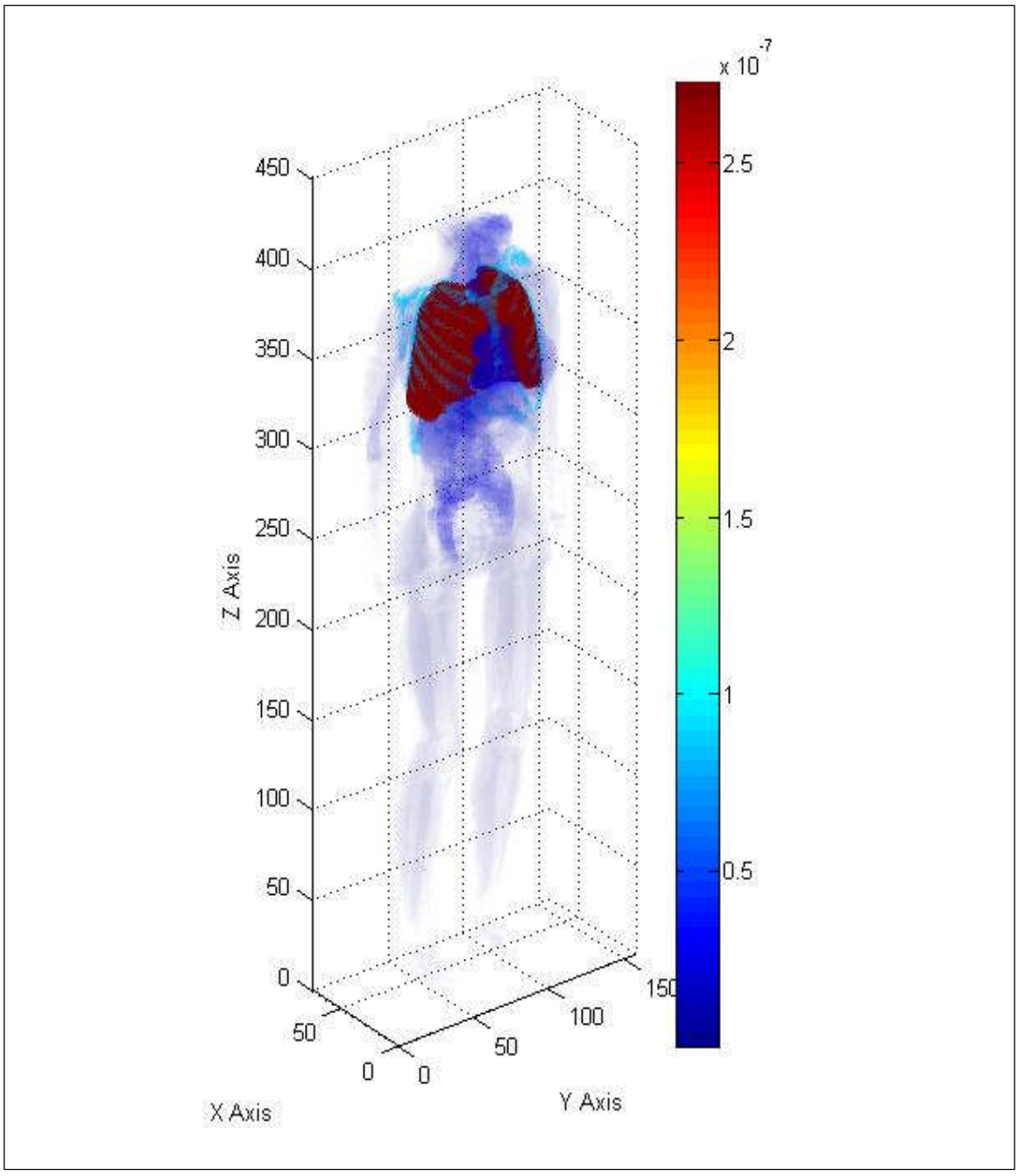

Fig. 12.4. Three-dimensional human dose profile from a 0.66 MeV Ir-192 electron source located within the lung.

Sr-90 organ dose profile

A Sr-90 source located within the lung would deliver a dose to the selected organs that ranges from a high of 2.65 x 10^{-7} MeV/g for the lung and a low of 6.34 x 10^{-12} MeV/g for the skin. This organ dose contribution is from a single beta particle with a maximum energy of 0.55 MeV. The beta particle is produced with a yield of about 100%. Table 12.4 provides the calculated dose conversions for each of the selected organs that will be considered in this problem.

Table 12.4. Organ doses from a Sr-90 volume source in the female lung.

Organs	MCNP Dose (MeV/g)	Std Deviation	MCNP Wght (g)	En Dep (MeV/his)	Organ Wt (g)	Organ Dose (MeV/g)	Organ Dose (Gy)
Skin	3.54E-07	1.21E-13	5.09E-02	1.80E-08	2830	6.36E-12	1.02E-21
Rib Bone Group	1.10E-03	5.70E-10	6.58E-02	7.23E-05	2167	3.34E-08	5.34E-18
Small Int	2.60E-05	2.58E-10	4.81E-02	1.25E-06	640	1.95E-09	3.12E-19
Breasts	4.78E-06	1.27E-09	4.85E-02	2.32E-07	26	8.91E-09	1.43E-18
Thyroid	3.75E-06	2.02E-09	4.90E-02	1.84E-07	19.6	9.37E-09	1.50E-18
Ovaries	0.00E+00	0.00E+00	4.90E-02	0.00E+00	16	0.00E+00	0.00E+00
Lung	2.18E-02	1.88E-09	1.21E-02	2.65E-04	999	2.65E-07	4.24E-17
Eyes	3.51E-08	1.09E-10	4.90E-02	1.72E-09	15	1.15E-10	1.84E-20
Trachea	2.51E-05	1.14E-08	4.90E-02	1.23E-06	10	1.23E-07	1.97E-17
Colon	3.00E-05	3.87E-10	4.90E-02	1.47E-06	369	3.98E-09	6.38E-19
Stomach	1.26E-04	2.69E-09	4.90E-02	6.15E-06	150	4.10E-08	6.57E-18

As expected, the lung and trachea receive the greatest dose from a moderately energetic beta particle source located within the lung. The stomach and thyroid, due to their close proximity to the source organ, receive less than half the dose of the lung. Statistical checks on the Sr-90 Dose output file were performed. The same warnings present with Co-60 were observed. The 10 statistical checks for tally-four fluence missed three of the 10 checks. The relative error was 0.22, VoV was 0.13 and increased and the pdf was 0. The 10 statistical checks for tally-six dose passed. Of the 61 tally bins, 9 bins had no dose and 25 bins had relative errors exceeding 0.10 for the 0.55 MeV beta particle. Figure 12.5 provides a simulated 3-dimensional view of the human body

with a color profile that equates to the MCNP dose for the beta radiation of Sr-90 absorbed by each organ. The color bar units to the right of the phantom are in MeV/organ weight in grams.

Y-90 organ dose profile

A Y-90 source located within the lung would deliver a dose to the selected organs that ranges from a high of 1.52×10^{-6} MeV/g for the lung and a low of 1.06×10^{-10} MeV/g for the skin. This organ dose contribution is from a single beta particle with a maximum energy of 2.28MeV. The beta radiation is produced with a yield of about 100%. The energy dose and relative errors are provided in Table 12.5.

Table 12.5. Organ doses from a Y-90 volume source in the female lung.

Organs	MCNP Dose (MeV/g-his)	Std Deviation	MCNP Wght (g)	En Dep (MeV/his)	Organ Wt (g)	Organ Dose (MeV/g-his)	Organ Dose (Gy/his)
Skin	5.07E-06	7.66E-13	5.09E-02	2.58E-07	2830	9.11E-11	1.46E-20
Rib Bone Group	2.77E-02	3.87E-09	6.58E-02	1.82E-03	2167	8.40E-07	1.35E-16
Gonads	3.14E-07	3.98E-10	4.85E-02	1.52E-08	37.1	4.11E-10	6.58E-20
Small Int	1.12E-03	3.61E-09	4.81E-02	5.36E-05	640	8.38E-08	1.34E-17
Rectum	7.12E-06	1.57E-09	4.90E-02	3.49E-07	63	5.53E-09	8.87E-19
Thyroid	2.48E-04	2.87E-08	4.90E-02	1.21E-05	19.6	6.19E-07	9.92E-17
Lung	1.44E-01	6.82E-09	1.21E-02	1.75E-03	999	1.75E-06	2.80E-16
Eyes	6.15E-06	6.41E-09	4.90E-02	3.01E-07	15	2.01E-08	3.22E-18
Trachea	6.99E-04	9.93E-08	4.90E-02	3.42E-05	10	3.42E-06	5.49E-16
Colon	7.12E-04	4.06E-09	4.90E-02	3.49E-05	369	9.45E-08	1.51E-17
Stomach	3.03E-03	1.90E-08	4.90E-02	1.48E-04	150	9.90E-07	1.59E-16

As with Sr-90, the lung and trachea received the highest dose from a highly-energetic, beta particle source located within the lung. The stomach and thyroid, due to their close proximity to the source organ, received approximately 50% of the dose to the lung. The Y-90 lung dose was approximately 10 times greater than the dose delivered by the Sr-90 beta particle even though the energy of the Y-90 beta particle was approximately 4 times greater than the Sr-90. The difference in dose is attributed to the

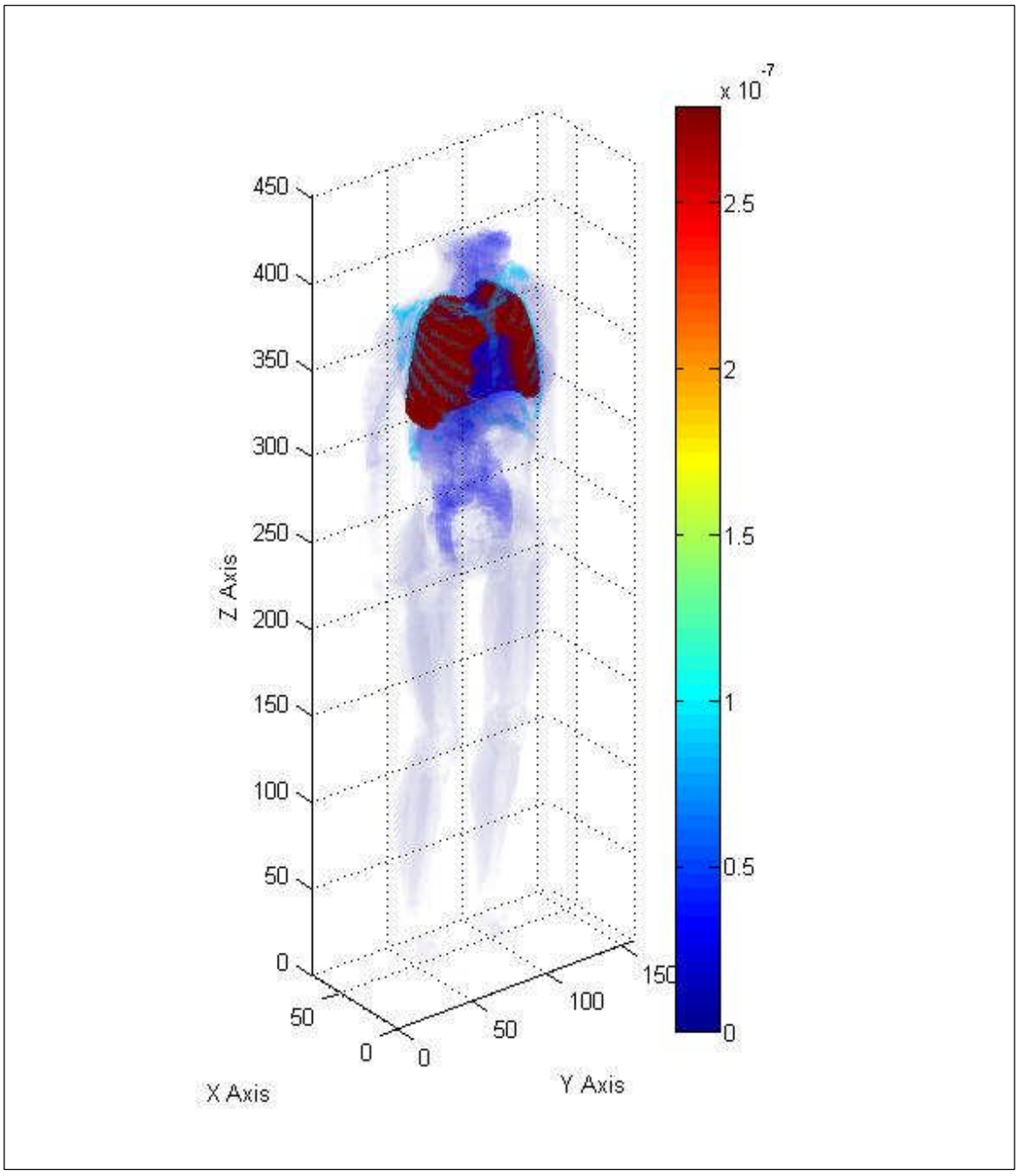

Fig. 12.5. Three-dimensional human dose profile from a Sr-90 beta source located within the lung.

difference in energy dependent stopping power as well as the energy and type of secondary radiations. The female lung dose was slightly less than the male lung dose. Statistical checks on the Y-90 dose output file were performed. The same warnings present with Co-60 were observed. The 10 statistical checks for tally-four fluence passed all checks except two. The VoV did not decrease at a rate of inverse the number of histories and the pdf was 0. The 10 statistical checks for tally-six passed all but one check. The figure of merit did not exhibit a random behavior. Of the 61 tally bins, one bin had a zero dose and 21 bins had relative errors exceeding 0.10 for the 2.28 MeV beta particle. Figure 12.6 provides a simulated 3-dimensional view of the human body with a color profile that equates the MCNP organ dose for the an Y-90 source in the lung. The color bar units to the right of the phantom are in MeV/organ weight in grams.

Results from lung volume source

Figure 12.7 provides a graph of all of the potential sources distributed in the lung and their organ doses. As with the male phantom, the results of the observed simulations indicate that Co-60 is the most limiting radionuclide. The trachea and lungs appear to be the most sensitive organs based upon a single decay from a source located within the lung. Even though the trachea shows the highest sensitivity, the dose is a little deceiving. The observed dose for the trachea is based on the number of voxels which include the air encircled by the trachea. The actual dose, based on the weight of the organ, is less than that for the lung. Figure 12.8 shows a dose comparison between the male and female phantoms for Co-60 and Sr-90.

Based on the data, the Co-60 dose from the male phantom appears to be slightly more sensitive than the female phantom. The Thyroid shows the largest difference between the two. The male dose is 5.26×10^{-5} MeV/g and for the female it is

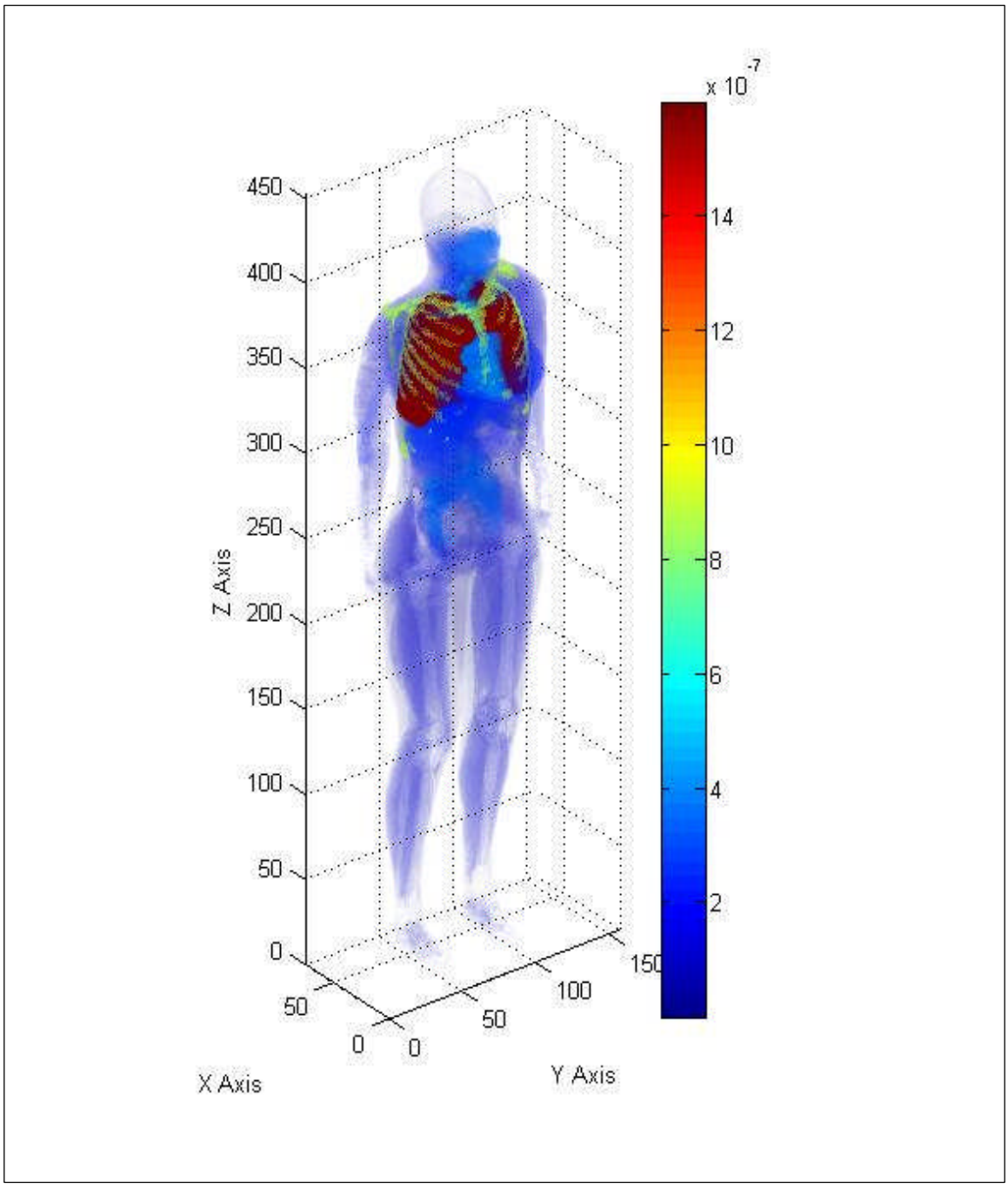

Fig. 12.6. Three-dimensional human dose profile from a Y-90 beta source located within the female lung.

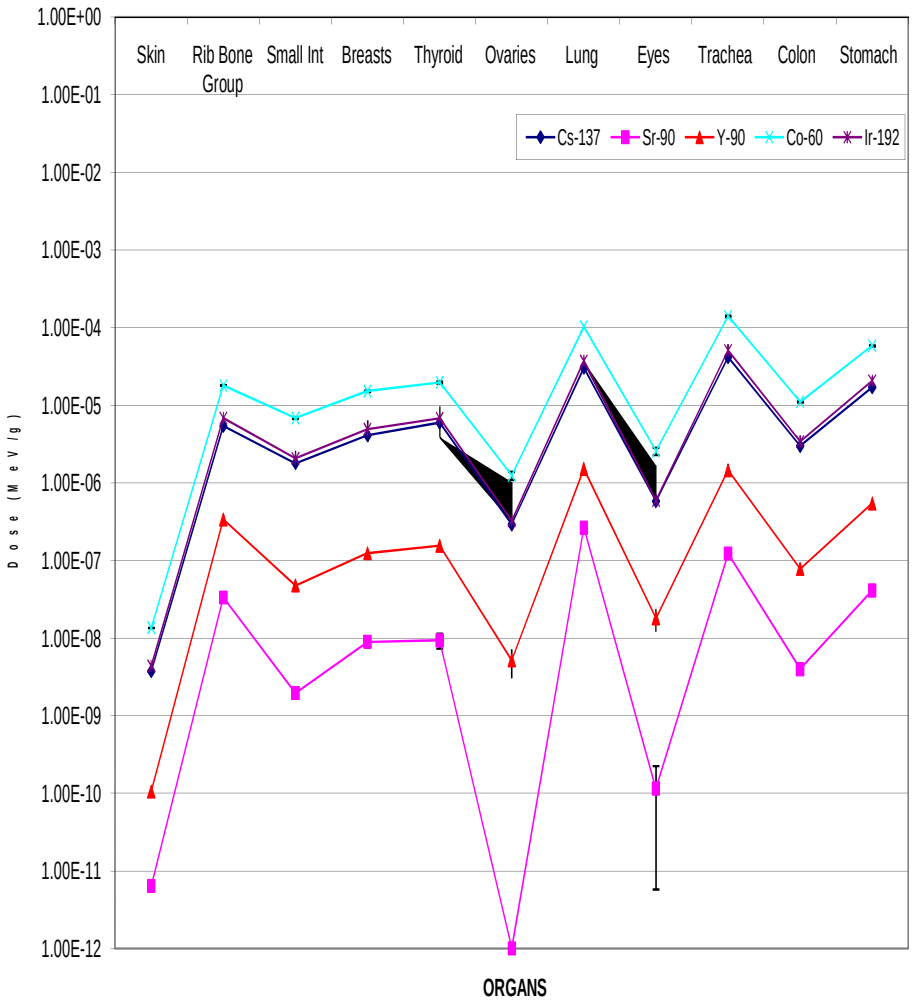

Fig. 12.7. Summary graph of organ doses for the five potential lung sources.

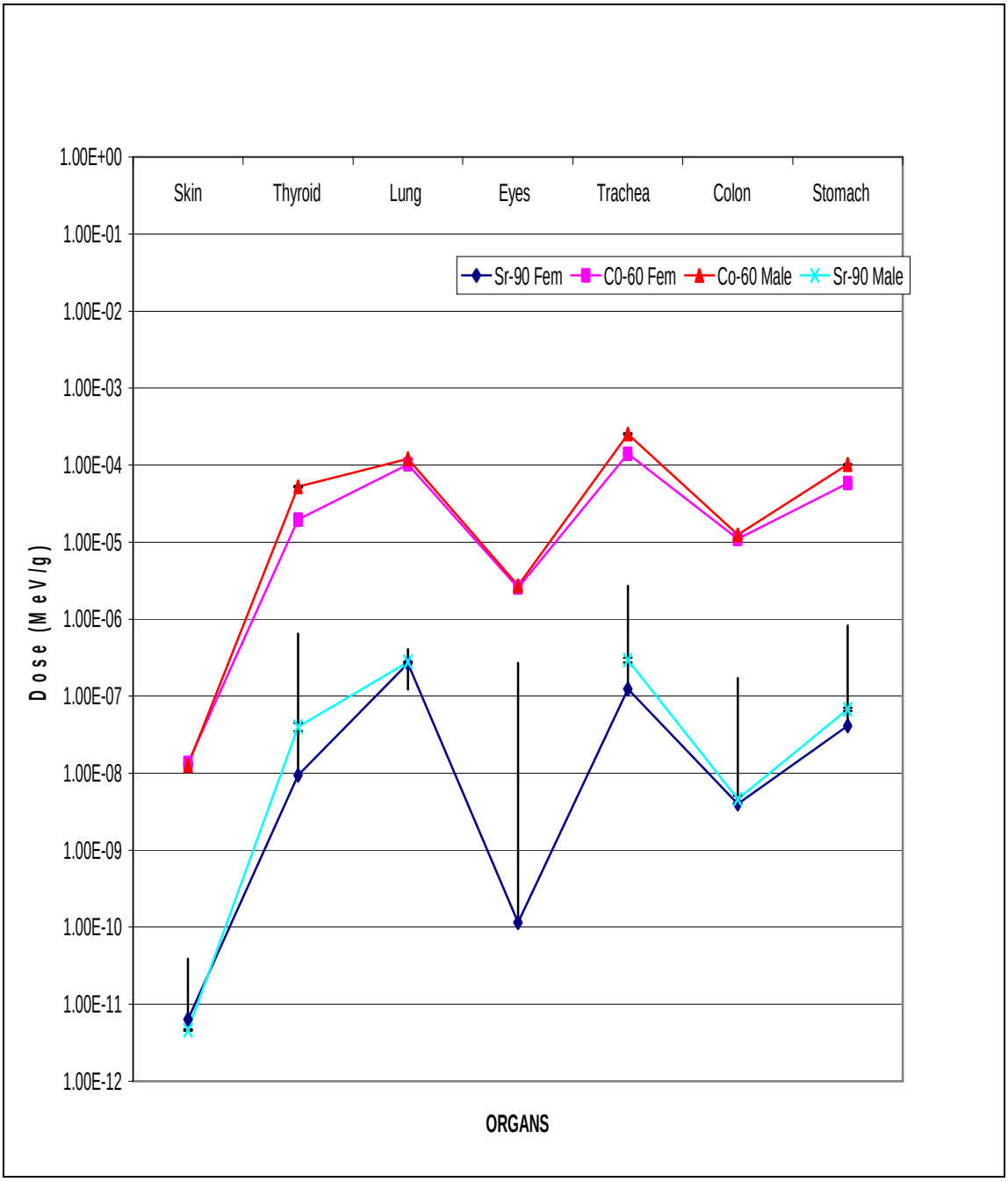

Fig. 12.8. Summary comparison of male and female organ doses for Co-60 and Sr-90.

1.96×10^{-5} MeV/g. The stomach and trachea show a slightly smaller difference between the two genders. This is probably due to the difference in volume since the mass remains the same. The volume for the male thyroid is 18.89 cm^3 and for the female it is 16.19 cm^3.

Based on the Sr-90 data, the female leg bone is more sensitive than the male. The male sensitivity holds for the thyroid, trachea and stomach with the largest difference in the thyroid. The dose to leg bone for the female is 2.99×10^{-9} MeV/g and that for the male is 2.15×10^{-10} MeV/g. A key thing to note is that both male and female dose falls within the margin of error for the female dose. The same is true for the trachea and stomach where both genders are within the margin of error.

CHAPTER XIII
ESTIMATING ORGAN DOSE BASED ON VOLUME SOURCE IN THE STOMACH

Organ data verification

The number of source voxels for additional organs will be based on the ratio of MAX lung source voxels divided by the total number of MAX lung voxels. This fraction will than be multiplied by the total number of organ voxels to determine the number of source voxels in the organ. The number of source voxels calculated for the stomach were 1,295. This number would represent a volume source based on the dimension of the stomach. Volumes and masses were checked against ICRU-46 established values for both simulations (ICRU 1990). Using the provided values from Table A-2 of Appendix A, the hand calculated volume of stomach was 380.95 cm^3, the volume of a single voxel was 4.67 x 10^{-2} cm^3 (Kramer 2003). According to figure A-1 of Appendix A, the MCNPX code calculated a volume of 4.67E-2 cm^3 for a single voxel. The hand calculated mass of the stomach was 400 g and the mass per voxel was 4.89 x 10^{-2} g which includes the stomach and its contents. The stomach alone weighs 150 g and the mass per voxel would be 1.83 x 10^{-2} g. Based on Figure A-1 of Appendix A, the code calculated a mass of 4.90 x 10^{-2} g in a single voxel. Therefore, the phantom stomach provided a good simulation that was representative of standard man.

Co-60 organ dose profile

A Co-60 source located within the stomach would deliver a dose to the selected organs that ranges from a high of 1.33 x 10^{-03} MeV/g for the stomach and a low of 1.25 x 10^{-8} MeV/g for the skin. This organ dose contribution is the sum of two photons emitted from Co-60 that occur with a yield of about100 percent. Table 13.1 provides the calculated dose conversions for each of the selected organs that will be considered in this problem.

Table 13.1. Organ doses from a Co-60 volume source in the stomach.

Organs	MCNP Dose (MeV/g)	Std Deviation	MCNP Wght (g)	En Dep (MeV/his)	Organ Wt (g)	Organ Dose (MeV/g)	Organ Dose (Gy)
Skin	6.98E-04	3.01E-11	5.09E-02	3.55E-05	2830	1.25E-08	2.01E-18
Rib Bone Group	8.25E-01	2.75E-08	6.58E-02	5.43E-02	2167	2.50E-05	4.01E-15
Small Int	5.96E-01	3.67E-07	4.81E-02	2.86E-02	640	4.47E-05	7.17E-15
Gonads	4.75E-04	9.59E-08	4.85E-02	2.30E-05	37.1	6.21E-07	9.94E-17
Rectum	2.59E-03	1.32E-07	4.90E-02	1.27E-04	63	2.02E-06	3.23E-16
Thyroid	3.60E-03	4.30E-07	4.90E-02	1.76E-04	19.6	8.99E-06	1.44E-15
Lung	3.42E+00	1.50E-07	1.21E-02	4.15E-02	999	4.15E-05	6.66E-15
Eyes	3.65E-04	1.97E-07	4.90E-02	1.79E-05	15	1.19E-06	1.91E-16
Trachea	8.88E-03	1.76E-06	4.90E-02	4.35E-04	10	4.35E-05	6.97E-15
Colon	2.24E-01	3.03E-07	4.90E-02	1.10E-02	369	2.97E-05	4.76E-15
Stomach	4.08E+00	2.26E-06	4.90E-02	2.00E-01	150	1.33E-03	2.13E-13

As expected, the largest dose concentration was to the stomach. The small intestine, colon, lung and trachea received the next highest doses, which is not surprising due to their central location to the stomach. The dose to the skin is reduced by a factor of 100,000. The assumption applied to the skin dose is that the dose is uniform across the entire volume of skin. The actual skin dose is delivered on a gradient depending upon the distance from the source as well as the amount and type of material between the source and the skin.

Statistical analysis of output file

The tally-four fluence analysis for each simulated detector, setup in accordance with chapter VII provided a random behavior for the mean. The desired relative error should be less than 0.10 and the observed relative error was 0.05. The desired and observed relative errors decreased according to the inverse of the square root of the number of histories. The desired variance of the variance should be less than 0.10 and the observed VoV was 0.01. The figure of merit value was constant and the behavior was random. The probability density function (pdf) desired should be greater than three,

the observed pdf was 10. The tally-four fluence passed all 10 statistical checks. Out of 10 tally-four bins, no bin had a zero dose value and no bins contained relative errors greater than 0.10. The second 1.33 MeV photon simulation provided similar statistical results.

The tally-six dose analysis for each material showed a random behavior for the mean. The desired relative error should be less than 0.10 and the observed relative error was 0.00 for both the 1.17 MeV and 1.33 MeV photons. The desired and observed relative errors decreased in relation to the inverse of the square root of the number of histories. The desired variance of the variance should be less than 0.10 and the observed VoV was 0.00. The figure of merit value was constant and the behavior was random. The desired probability density function (pdf) should be greater than 3.00 and the observed value was 4.68 for the 1.17 MeV photon and 5.66 for the 1.33 MeV photon. The tally-six dose passed all 10 statistical checks. Out of 61 tally-six bins, no bin had a zero value and only 5 bins contained relative errors greater than 0.10.

Figure 13.1 provides a simulated 3-dimensional view of the human body with a color profile that shows the organ dose for the 1.33 MeV photon of Co-60. The color bar units to the right of the phantom are in MeV/organ weight in grams. Each axis is represented in the figure along with a color bar that indicates the organ dose in MeV/g provided by the MCNPX output file. In the MCNPX output file, the stomach receives the highest dose followed by the small intestine. The dose to the stomach is over 13 times that of the small intestine. The lung and trachea are closely matched.

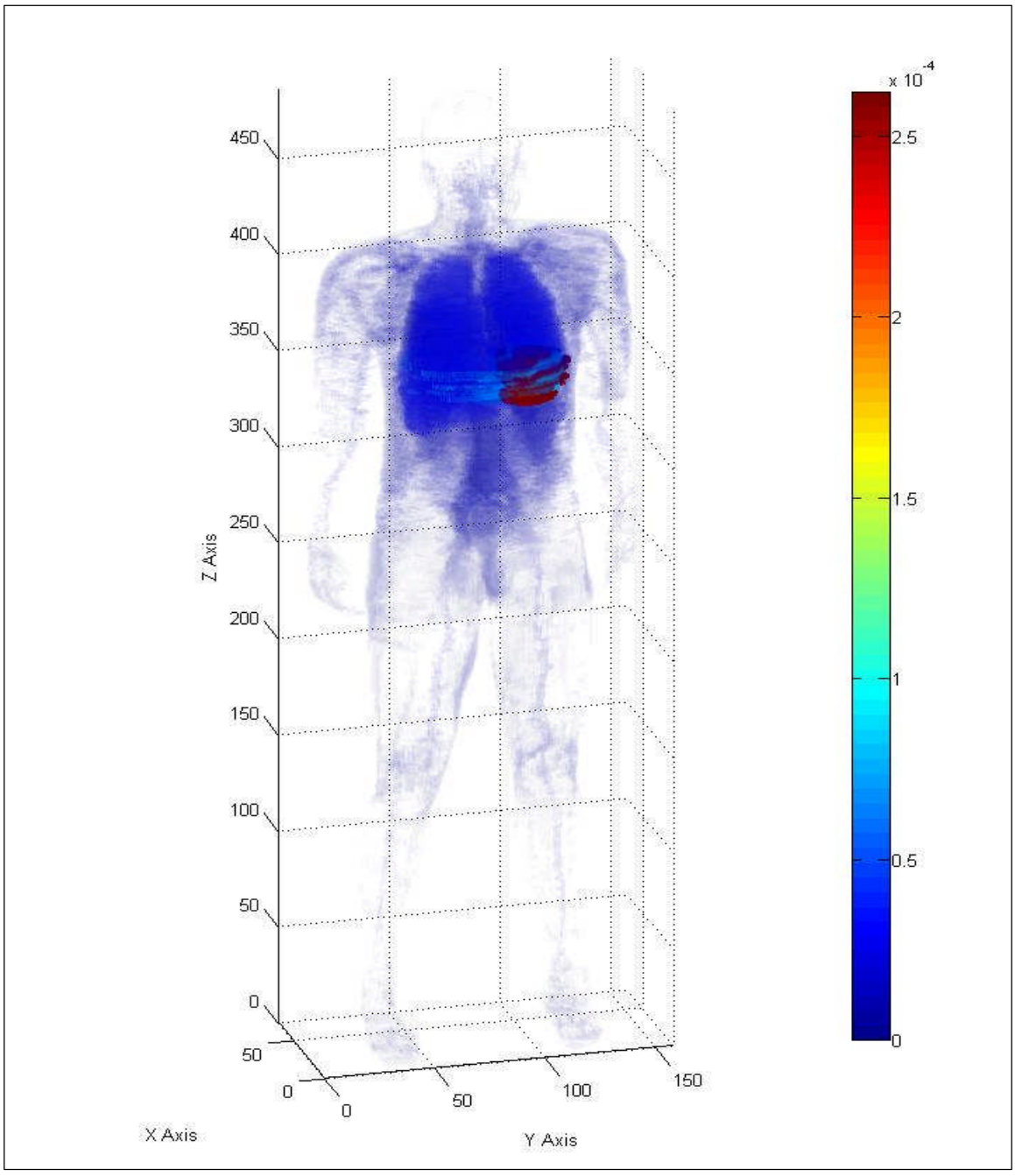

Fig. 13.1. Three-dimensional human dose profile from a 1.33 MeV photon source located within the stomach.

Cs-137 organ dose profile

A Cs-137 source located within the stomach would deliver a dose to the selected organs that ranges from a high of 3.90 x 10^{-4} MeV/g for the stomach and a low of 3.37 x 10^{-9} MeV/g for the skin. This organ dose contribution is from a 0.66 MeV photon emitted from Cs-137 that occur with a yield of about 86 percent. Table 13.2 provides the dose output to the selected organs from the 0.66 MeV photon.

Table 13.2. Organ doses for a Cs-137 volume source in the stomach.

Organs	MCNP Dose (MeV/g)	Std Deviation	MCNP Wght (g)	En Dep (MeV/his)	Organ Wt (g)	Organ Dose (MeV/g)	Organ Dose (Gy)
Skin	1.87E-04	4.04E-12	5.09E-02	9.53E-06	2830	3.37E-09	5.40E-19
Rib Bone Group	2.47E-01	8.26E-09	6.58E-02	1.63E-02	2167	7.51E-06	1.20E-15
Small Int	1.73E-01	5.06E-08	4.81E-02	8.30E-03	640	1.30E-05	2.08E-15
Gonads	9.19E-05	1.06E-08	4.85E-02	4.46E-06	37.1	1.20E-07	1.93E-17
Rectum	5.72E-04	1.57E-08	4.90E-02	2.80E-05	63	4.44E-07	7.12E-17
Thyroid	1.04E-03	6.07E-08	4.90E-02	5.11E-05	19.6	2.60E-06	4.17E-16
Lung	1.01E+00	2.21E-08	1.21E-02	1.23E-02	999	1.23E-05	1.97E-15
Eyes	8.14E-05	2.46E-08	4.90E-02	3.99E-06	15	2.66E-07	4.26E-17
Trachea	2.61E-03	2.46E-07	4.90E-02	1.28E-04	10	1.28E-05	2.05E-15
Colon	6.36E-02	4.22E-08	4.90E-02	3.11E-03	369	8.44E-06	1.35E-15
Stomach	1.20E+00	3.12E-07	4.90E-02	5.86E-02	150	3.90E-04	6.25E-14

As expected, the dose to the selected organs is similar to the dose produced by the Co-60 photons. The largest dose concentration remains among the organs in the immediate vicinity of the stomach. The stomach dose is reduced by an approximate factor of two. This reduction is expected based on the energy reduction between the 1.17 MeV Co-60 photon and the 0.66 MeV photon from Cs-137.

Statistical checks were performed on the Cs-137 dose output file. The same warnings present with Co-60 were observed. The 10 statistical checks for tally-four fluence passed and produced similar results. The 10 statistical checks for tally-six dose passed and produced similar results as with Co-60. Of the 61 tally bins, no bin had a zero dose and 9 bins had relative errors exceeding 0.10. Figure 13.2 provides a

simulated 3-dimensional view of the human body with a color profile that shows the MCNP dose for the single photon of Cs-137 absorbed by each organ. The color bar units to the right of the phantom are in MeV/organ weight in grams.

The Co-60 stomach dose was 6.33×10^{-4} MeV/g for the 1.17 MeV photon compared with the Cs-137 stomach dose of 3.90×10^{-4} MeV/g for the 0.66 MeV photon. As expected, the dose profile is similar to that of the photons emitted by Co-60. The dose to each individual organ is proportionally reduced based on the lower-energy of the source photon and the energy dependent stopping power of the material within the phantom.

Ir-192 organ dose profile

An Ir-192 source located within the stomach would deliver a dose to the selected organs that ranges from a high of 4.79×10^{-04} MeV/g for the stomach and a low of 3.89×10^{-9} MeV/g for the skin. This organ dose is the sum of two photons with energies of 0.47 MeV and 0.32 MeV along with two electrons with maximum energies of 0.66 MeV and 0.54 MeV. All four emissions are produced with a yield of 26.2%, 22.4%, 10.1% and 6.7%, respectively. Table 13.3 provides the calculated dose conversions for each of the selected organs.

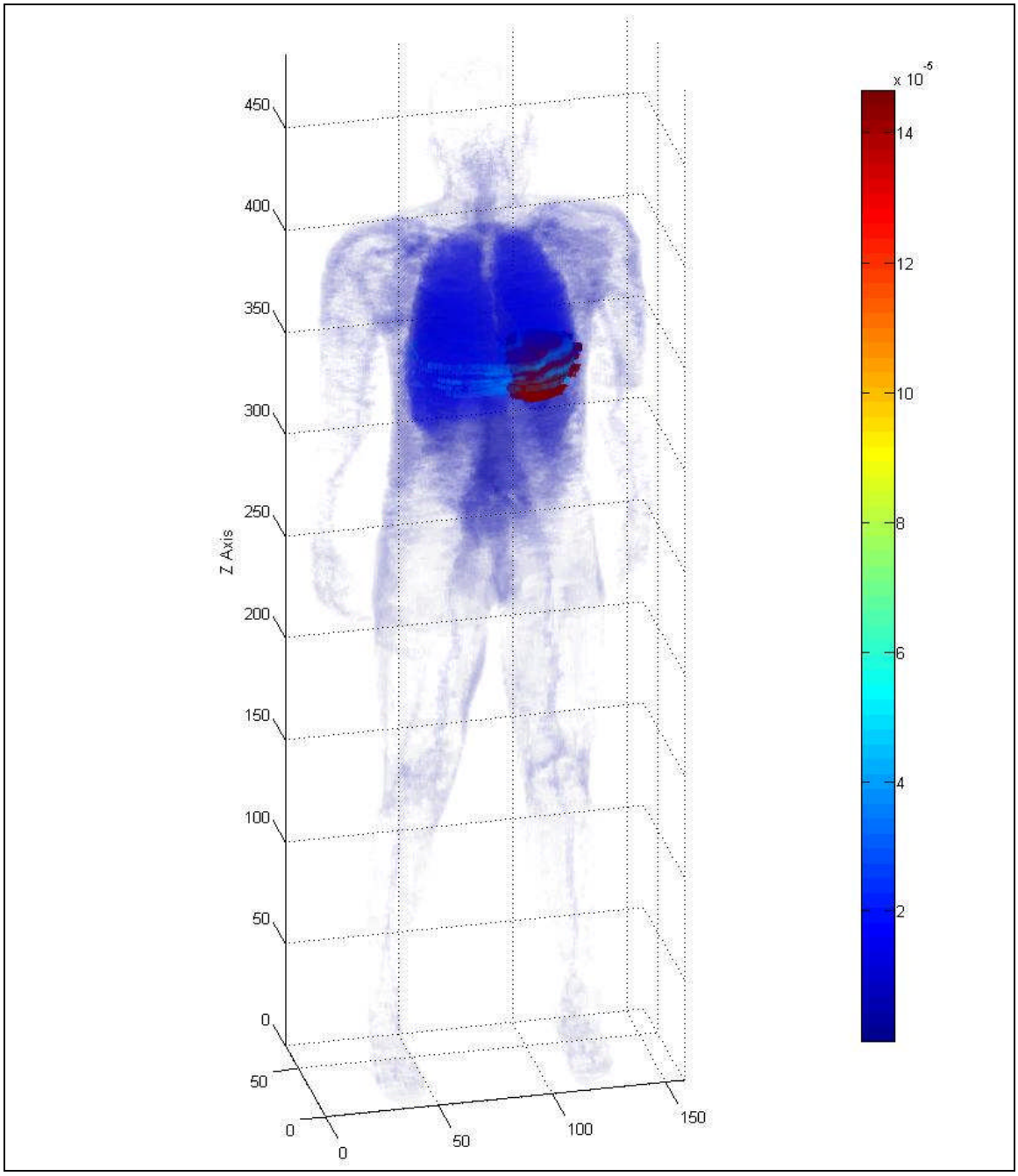

Fig. 13.2. Three-dimensional human dose profile from a Cs-137 photon source located within the stomach.

Table 13.3. Organ doses for an Ir-192 volume source in the stomach.

Organs	MCNP Dose (MeV/g)	Std Deviation	MCNP Wght (g)	En Dep (MeV/his)	Organ Wt (g)	Organ Dose (MeV/g)	Organ Dose (Gy)
Skin	2.16E-04	1.73E-10	5.09E-02	1.10E-05	2830	3.89E-09	6.23E-19
Rib Bone Group	3.27E-01	1.09E-08	6.58E-02	2.15E-02	2167	9.93E-06	1.59E-15
Small Int	2.15E-01	1.55E-06	4.81E-02	1.03E-02	640	1.62E-05	2.59E-15
Gonads	7.83E-05	1.01E-07	4.85E-02	3.80E-06	37.1	1.02E-07	1.64E-17
Rectum	5.97E-04	5.84E-07	4.90E-02	2.93E-05	63	4.64E-07	7.44E-17
Thyroid	1.34E-03	1.77E-06	4.90E-02	6.55E-05	19.6	3.34E-06	5.35E-16
Lung	1.27E+00	6.94E-07	1.21E-02	1.54E-02	999	1.54E-05	2.46E-15
Eyes	8.72E-05	5.44E-08	4.90E-02	4.27E-06	15	2.85E-07	4.56E-17
Trachea	3.33E-03	6.52E-06	4.90E-02	1.63E-04	10	1.63E-05	2.61E-15
Colon	7.82E-02	1.28E-06	4.90E-02	3.83E-03	369	1.04E-05	1.66E-15
Stomach	1.47E+00	7.52E-06	4.90E-02	7.18E-02	150	4.79E-04	7.67E-14

As expected, the organ dose was driven by the two photons over the two electrons by a factor of 100 or greater. Compared to the Co-60 and Cs-137 organ dose, the most sensitive organs for Ir-192 were the stomach, small intestine, lung, trachea and colon. The dose to the stomach is slightly greater than the Cs-137 stomach dose. The sum of the two Ir-192 photons dose is comparable to the dose from the energy of the Cs-137 photon.

Statistical checks on the Ir-192 Dose output file were performed. The same warnings present with Co-60 were observed. The 10 statistical checks for tally-four fluence passed and produced similar results. The 10 statistical checks for tally-six dose passed and produced similar results as with Co-60. Of the 61 tally bins, no bins contained a zero dose and 10 bins had relative errors exceeding 0.10 for the 0.47 MeV photon. The 0.32 MeV photon produced similar results with the exception that the testes did not exceed the relative error of 0.10.

The tallies for the electron sources in the stomach had to be evaluated in a slightly different manner based on their lack of ability to penetrate uniformly throughout the phantom. Secondary emissions, such as bremsstrahlung and characteristics x rays and delta rays were the primary radiation source for organs outside of the stomach. Three of the 10 statistical checks did not pass. The relative error was 0.49, the VoV was

0.30 and the pdf was 0. This reflects a large number of zero doses and slightly greater than zero doses based on the volume electron source in the stomach. For the electron source, only the selected organs were reviewed for their relative error.

Figures 13.3 and 13.4 provide a simulated 3 dimensional view of the human body with a color profile that equates to the MCNP dose for the 0.47 MeV photon of Ir-192 and the 0.66 MeV of Ir-192 absorbed by each organ, respectively. The color bar units to the right of the phantom are in MeV/organ weight in grams.

Sr-90 organ dose profile

A Sr-90 source located within the stomach would deliver a dose to the selected organs that ranges from a high of 2.21 x 10^{-6} MeV/g for the stomach and a low of 4.06 x 10^{-12} MeV/g for the skin. This organ dose contribution is from a single beta radiation with a maximum energy of 0.55 MeV. The beta radiation is produced with a yield of about 100%. Table 13.4 provides the calculated dose conversions for each of the selected organs that will be considered in this problem.

Table 13.4. Organ doses from a Sr-90 volume source in the stomach.

Organs	MCNP Dose (MeV/g)	Std Deviation	MCNP Wght (g)	En Dep (MeV/his)	Organ Wt (g)	Organ Dose (MeV/g)	Organ Dose (Gy)
Skin	2.26E-07	8.98E-14	5.09E-02	1.15E-08	2830	4.06E-12	6.51E-22
Rib Bone Group	1.06E-03	3.53E-11	6.58E-02	6.96E-05	2167	3.21E-08	5.14E-18
Small Int	3.03E-04	1.00E-09	4.81E-02	1.46E-05	640	2.28E-08	3.65E-18
Gonads	0.00E+00	0.00E+00	4.85E-02	0.00E+00	37.1	0.00E+00	0.00E+00
Rectum	5.81E-07	2.02E-10	4.90E-02	2.85E-08	63	4.52E-10	7.24E-20
Thyroid	1.91E-06	1.46E-09	4.90E-02	9.38E-08	19.6	4.78E-09	7.66E-19
Lung	2.34E-03	6.22E-10	1.21E-02	2.84E-05	999	2.84E-08	4.55E-18
Eyes	0.00E+00	0.00E+00	4.90E-02	0.00E+00	15	0.00E+00	0.00E+00
Trachea	4.52E-06	4.89E-09	4.90E-02	2.21E-07	10	2.21E-08	3.55E-18
Colon	1.12E-04	9.40E-10	4.90E-02	5.47E-06	369	1.48E-08	2.38E-18
Stomach	6.78E-03	1.66E-08	4.90E-02	3.32E-04	150	2.21E-06	3.55E-16

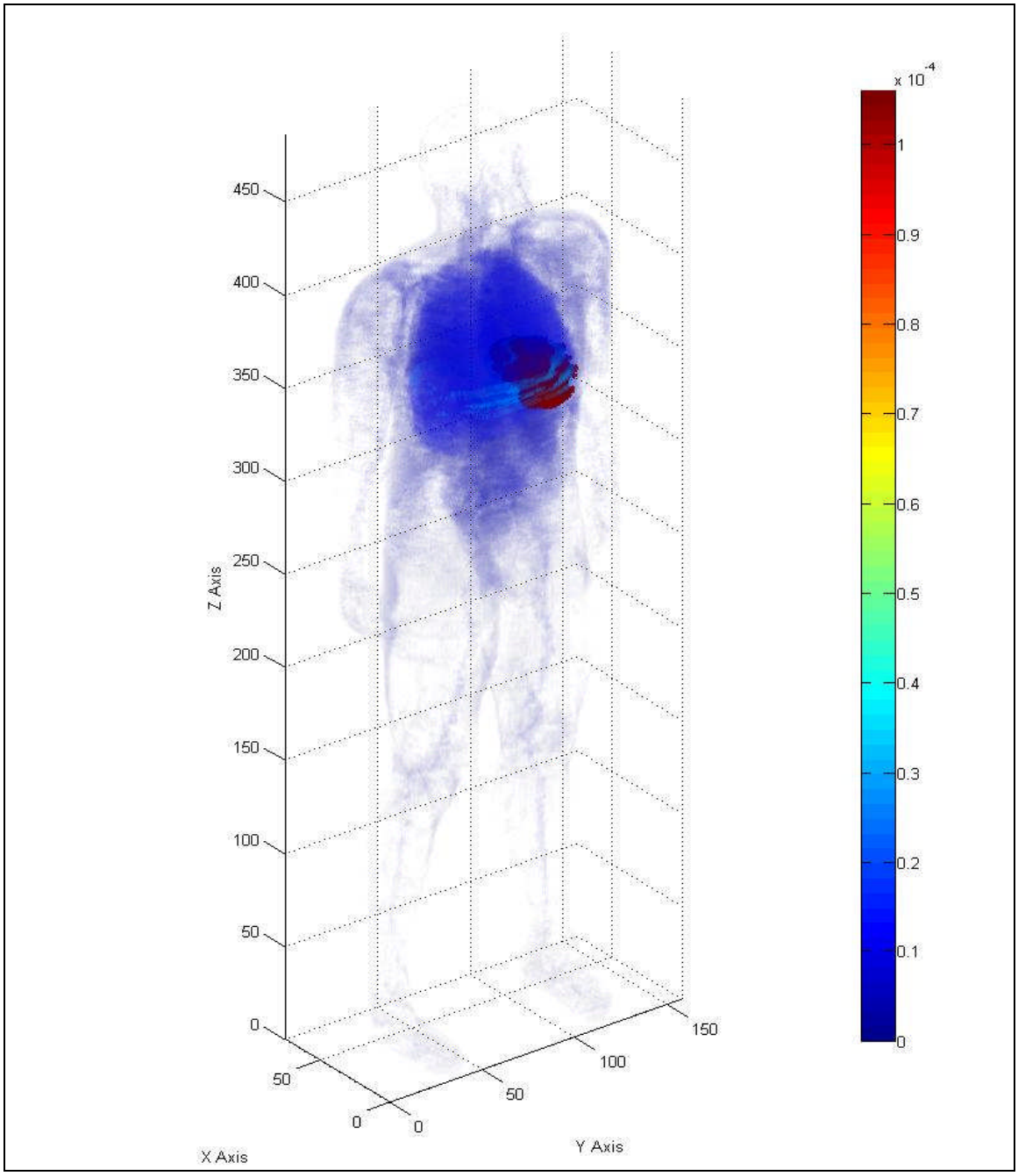

Fig. 13.3. Three-dimensional human dose profile from the 0.47 MeV Ir-192 photon source located within the stomach.

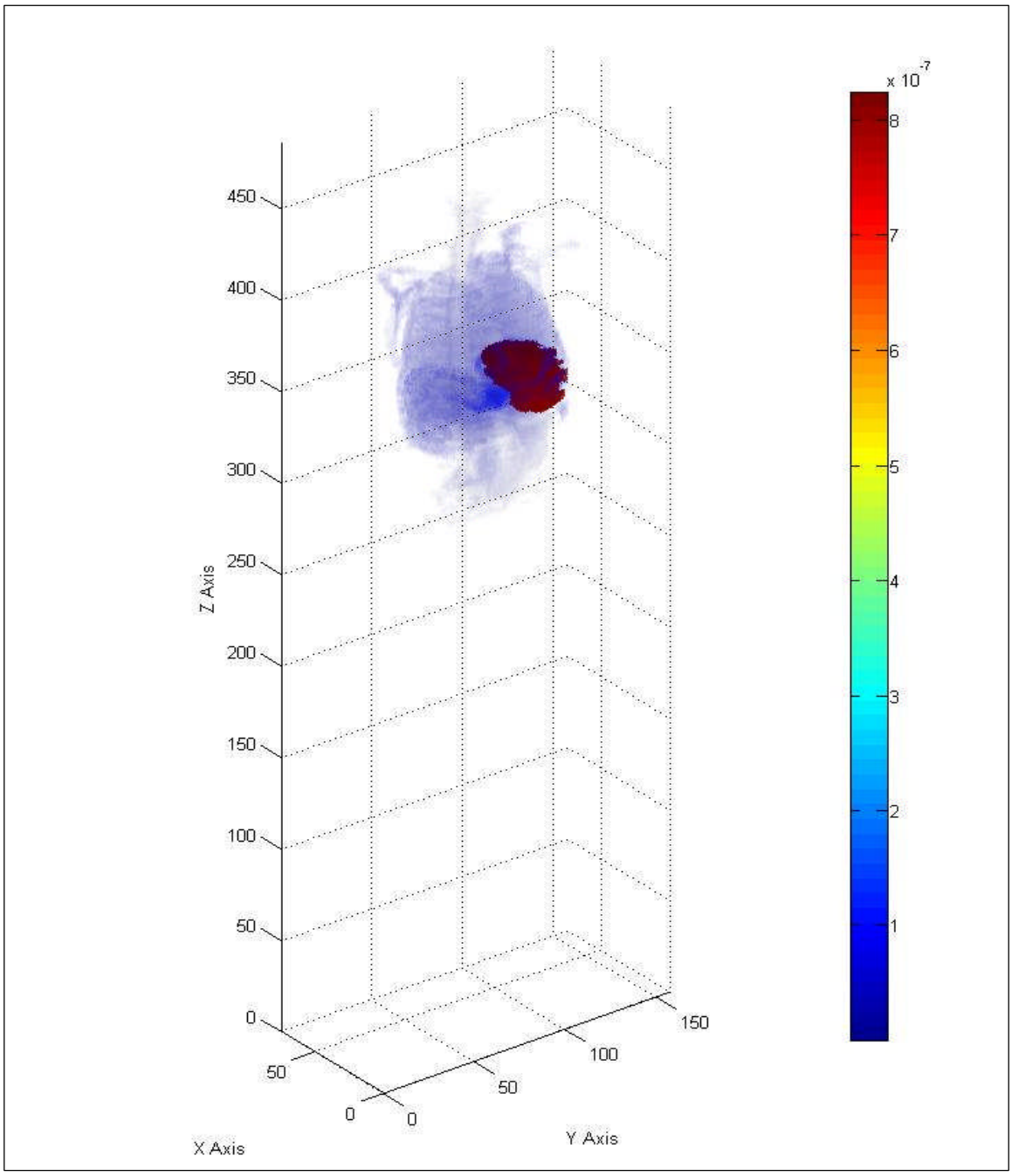

Fig. 13.4. Three-dimensional human dose profile from the 0.66 MeV Ir-192 electron source located within the stomach.

As expected, the stomach received the greatest dose from a moderately energetic beta radiation source located within the stomach. The lung, small intestine and colon received a dose that was 100 times smaller than the dose to the stomach.

Statistical checks on the Sr-90 dose output file were performed. The same warnings present with Co-60 were observed. The 10 statistical checks for tally-four fluence missed three of the 10 checks. The relative error was 0.38, VoV was 0.25 and the pdf was 0. The 10 statistical checks for tally-six passed. Of the 61 tally bins, 11 bins had a zero dose and 27 bins had relative errors exceeding 0.10 for the 0.55 MeV beta radiation. Figure 13.5 provides a simulated 3-dimensional view of the human body with a color profile that shows the MCNP dose for the beta radiation of Sr-90 absorbed by each organ. The color bar units to the right of the phantom are in MeV/organ weight in grams.

Y-90 organ dose profile

A Y-90 source located within the stomach would deliver a dose to the selected organs that ranges from a high of 1.70×10^{-5} MeV/g for the stomach and a low of 9.00×10^{-11} MeV/g for the skin. This organ dose contribution is from a single beta radiation with a maximum energy of 2.28 MeV. The beta radiation is produced with a yield of about 100%. The energy dose and relative errors are provided in Table 13.5.

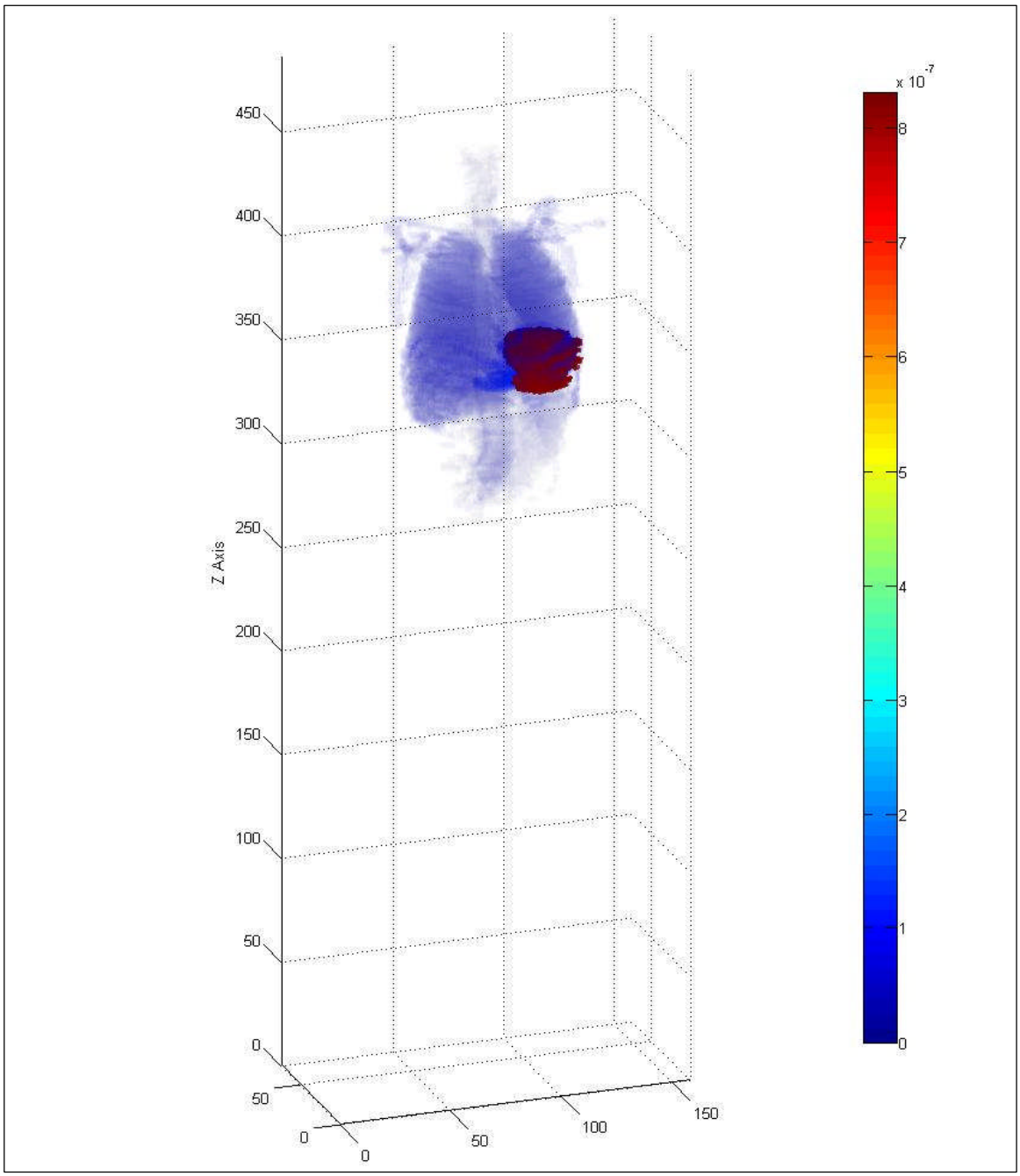

Fig. 13.5. Three-dimensional human dose profile from a Sr-90 beta source located within the stomach.

Table 13.5. Organ doses from a Y-90 volume source in the stomach.

Organs	MCNP Dose (MeV/g)	Std Deviation	MCNP Wght (g)	En Dep (MeV/his)	Organ Wt (g)	Organ Dose (MeV/g)	Organ Dose (Gy)
Skin	5.01E-06	7.65E-13	5.09E-02	2.55E-07	2830	9.00E-11	1.44E-20
Rib Bone Group	1.18E-02	3.95E-10	6.58E-02	7.78E-04	2167	3.59E-07	5.75E-17
Small Int	5.36E-03	7.60E-09	4.81E-02	2.57E-04	640	4.02E-07	6.44E-17
Gonads	8.63E-07	5.29E-10	4.85E-02	4.19E-08	37.1	1.13E-09	1.81E-19
Rectum	1.74E-05	2.77E-09	4.90E-02	8.50E-07	63	1.35E-08	2.16E-18
Thyroid	3.29E-05	8.47E-09	4.90E-02	1.61E-06	19.6	8.24E-08	1.32E-17
Lung	3.45E-02	3.68E-09	1.21E-02	4.18E-04	999	4.19E-07	6.71E-17
Eyes	9.38E-07	1.28E-09	4.90E-02	4.59E-08	15	3.06E-09	4.91E-19
Trachea	7.90E-05	3.22E-08	4.90E-02	3.87E-06	10	3.87E-07	6.20E-17
Colon	1.82E-03	5.76E-09	4.90E-02	8.90E-05	369	2.41E-07	3.86E-17
Stomach	5.22E-02	7.33E-08	4.90E-02	2.56E-03	150	1.70E-05	2.73E-15

As with Sr-90, the stomach received the highest dose from a highly-energetic, beta radiation source located within the stomach. The small intestine, trachea, lung and colon, due to their close proximity to the source organ, received approximately one percent of the dose absorbed by the stomach. The Y-90 stomach dose was approximately 10 times greater than the dose delivered by the Sr-90 beta radiation even though the energy of the Y-90 beta radiation was approximately 4 times greater than the Sr-90. The difference in dose is attributed to the difference in energy dependent stopping power as well as the energy and type of secondary radiations.

Statistical checks on the Y-90 Dose output file were performed. The same warnings present with Co-60 were observed. The 10 statistical checks for tally-four fluence passed all but two checks. The relative error was 0.16 and the pdf was 0. The 10 statistical checks for tally-six dose passed. Of the 61 tally bins, no bins had a zero dose and 33 bins had relative errors exceeding 0.10 for the 2.28 MeV beta radiation. Figure 13.6 provides a simulated 3-dimensional view of the human body with a color profile that shows the MCNP organ dose for an Y-90 source in the stomach. The color bar units to the right of the phantom are in MeV/organ weight in grams.

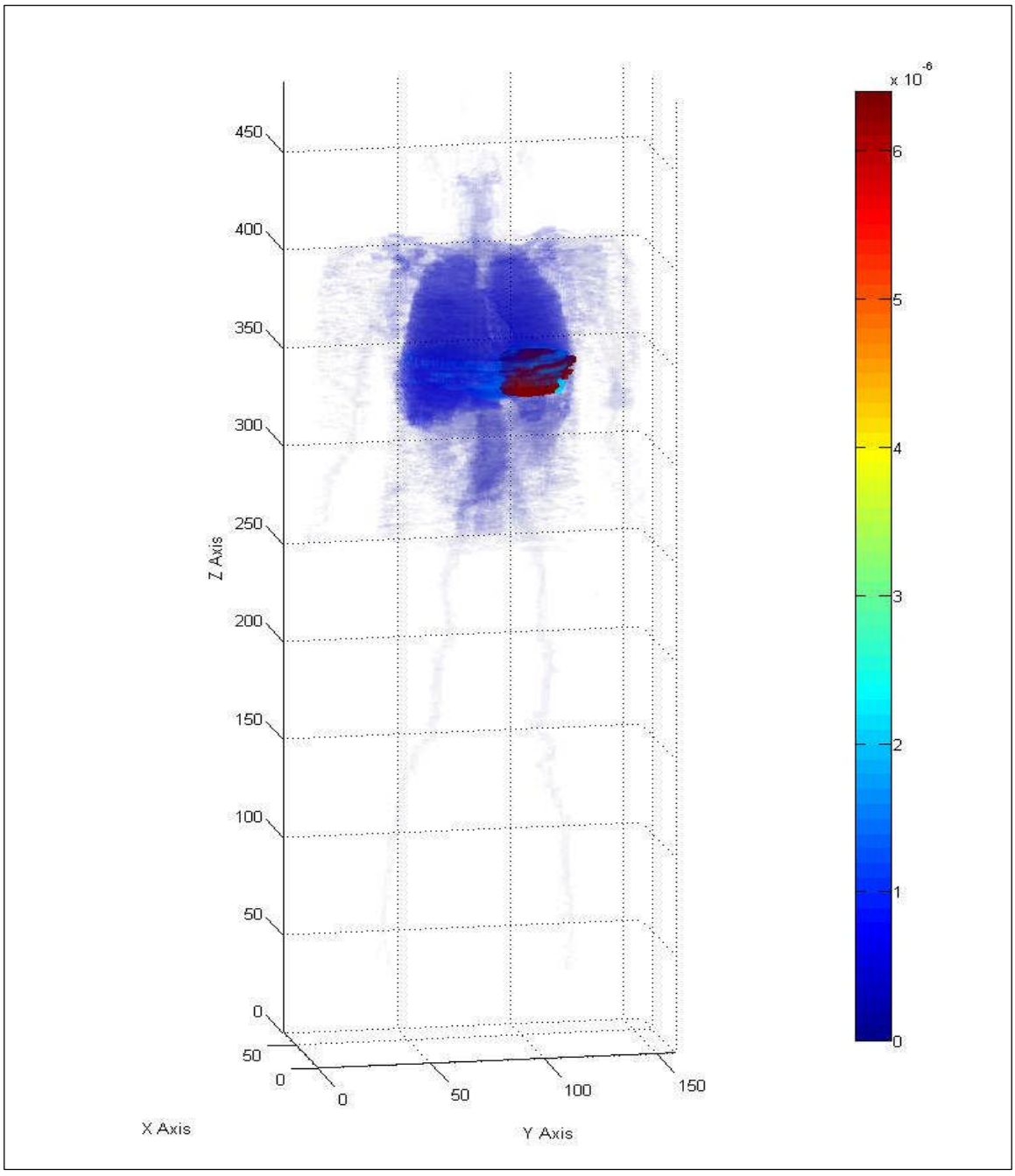

Fig. 13.6. Three-dimensional human dose profile from a Y-90 beta source located within the stomach.

Results from stomach volume source

Figure 13.7 provides a graph of all of the potential sources distributed in the stomach and their organ doses. Based upon the results of the observed programs, Co-60 is the most limiting radionuclide. The stomach and lungs appear to be the most sensitive organs based upon a single decay from a source located within the stomach. Even though the trachea shows a higher sensitivity than the lung, the dose is a little deceiving. The observed dose for the trachea is based on the number of voxels which include the air encircled by the trachea. The actual dose, based on the weight of the organ, is less than the dose for the lung. The dose to all of the selected organs from Sr-90 and Y-90 appears to be almost 100 times lower than the other three radionuclides. Ir-192 and Cs-137 appear to deliver an almost identical dose to the selected organs.

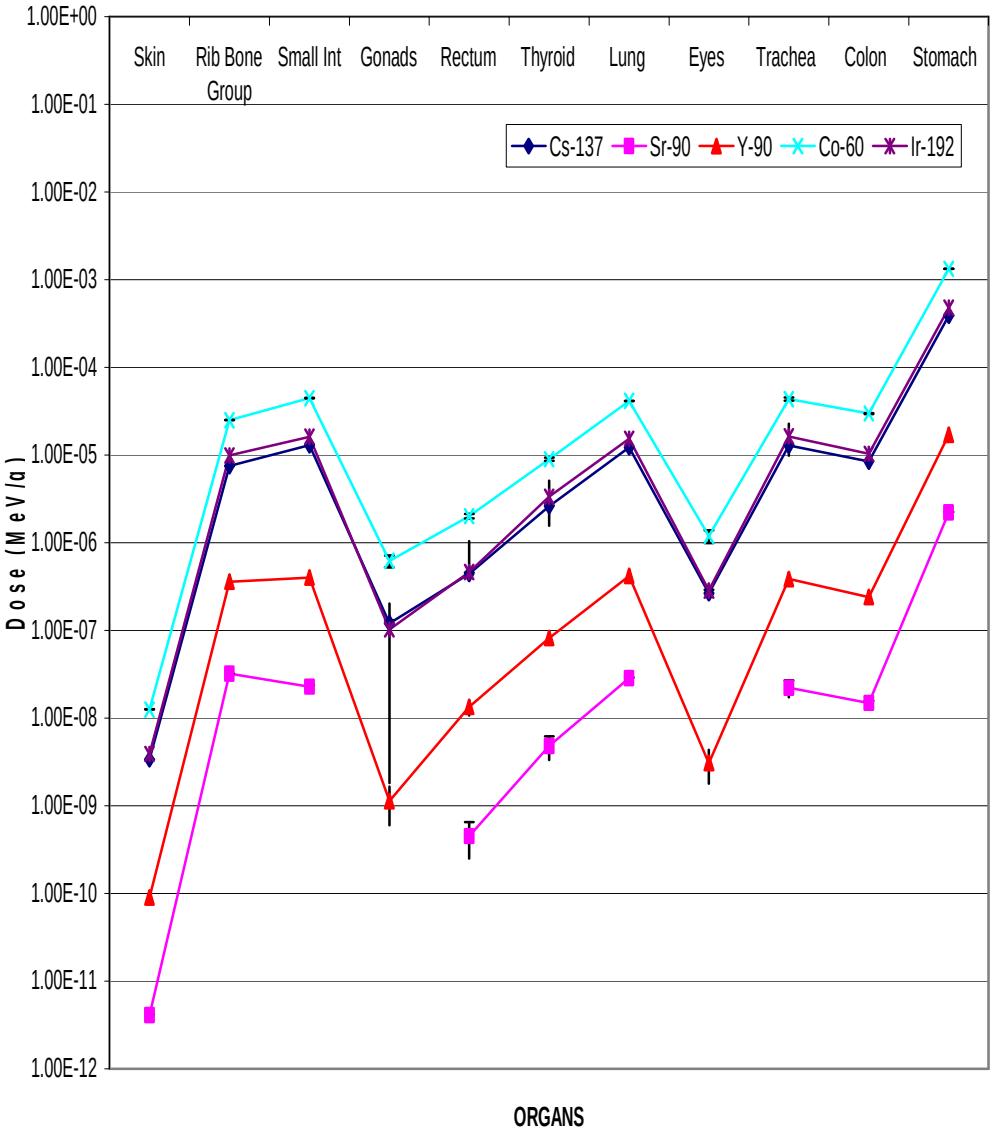

Fig. 13.7. Summary graph of organ doses for the five potential stomach sources.

CHAPTER XIV
ESTIMATING ORGAN DOSE BASED ON VOLUME SOURCE IN THE COLON

Organ data verification

The number of source voxels for additional organs will be based on the ratio of MAX lung source voxels divided by the total number of MAX lung voxels. This fraction will than be multiplied by the total number of organ voxels to determine the number of source voxels in the organ. Based on the lung fraction, the number of sources calculated for the colon was 2,379. This number would represent a volume source based on the dimension of the colon. Volumes and masses were checked against ICRU-46 established values for both simulations (ICRU 1990). Using the values from Table A-2 of Appendix A, the hand calculated colon volume was 578.11 cm^3, the volume of a single voxel was 4.67 x 10^{-2} cm^3 (Kramer 2003). According to figure A-1 of Appendix A, the MCNPX code calculated a volume of 4.67 x 10^{-2} cm^3 for a single voxel. The hand calculated mass of the colon was 590 g and the mass per voxel was 4.76 x 10^{-2} g which includes the stomach and its contents. The stomach alone weighs 370g and the mass per voxel would be 2.99 x 10^{-2}g. Based on Figure A-1 of Appendix A, the code calculated a mass of 4.90 x 10^{-2} g in a single voxel. Therefore, the phantom colon provided a good simulation that was representative of standard man.

Co-60 organ dose profile

A Co-60 source located within the colon would deliver a dose to the selected organs that ranges from a high of 4.81 x 10^{-4} MeV/g for the colon and a low of 1.22 x 10^{-8} MeV/g for the skin. This organ dose contribution is the sum of two photons emitted from Co-60 that occur with a yield of about 100 percent. Table 14.1 provides the calculated dose conversions for each of the selected organs that will be considered in this problem.

Table 14.1. Organ doses from a Co-60 volume source in the colon.

Organs	MCNP Dose (MeV/g)	Std Deviation	MCNP Wght (g)	En Dep (MeV/his)	Organ Wt (g)	Organ Dose (MeV/g)	Organ Dose (Gy)
Skin	3.19E-04	6.89E-12	5.09E-02	1.62E-05	2830	5.74E-09	9.20E-19
Rib Bone Group	1.43E-01	1.17E-08	6.58E-02	9.39E-03	2167	4.33E-06	6.94E-16
Small Int	6.70E-01	1.21E-07	4.81E-02	3.22E-02	640	5.03E-05	8.06E-15
Gonads	1.02E-03	4.82E-08	4.85E-02	4.97E-05	37.1	1.34E-06	2.15E-16
Rectum	1.13E-02	1.00E-07	4.90E-02	5.53E-04	63	8.78E-06	1.41E-15
Thyroid	5.41E-04	5.60E-08	4.90E-02	2.65E-05	19.6	1.35E-06	2.17E-16
Lung	3.12E-01	1.67E-08	1.21E-02	3.78E-03	999	3.79E-06	6.07E-16
Eyes	8.05E-05	3.35E-08	4.90E-02	3.94E-06	15	2.63E-07	4.21E-17
Trachea	1.28E-03	2.36E-07	4.90E-02	6.27E-05	10	6.27E-06	1.00E-15
Colon	1.72E+00	2.06E-07	4.90E-02	8.45E-02	369	2.29E-04	3.67E-14
Stomach	6.84E-02	1.43E-07	4.90E-02	3.35E-03	150	2.23E-05	3.58E-15

As expected, the largest dose concentration is to the organs in the immediate vicinity of the colon which includes the small intestine and stomach. The dose to the skin is smaller than the dose to the colon by a factor of 10,000. The assumption applied to the skin dose is that the dose is uniform across the entire volume of skin. The actual skin dose is delivered on a gradient depending upon the distance from the source as well as the amount and type of material between the source and the skin.

Statistical analysis of output file

The tally-four fluence analysis for each detector setup, as described in chapter VII, provided a random behavior for the mean. The desired relative error should be less than 0.10 and the observed relative error was 0.08. The desired and observed relative errors decreased according to the inverse of the square root of the number of histories. The desired variance of the variance should be less than 0.10 and the observed VoV was 0.02. The figure of merit value was constant and the behavior was random. The probability density function (pdf) desired should be greater than three, the observed pdf value was 0. There was insufficient tfc bin tally information to estimate the large tally

slope reliably. The tally-four fluence passed all 10 statistical checks except the pdf. Out of 10 tally-four bins, one had a zero value and no bins contained relative errors greater than 0.10. The second 1.33 MeV photon simulation provided similar results.

The tally-six dose analysis for each material showed a random behavior for the mean. The desired relative error should be less than 0.10 and the observed relative error was 0.00 for both photons. The desired and observed relative error decreased at a rate of inverse square root of the number of histories. The desired variance of the variance should be less than 0.10 and the observed VoV was 0.00. The figure of merit value was constant and the behavior was random. The desired probability density function (pdf) should be greater than 3.00 and the observed value was 10.0 for both photons. The tally-six dose passed all 10 statistical checks. Out of 61 tally-six bins, no bin had a zero value and only 11 bins contained relative errors greater than 0.10.

Figure 14.1 provides a simulated 3-dimensional view of the human body with a color profile that equates to the organ dose for the 1.33 MeV photon of Co-60. The color bar units to the right of the phantom are in MeV/organ weight in grams. Each axis is represented in the figure along with a color bar that indicates the organ dose in MeV/g provided by the MCNPX output file. In the MCNPX output file, the colon receives the highest dose followed by the small intestine. The dose to the colon is roughly 5 times that of the small intestine. The stomach and trachea are closely matched.

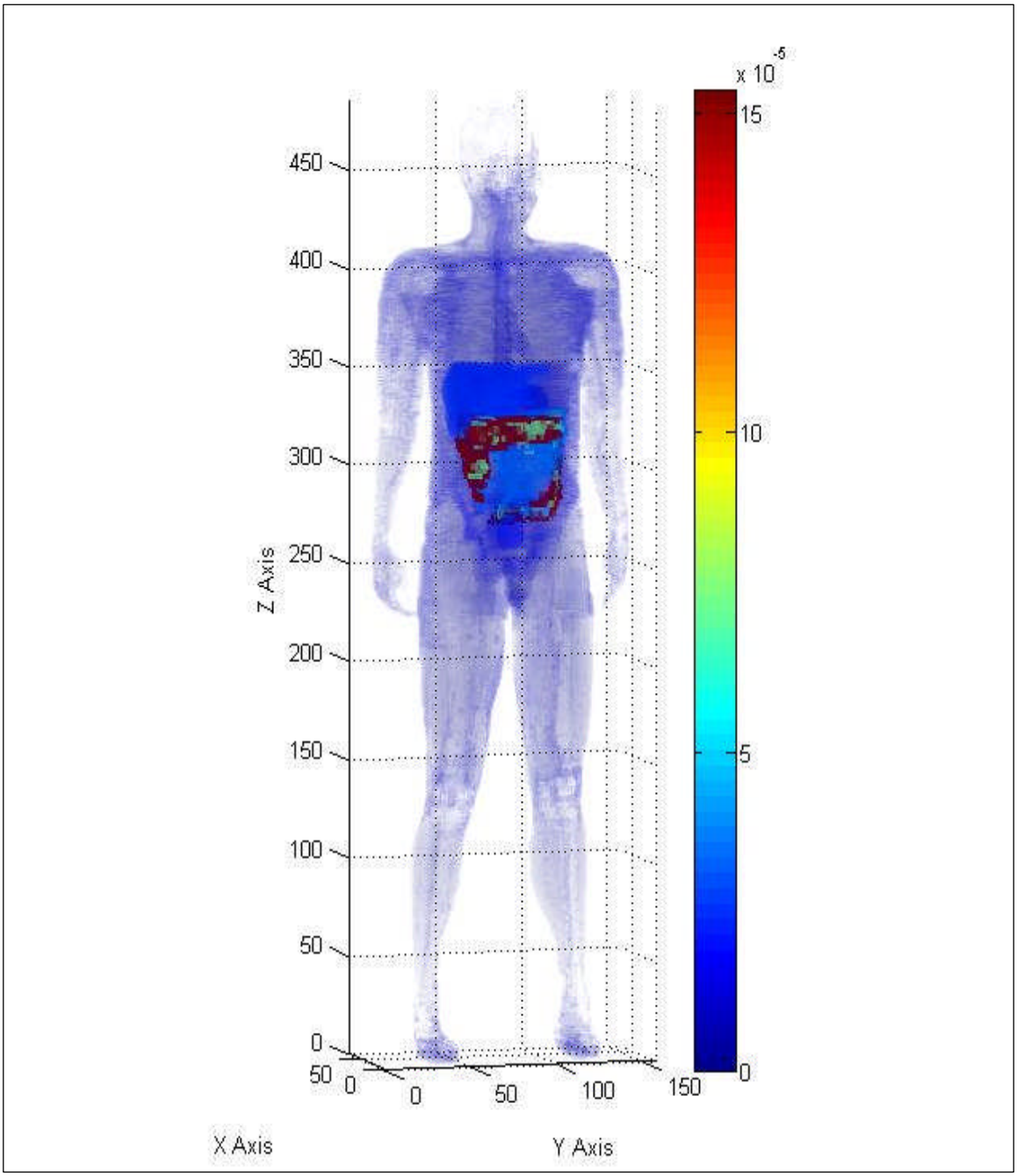

Fig. 14.1. Three-dimensional human dose profile from a 1.33 MeV photon source located within the colon.

Cs-137 organ dose profile

A Cs-137 source located within the colon would deliver a dose to the selected organs that ranges from a high of 1.42 x 10^{-4} MeV/g for the colon and a low of 3.25 x 10^{-9} MeV/g for the skin. This organ dose contribution is from 0.66 MeV photon emitted from Cs-137 that occurs with a yield of about 86 percent. Table 14.2 provides the dose output to the selected organs from the 0.66 MeV photon.

Table 14.2. Organ doses for a Cs-137 volume source in the colon.

Organs	MCNP Dose (MeV/g)	Std Deviation	MCNP Wght (g)	En Dep (MeV/his)	Organ Wt (g)	Organ Dose (MeV/g)	Organ Dose (Gy)
Skin	3.59E-04	7.75E-12	5.09E-02	1.83E-05	2830	6.46E-09	1.03E-18
Rib Bone Group	1.59E-01	1.30E-08	6.58E-02	1.05E-02	2167	4.83E-06	7.73E-16
Small Int	7.40E-01	1.33E-07	4.81E-02	3.55E-02	640	5.55E-05	8.90E-15
Gonads	1.19E-03	5.50E-08	4.85E-02	5.78E-05	37.1	1.56E-06	2.50E-16
Rectum	1.25E-02	1.11E-07	4.90E-02	6.12E-04	63	9.72E-06	1.56E-15
Thyroid	5.92E-04	6.23E-08	4.90E-02	2.90E-05	19.6	1.48E-06	2.37E-16
Lung	3.49E-01	1.86E-08	1.21E-02	4.23E-03	999	4.24E-06	6.79E-16
Eyes	1.02E-04	4.10E-08	4.90E-02	5.02E-06	15	3.35E-07	5.36E-17
Trachea	1.37E-03	2.59E-07	4.90E-02	6.70E-05	10	6.70E-06	1.07E-15
Colon	1.90E+00	2.27E-07	4.90E-02	9.31E-02	369	2.52E-04	4.04E-14
Stomach	7.63E-02	1.59E-07	4.90E-02	3.74E-03	150	2.49E-05	3.99E-15

As expected, the dose to the selected organs is similar to the dose produced by the Co-60 photons. The largest dose concentration remains with organs in the immediate vicinity of the colon. The colon dose from Cs-137 is reduced by approximately a factor of two compared to the colon dose from the 1.17 MeV photon from Co-60. This reduction is expected based on the energy reduction between the low-energy Co-60 photon and that of Cs-137.

Statistical checks were performed on the Cs-137 Dose output file. The same warnings present with Co-60 were observed. The 10 statistical checks for tally-four fluence passed with the exception of the pdf. There was insufficient tfc bin tally information to estimate the large tally slope reliably. The 10 statistical checks for tally-

six dose passed and produced similar results as with Co-60. Of the 61 tally bins, no bins contained zero dose and 11 bins had relative errors exceeding 0.10. Figure 11.2 provides a simulated 3-dimensional view of the human body with a color profile that shows the MCNP dose for the single photon of Cs-137. The color bar units to the right of the phantom are in MeV/organ weight in grams.

The Co-60 colon dose was 2.29×10^{-4} MeV/g for the 1.17 MeV photon compared with the Cs-137 colon dose of 1.42×10^{-4} MeV/g for the 0.66 MeV photon. As expected, the dose profile is similar to that of the photons emitted by Co-60. The dose to each individual organ is proportionally reduced based on the lower-energy of the source photon and the energy dependent stopping power of the material within the phantom.

Ir-192 organ dose profile

An Ir-192 source located within the colon would deliver a dose to the selected organs that ranges from a high of 7.38×10^{-5} MeV/g for the colon and a low of 3.03×10^{-9} MeV/g for the skin. This organ dose contribution is the sum of two photons with energies of 0.47 MeV and 0.32 MeV along with two electrons with maximum energies of 0.66 MeV and 0.54 MeV. All four emissions are produced with a yield of 26.2%, 22.4%, 10.1% and 6.7%, respectively. Table 14.3 provides the calculated dose conversions for each of the selected organs.

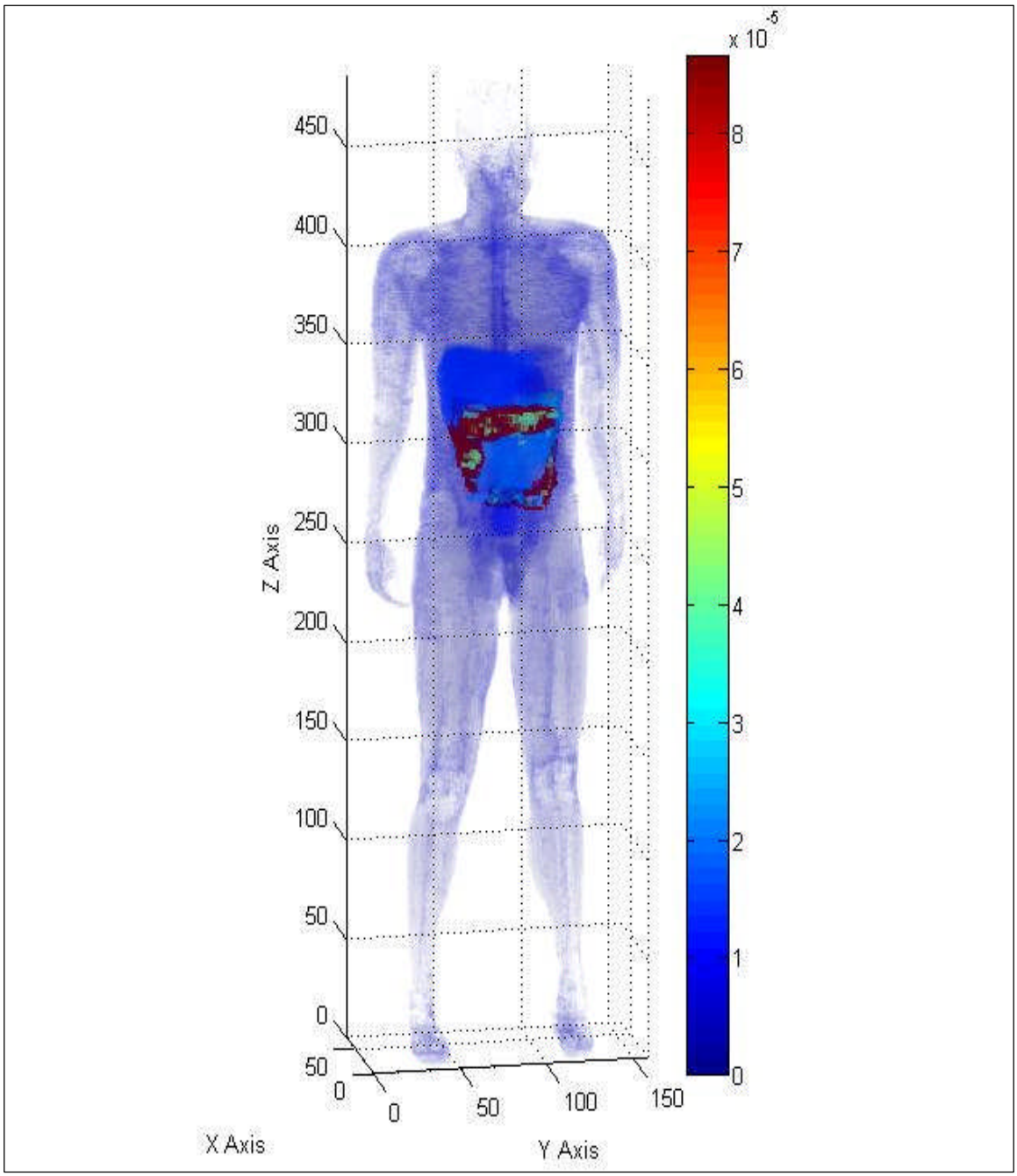

Fig. 14.2. Three-dimensional human dose profile from a Cs-137 photon source located within the colon.

Table 14.3. Organ doses for an Ir-192 volume source in the colon.

Organs	MCNP Dose (MeV/g)	Std Deviation	MCNP Wght (g)	En Dep (MeV/his)	Organ Wt (g)	Organ Dose (MeV/g)	Organ Dose (Gy)
Skin	8.69E-05	1.87E-12	5.09E-02	4.42E-06	2830	1.56E-09	2.50E-19
Rib Bone Group	2.51E-01	8.37E-09	6.58E-02	1.65E-02	2167	7.60E-06	1.22E-15
Small Int	3.04E-01	5.26E-08	4.81E-02	1.46E-02	640	2.29E-05	3.66E-15
Gonads	1.03E-05	2.15E-09	4.85E-02	5.01E-07	37.1	1.35E-08	2.16E-18
Rectum	8.84E-05	4.27E-09	4.90E-02	4.33E-06	63	6.87E-08	1.10E-17
Thyroid	3.22E-03	8.54E-08	4.90E-02	1.58E-04	19.6	8.06E-06	1.29E-15
Lung	1.48E+00	1.26E-08	1.21E-02	1.79E-02	999	1.80E-05	2.88E-15
Eyes	6.85E-05	1.49E-08	4.90E-02	3.36E-06	15	2.24E-07	3.58E-17
Trachea	7.87E-03	2.81E-07	4.90E-02	3.86E-04	10	3.86E-05	6.18E-15
Colon	1.24E-02	1.30E-08	4.90E-02	6.09E-04	369	1.65E-06	2.65E-16
Stomach	4.70E-02	6.29E-08	4.90E-02	2.30E-03	150	1.53E-05	2.46E-15

As expected, the organ dose was driven by the two photons over the two electrons by a factor of 100 or greater. Compared to the Co-60 and Cs-137 organ dose, the most sensitive organs for Ir-192 were the colon, small intestine and trachea. The dose to the colon is slightly less than the dose to the colon from Cs-137. The sum of the two Ir-192 photons is comparable to the energy of the single 0.66 MeV Cs-137 photon.

Statistical checks on the Ir-192 photon dose output file were performed. The same warnings present with Co-60 were observed. The 10 statistical checks for tally-four fluence passed with the exception of the pdf. There was insufficient tfc bin tally information to estimate the large tally slope reliably. The 10 statistical checks for tally-six dose passed and produced similar results as with Co-60. Of the 61 tally bins, no bins contained a zero dose result and 11 bins had relative errors exceeding 0.10 for the 0.32 MeV photon. The 0.47 MeV photon produced similar results.

The tallies for the electron sources in the colon had to be evaluated in a slightly different manner based on their inability to penetrate throughout the entire phantom. Secondary emissions, such as bremsstrahlung and characteristics x rays were the primary radiation source for organs outside of the colon. All of the 10 tally-four fluence statistical checks passed. The relative error was 0.02, the VoV was 0.01 and the pdf was

7.50. In the case of an electron source, only the selected organs were reviewed for their relative error.

Figures 14.3 and 14.4 provide a simulated 3-dimensional view of the human body with a color profile that shows the MCNP dose for the 0.47 MeV photon of Ir-192 and the 0.66 MeV electron of Ir-192 absorbed by each organ, respectively. The color bar units to the right of the phantom are in MeV/organ weight in grams.

Sr-90 organ dose profile

A Sr-90 source located within the colon would deliver a dose to the selected organs that ranges from a high of 3.31×10^{-4} MeV/g for the colon and a low of 4.35×10^{-12} MeV/g for the skin. This organ dose contribution is from a single beta radiation with a maximum energy of 0.55 MeV. The beta radiation is produced with a yield of about 100%. Table 14.4 provides the calculated dose conversions for each of the selected organs that will be considered in this problem.

Table 14.4. Organ doses from a Sr-90 volume source in the colon.

Organs	MCNP Dose (MeV/g)	Std Deviation	MCNP Wght (g)	En Dep (MeV/his)	Organ Wt (g)	Organ Dose (MeV/g)	Organ Dose (Gy)
Skin	3.72E-07	1.27E-13	5.09E-02	1.89E-08	2830	6.69E-12	1.07E-21
Rib Bone Group	3.85E-04	3.81E-10	6.58E-02	2.53E-05	2167	1.17E-08	1.87E-18
Small Int	1.42E-03	2.22E-09	4.81E-02	6.84E-05	640	1.07E-07	1.71E-17
Gonads	9.17E-07	5.23E-10	4.85E-02	4.45E-08	37.1	1.20E-09	1.92E-19
Rectum	1.77E-05	1.64E-09	4.90E-02	8.65E-07	63	1.37E-08	2.20E-18
Thyroid	2.02E-07	3.47E-10	4.90E-02	9.90E-09	19.6	5.05E-10	8.09E-20
Lung	3.45E-04	2.41E-10	1.21E-02	4.19E-06	999	4.19E-09	6.71E-19
Eyes	0.00E+00	0.00E+00	4.90E-02	0.00E+00	15	0.00E+00	0.00E+00
Trachea	2.39E-06	3.99E-09	4.90E-02	1.17E-07	10	1.17E-08	1.88E-18
Colon	8.81E-03	7.72E-09	4.90E-02	4.31E-04	369	1.17E-06	1.87E-16
Stomach	9.94E-05	2.19E-09	4.90E-02	4.87E-06	150	3.25E-08	5.20E-18

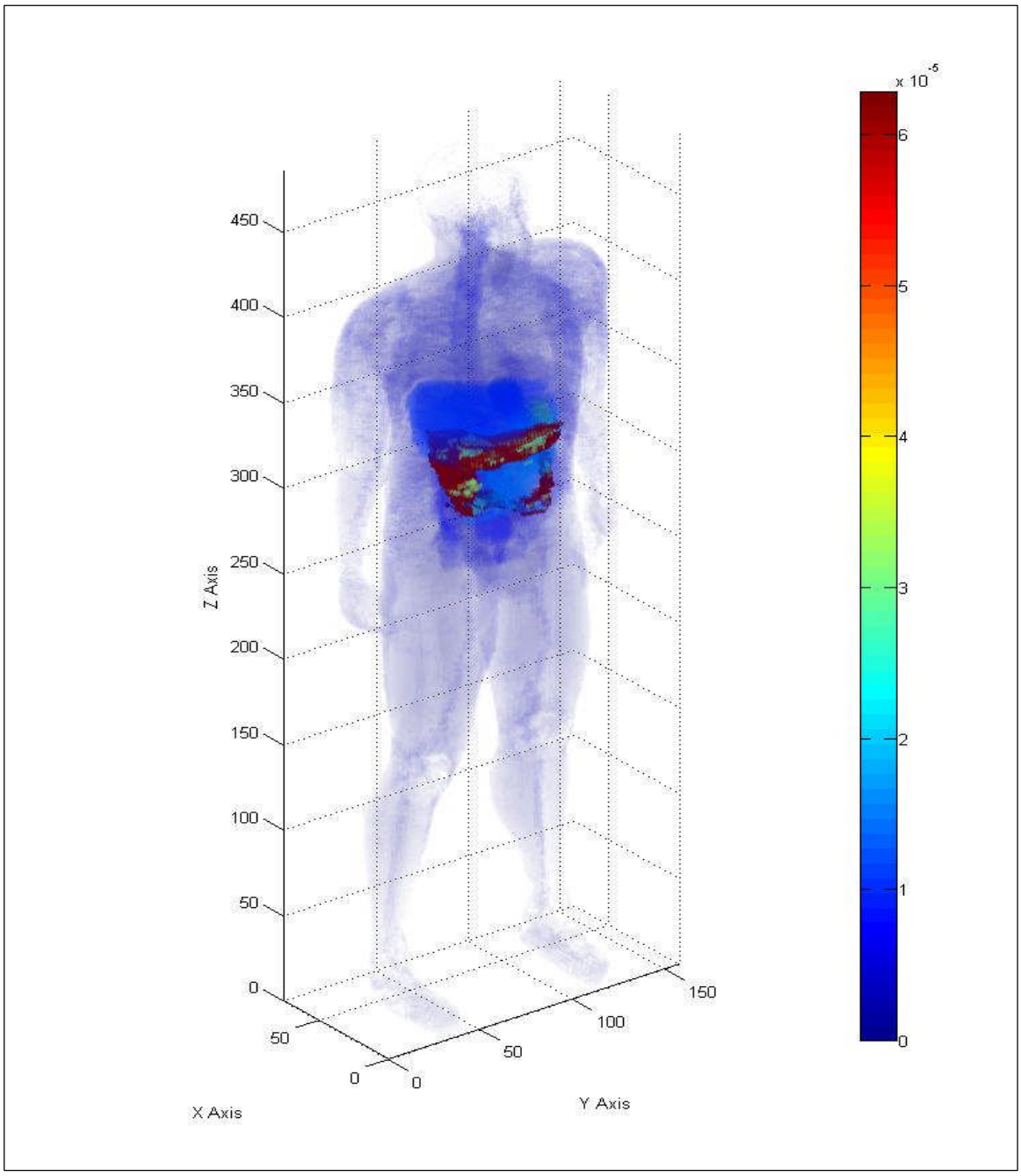

Fig. 14.3. Three-dimensional human dose profile from the 0.47 MeV Ir-192 photon source located within the colon.

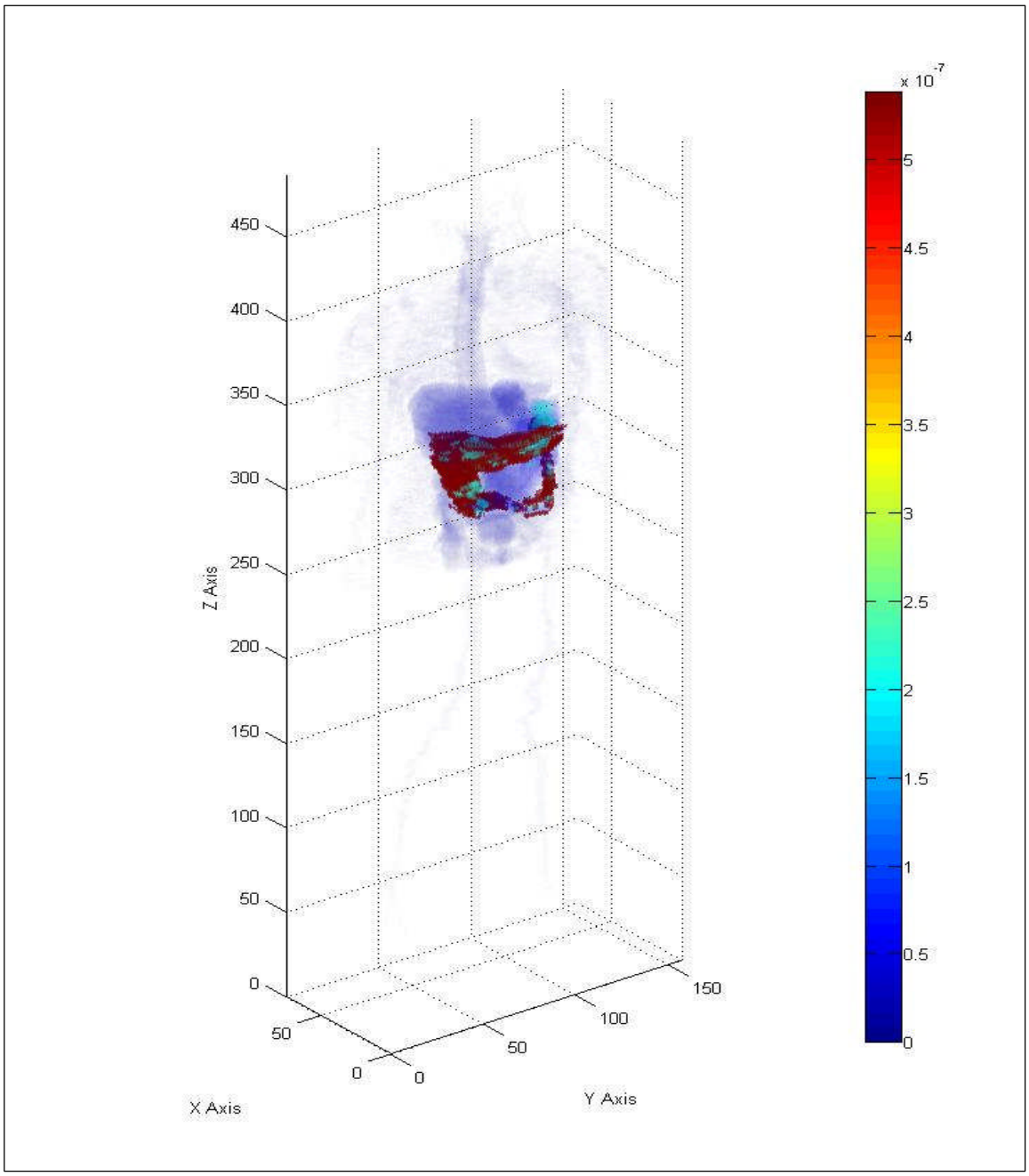

Fig. 14.4. Three-dimensional human dose profile from the 0.66 MeV Ir-192 beta source located within the colon.

As expected, the colon and small intestine received the greatest dose from a moderately energetic beta radiation source located within the colon. The stomach, due to its close proximity to the source organ received a smaller dose by a factor of 10 than the dose received by the colon.

Statistical checks on the Sr-90 dose output file were performed. The same warnings present with Co-60 were observed. No non-zero tallies were made in the tally fluctuation bin therefore no statistical checks could be made for tally-four. For tally-six, the relative error was 0.03, VoV was 0.00 and the pdf was 8.59. The 10 statistical checks for tally-six passed. Of the 61 tally bins, 20 bins had zero dose and 20 bins had relative errors exceeding 0.10 for the 0.55 MeV beta radiation. Figure 14.5 provides a simulated 3 dimensional view of the human body with a color profile that shows the MCNP dose for the beta radiation of Sr-90 absorbed by each organ. The color bar units to the right of the phantom are in MeV/organ weight in grams.

Y-90 organ dose profile

A Y-90 source located within the colon would deliver a dose to the 11 selected organs that ranges from a high of 6.41×10^{-6} MeV/g for the colon and a low of 8.59×10^{-11} MeV/g for the skin. This organ dose contribution is from a single beta radiation with a maximum energy of 2.28 MeV. The beta radiation is produced with a yield of about 100%. Table 14.5 provides the calculated dose conversions for each of the selected organs.

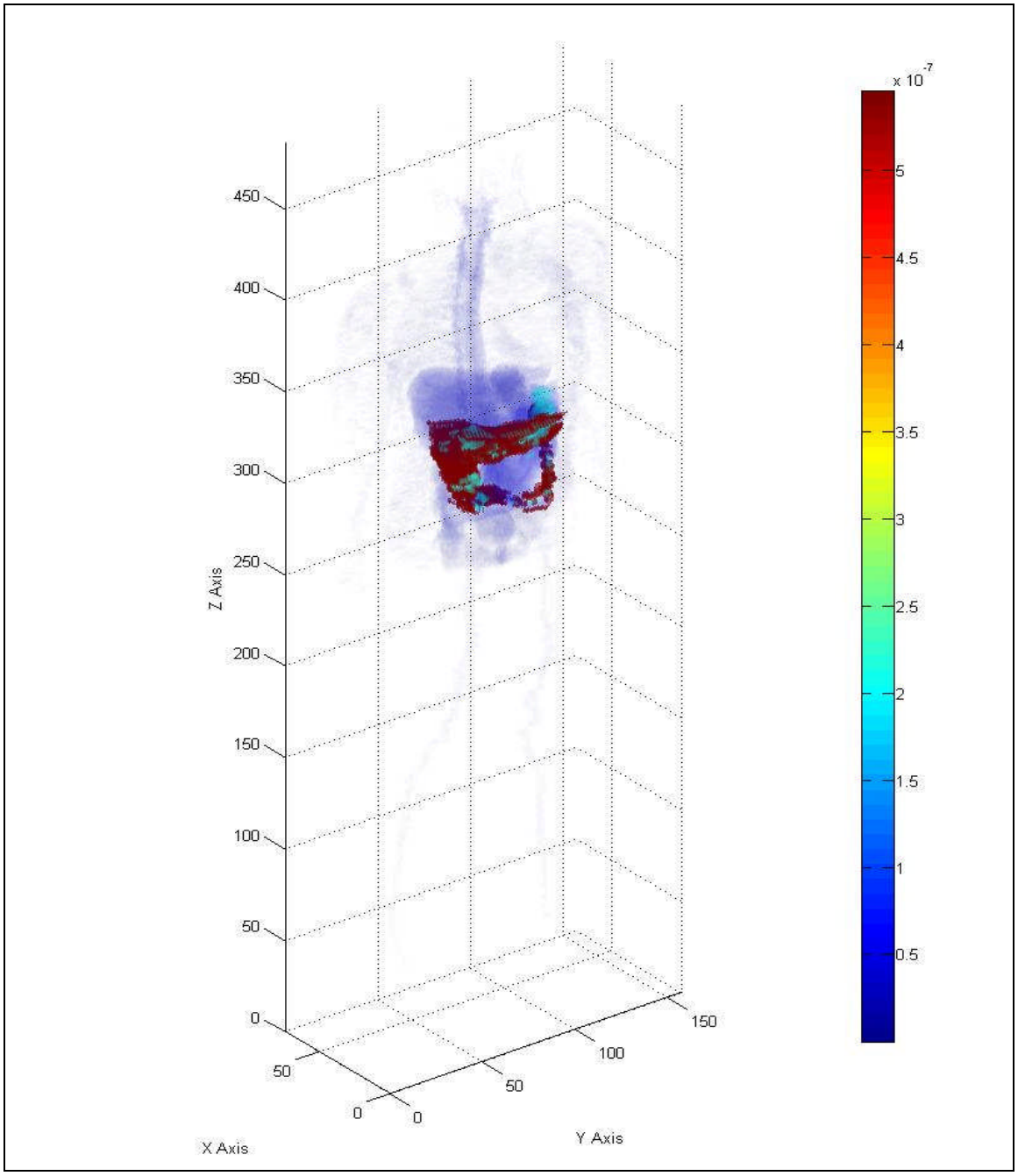

Fig. 14.5. Three-dimensional human dose profile from a Sr-90 beta source located within the colon.

Table 14.5. Organ doses from a Y-90 volume source in the colon.

Organs	MCNP Dose (MeV/g)	Std Deviation	MCNP Wght (g)	En Dep (MeV/his)	Organ Wt (g)	Organ Dose (MeV/g)	Organ Dose (Gy)
Skin	2.40E-07	9.50E-14	5.09E-02	1.22E-08	2830	4.32E-12	6.92E-22
Rib Bone Group	2.70E-04	3.12E-10	6.58E-02	1.78E-05	2167	8.19E-09	1.31E-18
Small Int	9.68E-04	1.78E-09	4.81E-02	4.65E-05	640	7.27E-08	1.16E-17
Gonads	2.27E-07	2.14E-10	4.85E-02	1.10E-08	37.1	2.97E-10	4.75E-20
Rectum	1.33E-05	1.38E-09	4.90E-02	6.49E-07	63	1.03E-08	1.65E-18
Thyroid	2.53E-07	3.67E-10	4.90E-02	1.24E-08	19.6	6.34E-10	1.01E-19
Lung	2.60E-04	2.15E-10	1.21E-02	3.16E-06	999	3.16E-09	5.06E-19
Eyes	0.00E+00	0.00E+00	4.90E-02	0.00E+00	15	0.00E+00	0.00E+00
Trachea	1.46E-06	3.81E-09	4.90E-02	7.17E-08	10	7.17E-09	1.15E-18
Colon	6.67E-03	6.64E-09	4.90E-02	3.27E-04	369	8.85E-07	1.42E-16
Stomach	5.98E-05	1.64E-09	4.90E-02	2.93E-06	150	1.95E-08	3.13E-18

As expected with Sr-90, the colon and small intestine received the highest dose from a highly energetic, beta radiation source located within the colon. The stomach, due to its close proximity to the source organ, received approximately 10% of the dose absorbed by the colon. The Y-90 colon dose was approximately 5 times greater than the dose absorbed by the Sr-90 beta radiation.

Statistical checks were performed on the Y-90 organ dose. The same warnings present with Co-60 were observed. The 10 statistical checks for tally-four fluence passed all but three checks. The relative error was 0.36, the VoV was 0.29 and the pdf was 0. The 10 statistical checks for tally-six dose passed. Of the 61 tally bins, 3 bins had a zero dose and 26 bins had relative errors exceeding 0.10 for the 2.28 MeV beta radiation. Figure 14.6 provides a simulated 3-dimensional view of the human body with a color profile that shows the MCNP organ dose for an Y-90 source in the colon. The color bar units to the right of the phantom are in MeV/organ weight in grams.

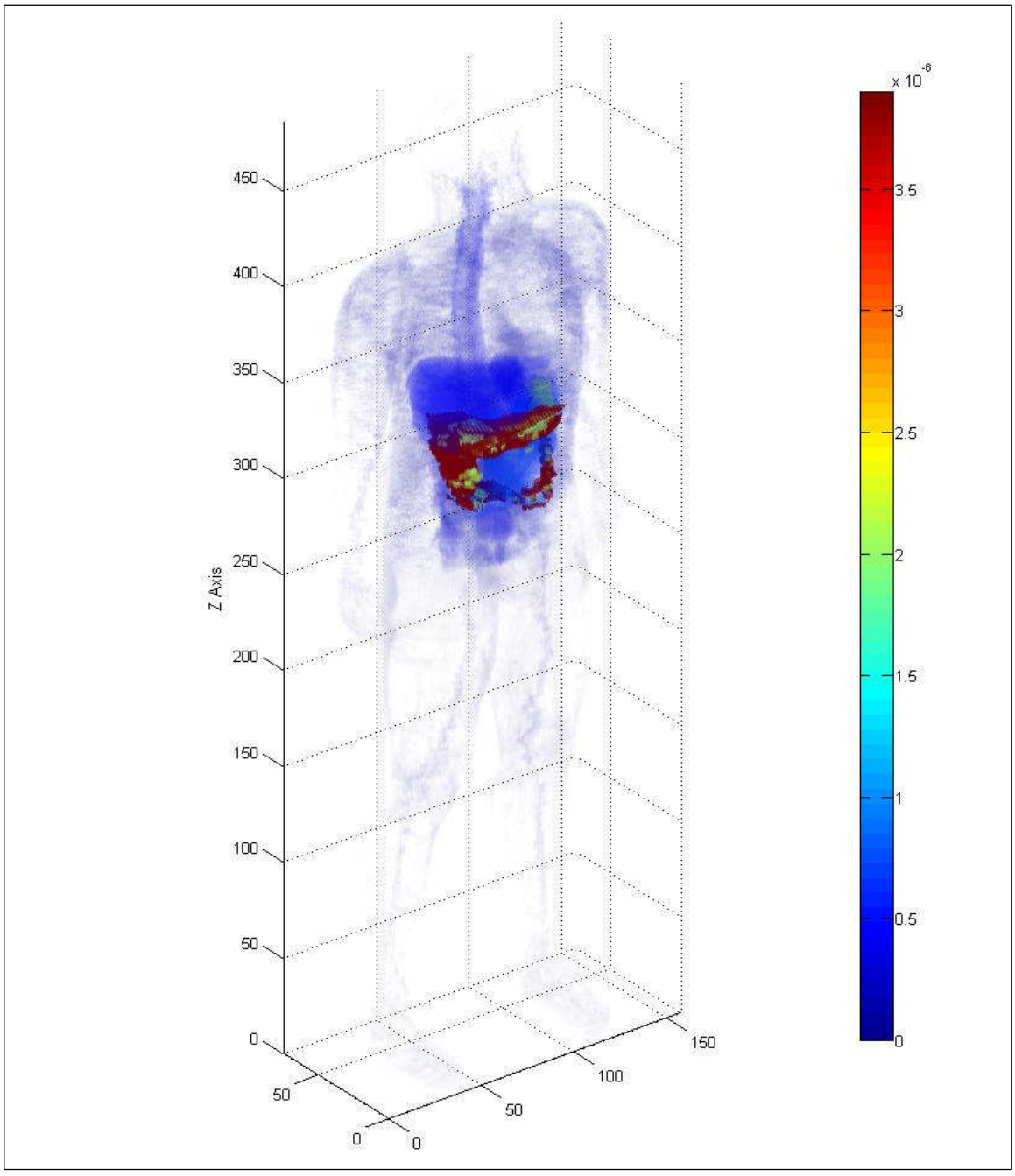

Fig. 14.6. Three-dimensional human dose profile from a 2.28 MeV Y-90 beta source located within the colon.

Results from colon volume source

Figure 14.7 provides an overview of all of the potential sources distributed in the colon and their organ doses. Based upon the results of the observed programs, Co-60 is the most limiting radionuclide with the exception of the thyroid, lung and trachea. It appears that Ir-192 becomes the most limiting radionuclide for those three organs. As expected, the colon followed by the small intestine and stomach appear to be the most sensitive organs based upon a single decay from a source located within the colon. Even though the trachea shows a higher sensitivity than the lung, the dose is a little deceiving. The observed dose for the trachea is based on the number of voxels which include the air encircled by the trachea. The actual dose, based on the weight of the organ, is less than that for the lung. As expected, the organ dose for the two beta sources was approximately 100 times smaller than the three gamma sources. An interesting note, Ir-192 and Cs-137 do not track the same for the thyroid, lung, trachea, colon and stomach. Cs-137 provides a higher dose than Ir-192 to the colon but a smaller dose to the stomach from a source located in the colon.

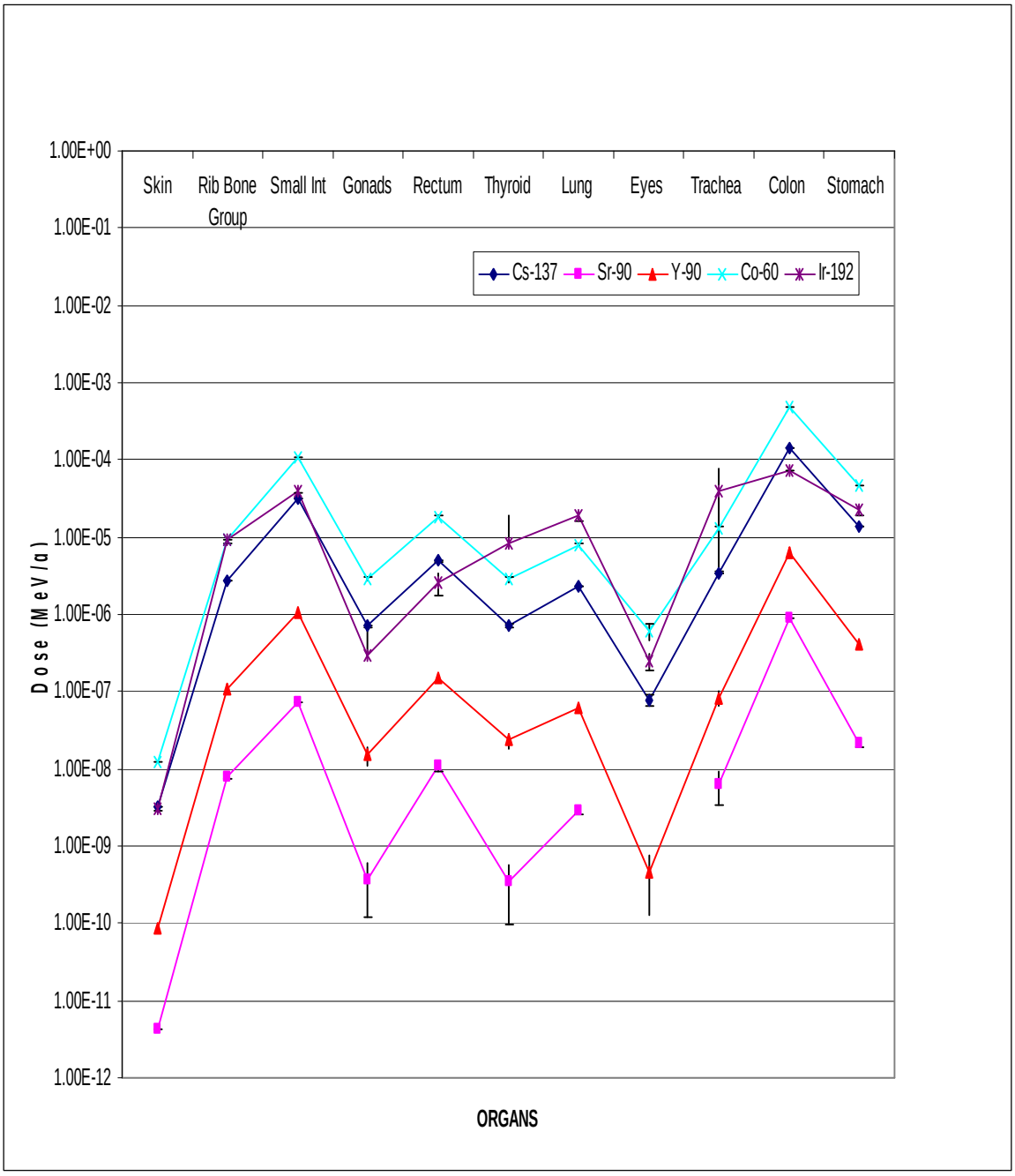

Fig. 14.7. Comprehensive graph of organ doses for the five potential colon sources.

CHAPTER XV
ESTIMATING ORGAN DOSE BASED ON VOLUME SOURCE IN THE SMALL INTESTINES

Organ data verification

The number of source voxels for additional organs will be based on the ratio of MAX lung source voxels divided by the total number of MAX lung voxels. This fraction will than be multiplied by the total number of organ voxels to determine the number of source voxels in the organ. Based on the fraction, the number of source voxels calculated for the small intestine was 3,499. This number would represent a volume source based on the dimension of the small intestine. Volumes and masses were checked against ICRU-46 established values for both simulations (ICRU 1990). Using the provided values from Table A-2 of Appendix A, the hand calculated volume of small intestine was 952.39 cm^3, the volume of a single voxel was 4.67×10^{-2} cm^3 (Kramer 2003). According to figure A-1 of Appendix A, the MCNPX code calculated a volume of 4.67×10^{-2} cm^3 for a single voxel. The hand calculated mass of the small intestine was 590 g and the mass per voxel was 5.09×10^{-2} g which includes the small intestine and its contents. The small intestine alone weighs 640 g and the mass per voxel without contents would be 3.14×10^{-2} g. Based on Figure A-1 of Appendix A, the code calculated a mass of 4.81×10^{-2} g in a single voxel. Therefore, the phantom small intestine provided a good simulation that was representative of standard man.

Co-60 organ dose profile

A Co-60 source located within the small intestine would deliver a dose to the selected organs that ranges from a high of 4.01×10^{-4} MeV/g for the small intestine and a low of 1.19×10^{-8} MeV/g for the skin. This organ dose contribution is the sum of two photons emitted from Co-60 that occur with a yield of about 100 percent. Table 15.1

provides the calculated dose conversions for each of the selected organs that will be considered in this problem.

Table 15.1. Organ doses from a Co-60 volume source in the small intestine.

Organs	MCNP Dose (MeV/g)	Std Deviation	MCNP Wght (g)	En Dep (MeV/his)	Organ Wt (g)	Organ Dose (MeV/g)	Organ Dose (Gy)
Skin	6.62E-04	2.86E-11	5.09E-02	3.37E-05	2830	1.19E-08	1.91E-18
Rib Bone Group	2.67E-01	4.54E-08	6.58E-02	1.76E-02	2167	8.11E-06	1.30E-15
Small Int	5.33E+00	6.41E-07	4.81E-02	2.56E-01	640	4.01E-04	6.42E-14
Gonads	2.28E-03	2.13E-07	4.85E-02	1.11E-04	37.1	2.98E-06	4.77E-16
Rectum	1.22E-02	2.89E-07	4.90E-02	5.99E-04	63	9.51E-06	1.52E-15
Thyroid	9.67E-04	2.13E-07	4.90E-02	4.74E-05	19.6	2.42E-06	3.87E-16
Lung	6.54E-01	7.06E-08	1.21E-02	7.93E-03	999	7.94E-06	1.27E-15
Eyes	1.09E-04	9.34E-08	4.90E-02	5.33E-06	15	3.56E-07	5.70E-17
Trachea	2.61E-03	9.93E-07	4.90E-02	1.28E-04	10	1.28E-05	2.05E-15
Colon	8.73E-01	5.33E-07	4.90E-02	4.28E-02	369	1.16E-04	1.86E-14
Stomach	2.43E-01	6.81E-07	4.90E-02	1.19E-02	150	7.92E-05	1.27E-14

As expected, the largest dose concentration is to the small intestine and the organs in the immediate vicinity of the small intestine. The dose to the skin is smaller by a factor of 10,000. The assumption applied to the skin dose is that the dose is uniform across the entire volume of skin. The actual skin dose is delivered on a gradient depending upon the distance from the source as well as the amount and type of material between the source and the skin.

Statistical analysis of output file

The tally-four fluence analysis for each detector, setup as described in chapter VII provided a random behavior for the mean. The desired relative error should be less than 0.10 and the observed relative error was 0.08. The desired and observed relative error decreased according to the inverse of the square root of the number of histories. The desired variance of the variance should be less than 0.10 and the observed VoV was 0.02. The figure of merit value was constant and the behavior was random. The

probability density function (pdf) desired should be greater than three, the observed pdf was 0. There was insufficient tfc bin tally information to estimate the large tally slope reliably. The tally-four fluence passed all 10 statistical checks except the pdf. Out of 10 tally-four bins, one had a zero value and no bins contained relative errors greater than 0.10. The second 1.33 MeV photon simulation provided similar results.

The tally-six dose analysis for each material showed a random behavior for the mean. The desired relative error should be less than 0.10 and the observed relative error was 0.00 for both photons. The desired and observed relative errors decreased according to the inverse of the square root of the number of histories. The desired variance of the variance should be less than 0.10 and the observed VoV was 0.00. The figure of merit value was constant and the behavior was random. The desired probability density function (pdf) should be greater than 3.00 and the observed value was 10.0 for the 1.17 MeV photon and 6.35 for the 1.33 MeV photon. The tally-six dose passed all 10 statistical checks. Out of 61 tally-six bins, no bin had a zero dose value and only 11 bins contained relative errors greater than 0.10.

Figure 15.1 provides a simulated 3-dimensional view of the human body with a color profile that shows the organ dose for the 1.33 MeV photon of Co-60. The color bar units to the right of the phantom are in MeV/organ weight in grams. Each axis is represented in the figure along with a color bar that indicates the organ dose in MeV/g provided by the MCNPX output file. In the MCNPX output file, the small intestine received the highest dose followed by the colon. The dose to the small intestine is roughly 2 times that of the colon. The stomach dose is within a factor of 3 compared to the dose from the small intestine.

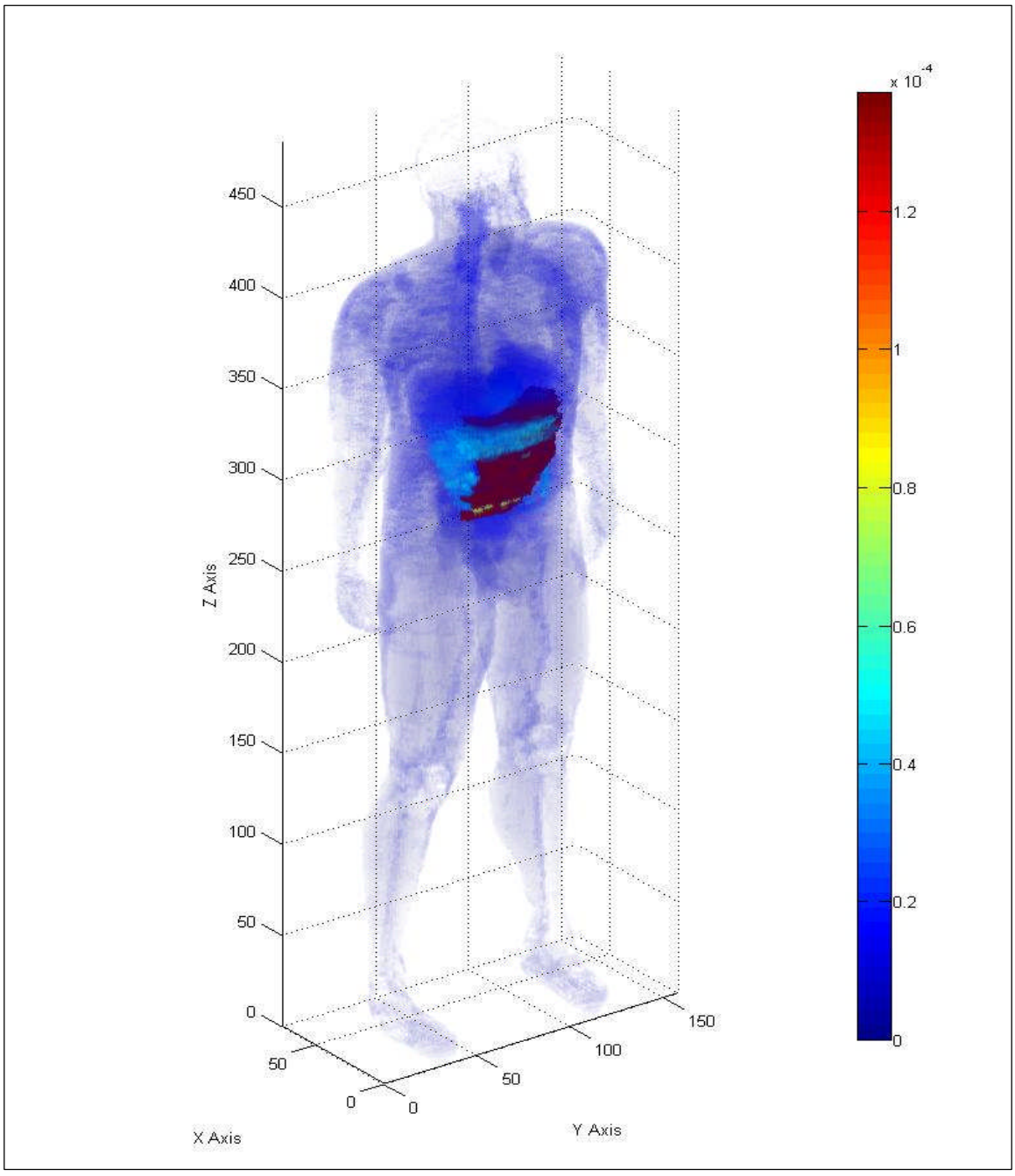

Fig. 15.1. Three-dimensional human dose profile from a 1.33 MeV photon source located within the small intestine.

Cs-137 organ dose profile

A Cs-137 source located within the small intestine would deliver a dose to the selected organs that ranges from a high of 1.17 x 10^{-4} MeV/g for the small intestine and a low of 3.16 x 10^{-9} MeV/g for the skin. This organ dose contribution is from a 0.66 MeVphoton emitted from Cs-137 that occurs with a yield of about 86 percent. Table 15.2 provides the dose output to the selected organs from the 0.66 MeV photon.

Table 15.2. Organ doses for a Cs-137 volume source in the small intestine.

Organs	MCNP Dose (MeV/g)	Std Deviation	MCNP Wght (g)	En Dep (MeV/his)	Organ Wt (g)	Organ Dose (MeV/g)	Organ Dose (Gy)
Skin	1.76E-04	4.11E-12	5.09E-02	8.94E-06	2830	3.16E-09	5.06E-19
Rib Bone Group	7.73E-02	6.57E-09	6.58E-02	5.08E-03	2167	2.34E-06	3.76E-16
Small Int	1.56E+00	9.38E-08	4.81E-02	7.50E-02	640	1.17E-04	1.88E-14
Gonads	5.33E-04	2.59E-08	4.85E-02	2.59E-05	37.1	6.97E-07	1.12E-16
Rectum	3.51E-03	4.01E-08	4.90E-02	1.72E-04	63	2.73E-06	4.37E-16
Thyroid	2.58E-04	2.86E-08	4.90E-02	1.26E-05	19.6	6.45E-07	1.03E-16
Lung	1.78E-01	9.73E-09	1.21E-02	2.16E-03	999	2.16E-06	3.47E-16
Eyes	2.54E-05	1.31E-08	4.90E-02	1.24E-06	15	8.29E-08	1.33E-17
Trachea	6.36E-04	1.21E-07	4.90E-02	3.12E-05	10	3.12E-06	4.99E-16
Colon	2.53E-01	7.73E-08	4.90E-02	1.24E-02	369	3.36E-05	5.38E-15
Stomach	6.97E-02	9.79E-08	4.90E-02	3.42E-03	150	2.28E-05	3.65E-15

As expected, the dose to the selected organs is similar to the dose produced by the Co-60 photons. The largest dose concentration remains with organs in the immediate vicinity of the small intestine. The small intestine dose is reduced by approximately a factor of two from the 1.17 MeV Co-60 photon dose. This reduction is expected based on the energy reduction between the 1.17 MeV Co-60 photon and that of Cs-137.

Statistical checks were performed on the Cs-137 dose output file. The same warnings present with Co-60 were observed. The 10 statistical checks for tally-four fluence passed with the exception of the pdf. There was insufficient tfc bin tally information to estimate the large tally slope reliably. The 10 statistical checks for tally-

six dose passed and produced similar results as with Co-60. Of the 61 tally bins, no bins contained a zero dose and 11 bins had relative errors exceeding 0.10. Figure 15.2 provides a simulated 3-dimensional view of the human body with a color profile that shows the organ dose for the single photon of Cs-137. The color bar units to the right of the phantom are in MeV/organ weight in grams.

The Co-60 small intestine dose was 1.90×10^{-4} MeV/g for the 1.17 MeV photon compared with the Cs-137 small intestine dose of 1.17×10^{-4} MeV/g for the 0.66 MeV photon. As expected, the dose profile is similar to that of the photons emitted by Co-60. The dose to each individual organ is proportionally reduced based on the lower-energy of the source photon and the energy dependent stopping power of the material within the phantom.

Ir-192 organ dose profile

An Ir-192 source located within the small intestine would deliver a dose to the selected organs that ranges from a high of 1.45×10^{-4} MeV/g for the small intestine and a low of 3.63×10^{-9} MeV/g for the skin. This organ dose contribution is from the sum of two photons with energies of 0.47 MeV and 0.32 MeV along with two electrons with maximum energies of 0.66 MeV and 0.54 MeV. All four emissions are produced with a yield of 26.2%, 22.4%, 10.1% and 6.7%, respectively. Table 15.3 provides the calculated dose conversions for each of the selected organs.

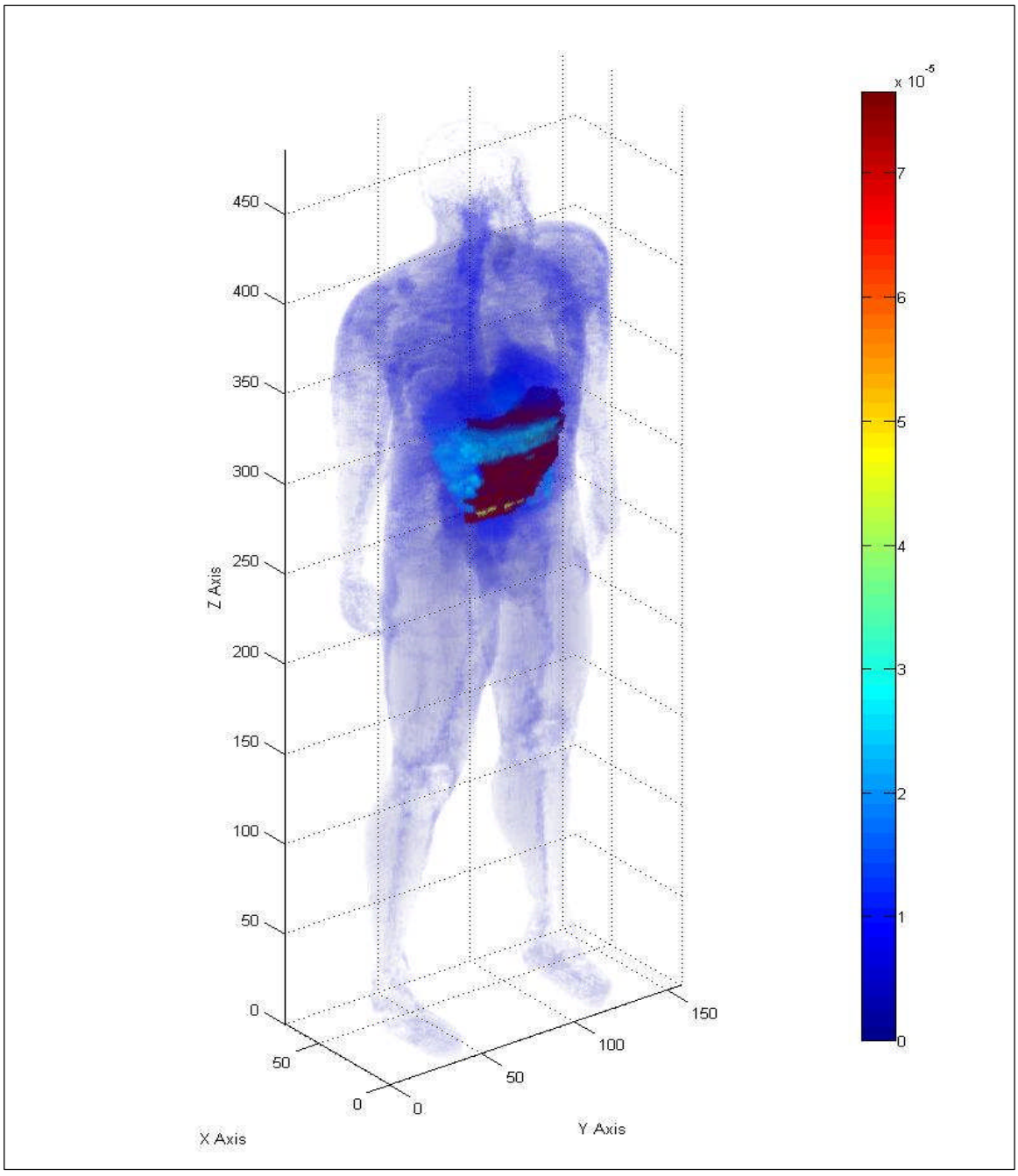

Fig. 15.2. Three-dimensional human dose profile from a Cs-137 photon source located within the small intestine.

Table 15.3. Organ doses for an Ir-192 volume source in the small intestine.

Organs	MCNP Dose (MeV/g)	Std Deviation	MCNP Wght (g)	En Dep (MeV/his)	Organ Wt (g)	Organ Dose (MeV/g)	Organ Dose (Gy)
Skin	2.02E-04	1.56E-10	5.09E-02	1.03E-05	2830	3.63E-09	5.81E-19
Rib Bone Group	1.00E-01	2.43E-07	6.58E-02	6.60E-03	2167	3.05E-06	4.88E-16
Small Int	1.93E+00	2.32E-06	4.81E-02	9.26E-02	640	1.45E-04	2.32E-14
Gonads	5.55E-04	6.65E-07	4.85E-02	2.69E-05	37.1	7.26E-07	1.16E-16
Rectum	4.21E-03	1.53E-06	4.90E-02	2.06E-04	63	3.27E-06	5.24E-16
Thyroid	2.98E-04	1.25E-06	4.90E-02	1.46E-05	19.6	7.44E-07	1.19E-16
Lung	2.10E-01	3.52E-07	1.21E-02	2.54E-03	999	2.55E-06	4.08E-16
Eyes	2.02E-05	2.44E-08	4.90E-02	9.89E-07	15	6.59E-08	1.06E-17
Trachea	7.13E-04	5.13E-06	4.90E-02	3.49E-05	10	3.49E-06	5.59E-16
Colon	3.16E-01	2.12E-06	4.90E-02	1.55E-02	369	4.20E-05	6.73E-15
Stomach	8.66E-02	3.16E-06	4.90E-02	4.24E-03	150	2.83E-05	4.53E-15

As expected, the organ dose was driven by the two photons over the two electrons by a factor of 100 or greater. Compared to the Co-60 and Cs-137 organ dose, the most sensitive organs for Ir-192 were the small intestine and colon. The dose to the small intestine is slightly larger than the Cs-137 small intestine dose. The sum of the two Ir-192 photons is comparable to the energy of the single Cs-137 photon.

Statistical checks on the Ir-192 photon dose output file were performed. The same warnings present with Co-60 were observed. The 10 statistical checks for tally-four fluence passed with the exception of the pdf. There was insufficient tfc bin tally information to estimate the large tally slope reliably. The 10 statistical checks for tally-six dose passed and produced similar results as with Co-60. Of the 61 tally bins, no bins contained a zero dose and 12 bins had relative errors exceeding 0.10 for the 0.32 MeV photon. The 0.47 MeV photon produced similar results.

The tallies for the electron sources within the small intestine had to be evaluated in a slightly different manner based on their inability to penetrate uniformly throughout the phantom. Secondary emissions, such as bremsstrahlung and characteristics x rays were the primary radiation source for organs outside of the small intestine. All but three of the 10 tally-four fluence statistical checks passed. The relative error was 1.00, the VoV was 1.00 and the pdf was 0. This reflects a large number of zero doses and slightly

greater than zero dose based on the electron source. In the case of an electron source, only the selected organs were reviewed for their relative error.

Figures 15.3 and 15.4 provide a simulated 3 dimensional view of the human body with a color profile that shows the MCNP dose for the 0.14 MeV photon of Ir-192 and the 0.66 MeV electron of Ir-192 absorbed by each organ, respectively. The color bar units to the right of the phantom are in MeV/organ weight in grams.

Sr-90 organ dose profile

A Sr-90 source located within the small intestine would deliver a dose to the selected organs that ranges from a high of 6.14×10^{-7} MeV/g for the small intestine and a low of 4.17×10^{-12} MeV/g for the skin. This organ dose contribution is from a single beta emission with a maximum energy of 0.55 MeV. The beta emission is produced with a yield of about 100%. Table 15.4 provides the calculated dose conversions for each of the selected organs that will be considered in this problem.

Table 15.4. Organ doses from a Sr-90 volume source in the small intestine.

Organs	MCNP Dose (MeV/g)	Std Deviation	MCNP Wght (g)	En Dep (MeV/his)	Organ Wt (g)	Organ Dose (MeV/g)	Organ Dose (Gy)
Skin	2.32E-07	8.85E-14	5.09E-02	1.18E-08	2830	4.17E-12	6.69E-22
Rib Bone Group	2.20E-04	2.68E-10	6.58E-02	1.45E-05	2167	6.69E-09	1.07E-18
Small Int	8.17E-03	4.66E-09	4.81E-02	3.93E-04	640	6.14E-07	9.83E-17
Gonads	2.25E-07	1.97E-10	4.85E-02	1.09E-08	37.1	2.95E-10	4.72E-20
Rectum	4.98E-06	6.81E-10	4.90E-02	2.44E-07	63	3.87E-09	6.21E-19
Thyroid	1.31E-07	2.76E-10	4.90E-02	6.44E-09	19.6	3.29E-10	5.26E-20
Lung	2.19E-04	1.88E-10	1.21E-02	2.66E-06	999	2.66E-09	4.26E-19
Eyes	0.00E+00	0.00E+00	4.90E-02	0.00E+00	15	0.00E+00	0.00E+00
Trachea	4.33E-07	1.53E-09	4.90E-02	2.12E-08	10	2.12E-09	3.40E-19
Colon	5.98E-04	2.03E-09	4.90E-02	2.93E-05	369	7.93E-08	1.27E-17
Stomach	1.15E-04	2.32E-09	4.90E-02	5.62E-06	150	3.75E-08	6.01E-18

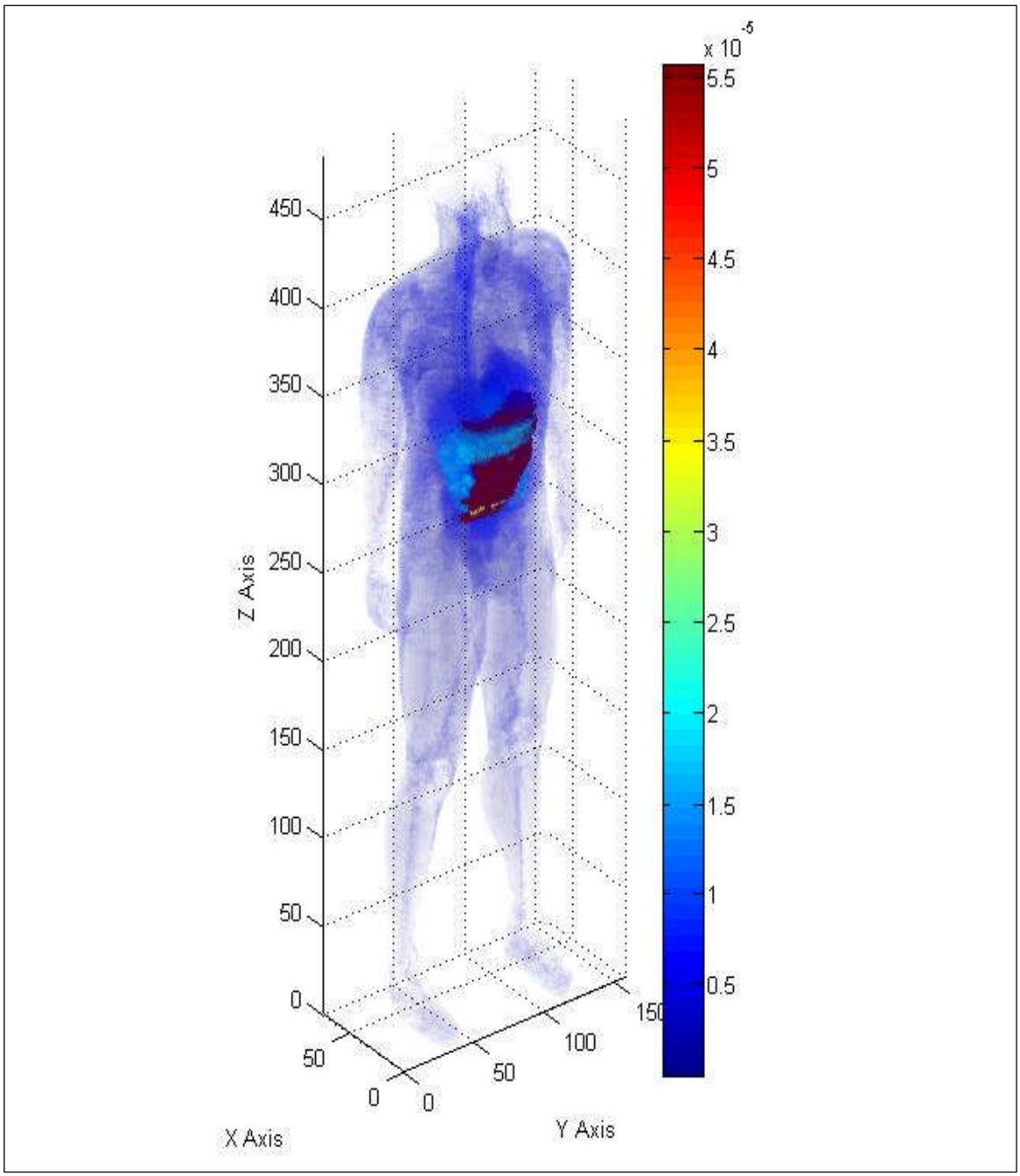

Fig. 15.3. Three-dimensional human dose profile from the 0.47 MeV Ir-192 photon source located within the small intestine.

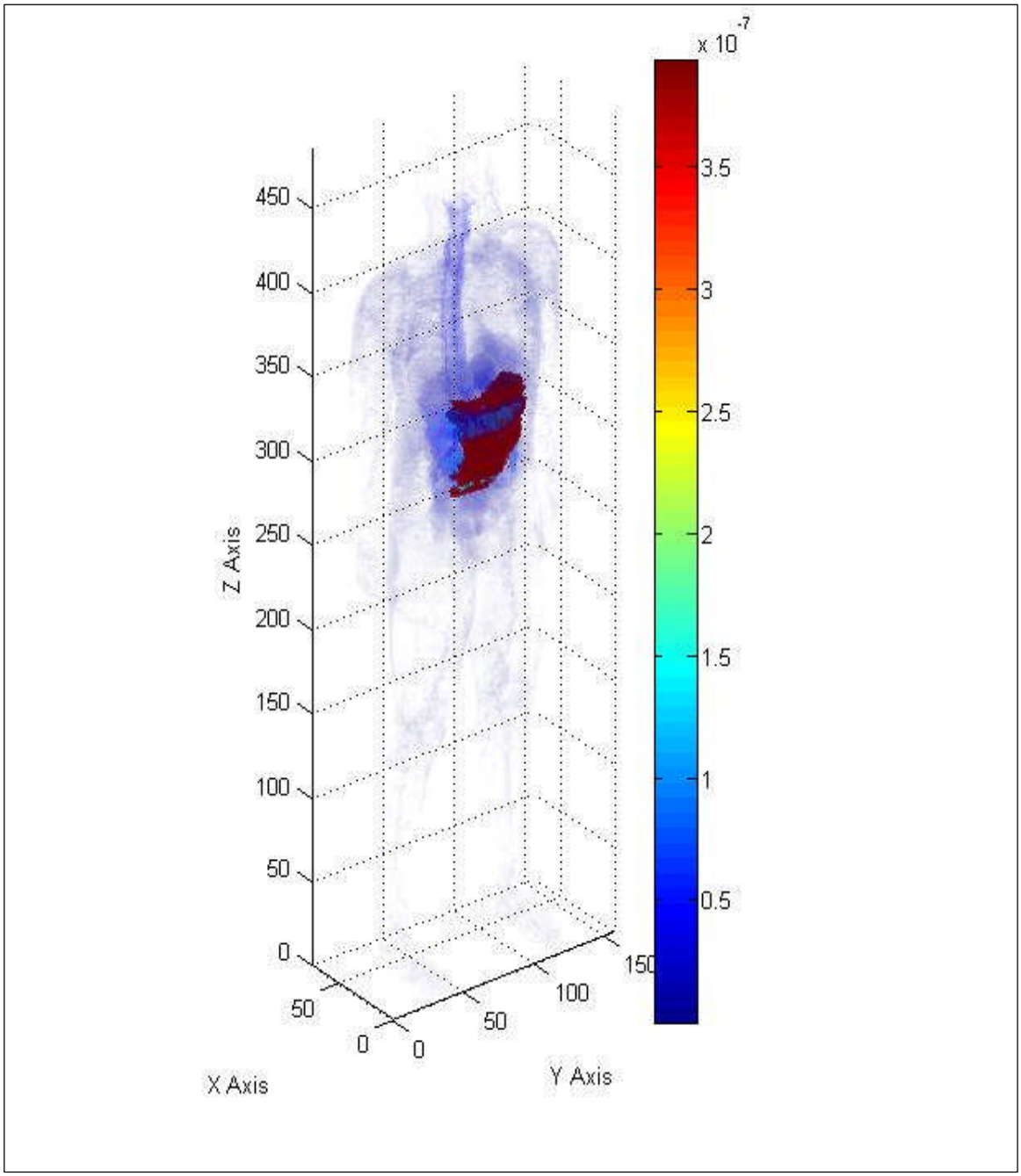

Fig. 15.4. Three-dimensional human dose profile from the 0.66 MeV Ir-192 electron source located within the small intestine.

As expected, the small intestine received the greatest dose from a moderately energetic beta radiation source located within the small intestine. The colon and stomach, due to their close proximity to the source organ received approximately 10 percent of the dose to the small intestine.

Statistical checks were performed on the Sr-90 dose output file. The same warnings present with Co-60 were observed. The tally-four fluence passed all but three of the 10 statistical checks. The relative error was 1.00, the VoV was 1.00 and the pdf was 0. For tally-six dose, the relative error was 0.02, VoV was 0.00 and the pdf was 5.01. The 10 statistical checks for tally-six dose passed. Of the 61 tally bins, 14 bins had zero dose and 25 bins had relative errors exceeding 0.10 for the 0.55 MeV beta radiation. Figure 15.5 provides a simulated 3-dimensional view of the human body with a color profile that shows the organ dose for the beta radiation of Sr-90 absorbed by each organ. The color bar units to the right of the phantom are in MeV/organ weight in grams.

Y-90 organ dose profile

A Y-90 source located within the small intestine would deliver a dose to the selected organs that ranges from a high of 5.06×10^{-6} MeV/g for the small intestine and a low of 8.46×10^{-11} MeV/g for the skin. This organ dose contribution is from a single beta emission with a maximum energy of 2.28 MeV. The beta emission is produced with a yield of about 100%. Table 15.5 provides the calculated dose conversions for each of the selected organs.

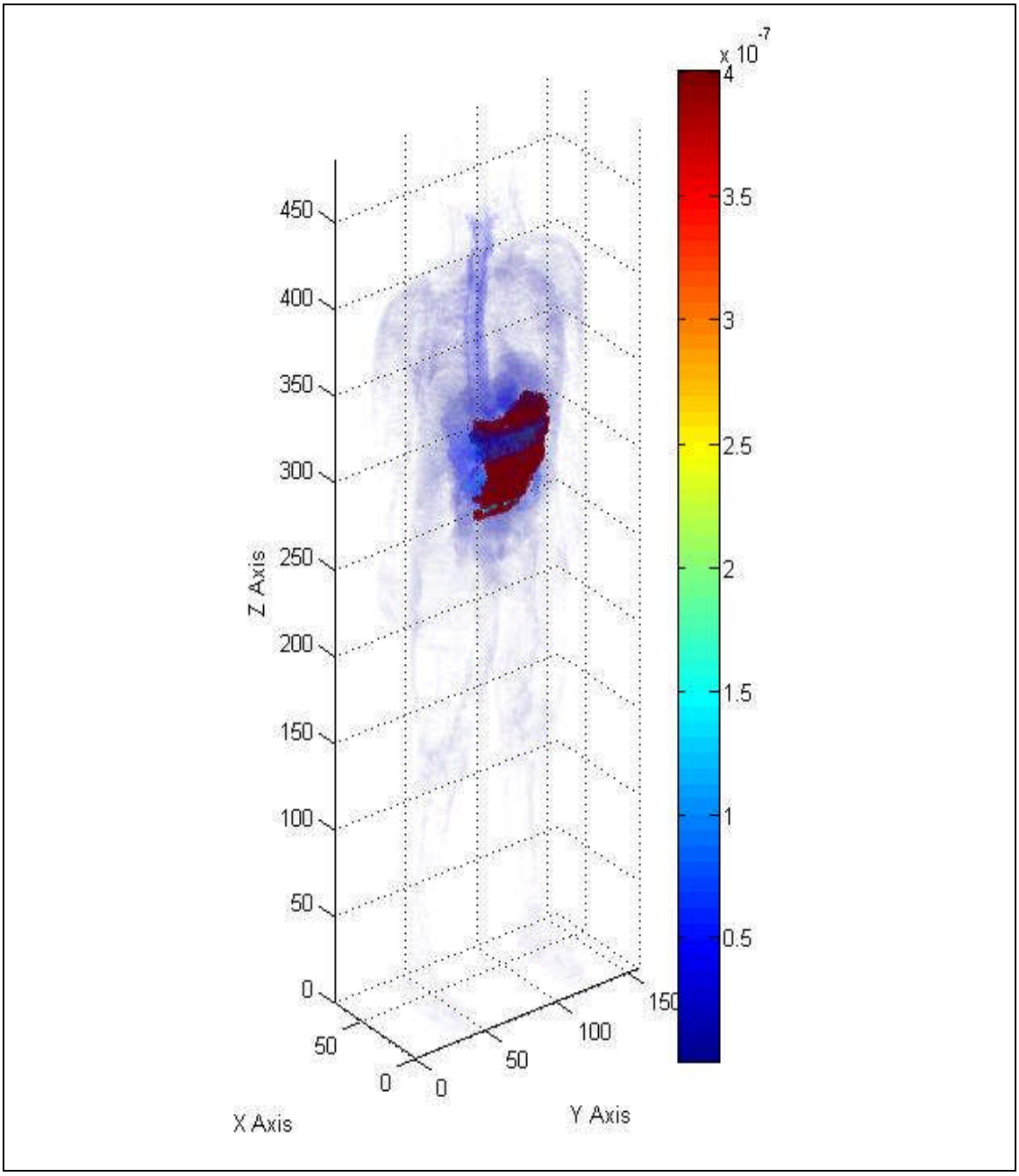

Fig. 15.5. Three-dimensional human dose profile from a Sr-90 beta source located within the small intestine.

Table 15.5. Organ doses from a Y-90 volume source in the small intestine.

Organs	MCNP Dose (MeV/g)	Std Deviation	MCNP Wght (g)	En Dep (MeV/his)	Organ Wt (g)	Organ Dose (MeV/g)	Organ Dose (Gy)
Skin	4.71E-06	7.53E-13	5.09E-02	2.40E-07	2830	8.46E-11	1.36E-20
Rib Bone Group	3.02E-03	1.22E-09	6.58E-02	1.99E-04	2167	9.17E-08	1.47E-17
Small Int	6.74E-02	2.18E-08	4.81E-02	3.24E-03	640	5.06E-06	8.11E-16
Gonads	1.09E-05	2.77E-09	4.85E-02	5.27E-07	37.1	1.42E-08	2.28E-18
Rectum	9.30E-05	5.32E-09	4.90E-02	4.56E-06	63	7.23E-08	1.16E-17
Thyroid	5.32E-06	3.13E-09	4.90E-02	2.61E-07	19.6	1.33E-08	2.13E-18
Lung	4.56E-03	1.38E-09	1.21E-02	5.53E-05	999	5.53E-08	8.86E-18
Eyes	1.34E-06	3.35E-09	4.90E-02	6.58E-08	15	4.39E-09	7.03E-19
Trachea	1.45E-05	1.23E-08	4.90E-02	7.10E-07	10	7.10E-08	1.14E-17
Colon	8.68E-03	1.19E-08	4.90E-02	4.25E-04	369	1.15E-06	1.85E-16
Stomach	2.12E-03	1.47E-08	4.90E-02	1.04E-04	150	6.91E-07	1.11E-16

As with Sr-90, the small intestine received the highest dose from a highly-energetic beta particle source located within the small intestine. The colon and stomach, due to their close proximity to the source organ, received approximately 10 percent of the dose to the small intestine. The Y-90 small intestine dose was approximately 10 times greater than the dose delivered by the Sr-90 beta radiation even though the energy of the Y-90 beta radiation was approximately 4 times greater than the energy of the Sr-90 beta radiation.

Statistical checks on the Y-90 dose output file were performed. The same warnings present with Co-60 were observed. The 10 statistical checks for tally-four fluence passed all but three checks. The relative error was 0.41, the VoV was 0.47 and the pdf was 0. The 10 statistical checks for tally-six dose passed. Of the 61 tally bins, 3 bins had zero dose and 26 bins had relative errors exceeding 0.10 for the 2.28 MeV beta radiation. Figure 15.6 provides a simulated 3-dimensional view of the human body with a color profile that shows the organ dose for an Y-90 source in the small intestine. The color bar units to the right of the phantom are in MeV/organ weight in grams.

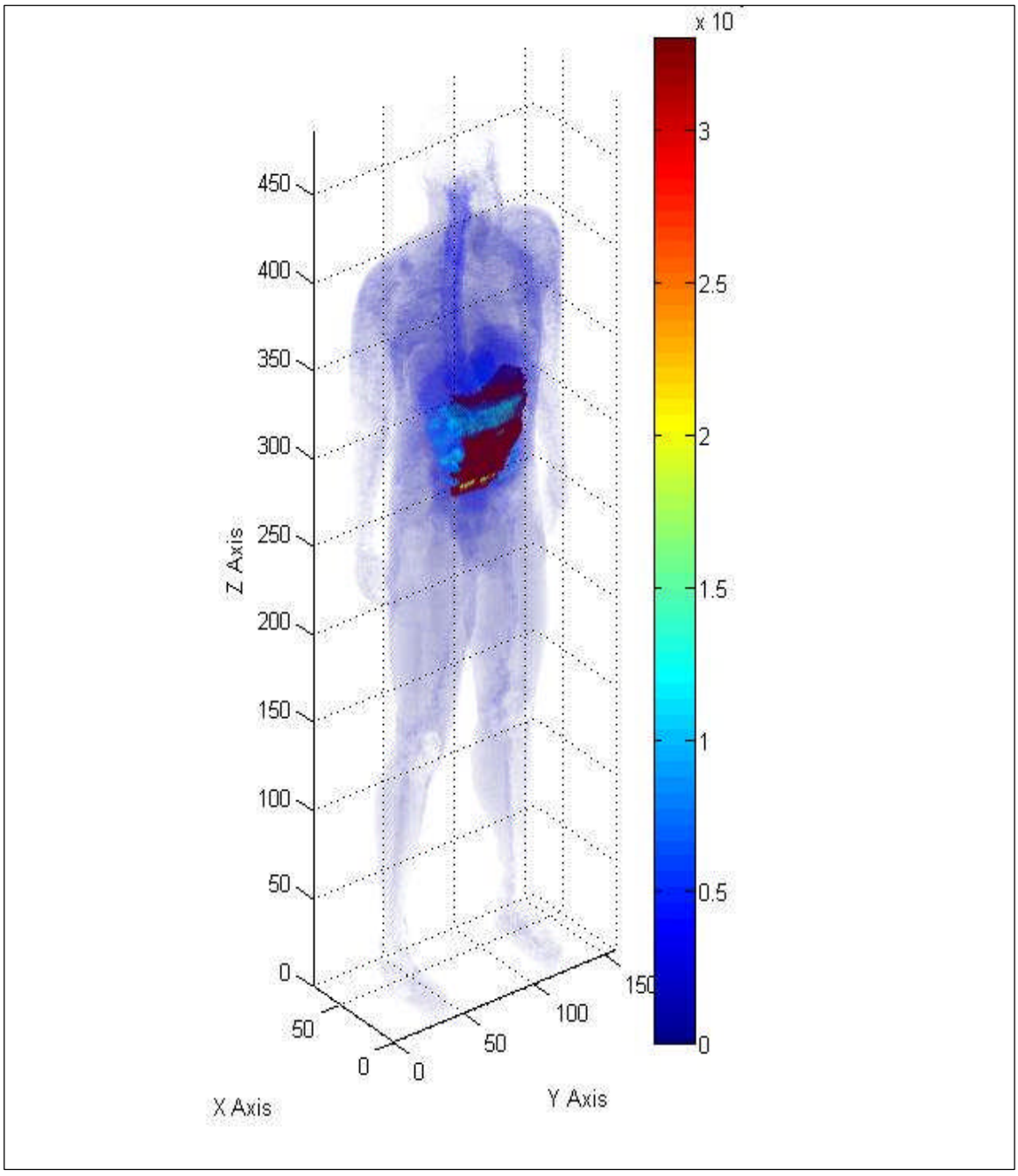

Fig. 15.6. Three-dimensional human dose profile from a Y-90 beta source located within the small intestine.

Results from small intestine volume source

Figure 15.7 provides a graph of all of the potential sources distributed in the small intestine. Based upon the results of the observed programs, Co-60 is the most limiting radionuclide. The small intestine, followed by the colon appear to be the most sensitive organs based upon a single emission from a source located within the small intestine. Even though the trachea shows a higher sensitivity than the lung, the dose is a little deceiving. The observed dose for the trachea is based on the number of voxels which include the air encircled by the trachea. The actual dose, based on the weight of the organ, is less than that for the lung.

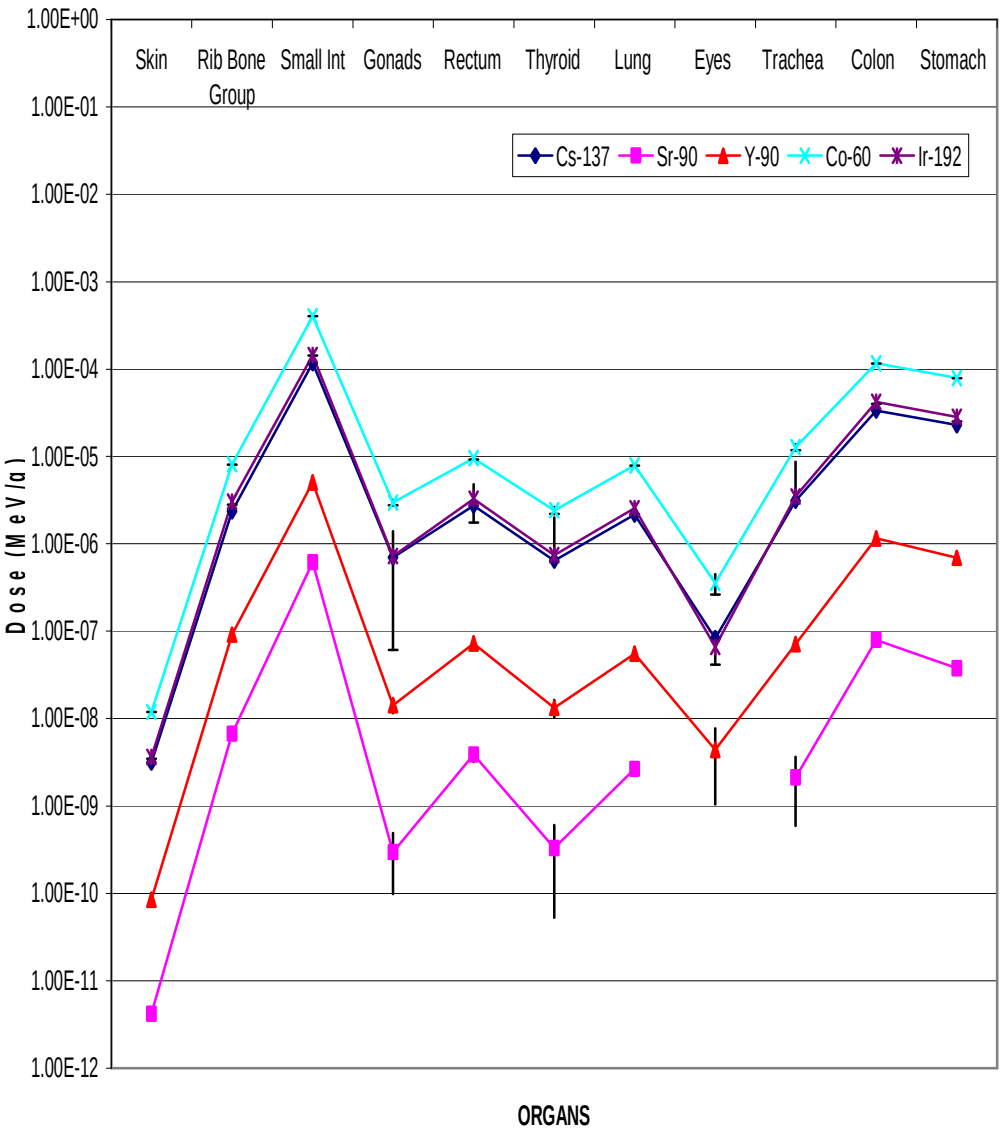

Fig. 15.7. Summary graph of organ doses for the five potential small intestine sources.

CHAPTER XVI
ESTIMATING ORGAN DOSE BASED ON VOLUME SOURCE IN THE SKIN

Organ data verification

The number of source voxels for additional organs will be based on the ratio of MAX lung source voxels divided by the total number of MAX lung voxels. This fraction will than be multiplied by the total number of organ voxels to determine the number of source voxels in the organ. Based on the fraction, the number of sources calculated for the skin was 21,082. This number would represent a volume source based on the dimension of the skin. Volumes and masses were checked against ICRU-46 established values for both simulations (ICRU 1990). Using the values from Table A-2 of Appendix A, the hand calculated volume of skin was 5,737.94 cm^3, the volume of a single voxel was 4.67 x 10^{-2} cm^3 (Kramer 2003). According to figure A-1 of Appendix A, the MCNPX code calculated a volume of 4.67 x 10^{-2} cm^3 for a single voxel. The hand calculated mass of the skin was 2,600 g and the mass per voxel was 2.11 x 10^{-2} g. Based on Figure A-1 of Appendix A, the code calculated a mass of 5.01 x 10^{-2} g in a single voxel. The skin mass is off by a factor of two but can be compensated by a slightly lower density. Therefore, the phantom skin provided a fair simulation that is representative of standard man.

Co-60 organ dose profile

A Co-60 source located within the skin would deliver a dose to the selected organs that ranges from a high of 9.29 x 10^{-5} MeV/g for the gonads and a low of 3.34 x 10^{-8} MeV/g for the skin. This organ dose contribution is the sum of two photons emitted from Co-60 that occur with a yield of about 100 percent. Table 16.1 provides calculated dose conversions for each of the selected organs that will be considered in this problem.

Table 16.1. Organ doses from a Co-60 volume source in the skin.

Organs	MCNP Dose (MeV/g)	Std Deviation	MCNP Wght (g)	En Dep (MeV/his)	Organ Wt (g)	Organ Dose (MeV/g)	Organ Dose (Gy)
Skin	1.86E-03	8.02E-11	5.09E-02	9.46E-05	2830	3.34E-08	5.35E-18
Rib Bone Group	1.95E-01	5.81E-08	6.58E-02	1.29E-02	2167	5.93E-06	9.50E-16
Small Int	1.05E-01	1.51E-07	4.81E-02	5.06E-03	640	7.91E-06	1.27E-15
Gonads	9.18E-03	4.82E-07	4.85E-02	4.46E-04	37.1	1.20E-05	1.92E-15
Rectum	7.36E-03	2.55E-07	4.90E-02	3.61E-04	63	5.72E-06	9.17E-16
Thyroid	2.16E-03	3.93E-07	4.90E-02	1.06E-04	19.6	5.41E-06	8.66E-16
Lung	4.69E-01	6.95E-08	1.21E-02	5.69E-03	999	5.69E-06	9.12E-16
Eyes	1.96E-03	4.61E-07	4.90E-02	9.58E-05	15	6.39E-06	1.02E-15
Trachea	6.15E-03	1.28E-06	4.90E-02	3.01E-04	10	3.01E-05	4.83E-15
Colon	6.63E-02	1.71E-07	4.90E-02	3.25E-03	369	8.81E-06	1.41E-15
Stomach	4.38E-02	3.60E-07	4.90E-02	2.14E-03	150	1.43E-05	2.29E-15

The largest dose concentration is to the gonads and stomach. The trachea received an equivalent dose when the air inside the trachea is added to the mass of the trachea.

Statistical analysis of output file

The tally-four fluence analysis for each detector, setup as described in chapter VII, provided a random behavior for the mean. The desired relative error should be less than 0.10 and the observed relative error was 0.05. The desired and observed relative errors decreased according to the inverse of the square root of the number of histories. The desired variance of the variance should be less than 0.10 and the observed VoV was 0.01. The figure of merit value was constant and the behavior was random. The probability density function (pdf) desired should be greater than three, the observed pdf value was 10.0. The tally-four fluence passed all 10 statistical checks. Out of 10 tally-four bins, one had a zero dose value and no bins contained relative errors greater than 0.10. The second 1.33 MeV photon simulation provided similar results.

The tally-six dose analysis for each material showed a random behavior for the mean. The desired relative error should be less than 0.10 and the observed relative error

was 0.00 for both photons. The desired and observed relative errors decreased according to the inverse of the square root of the number of histories. The desired variance of the variance should be less than 0.10 and the observed VoV was 0.00. The figure of merit value was constant and the behavior was random. The desired probability density function (pdf) should be greater than 3.00 and the observed value was 10.0 for both photons. The tally-six dose passed all 10 statistical checks. Out of 61 tally-six bins, no bins had a zero value and no bins contained relative errors greater than 0.10.

Figure 16.1 provides a simulated 3-dimensional view of the human body with a color profile that shows the organ dose for the 1.33 MeV photon of Co-60. Each axis is represented in the figure along with a color bar that indicates the organ dose in MeV/organ in grams provided by the MCNPX output file. In the MCNPX output file, the gonads received the highest dose followed by the stomach and trachea. The dose to the gonads is roughly 1000 times the dose of the skin.

Cs-137 organ dose profile

A Cs-137 source located within the skin would deliver a dose to the selected organs that ranges from a high of 8.24×10^{-6} MeV/g for the trachea and a low of 9.53×10^{-9} MeV/g for the skin. This organ dose contribution is from a 0.66 MeV photon emitted from Cs-137 that occurs with a yield of about 86 percent. Table 16.2 provides the dose output to selected organs from the 0.66 MeV photon.

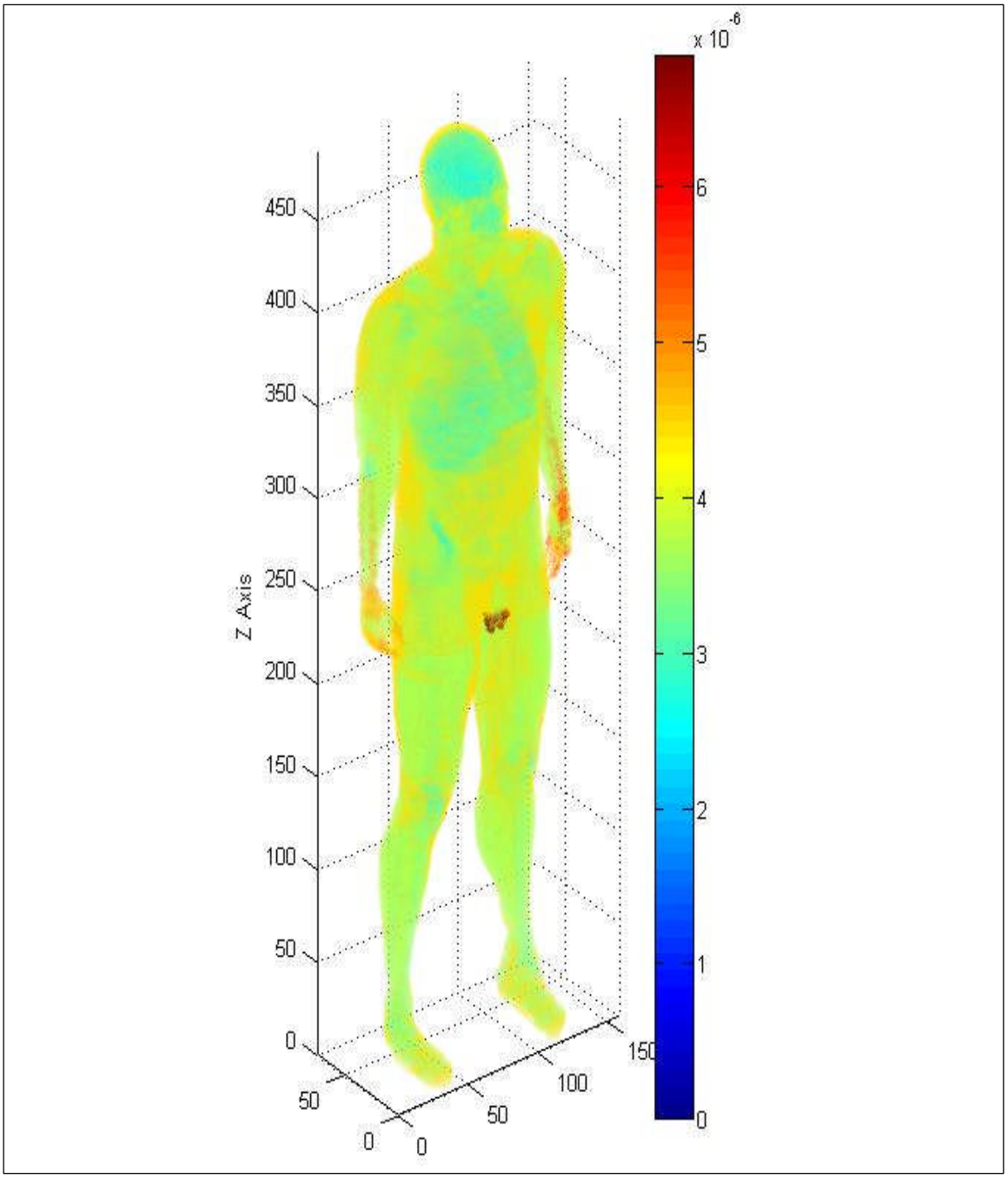

Fig. 16.1. Three-dimensional human dose profile from a 1.33 MeV photon source located within the skin.

Table 16.2. Organ doses for a Cs-137 volume source in the skin.

Organs	MCNP Dose (MeV/g)	Std Deviation	MCNP Wght (g)	En Dep (MeV/his)	Organ Wt (g)	Organ Dose (MeV/g)	Organ Dose (Gy)
Skin	5.31E-04	1.14E-11	5.09E-02	2.70E-05	2830	9.53E-09	1.53E-18
Rib Bone Group	5.45E-02	8.10E-09	6.58E-02	3.58E-03	2167	1.65E-06	2.65E-16
Small Int	2.82E-02	2.06E-08	4.81E-02	1.36E-03	640	2.12E-06	3.40E-16
Gonads	2.65E-03	6.92E-08	4.85E-02	1.28E-04	37.1	3.46E-06	5.54E-16
Rectum	1.97E-03	3.47E-08	4.90E-02	9.66E-05	63	1.53E-06	2.46E-16
Thyroid	6.11E-04	5.54E-08	4.90E-02	2.99E-05	19.6	1.53E-06	2.45E-16
Lung	1.29E-01	9.83E-09	1.21E-02	1.56E-03	999	1.56E-06	2.50E-16
Eyes	5.52E-04	6.47E-08	4.90E-02	2.70E-05	15	1.80E-06	2.89E-16
Trachea	1.68E-03	1.79E-07	4.90E-02	8.24E-05	10	8.24E-06	1.32E-15
Colon	1.77E-02	2.32E-08	4.90E-02	8.66E-04	369	2.35E-06	3.76E-16
Stomach	1.18E-02	4.93E-08	4.90E-02	5.78E-04	150	3.85E-06	6.18E-16

As expected, the dose to the selected organs is similar to the dose produced by the Co-60 photons. The largest dose concentration remains in the trachea. The stomach and gonads received a dose approximately two times less than the dose to the trachea. The 1.17 MeV photon from Co-60 produced a trachea dose of 3.01×10^{-5} MeV/g compared to the Cs-137 trachea dose of 8.24×10^{-6} MeV/g. The Cs-137 trachea dose was approximately one-fourth the dose of the Co-60 trachea dose.

Statistical checks were performed on the Cs-137 dose output file. The same warnings present with Co-60 were observed. The 10 statistical checks for tally-four fluence passed. The 10 statistical checks for tally-six dose passed all but one statistical check and produced similar results as with Co-60. The figure of merit has a trend during the last half of the problem. Of the 61 tally bins, no bins contained zero dose and no bins had relative errors exceeding 0.10. Figure 16.2 provides a simulated 3-dimensional view of the human body with a color profile that shows the organ dose for the single photon of Cs-137 absorbed by each organ.

The Co-60 skin dose was 1.58×10^{-8} MeV/g for the 1.17 MeV photon compared with the Cs-137 skin dose of 9.53×10^{-9} MeV/g for the 0.66 MeV photon. As expected, the dose profile is similar to that of the photons emitted by Co-60. The dose to each

individual organ is proportionally reduced based on the lower-energy of the source photon and the energy dependent stopping power of the material within the phantom.

Ir-192 organ dose profile

An Ir-192 source located within the skin would deliver a dose to the selected organs that ranges from a high of 9.65 x 10^{-6} MeV/g for the trachea and a low of 1.14 x 10^{-8} MeV/g for the skin. This organ dose contribution is from the sum of two photons with energies of 0.47 MeV and 0.32 MeV along with two electrons with maximum energies of 0.66 MeV and 0.54 MeV. All four emissions are produced with a yield of 26.2%, 22.4%, 10.1% and 6.7%, respectively. Table 16.3 provides the total dose output calculated conversions for each of the 11 selected organs.

Table 16.3. Organ doses for an Ir-192 volume source in the skin.

Organs	MCNP Dose (MeV/g)	Std Deviation	MCNP Wght (g)	En Dep (MeV/his)	Organ Wt (g)	Organ Dose (MeV/g)	Organ Dose (Gy)
Skin	6.34E-04	1.10E-09	5.09E-02	3.22E-05	2830	1.14E-08	1.83E-18
Rib Bone Group	6.65E-02	2.66E-07	6.58E-02	4.37E-03	2167	2.02E-06	3.23E-16
Small Int	3.26E-02	7.80E-07	4.81E-02	1.56E-03	640	2.45E-06	3.92E-16
Gonads	3.12E-03	1.43E-06	4.85E-02	1.51E-04	37.1	4.08E-06	6.53E-16
Rectum	2.23E-03	9.81E-07	4.90E-02	1.09E-04	63	1.73E-06	2.77E-16
Thyroid	6.89E-04	1.85E-06	4.90E-02	3.38E-05	19.6	1.72E-06	2.76E-16
Lung	1.49E-01	3.80E-07	1.21E-02	1.81E-03	999	1.81E-06	2.90E-16
Eyes	6.29E-04	2.52E-06	4.90E-02	3.08E-05	15	2.05E-06	3.29E-16
Trachea	1.97E-03	6.21E-06	4.90E-02	9.65E-05	10	9.65E-06	1.55E-15
Colon	2.04E-02	8.21E-07	4.90E-02	9.98E-04	369	2.71E-06	4.33E-16
Stomach	1.37E-02	1.88E-06	4.90E-02	6.73E-04	150	4.49E-06	7.19E-16

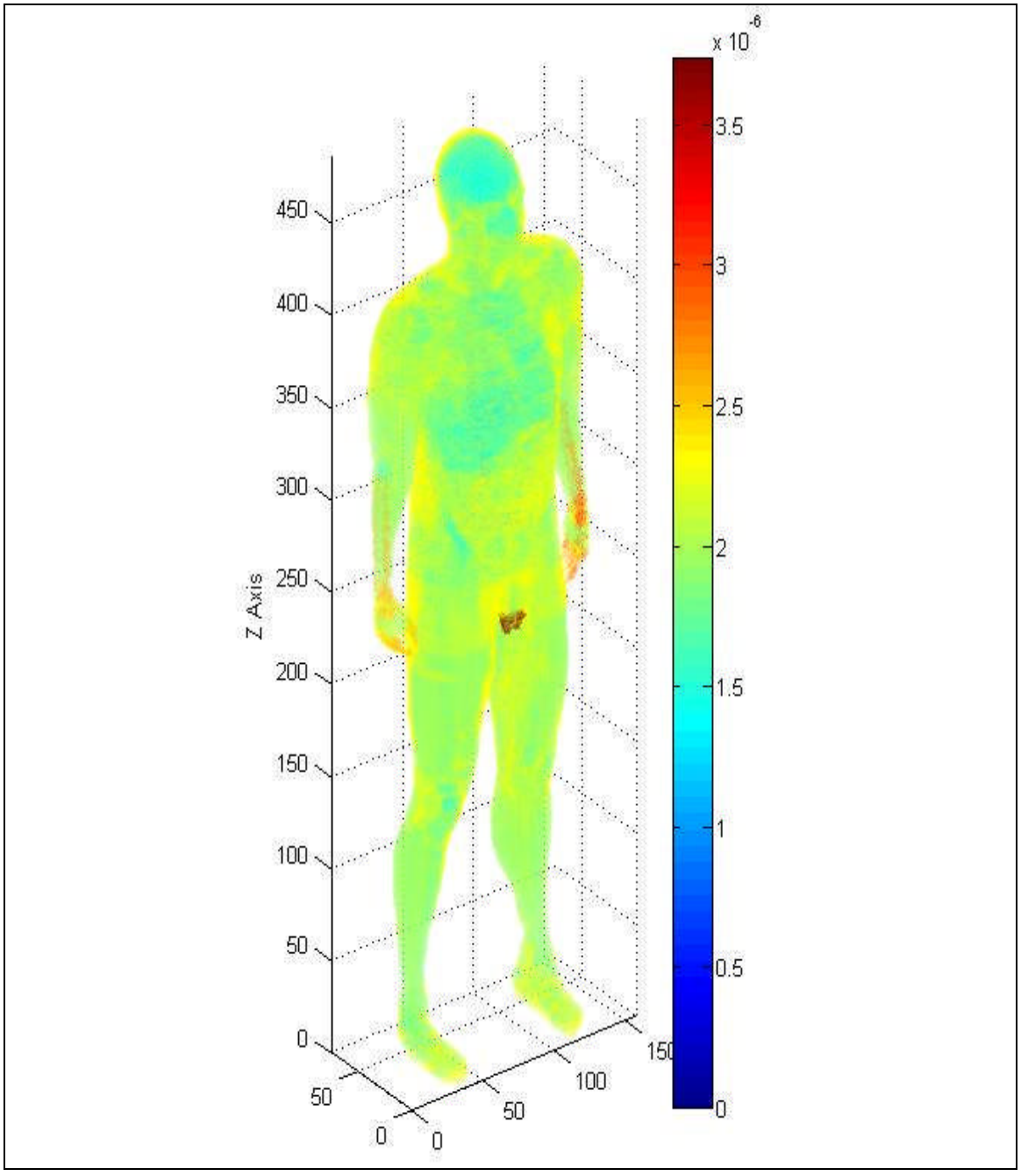

Fig. 16.2. Three-dimensional human dose profile from a Cs-137 photon source located within the skin.

As expected, the organ dose was driven by the two photons over the two electrons by a factor of 100 or greater. Compared to the Co-60 and Cs-137 organ dose, the most sensitive organs for Ir-192 were the trachea, gonads and stomach. The dose to the trachea from Ir-192 was slightly greater than the dose to the trachea from Cs-137. The sum of the two Ir-192 photons is comparable to the energy of the single Cs-137 photon.

Statistical checks were performed on the Ir-192 photon dose output file. The same warnings present with Co-60 were observed. The 10 statistical checks for tally-four fluence passed. The 10 statistical checks for tally-six passed all but one check. The figure of merit had a trend during the last half of the problem. The tally-six checks produced similar results as with Co-60. Of the 61 tally bins, no bin contained a zero dose and no bins had relative errors exceeding 0.10 for the 0.32 MeV photon. The 0.47 MeV photon produced similar results.

The tallies for the electron sources within the skin had to be evaluated in a slightly different manner based on their lack inability to penetrate uniformly throughout the phantom. Secondary radiations, such as bremsstrahlung and characteristics x rays were the primary radiation source for organs inside of the skin. Four of the 10 statistical checks failed. The relative error was 0.41, the VoV was 0.24, the VoV did not decrease according to the inverse of the number of histories and the pdf was 0. This reflects a large number of zero and slightly greater than zero dose based on the electron source. In the case of an electron source, only the selected organs were reviewed for their relative error.

Figures 16.3 and 16.4 provide a simulated 3-dimensional view of the human body with a color profile that shows the MCNP dose for the 0.47 MeV photon of Ir-192 and the 0.66 MeV electron of Ir-192 absorbed by each organ, respectively. The color bar units to the right of the phantom are in MeV/organ weight in grams.

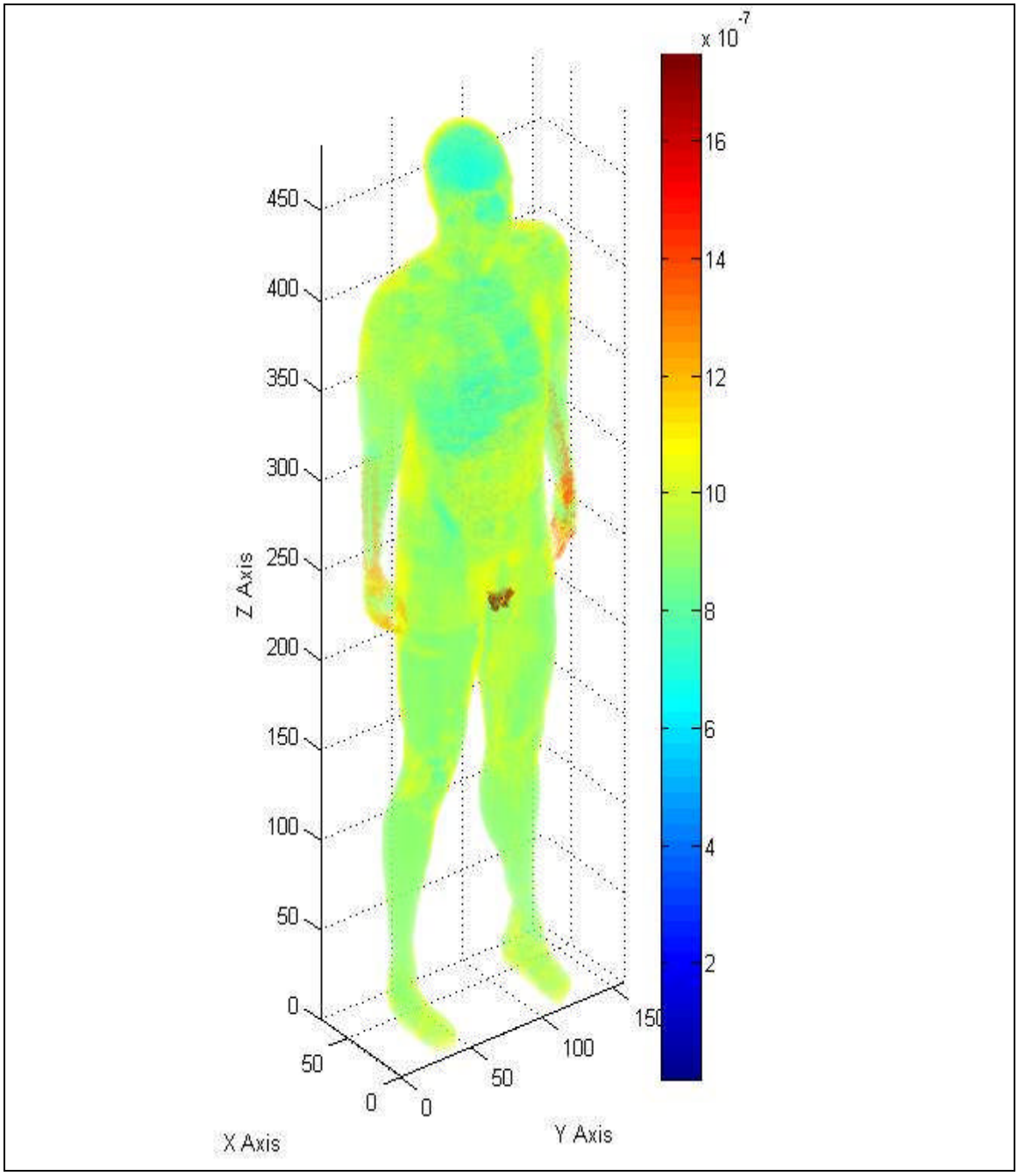

Fig. 16.3. Three-dimensional human dose profile from a 0.47 MeV Ir-192 photon source located within the skin.

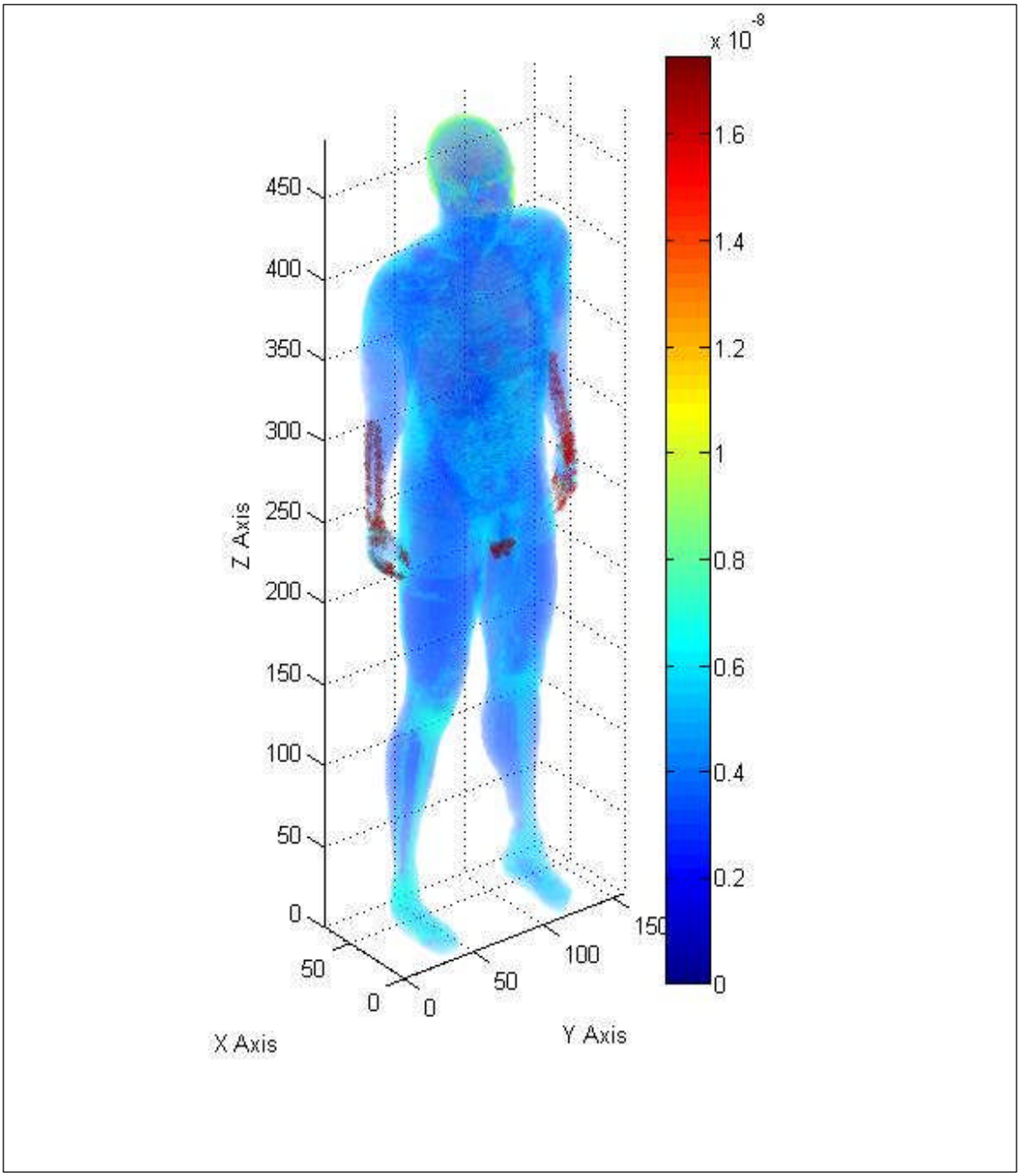

Fig. 16.4. Three-dimensional human dose profile from a 0.66 MeV Ir-192 electron source located within the skin.

Sr-90 organ dose profile

A Sr-90 source located within the skin would deliver a dose to the selected organs that ranges from a high of 1.42 x 10^{-8} MeV/g for the trachea and a low of 7.29 x 10^{-11} MeV/g for the skin. This organ dose contribution is from a single beta radiation with a maximum energy of 0.55 MeV. The beta radiation is produced with a yield of about 100%. Table 16.4 provides the calculated dose conversions for each of the selected organs that will be considered in this problem.

Table 16.4. Organ doses from a Sr-90 volume source in the skin.

Organs	MCNP Dose (MeV/g)	Std Deviation	MCNP Wght (g)	En Dep (MeV/his)	Organ Wt (g)	Organ Dose (MeV/g)	Organ Dose (Gy)
Skin	4.06E-06	3.07E-12	5.09E-02	2.06E-07	2830	7.29E-11	1.17E-20
Rib Bone Group	1.04E-04	2.26E-10	6.58E-02	6.87E-06	2167	3.17E-09	5.08E-19
Small Int	2.28E-05	2.57E-10	4.81E-02	1.10E-06	640	1.71E-09	2.75E-19
Gonads	9.43E-06	1.78E-09	4.85E-02	4.58E-07	37.1	1.23E-08	1.98E-18
Rectum	2.16E-06	6.14E-10	4.90E-02	1.06E-07	63	1.68E-09	2.69E-19
Thyroid	3.73E-07	4.27E-10	4.90E-02	1.83E-08	19.6	9.32E-10	1.49E-19
Lung	1.20E-04	1.55E-10	1.21E-02	1.46E-06	999	1.46E-09	2.34E-19
Eyes	1.15E-06	1.47E-09	4.90E-02	5.63E-08	15	3.75E-09	6.01E-19
Trachea	2.90E-06	3.52E-09	4.90E-02	1.42E-07	10	1.42E-08	2.28E-18
Colon	1.30E-05	2.89E-10	4.90E-02	6.38E-07	369	1.73E-09	2.77E-19
Stomach	9.55E-06	7.47E-10	4.90E-02	4.68E-07	150	3.12E-09	4.99E-19

As expected, the trachea received the greatest dose from a moderately energetic beta particle source located within the skin. The gonads received approximately 80 percent of the dose compared to the dose received by the trachea.

Statistical checks were performed on the Sr-90 dose output file. The same warnings present with Co-60 were observed. The 10 statistical checks for tally-four missed five of the 10 checks. The relative error was 0.51, VoV did not decrease according to the inverse of the number of histories and the value was 0.3, the FOM was not constant and increased, and the pdf was 0. The 10 statistical checks for tally-six passed. Of the 61 tally bins, one bin had a zero value and 48 bins had relative errors

exceeding 0.10 for the 0.55 MeV beta particle. Figure 16.5 provides a simulated 3-dimensional view of the human body with a color profile that shows the organ dose for the beta radiation of Sr-90. The color bar units to the right of the phantom are in MeV/organ weight in grams.

Y-90 organ dose profile

A Y-90 source located within the skin would deliver a dose to the selected organs that ranges from a high of 1.42×10^{-8} MeV/g for the trachea and a low of 1.90×10^{-10} MeV/g for the skin. This organ dose contribution is from a single beta radiation with a maximum energy of 2.28 MeV. The beta radiation is produced with a yield of about 100%. Table 16.5 provides the calculated dose conversions for each of the selected organs that will be considered in this problem.

Table 16.5. Organ doses from a Y-90 volume source in the skin.

Organs	MCNP Dose (MeV/g)	Std Deviation	MCNP Wght (g)	En Dep (MeV/his)	Organ Wt (g)	Organ Dose (MeV/g)	Organ Dose (Gy)
Skin	1.06E-05	3.45E-12	5.09E-02	5.39E-07	2830	1.90E-10	3.05E-20
Rib Bone Group	1.73E-03	1.24E-09	6.58E-02	1.14E-04	2167	5.26E-08	8.43E-18
Small Int	6.08E-04	2.67E-09	4.81E-02	2.92E-05	640	4.57E-08	7.32E-18
Gonads	1.15E-04	1.21E-08	4.85E-02	5.57E-06	37.1	1.50E-07	2.41E-17
Rectum	3.91E-05	3.80E-09	4.90E-02	1.92E-06	63	3.04E-08	4.88E-18
Thyroid	1.33E-05	6.23E-09	4.90E-02	6.52E-07	19.6	3.32E-08	5.33E-18
Lung	2.83E-03	1.40E-09	1.21E-02	3.44E-05	999	3.44E-08	5.51E-18
Eyes	1.62E-05	1.10E-08	4.90E-02	7.93E-07	15	5.28E-08	8.47E-18
Trachea	3.64E-05	1.91E-08	4.90E-02	1.78E-06	10	1.78E-07	2.86E-17
Colon	4.22E-04	3.50E-09	4.90E-02	2.07E-05	369	5.60E-08	8.97E-18
Stomach	2.31E-04	6.53E-09	4.90E-02	1.13E-05	150	7.54E-08	1.21E-17

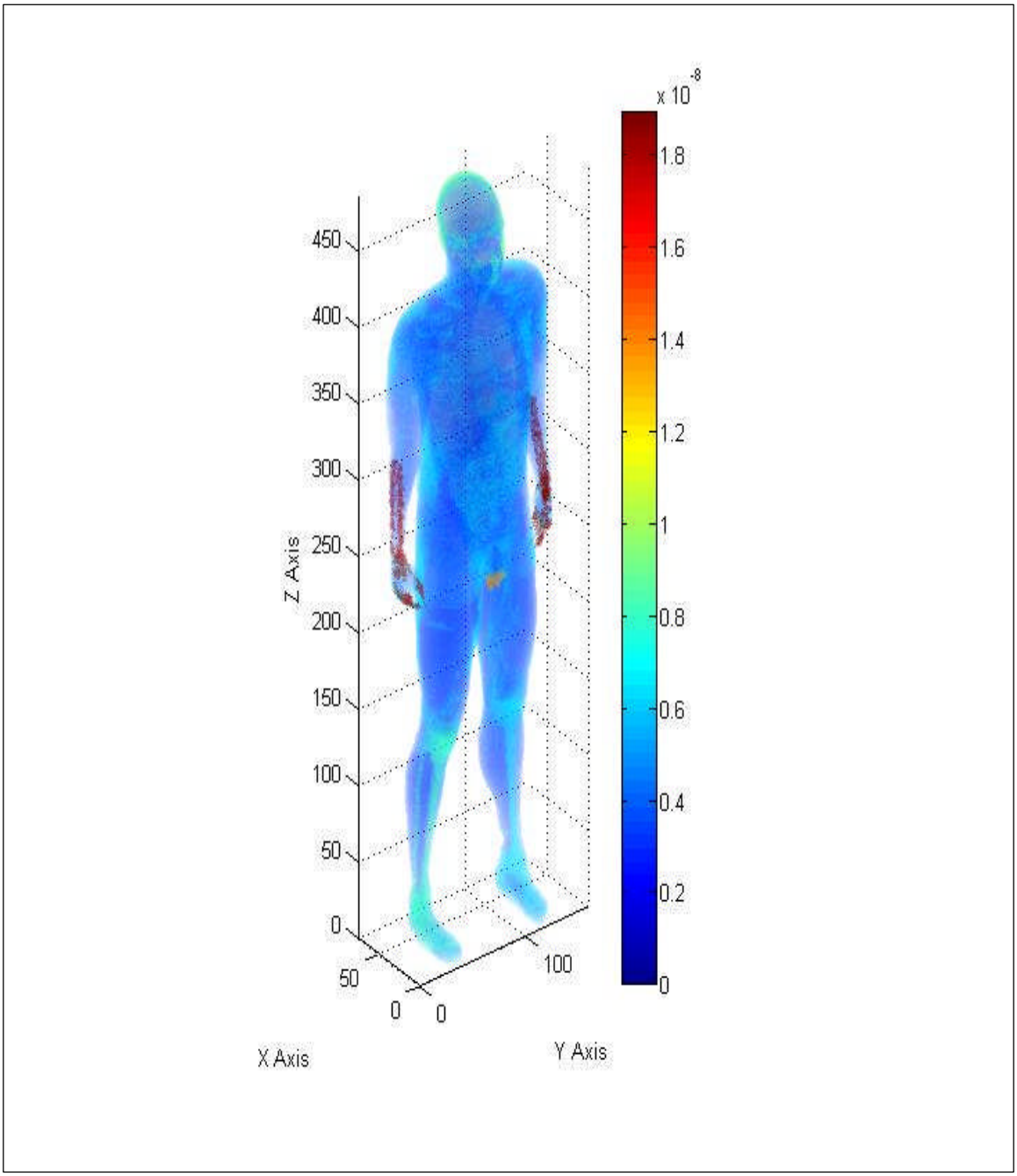

Fig. 16.5. Three-dimensional human dose profile from a Sr-90 beta source located within the skin.

As expected with Sr-90, the trachea received the highest dose from a highly-energetic beta radiation source located within the skin. The stomach received approximately twenty percent less dose than the dose to the trachea. The Y-90 skin dose was approximately three times the dose to the skin from Sr-90.

Statistical checks were performed on the Y-90 dose output file. The same warnings present with Co-60 were observed. The 10 statistical checks for tally-four fluence passed all but four checks. The relative error was 0.27, The VoV was 0.25, the VoV did not decrease according to the inverse of the number of histories and the pdf was 0. The 10 statistical checks for tally-six dose passed. Of the 61 tally bins, no bin had a zero dose and 24 bins had relative errors exceeding 0.10 for the 2.28 MeV beta radiation. Figure 16.6 provides a simulated 3-dimensional view of the human body with a color profile that shows the organ dose for the 0.55 MeV beta radiation of Sr-90. The color bar units to the right of the phantom are in MeV/organ weight in grams.

Results from skin volume source

Figure 16.7 provides an overview of all of the potential sources distributed in the skin. Based upon the results of the observed programs, Co-60 is the most limiting radionuclide. The trachea followed by the gonads and stomach appears to be the most sensitive organs based upon a single emission from a source located within the skin. The dose delivered to the organs from Ir-192 and Cs-137 appears to be equivalent within their respective error of margin. The overall organ dose from the three photon sources appear to deliver a dose that is approximately 100 times the dose delivered from the highest beta source of Y-90. Even though the trachea shows a higher sensitivity than the lung, the dose is a little deceiving. The observed dose for the trachea is based on the number of voxels which include the air encircled by the trachea.

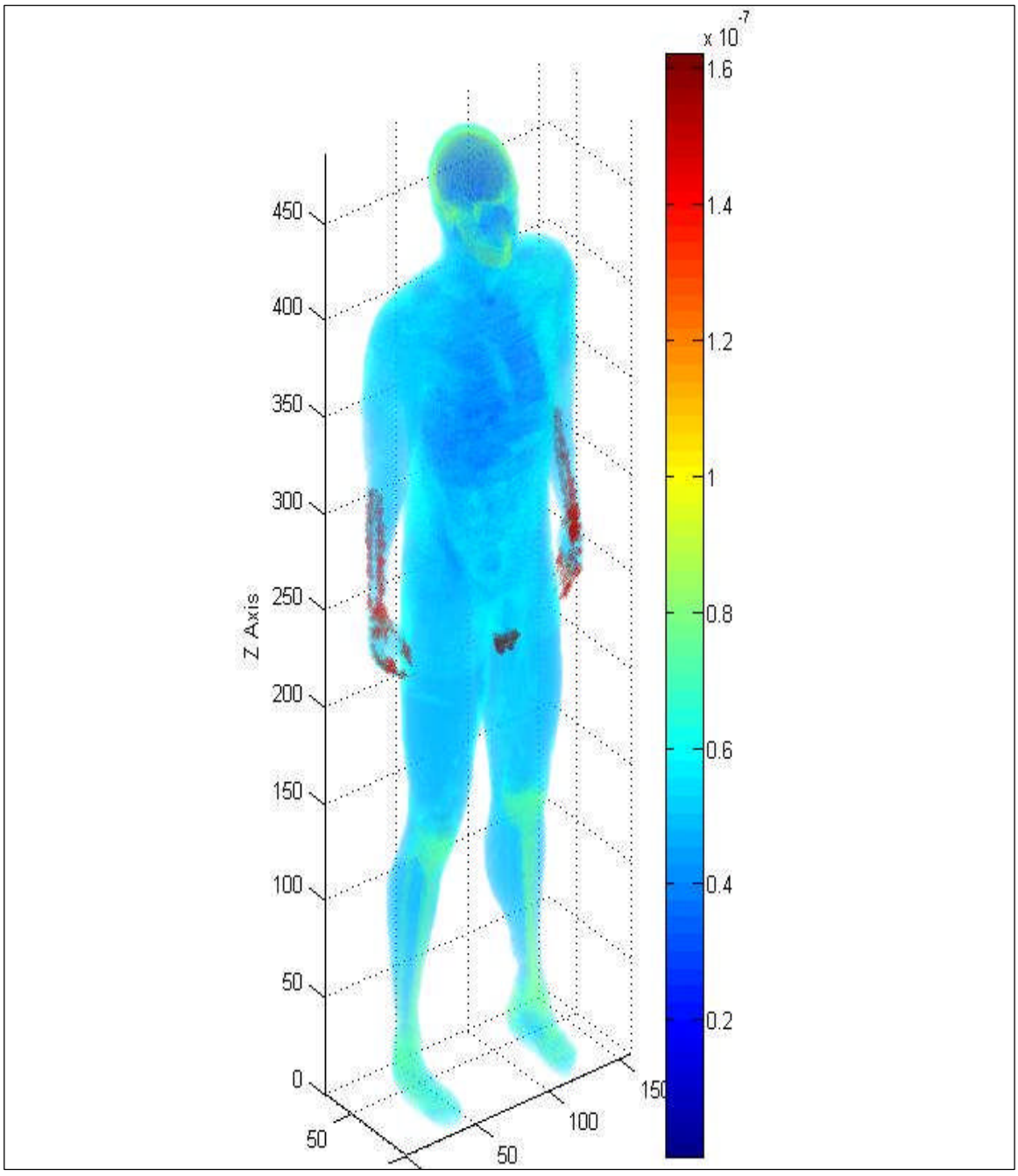

Fig. 16.6. Three-dimensional human dose profile from a Y-90 electron source located within the skin.

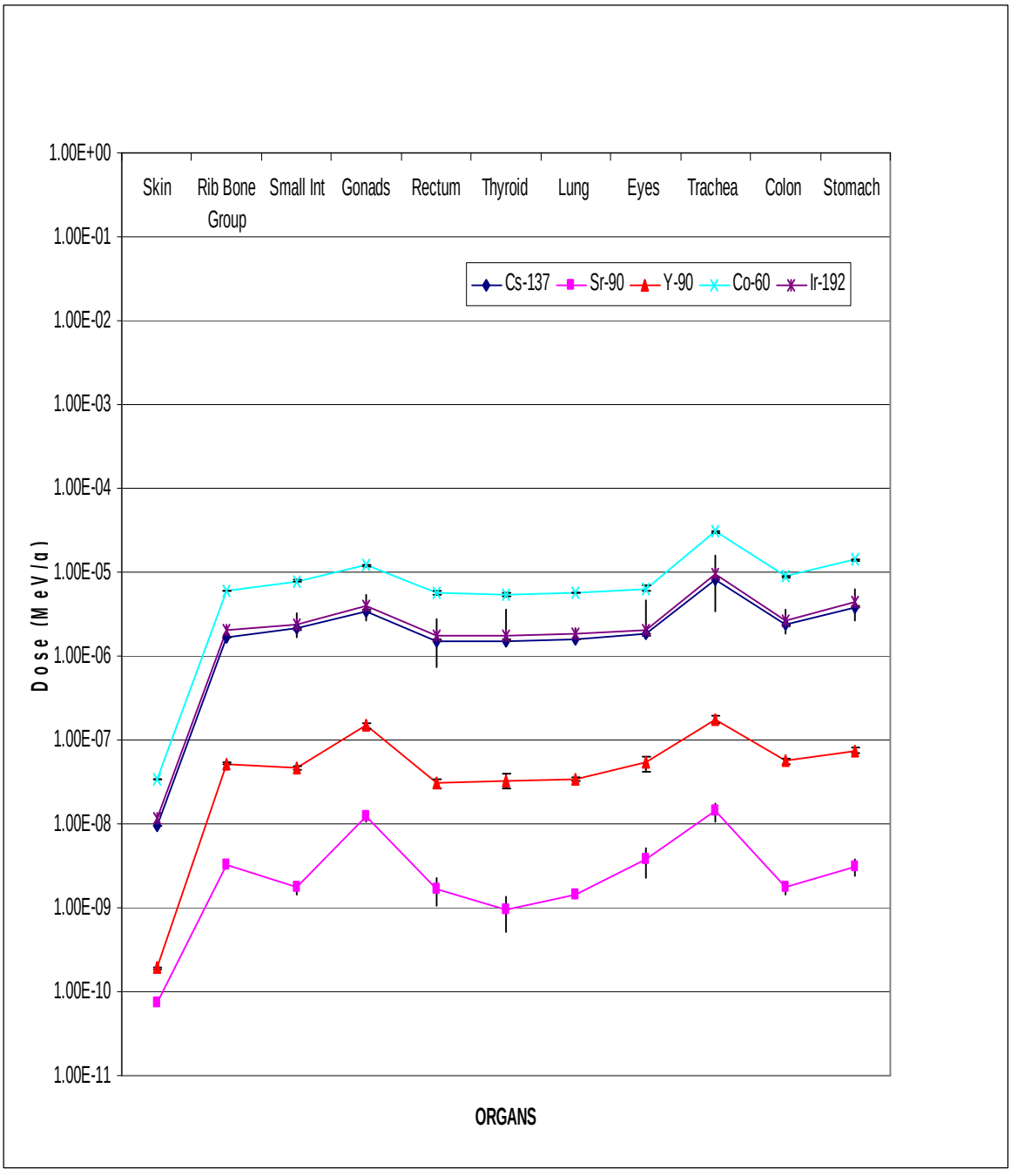

Fig. 16.7. Comprehensive graph of organ doses for the five potential skin sources.

CHAPTER XVII
ESTIMATING ORGAN DOSE BASED ON VOLUME SOURCES IN THE LUNG, STOMACH, SMALL INTESTINE AND COLON ONE HOUR AFTER A LUNG INHALATION

Dose to multiple organ verification

The MATLAB subprogram Simulink was used to build a time dependant activity profile program that would calculate organ activities over time (MathWorks 2007). Based on the most probable exposure route for an RDD event, the program was simulated to calculate activity over time using the current ICRP-30 internal dose model (ICRP 1978). By utilizing typical response times for emergency responders, time frames of one, six, 12 and 24 hour post detonation where chosen to provide dose and organ activities at specific times to assist emergency responders in assessing injured personnel as well as establishing response time limits for emergency responders. Total activity for each organ was established based on the pre-selected time intervals. The MATLAB program file named Shannon, normalizes the activity in each source organ to one disintegration per second. Based on the number of source voxels in each source organ, a probability is calculated from the normalized activity for each organ. The number of source voxels in each source organ is based on the fraction of source voxels in the lung, a source volume of 15,000 lung voxels per 87,506 total lung voxels was selected and the number of source particles chosen was one million. Being the most limiting of the five sources, Co-60 was chosen as the first test source for our phantom model. To keep things simple, two simulations were set up. The first simulation analyzed the lower energy photon of 1.17 MeV and the second simulation tracked a 1.33 MeV photon. Volumes and masses were checked against ICRU-46 established values for both simulations (ICRU 1990).

The MCNP output file provides a dose to all tissues defined within the phantom. The dose is listed in g/cm3 and applies to a single voxel. The dose is based on the

average energy deposited per unit mass for a single history. In this case, a single 1.17MeV photon would deliver an average dose of 4.56 ± 0.0008 MeV/g of tissue contained in a single voxel. In order to derive any meaningful information from this value, simple calculated dose conversions were applied to create a dose in gray (Gy) for each organ. The above value provides an average lung dose of 8.87×10^{-15} Gy from a single 1.17 MeV photon when the photons originate within a lung, stomach, small intestine, liver and colon volume source. Because of the extremely small dose from a single photon, the dose graphs are in units of MeV/g. Table 17.1 provides calculated dose conversions for each of the selected organs at time (T) plus one hour from detonation.

Table 17.1. Organ doses from Co-60 volume source in multiple organs at T plus one hour.

Organs	No. of Sources in Organ	Activity normalized to 1	MCNP Dose (MeV/g)/his	Std Deviation	Organ Dose (MeV/g)/his	Organ Dose (Gy)/his
Skin	0	0.00E+00	6.97E-04	3.00E-11	1.25E-08	2.01E-18
Rib Bone Group	0	0.00E+00	1.48E+00	9.85E-08	4.48E-05	7.17E-15
Small Int	3499	1.10E-02	2.57E-01	2.35E-07	1.93E-05	3.09E-15
Gonads	0	0.00E+00	3.23E-04	7.79E-08	4.22E-07	6.76E-17
Rectum	0	0.00E+00	1.63E-03	1.04E-07	1.27E-06	2.03E-16
Thyroid	0	0.00E+00	2.04E-02	1.19E-06	5.09E-05	8.15E-15
Lung	15000	5.95E-01	9.58E+00	1.86E-07	1.16E-04	1.86E-14
Eyes	0	0.00E+00	7.08E-04	2.78E-07	2.31E-06	3.7E-16
Trachea	0	0.00E+00	4.98E-02	4.00E-06	2.44E-04	3.91E-14
Colon	2124	1.02E-03	1.19E-01	2.29E-07	1.58E-05	2.53E-15
Stomach	1400	2.00E-02	4.35E-01	1.05E-06	1.42E-04	2.27E-14

As expected, the majority of the activity remains in the lung at time T plus one hour. The stomach contains the second highest activity. For Co-60, the most sensitive organ is the trachea followed by the stomach, lung and small intestine. Compared to the Co-60 dose with a source located in just the lung, the lung dose was 1.21×10^{-4} MeV/g and from multiple source organs the lung dose was 1.16×10^{-4} MeV/g. The stomach dose from Co-60 with a source located only in the stomach was 1.33×10^{-3} MeV/g and

from multiple source organs the stomach dose was 1.42 x 10^{-4} MeV/g or approximately 10 percent of the stomach dose with the source located only in the stomach.

Statistical analysis of output file

The tally-four fluence analysis for each detector, setup as described in chapter VII, provided a random behavior for the mean. The desired relative error should be less than 0.10 and the observed relative error was 0.02. The desired and observed relative errors decreased according to the inverse of the square root of the number of histories. The desired variance of the variance should be less than 0.10 and the observed VoV was 0.00. The figure of merit value was constant and the behavior was random. The probability density function (pdf) desired should be greater than three, the observed pdf value was 10. The tally-four fluence passed all 10 statistical checks. Out of 10 tally-four bins, only one had a zero dose value and no bins contained relative errors greater than 0.10. The second 1.33 MeV photon simulation provided similar results.

The tally-six dose analysis for each material provided a random behavior for the mean. The desired relative error should be less than 0.10 and the observed relative error was 0.00 for the 1.17 MeV photon and 0.00 for the 1.33 MeV photon. The desired and observed relative errors decreased according to the inverse of the square root of the number of histories. The desired variance of the variance should be less than 0.10 and the observed VoV was 0.00. The figure of merit value was constant and the behavior was random. The desired probability density function (pdf) should be greater than 3.00 and the observed value was 5.51 for the 1.17 MeV photon and 5.57 for the 1.33 MeV photon. The tally-six dose passed all 10 statistical checks. Out of 61 tally-six bins, no bin had a zero dose and only 6 bins contained relative errors greater than 0.10.

Co-60 organ dose Profile

A Co-60 source located within the multiple organs specified above would deliver a dose to the selected organs that ranges from a high or 1.42×10^{-4} MeV/g for the stomach and a low of 1.25×10^{-8} MeV/g for the skin after one hour from initial exposure. This organ dose contribution is the sum of two photons emitted from Co-60 that occur with a yield of about 100 percent. Figure 17.1 provides a simulated 3-dimensional view of the human body with a color profile that equates the organ dose for the 1.33 MeV photon of Co-60. Each axis is represented in the figure along with a color bar that indicates the organ dose in MeV/organ in grams provided by the MCNPX output file. In the MCNPX output file, the trachea receives a slightly lesser dose than the lung based upon the number of voxels versus the measured gram weight of the trachea. The phantom includes the airway as part of the trachea. The stomach becomes the most sensitive organ.

Cs-137 organ dose profile

A Cs-137 source located within the lung, stomach, liver, small intestine and colon would deliver a dose to the selected organs at T plus one hour that ranges from a high of 1.08×10^{-4} MeV/g for the stomach and a low of 3.41×10^{-9} MeV/g for the skin. This organ dose contribution is from a 0.66 MeV photon emitted from Cs-137 that occurs with a yield of about 86 percent. Table 17.2 provides the dose output to the selected organs at time (T) plus one hour after exposure.

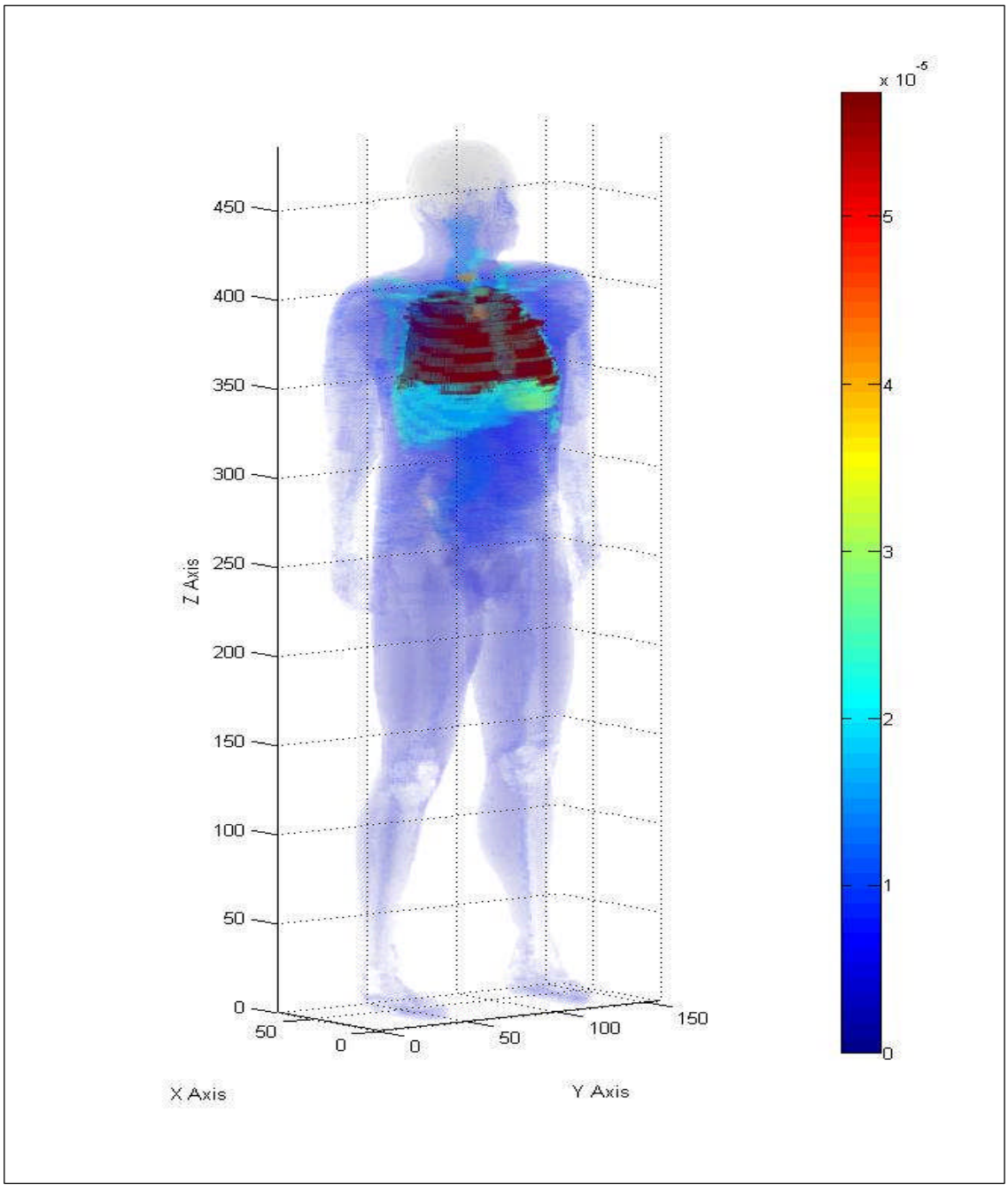

Fig. 17.1. Three-dimensional human dose profile from a 1.33 MeV photon source located within multiple organs after time T plus one hour.

Table 17.2. Organ doses for a Cs-137 volume source in multiple organs at T plus one hour.

Organs	No. of Sources in Organ	Activity normalized to 1	MCNP Dose (MeV/g)/his	Std Deviation	Organ Dose (MeV/g)/his	Organ Dose (Gy)/his
Skin	0	0.00E+00	1.90E-04	4.10E-12	3.41E-09	5.47E-19
Rib Bone Group	0	0.00E+00	4.14E-01	1.38E-08	1.26E-05	2.01E-15
Small Int	3499	0.00E+00	6.91E-02	3.22E-08	5.19E-06	8.32E-16
Gonads	0	0.00E+00	5.18E-05	8.69E-09	6.78E-08	1.09E-17
Rectum	0	0.00E+00	3.40E-04	1.26E-08	2.65E-07	4.24E-17
Thyroid	0	0.00E+00	5.22E-03	1.58E-07	1.30E-05	2.09E-15
Lung	15000	2.63E-01	2.54E+00	2.78E-08	3.09E-05	4.95E-15
Eyes	0	0.00E+00	1.53E-04	3.29E-08	4.98E-07	7.98E-17
Trachea	0	0.00E+00	1.28E-02	5.31E-07	6.25E-05	1E-14
Colon	2124	0.00E+00	3.42E-02	3.18E-08	4.55E-06	7.28E-16
Stomach	1400	7.12E-02	3.30E-01	2.37E-07	1.08E-04	1.73E-14

As expected, unlike Co-60, the majority of the activity has been absorbed by the body at time T plus one hour. Of the activity that remains, the lung contains the largest percent followed by the stomach. For Cs-137, the most sensitive organ is the stomach followed by the trachea and lung. Compared to the Cs-137 dose with a source located in just the lung, the lung dose was 3.60×10^{-5} MeV/g and from multiple source organs the lung dose was 3.09×10^{-5} MeV/g. The stomach dose from Cs-137 with a source located only in the stomach was 3.90×10^{-4} MeV/g and from multiple source organs the dose was 1.08×10^{-4} MeV/g. This produced a reduction in the stomach dose by approximately 25 percent. The Co-60 multiple source organ dose to the lung dose was 1.16×10^{-4} MeV/g and from Cs-137, the multiple source organ dose to the lung was 3.09×10^{-5} MeV/g. The lung dose was reduced by approximately 25 percent. The stomach dose from multiple source organs containing Co-60 was 1.42×10^{-4} MeV/g and for Cs-137 it was 1.08×10^{-4} MeV/g or reduced by approximately 33 percent, respectively.

Statistical checks were performed on the Cs-137 dose output file. The same warnings present with Co-60 were observed. The 10 statistical checks for tally-four fluence passed and produced similar results. The 10 statistical checks for tally-six dose passed and produced similar results as with Co-60. Of the 61 tally bins, no bins had a zero dose and 8 bins had relative errors exceeding 0.10. Figure 17.2 provides a

simulated 3-dimensional view of the human body with a color profile that shows the MCNP dose for the single photon of Cs-137. The color bar units to the right of the phantom are in MeV/organ weight in grams.

At T plus one hour, the most sensitive organ for a Co-60 exposure was the trachea that received a dose of 1.16×10^{-4} MeV/g. For a Cs-137 exposure, the most sensitive organ was the stomach which received a dose of 1.08×10^{-4} MeV/g. The change in organ sensitivity can be attributed to the difference in activity present in the lung and stomach at T plus one hour. For Co-60, 59 percent of the activity remains in the lung while only 26 percent of the activity remains in the lung for Cs-137. Co-60 transfers 2.0 percent of the activity to the stomach while Cs-137 transfers 7.1 percent of the activity to the stomach.

Ir-192 organ dose profile

An Ir-192 source located within the lung, stomach, liver, small intestine and colon would deliver a dose to the selected organs at T plus one hour that ranges from a high of 1.15×10^{-4} MeV/g for the stomach and a low of 3.89×10^{-9} MeV/g for the skin. This organ dose contribution is from the sum of two photons with energies of 0.47 MeV and 0.32 MeV along with two electrons with maximum energies of 0.66 MeV and 0.54 MeV. All four particles are produced with a yield of 26.2%, 22.4%, 10.1% and 6.7%, respectively. Table 17.3 provides the calculated dose conversions for each of the selected organs at time (T) plus one hour from detonation.

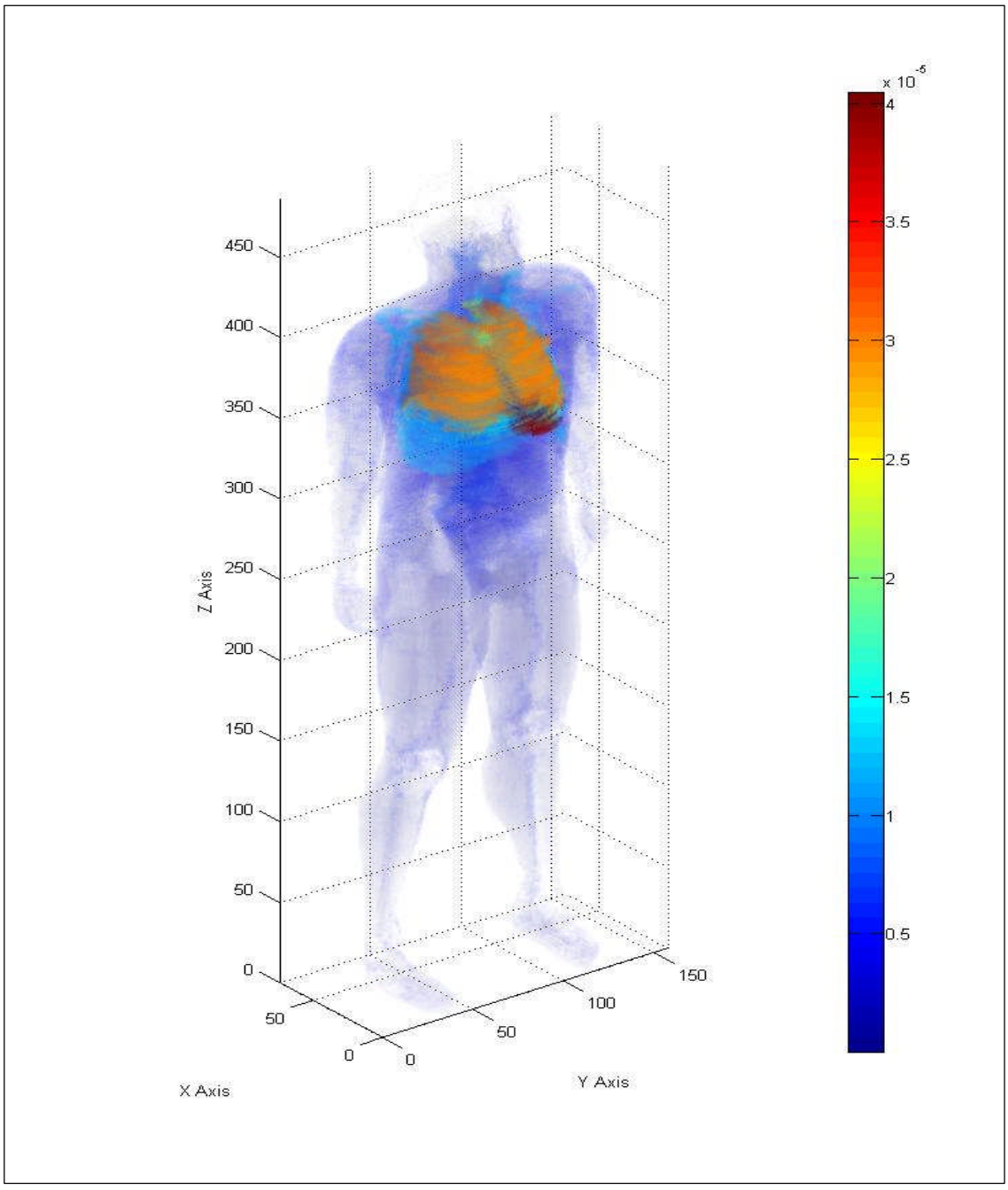

Fig. 17.2. Three-dimensional human dose profile from a Cs-137 photon source located within multiple organs after time T plus one hour.

Table 17.3. Organ doses for an Ir-192 volume source in multiple organs at T plus one hour.

Organs	No. of Sources in Organ	Activity normalized to 1	MCNP Dose (MeV/g)/his	Std Deviation	Organ Dose (MeV/g)/his	Organ Dose (Gy)/his
Skin	0	0.00E+00	2.16E-04	1.70E-10	3.89E-09	6.23E-19
Rib Bone Group	0	0.00E+00	4.64E-01	4.40E-07	1.41E-05	2.26E-15
Small Int	3499	6.30E-02	3.82E-01	1.17E-06	2.87E-05	4.59E-15
Gonads	0	0.00E+00	1.30E-04	1.97E-07	1.71E-07	2.73E-17
Rectum	0	0.00E+00	1.11E-03	6.56E-07	8.60E-07	1.38E-16
Thyroid	0	0.00E+00	5.32E-03	3.72E-06	1.33E-05	2.13E-15
Lung	15000	2.63E-01	2.65E+00	5.97E-07	3.21E-05	5.15E-15
Eyes	0	0.00E+00	1.48E-04	5.17E-07	4.82E-07	7.72E-17
Trachea	0	0.00E+00	1.31E-02	1.22E-05	6.41E-05	1.03E-14
Colon	2124	7.36E-03	1.08E-01	1.18E-06	1.44E-05	2.3E-15
Stomach	1400	7.12E-02	3.52E-01	4.29E-06	1.15E-04	1.84E-14

As expected and unlike Cs-137, the majority of the activity remains in the lung but has begun to pass through the stomach, small intestine and colon. Of the 63 percent of activity that started in the lung, the lung retains 26 percent, seven percent is in the stomach and approximately 6.3 percent is in the small intestine. The most sensitive organ for Ir-192 was the stomach followed by the lung, small intestine and colon. Compared to the Ir-192 dose with a source located in just the lung, the lung dose was 4.48×10^{-5} MeV/g and from multiple source organs the lung dose was 3.21×10^{-5} MeV/g. The stomach dose from Ir-192 with a source located only in the stomach was 3.76×10^{-5} MeV/g and from multiple source organs the dose was 1.15×10^{-4} MeV/g. This produced an increase in the stomach dose by approximately three times.

Statistical checks were performed on the Ir-192 dose output file. The same warnings present with Co-60 were observed. The 10 statistical checks for tally-four photons passed and produced similar results as with Co-60 were observed. The 10 statistical checks for tally-six photons passed and produced similar results as with Co-60. Of the 61 tally bins, no bins had a zero dose and 6 bins had relative errors exceeding 0.10 for the 0.47 MeV photon. The 0.32 MeV photon produced similar results. The tallies for the electron sources within the organs had to be evaluated in a slightly different manner based on their inability to penetrate uniformly throughout the phantom.

Secondary emissions, such as bremsstrahlung and characteristics x rays were the primary radiation source for organs outside of the source organs. Three of the 10 statistical checks did not pass. The relative error was 0.26, the VoV was 0.14 and the pdf was 0. This reflects a large number of zero doses and slightly greater than zero doses based on the volume electron sources.

Figure 17.3 and 17.4 provide a simulated 3-dimensional view of the human body with a color profile that shows the MCNP dose for the 0.47 MeV photon of Ir-192 and the 0.66 MeV electron of Ir-192 absorbed by each organ, respectively. The color bar units to the right of the phantom are in MeV/organ weight in grams.

Sr-90 organ dose profile

A Sr-90 source located within the lung, stomach, liver, small intestine and colon would deliver a dose to the selected organs at T plus one hour after exposure that ranges from a high of 4.41×10^{-7} MeV/g for the stomach and a low of 4.57×10^{-12} MeV/g for the skin. This organ dose contribution is from a single beta emission with a maximum energy of 0.57 MeV. The beta emission is produced with a yield of about 100%. Table 17.4 provides the calculated dose conversions for each of the selected organs that will be considered in this problem.

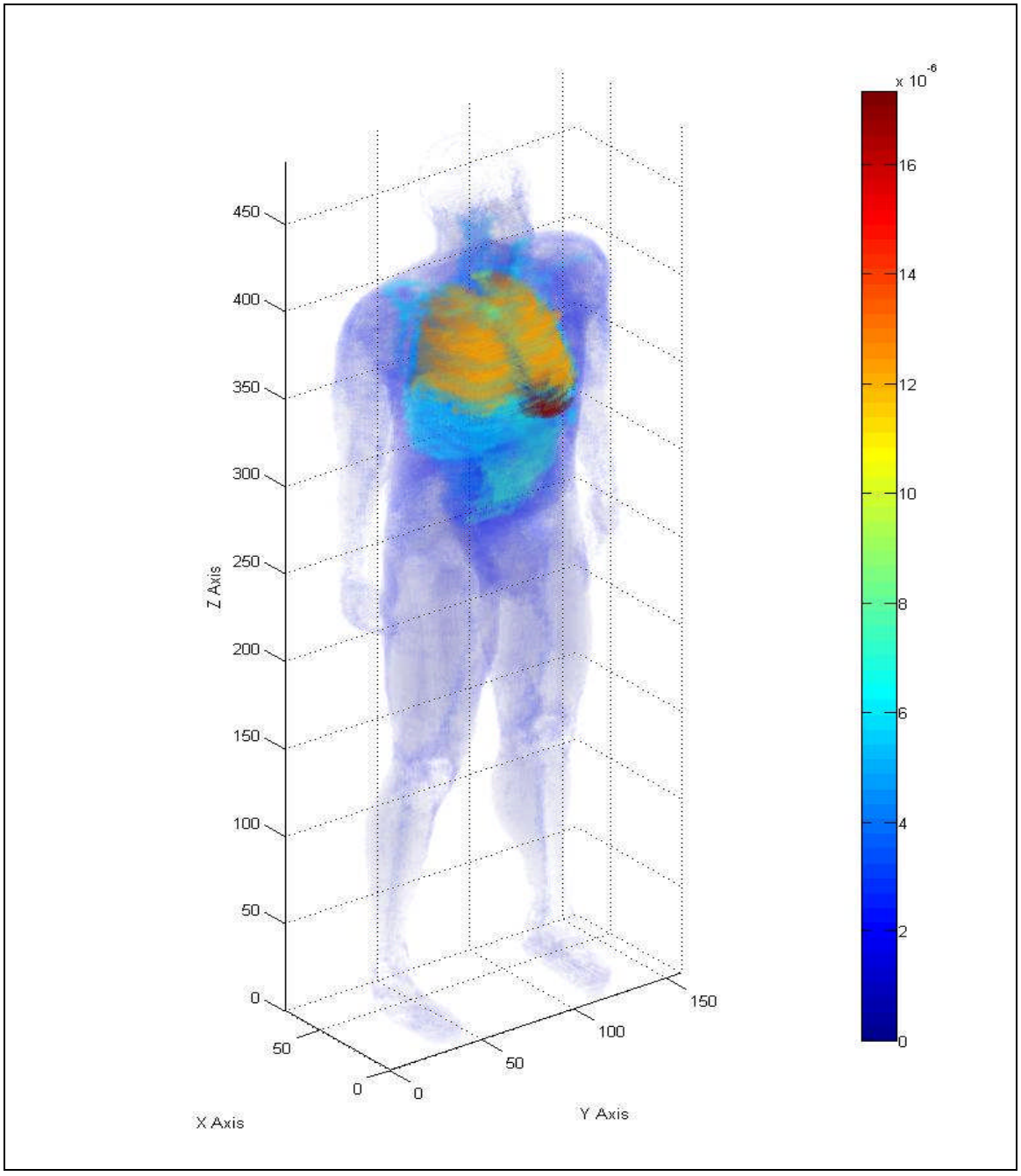

Fig. 17.3. Three-dimensional human dose profile from a 0.47 MeV Ir-192 photon source located within multiple organs after T plus one hour.

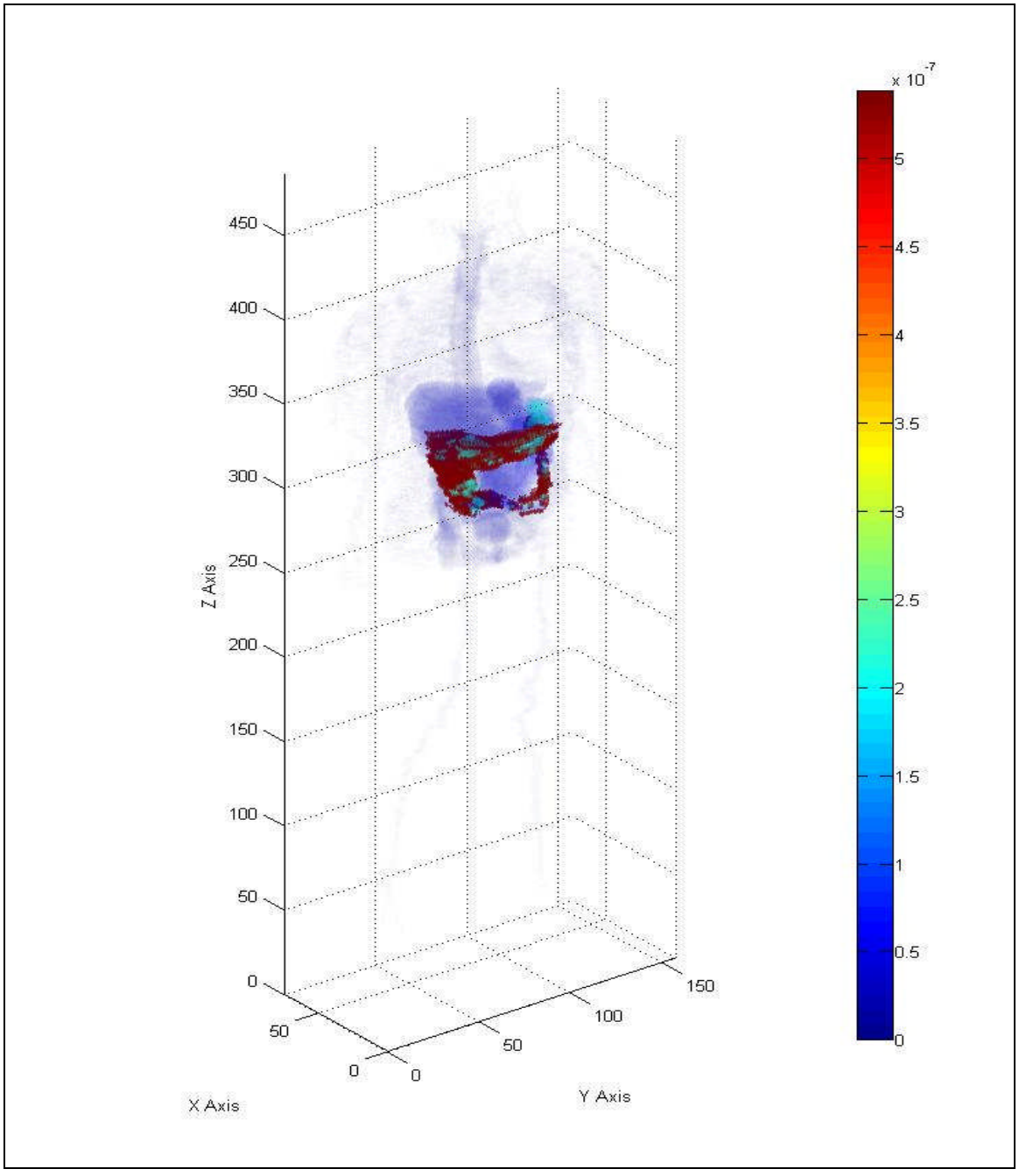

Fig. 17.4. Three-dimensional human dose profile from a 0.66 MeV Ir-192 electron source located within multiple organs after T plus one hour.

Table 17.4. Organ doses from a Sr-90 volume source in multiple organs at time T plus one hour.

Organs	No. of Sources in Organ	Activity normalized to 1	MCNP Dose (MeV/g)/his	Std Deviation	Organ Dose (MeV/g)/his	Organ Dose (Gy)/his
Skin	0	0.00E+00	2.54E-07	1.01E-13	4.57E-12	7.32E-22
Rib Bone Group	0	0.00E+00	1.96E-03	9.09E-10	5.94E-08	9.51E-18
Small Int	3499	6.10E-02	1.34E-03	1.91E-09	1.00E-07	1.61E-17
Gonads	0	0.00E+00	1.36E-07	1.78E-10	1.78E-10	2.85E-20
Rectum	0	0.00E+00	1.32E-06	3.15E-10	1.02E-09	1.64E-19
Thyroid	0	0.00E+00	1.07E-05	3.81E-09	2.68E-08	4.3E-18
Lung	15000	2.64E-01	1.54E-02	1.63E-09	1.87E-07	3E-17
Eyes	0	0.00E+00	1.15E-07	3.75E-10	3.75E-10	6E-20
Trachea	0	0.00E+00	3.72E-05	1.57E-08	1.82E-07	2.92E-17
Colon	2124	7.16E-03	2.51E-04	1.27E-09	3.34E-08	5.34E-18
Stomach	1400	7.18E-02	1.35E-03	7.46E-09	4.41E-07	7.07E-17

As expected, the most sensitive organ is the stomach followed by the lung, trachea and small intestine. Of the 63 percent of activity that started in the lung, the lung retained 26 percent. There was 7.1 percent of the activity in the stomach and approximately 6.1 percent in the small intestine. Compared to the Sr-90 dose with a source located in just the lung, the lung dose was 2.79×10^{-7} MeV/g and the lung dose from multiple source organs was 1.87×10^{-7} MeV/g. The stomach dose from Sr-90 with a source located only in the stomach was 6.76×10^{-8} MeV/g and the stomach dose from multiple source organs was 4.41×10^{-7} MeV/g. This produced an increase in the stomach dose by roughly seven times.

Statistical checks were performed on the Sr-90 dose output file. The same warnings present with Co-60 were observed. The 10 statistical checks for tally-four fluence missed three of the 10 checks. The relative error was 0.28, VoV was 0.16 and the pdf was 0. The 10 statistical checks for tally-six dose passed with the exception of the VoV that does not appear to decrease according to the inverse of the number of histories for the last half of the problem. Of the 61 tally bins, 4 bins had a zero dose and 34 bins had relative errors exceeding 0.10 for the 0.55 MeV beta emission. Figure 17.5 provides a simulated 3-dimensional view of the human body with a color profile that

shows the organ dose for the beta radiation of Sr-90. The color bar units to the right of the phantom are in MeV/organ weight in grams.

Y-90 organ dose profile

A Y-90 source located within the lung, stomach, liver, small intestine and colon would deliver a dose to the selected organs at T plus one hour after exposure that ranges from a high of 3.73×10^{-6} MeV/g for the stomach and a low of 9.08×10^{-11} MeV/g for the skin. This organ dose contribution is from a single beta emission with a maximum energy of 2.28 MeV. The beta emission is produced with a yield of about 100%. Table 17.5 provides the calculated dose conversions for each of the selected organs that will be considered in this problem.

Table 17.5. Organ doses from a Y-90 volume source in multiple organs at time T plus one hour.

Organs	No. of Sources in Organ	Activity normalized to 1	MCNP Dose (MeV/g)/his	Std Deviation	Organ Dose (MeV/g)/his	Organ Dose (Gy)/his
Skin	0	0.00E+00	5.05E-06	7.72E-13	9.08E-11	1.46E-20
Rib Bone Group	0	0.00E+00	2.10E-02	3.37E-09	6.37E-07	1.02E-16
Small Int	3499	6.10E-02	1.21E-02	9.75E-09	9.11E-07	1.46E-16
Gonads	0	0.00E+00	4.29E-06	2.14E-09	5.61E-09	8.98E-19
Rectum	0	0.00E+00	2.59E-05	2.52E-09	2.01E-08	3.22E-18
Thyroid	0	0.00E+00	1.54E-04	2.08E-08	3.86E-07	6.18E-17
Lung	15000	5.95E-01	1.01E-01	5.75E-09	1.22E-06	1.96E-16
Eyes	0	0.00E+00	5.70E-06	9.32E-09	1.86E-08	2.98E-18
Trachea	0	0.00E+00	4.23E-04	7.65E-08	2.07E-06	3.32E-16
Colon	2124	7.16E-03	3.03E-03	7.44E-09	4.02E-07	6.45E-17
Stomach	1400	7.18E-02	1.14E-02	3.51E-08	3.73E-06	5.98E-16

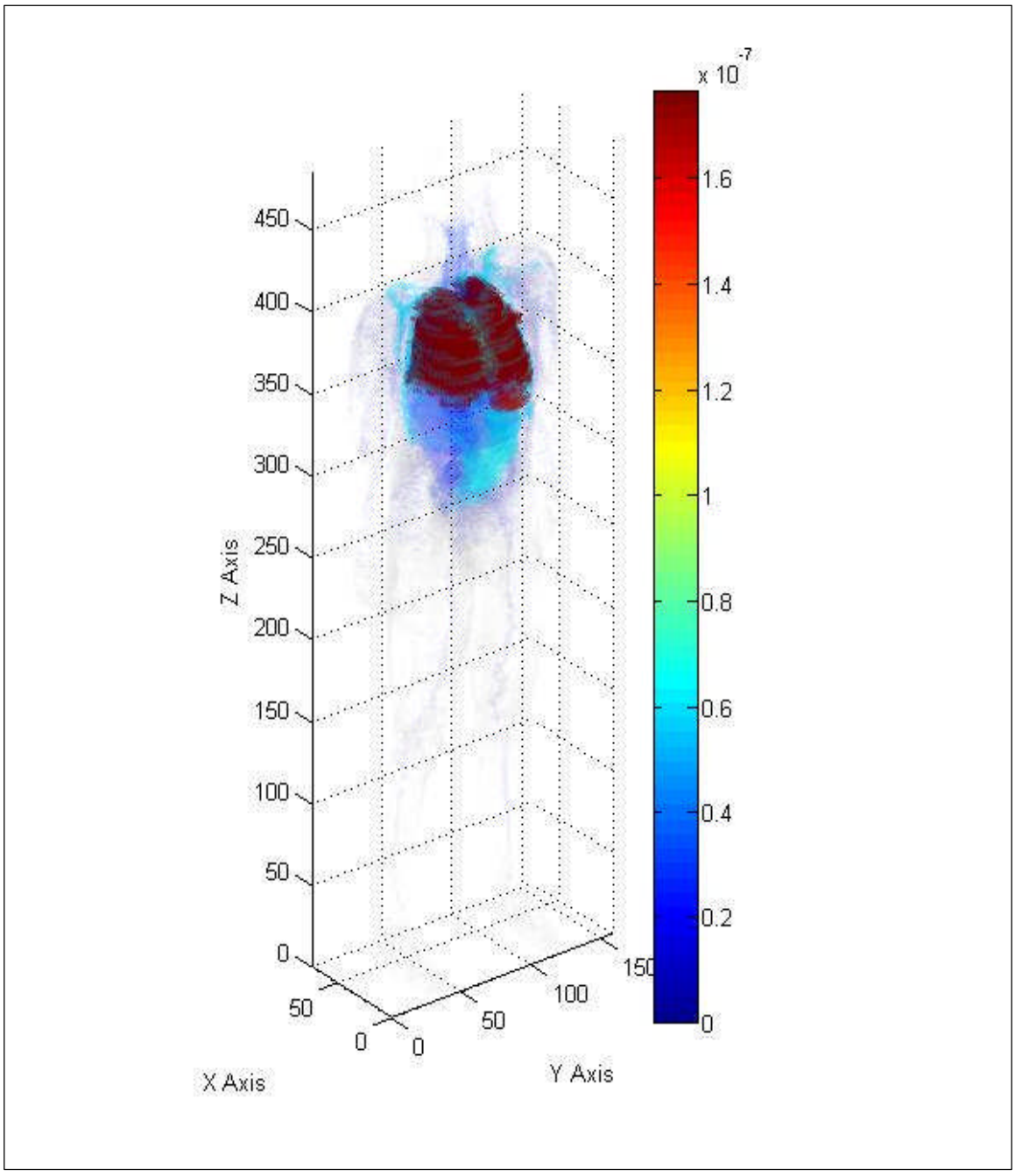

Fig. 17.5. Three-dimensional human dose profile from a Sr-90 beta source located within multiple organs after T plus one hour.

As expected and like Sr-90, the stomach, trachea and lung received the highest dose from a highly-energetic beta particle source located in multiple organs at time T plus one hour after exposure. Of the 63 percent of activity that started in the lung, the lung retained 26 percent. Based on the IRCP-30 methodology, the organ activity follows that of Sr-90. Compared to the Y-90 dose with a source located in just the lung, the lung dose was 1.75×10^{-6} MeV/g and the lung dose from multiple source organs was 1.22×10^{-6} MeV/g. The stomach dose from Y-90 with a source located only in the stomach was 1.70×10^{-5} MeV/g and the stomach dose from multiple source organs was 3.73×10^{-6} MeV/g. This produced a decrease in the stomach dose by roughly 25 percent.

Statistical checks were performed on the Y-90 dose output file. The same warnings present with Co-60 were observed. The 10 statistical checks for tally-four fluence passed all checks except the pdf which was 0. The 10 statistical checks for tally-six dose passed all but two of the checks. The VoV does not monotonically decrease over the last half of the problem nor does it decrease according to the inverse of the number of histories. Of the 61 tally bins, 1 bin had a zero dose and 27 bins had relative errors exceeding 0.10 for the 2.28 MeV beta emission. Figure 17.6 provides a simulated 3-dimensional view of the human body with a color profile that shows the MCNP dose for the beta radiation of Y-90. The color bar units to the right of the phantom are in MeV/organ weight in grams.

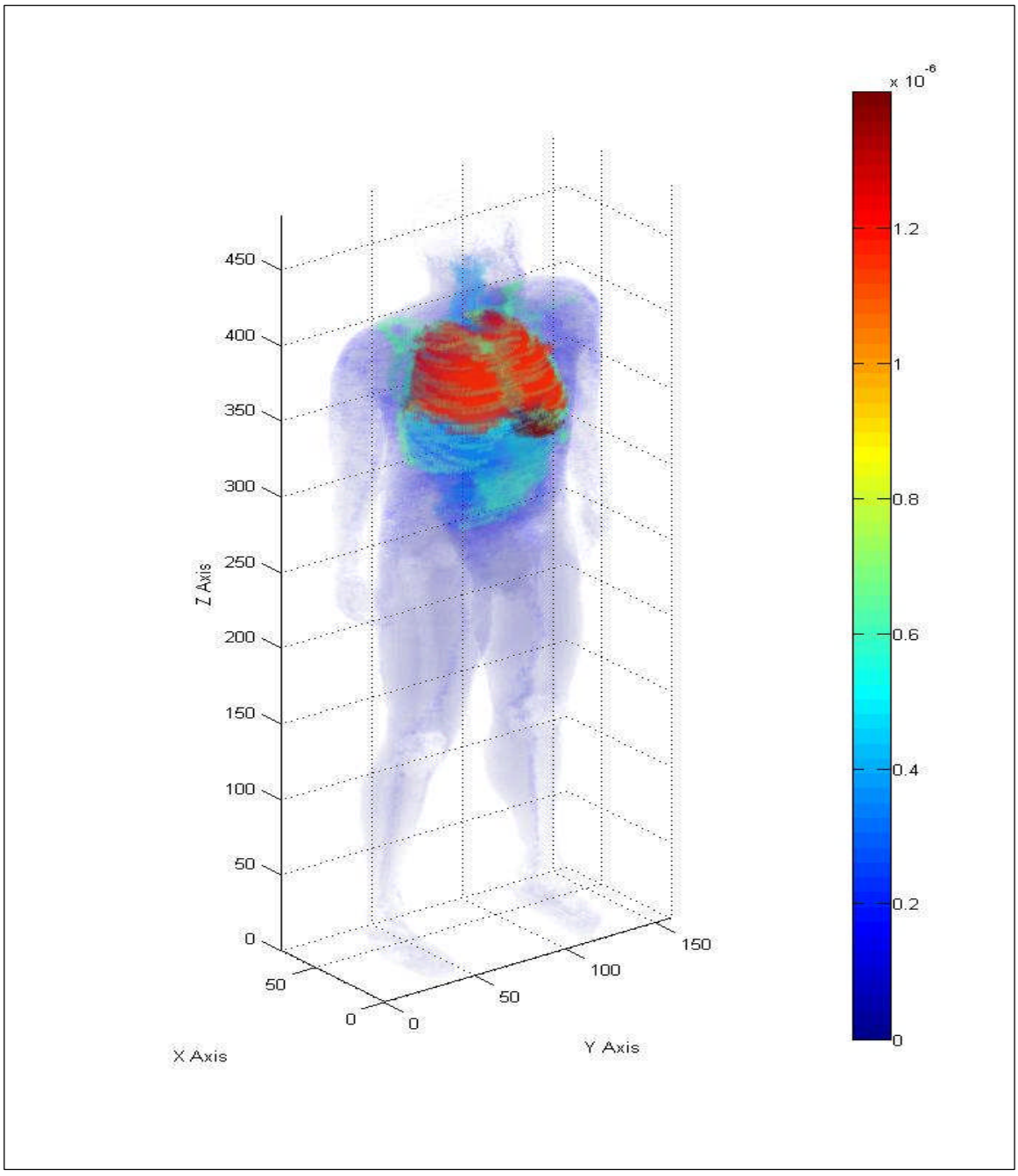

Fig. 17.6. Three-dimensional human dose profile from a Y-90 beta source located within multiple organs after T plus one hour.

Results from multi-organ lung, stomach, liver, small intestine and colon volume sources after one hour

Figure 17.7 provides a graph of all of the potential sources distributed in multiple organs at time T plus one hour. Based upon the results of the observed programs, after a one hour inhalation, Co-60 is the most limiting radionuclide of concern with the exception of the small intestine and stomach. Ir-192 appears to provide a higher dose to the small intestine. Ir-192, Co-60 and Cs-137 all appear to be within a margin of error for the stomach. The trachea appears to be the most sensitive organ based upon a single emission from a source distribution described above. Even though the trachea shows the highest sensitivity, the dose is a little deceiving. The observed dose for the trachea is based on the number of voxels which include the air encircled by the trachea. The actual dose based on the weight of the organ is less than that for the stomach and small intestine. Only Sr-90 appears to have a much lower dose for the trachea based upon the low energy beta. The stomach is the most sensitive organ for this material.

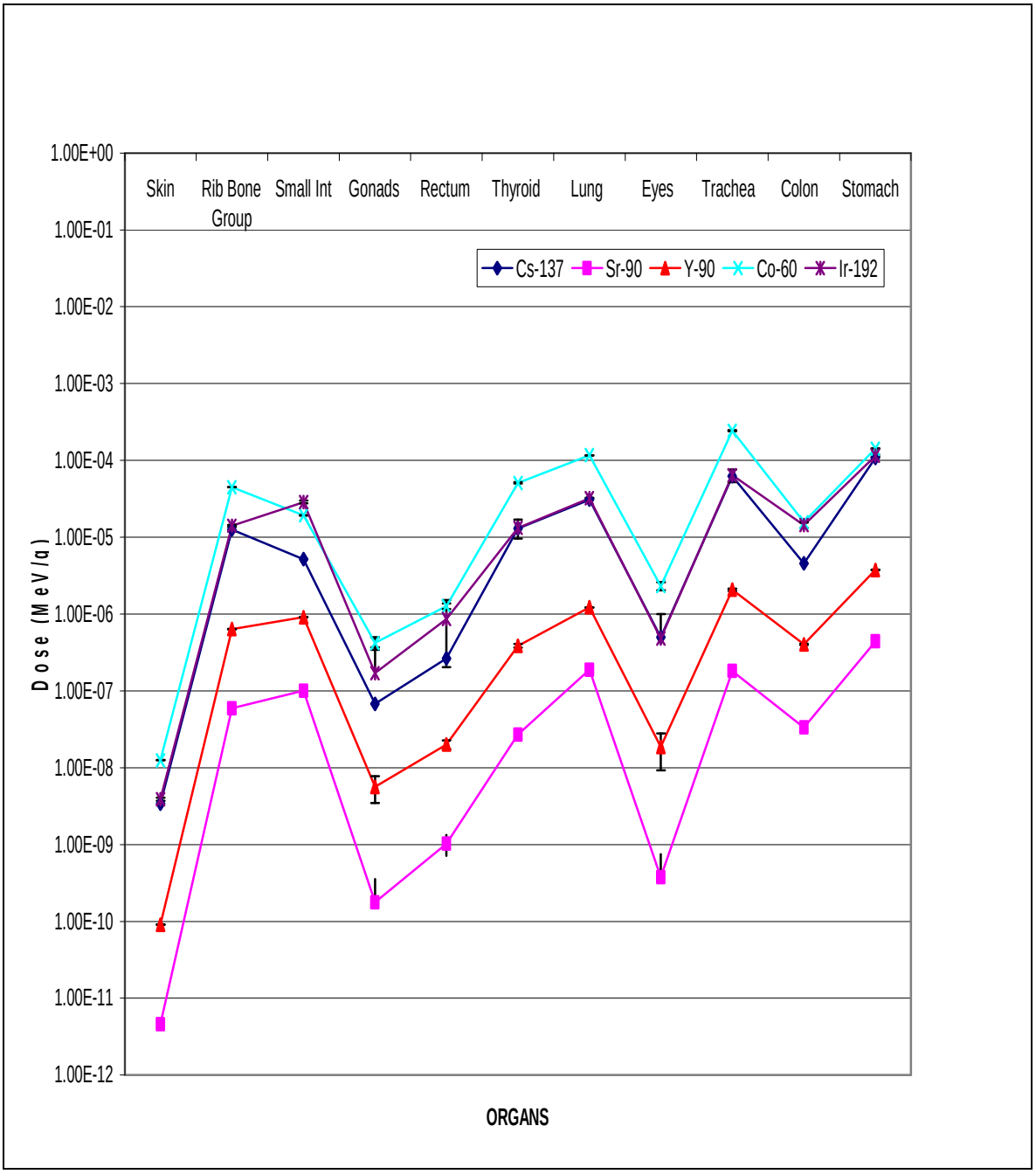

Fig. 17.7. Summary graph of organ doses for the five potential multi-organ sources located in multiple organs after time T plus one hour.

CHAPTER XVIII

ESTIMATING ORGAN DOSE BASED ON VOLUME SOURCES IN THE LUNG, STOMACH, SMALL INTESTINE AND COLON SIX HOURS AFTER A LUNG INHALATION

Co-60 organ dose profile

A Co-60 source located within the lung, stomach, liver, small intestine and colon would deliver a dose to the selected organs that ranges from a high of 2.10×10^{-4} MeV/g for the trachea and a low of 1.25×10^{-8} MeV/g for the skin six hours after initial exposure. This organ dose contribution is from the sum of two photon emissions that occur with a yield of about 100 percent. Table 18.1 provides the calculated dose conversions for each of the selected organs at time (T) plus six hours from detonation.

Table 18.1. Organ doses from a Co-60 volume source in multiple organs at time T plus six hours.

Organs	No. of Sources in Organ	Activity normalized to 1	MCNP Dose (MeV/g)/his	Std Deviation	Organ Dose (MeV/g)/his	Organ Dose (Gy)/his
Skin	0	0.00E+00	6.93E-04	2.99E-11	1.25E-08	2.00E-18
Rib Bone Group	0	0.00E+00	1.33E+00	9.66E-08	4.03E-05	6.45E-15
Small Int	3499	7.00E-02	8.18E-01	3.93E-07	6.14E-05	9.84E-15
Gonads	0	0.00E+00	4.86E-04	9.35E-08	6.36E-07	1.02E-16
Rectum	0	0.00E+00	3.03E-03	1.47E-07	2.36E-06	3.77E-16
Thyroid	0	0.00E+00	1.72E-02	1.09E-06	4.30E-05	6.89E-15
Lung	15000	4.73E-01	8.49E+00	1.86E-07	1.03E-04	1.65E-14
Eyes	0	0.00E+00	6.74E-04	2.71E-07	2.20E-06	3.53E-16
Trachea	0	0.00E+00	4.30E-02	3.70E-06	2.10E-04	3.37E-14
Colon	2124	6.08E-02	2.35E-01	3.12E-07	3.12E-05	4.99E-15
Stomach	1400	2.19E-02	4.48E-01	1.05E-06	1.46E-04	2.34E-14

As expected, the activity in the lung was reduced from 59 percent to 47 percent from time T plus one hour to time T plus six hours. The majority of activity remained in the lung at time T plus six hours. Unlike T plus one hour, the small intestine contains the second highest activity. The activity in the small intestine increased from 1.2 percent

to 41 percent. The activity in the stomach was reduced from 7.1 percent to 2.2 percent. The colon had an increase in activity from 0.7 percent to 6.1 percent. For Co-60, the most sensitive organs were the trachea and stomach followed by the lung and small intestine. Compared to the Co-60 dose at time T plus one hour, the lung dose was 1.16 x 10^{-4} MeV/g and the lung dose from multiple source organs was 1.03 x 10^{-4} MeV/g at T plus six hours. The stomach dose from Co-60 at T plus one hour was 1.42 x 10^{-4} MeV/g and the stomach dose at time T plus six hours was 1.46 x 10^{-4} MeV/g or roughly a 3 percent increase in dose to the stomach dose.

Statistical analysis of output file

The tally-four fluence analysis for each detector provided a random behavior for the mean. The desired relative error should be less than 0.10 and the observed relative error was 0.02. The desired and observed relative error decreased according to the inverse of the square root of the number of histories. The desired variance of the variance should be less than 0.10 and the observed VoV was 0.00. The figure of merit value was constant and the behavior was random. The probability density function (pdf) desired should be greater than three, the observed value was 10. The tally-four fluence passed all 10 statistical checks. Out of 10 tally-four bins, only one had a zero dose and no bins contained relative errors greater than 0.10. The 1.33 MeV photon simulation provided similar results. The same single bin had a zero value.

The tally-six dose analysis for each material provided a random behavior for the mean. The desired relative error should be less than 0.10 and the observed relative error was 0.00 for the 1.17 MeV photon and 0.00 for the 1.33 MeV photon. The desired and observed relative error decreased according to the inverse of the square root of the number of histories. The desired variance of the variance should be less than 0.10 and the observed VoV was 0.00. The figure of merit value was constant and the behavior was random. The desired probability density function (pdf) should be greater than 3.00 and the observed value was 7.64 for the 1.17 MeV photon and 6.74 for the 1.33 MeV

photon. The tally-six dose passed all 10 statistical checks. Out of 61 tally-six bins, no bin had a zero dose and only 5 bins contained relative errors greater than 0.10.

Figure 18.1 provides a simulated 3-dimensional view of the human body with a color profile that shows the organ dose for the 1.33 MeV photon of Co-60. Each axis is represented in the figure along with a color bar that indicates the organ dose in MeV/organ in grams provided by the MCNPX output file.

Cs-137 organ dose profile

A Cs-137 source located within the lung, stomach, liver, small intestine and colon would deliver a dose to the selected organs at T plus six hours from exposure that ranges from a high of 7.46×10^{-5} MeV/g for the trachea and a low of 3.41×10^{-9} MeV/g for the skin. This organ dose contribution is from a 0.66 MeV photon emitted from Cs-137 that occurs with a yield of about 86 percent. Table 18.2 provides the dose output to the selected organs at time (T) plus six hours from detonation.

Table 18.2. Organ doses for a Cs-137 volume source in multiple organs at time T plus six hours.

Organs	No. of Sources in Organ	Activity normalized to 1	MCNP Dose (MeV/g)/his	Std Deviation	Organ Dose (MeV/g)/his	Organ Dose (Gy)/his
Skin	0	0.00E+00	1.90E-04	4.09E-12	3.41E-09	5.47E-19
Rib Bone Group	0	0.00E+00	4.59E-01	1.53E-08	1.39E-05	2.23E-15
Small Int	3499	0.00E+00	4.25E-02	2.55E-08	3.19E-06	5.11E-16
Gonads	0	0.00E+00	4.09E-05	6.72E-09	5.35E-08	8.57E-18
Rectum	0	0.00E+00	2.69E-04	1.12E-08	2.09E-07	3.35E-17
Thyroid	0	0.00E+00	6.13E-03	1.73E-07	1.53E-05	2.45E-15
Lung	15000	1.92E-01	2.96E+00	2.51E-08	3.59E-05	5.75E-15
Eyes	0	0.00E+00	1.80E-04	3.62E-08	5.87E-07	9.41E-17
Trachea	0	0.00E+00	1.52E-02	5.82E-07	7.46E-05	1.19E-14
Colon	2124	0.00E+00	2.66E-02	2.86E-08	3.53E-06	5.65E-16
Stomach	1400	8.56E-04	9.84E-02	1.32E-07	3.21E-05	5.15E-15

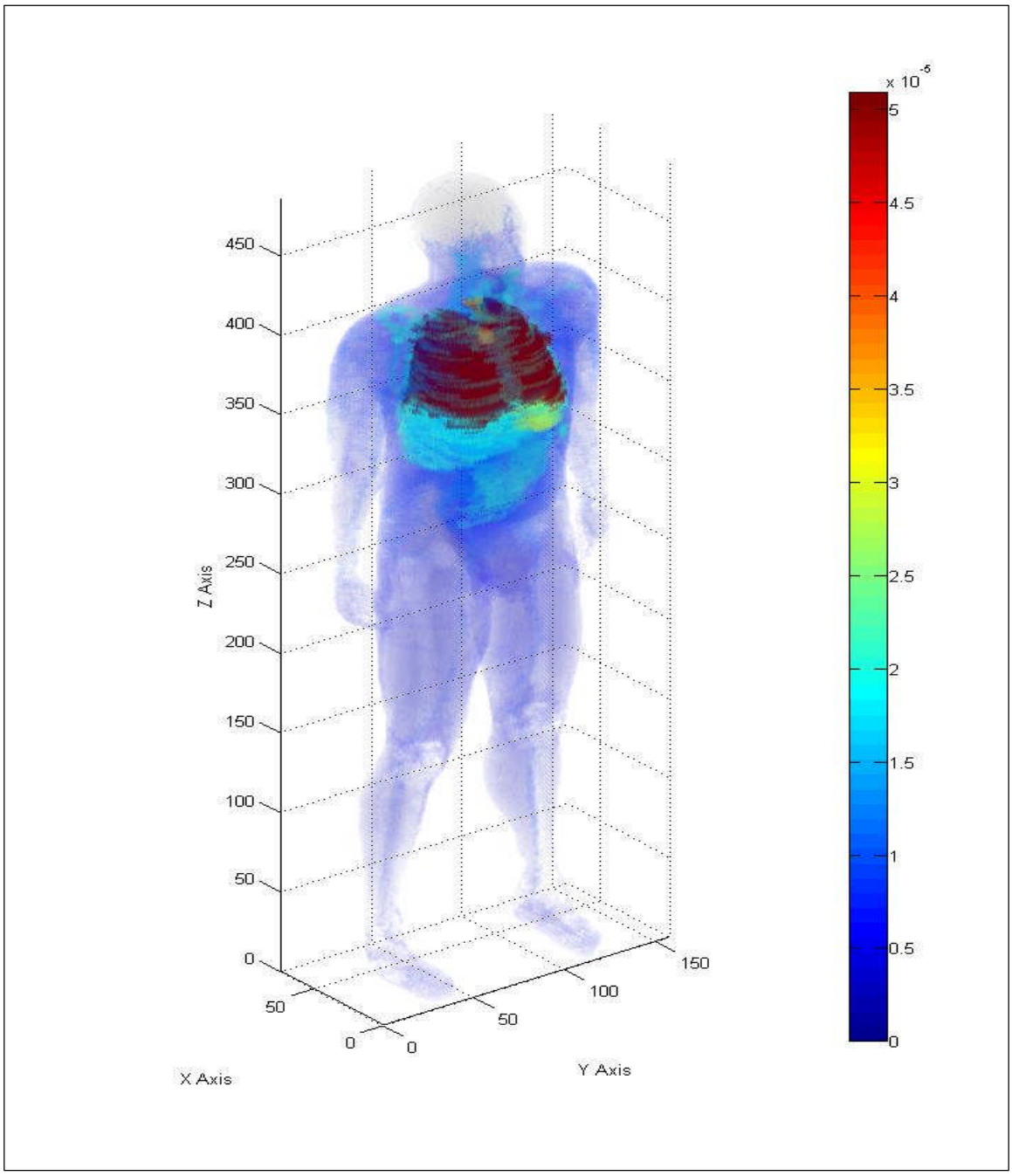

Fig. 18.1. Three-dimensional human dose profile from a 1.33 MeV photon source located within multiple organs after T plus six hours.

As expected, the activity in the lung was reduced from 26 percent to 19 percent from time T plus one hour to time T plus six hours. Based on the ICRP-30 methodology, the majority of the activity was absorbed by the body. The activity in the stomach is reduced from 7 percent to less than 0.1 percent. For Cs-137, the most sensitive organs were the trachea followed by the lung, colon and stomach. Compared to the Co-60 dose at time T plus one hour, the lung dose was 3.09×10^{-5} MeV/g and the lung dose from multiple source organs was 3.59×10^{-5} MeV/g at T plus six hours. The dose increase was due to the normalization of activity in the phantom. Even though the total lung activity decreased, the total percent of residual activity that remained was concentrated in the lung. The stomach dose from Co-60 at T plus one hour was 1.08×10^{-4} MeV/g and the stomach dose at time T plus six hours was 3.21×10^{-5} MeV/g or roughly a 3 fold decrease in dose to the stomach dose.

Statistical checks were performed on the Cs-137 dose output file. The same warnings present with Co-60 were observed. The 10 statistical checks for tally-four fluence passed and produced similar results. The 10 statistical checks for tally-six dose passed and produced similar results as with Co-60. Of the 61 tally bins, no bin had a zero dose and 8 bins had relative errors exceeding 0.10. Figure 19.2 provides a simulated 3-dimensional view of the human body with a color profile that shows the MCNP dose for the single photon of Cs-137. The color bar units to the right of the phantom are in MeV/organ weight in grams.

At T plus six hour, the most sensitive organ for a Co-60 and Cs-137 exposure was the trachea that received a dose of 2.10×10^{-4} MeV/g and 7.46×10^{-5} MeV/g, respectively. The change in organ sensitivity for Cs-137 can be attributed to the relative difference in activity present in the lung and stomach at T plus six hours. For Cs-137 18.2 percent of the activity remains in the lung at T plus six hours while 26 percent of the activity remains in the lung at T plus 1 hour. The key difference is the amount of activity present in the stomach. At T plus 6 hours, only 0.09 percent of the activity

remains in the stomach while at T plus 1 hour, 2.2 percent remains. The relative majority of activity remains in the lung.

Ir-192 organ dose profile

An Ir-192 source located within the lung, stomach, liver, small intestine and colon would deliver a dose to the selected organs at T plus six hours after exposure that ranges from a high of 6.05 x 10^{-5} MeV/g for the colon and a low of 3.83 x 10^{-9} MeV/g for the skin. This organ dose contribution is from the sum of two photons with energies of 0.47 MeV and 0.32 MeV along with two electrons with maximum energies of 0.66 MeV and 0.54 MeV. All four emissions are produced with a yield of 26.2%, 22.4%, 10.1% and 6.7%, respectively. Table 18.3 provides the calculated dose conversions for each of the selected organs at time (T) plus six hours from detonation.

Table 18.3. Organ doses for an Ir-192 volume source in multiple organs at time T plus six hours.

Organs	No. of Sources in Organ	Activity normalized to 1	MCNP Dose (MeV/g)/his	Std Deviation	Organ Dose (MeV/g)/his	Organ Dose (Gy)/his
Skin	0	0.00E+00	2.13E-04	1.64E-10	3.84E-09	6.15E-19
Rib Bone Group	0	0.00E+00	3.56E-01	3.94E-07	1.08E-05	1.73E-15
Small Int	3499	4.90E-02	3.56E-01	1.39E-06	2.67E-05	4.28E-15
Gonads	0	0.00E+00	2.85E-04	6.04E-07	3.73E-07	5.97E-17
Rectum	0	0.00E+00	3.83E-03	1.04E-06	2.98E-06	4.77E-16
Thyroid	0	0.00E+00	4.13E-03	3.24E-06	1.03E-05	1.65E-15
Lung	15000	1.91E-01	1.95E+00	5.18E-07	2.36E-05	3.79E-15
Eyes	0	0.00E+00	9.21E-05	5.51E-08	3.01E-07	4.82E-17
Trachea	0	0.00E+00	9.87E-03	1.10E-05	4.83E-05	7.74E-15
Colon	2124	1.01E-01	6.29E-01	2.01E-06	8.35E-05	1.34E-14
Stomach	1400	8.00E-04	8.55E-02	3.24E-06	2.79E-05	4.48E-15

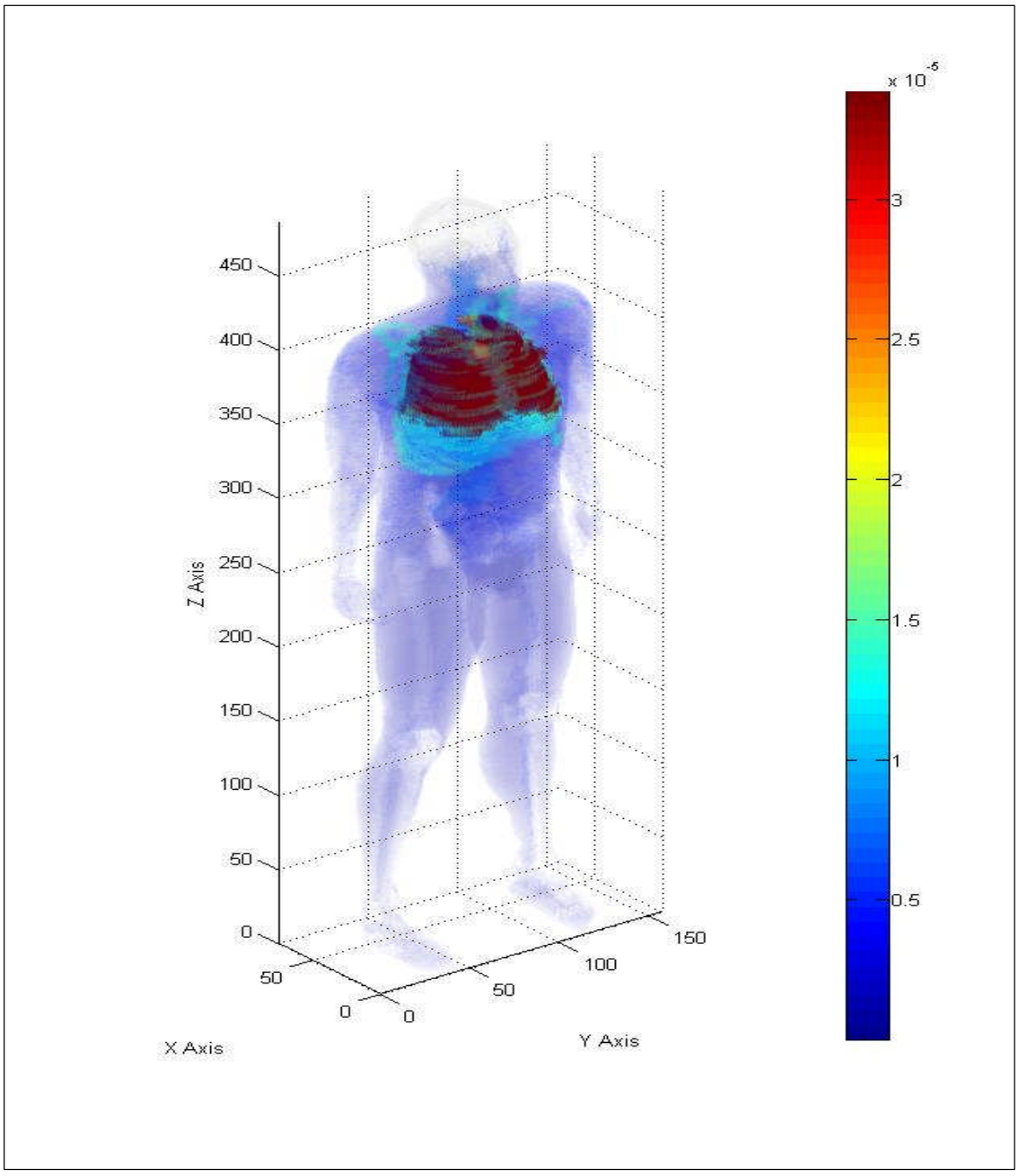

Fig. 18.2. Three-dimensional human dose profile from a Cs-137 photon source located within multiple organs at time T plus six hours.

As expected, like the Ir-192 multiple source organs at time T plus one hour, the majority of the activity remains in the lung but continues to pass through the stomach, small intestine and colon. Of the 26 percent of activity that remained in the lung at time T plus one hour, the lung contains 19 percent of the activity at time T plus six hours. The activity in the stomach is reduced from seven percent to less than 0.1 percent and the activity in the small intestine is reduced from 6.3 percent to 4.9 percent. The most sensitive organs for Ir-192 at time T plus six hours were the colon followed by the trachea, stomach and small intestine. The dose to the lung at time T plus one hour from Ir-192 was 3.21×10^{-5} MeV/g and the lung dose at time T plus six hours was 2.36×10^{-5} MeV/g. The colon dose at time T plus one hour from Ir-192 was 1.44×10^{-5} MeV/g and the colon dose at time T plus six hours was 8.35×10^{-5} MeV/g. This produced an increase in the stomach dose by approximately four times.

Statistical checks were performed on the Ir-192 dose output file. The same warnings present with Co-60 were observed. The 10 statistical checks for tally-four fluence photons passed and produced similar results. The 10 statistical checks for tally-six dose photons passed and produced similar results as with Co-60. Of the 61 tally bins, no bin had a zero dose and 6 bins had relative errors exceeding 0.10 for the 0.47 MeV photon. The second 0.32 MeV photon produced similar results.

The tallies for the electron sources within the lung had to be evaluated in a slightly different manner based on their inability to penetrate uniformly throughout the phantom. Secondary emissions, such as bremsstrahlung and characteristics x rays were the primary radiation source for organs outside of the source organs. Two of the 10 statistical checks did not pass. The relative error was 0.29 and the pdf was 0. This reflects a large number of zero doses and slightly greater than zero doses based on the volume electron source.

Figures 18.3 and 18.4 provide a simulated 3-dimensional view of the human body with a color profile that shows the MCNP dose for the 0.47 MeV photon of Ir-192 and the 0.66 MeV electron of Ir-192 absorbed by each organ, respectively. The color bar units to the right of the phantom are in MeV/organ weight in grams.

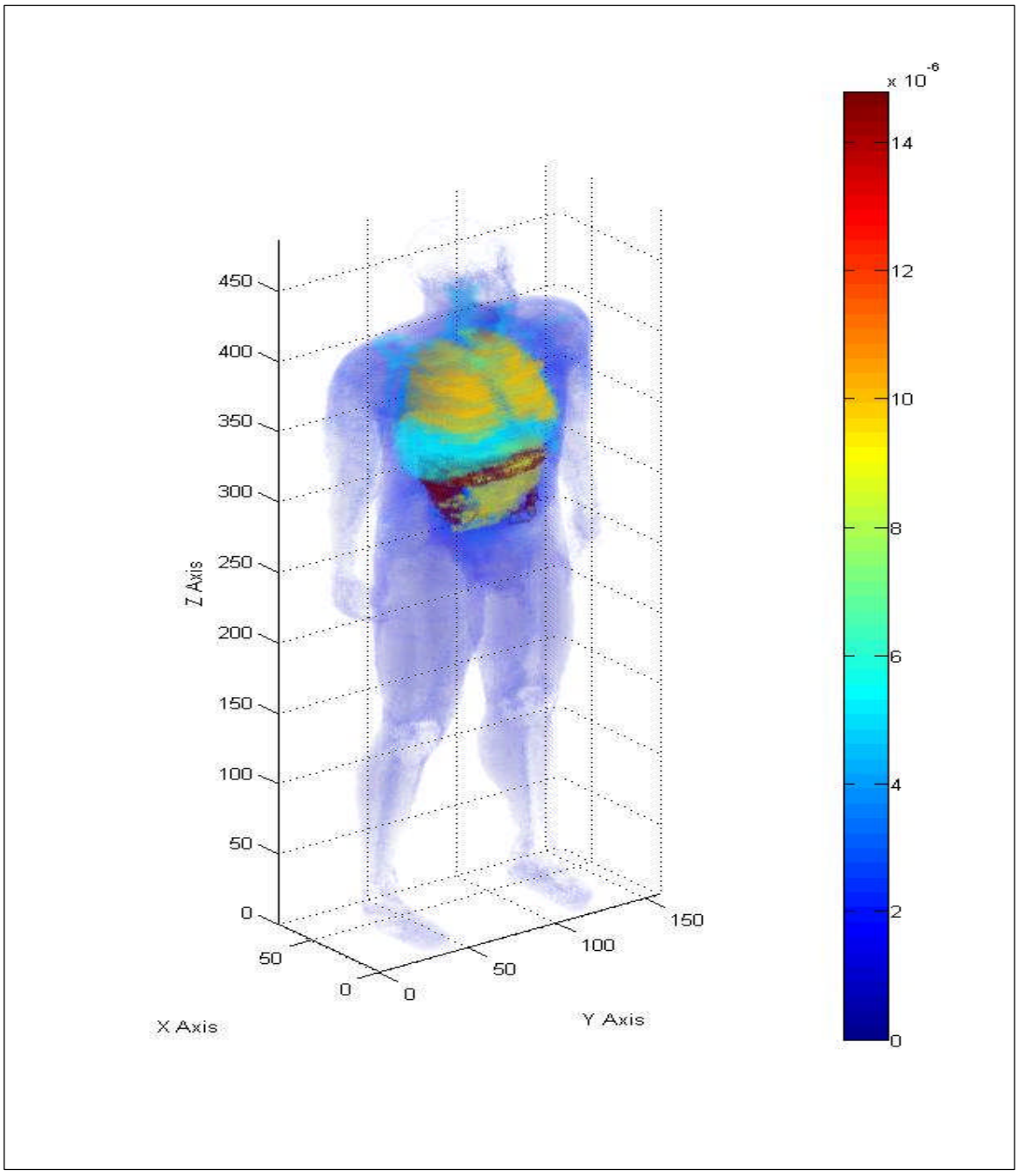

Fig. 18.3. Three-dimensional human dose profile from a 0.47 MeV Ir-192 photon source located within multiple organs after T plus six hours.

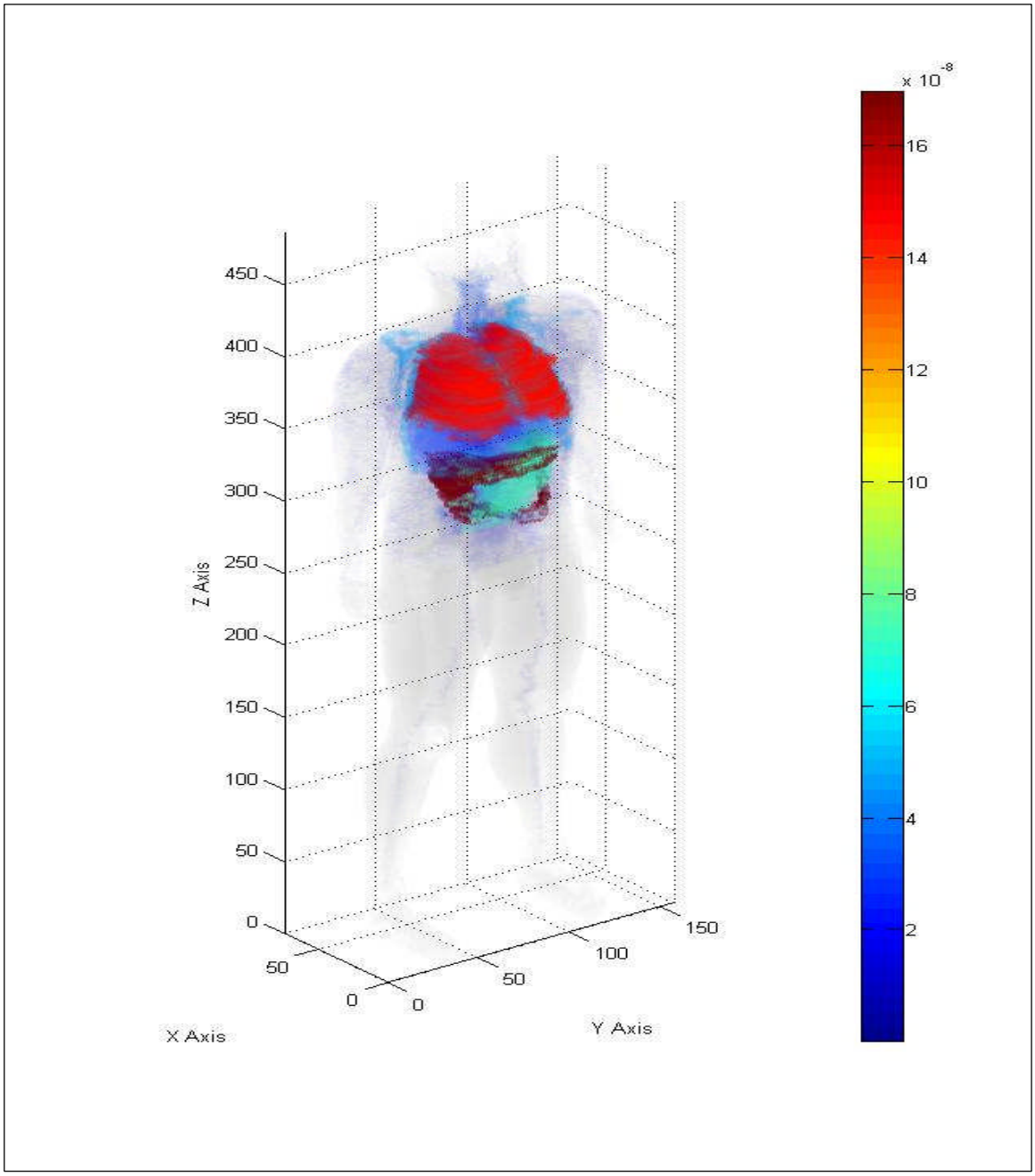

Fig. 18.4. Three-dimensional human dose profile from a 0.66 MeV Ir-192 beta source located within multiple organs after T plus six hours.

Sr-90 organ dose profile

A Sr-90 source located within the lung, stomach, liver, small intestine and colon would deliver a dose to the selected organs at T plus six hours after exposure that ranges from a high of 2.57 x 10^{-7} MeV/g for the colon and a low of 4.40 x 10^{-12} MeV/g for the skin. This organ dose contribution is from a single beta emission with a maximum energy of 0.55 MeV. The beta emission is produced with a yield of about 86 percent. Table 18.4 provides the calculated dose conversions for each of the selected organs that will be considered in this problem.

Table 18.4. Organ doses from a Sr-90 volume source in multiple organs at time T plus six hours.

Organs	No. of Sources in Organ	Activity normalized to 1	MCNP Dose (MeV/g)/his	Std Deviation	Organ Dose (MeV/g)/his	Organ Dose (Gy)/his
Skin	0	0.00E+00	2.45E-07	1.04E-13	4.40E-12	7.05E-22
Rib Bone Group	0	0.00E+00	1.71E-03	8.55E-10	5.18E-08	8.30E-18
Small Int	3499	3.20E-02	1.15E-03	1.85E-09	8.66E-08	1.39E-17
Gonads	0	0.00E+00	0.00E+00	0.00E+00	0.00E+00	0
Rectum	0	0.00E+00	4.38E-06	7.21E-10	3.41E-09	5.45E-19
Thyroid	0	0.00E+00	1.03E-05	3.73E-09	2.58E-08	4.13E-18
Lung	15000	1.92E-01	1.44E-02	1.59E-09	1.75E-07	2.8E-17
Eyes	0	0.00E+00	0.00E+00	0.00E+00	0.00E+00	0
Trachea	0	0.00E+00	3.65E-05	1.89E-08	1.79E-07	2.86E-17
Colon	2124	8.36E-02	1.93E-03	3.59E-09	2.57E-07	4.11E-17
Stomach	1400	8.00E-04	1.72E-04	2.76E-09	5.60E-08	8.97E-18

The most sensitive organ for a Sr-90 electron source at time T plus six hours after exposure has changed from the stomach to the colon. The trachea and lung follow the colon in sensitivity. The colon retained 0.7 percent of the activity at T plus one hour and 8.4 percent at T plus six hours. Of the 26 percent of activity that remained in the lung at T plus one hour, the lung retained 19.2 percent at T plus six hours. Compared to the Sr-90 dose to the lung at T plus one hour, which was 1.87 x 10^{-7} MeV/g, the lung dose at T plus six hours was 1.75 x 10^{-7} MeV/g.

Statistical checks were performed on the Sr-90 dose output file. The same warnings present with Co-60 were observed. The 10 statistical checks for tally-four fluence missed three of the 10 checks. The relative error was 0.30, VoV was 0.20 and the pdf was 0. The 10 statistical checks for tally-six dose passed. Of the 61 tally bins, 8 bins had a zero dose and 30 bins had relative errors exceeding 0.10 for the 0.55 MeV beta emission. Figure 18.5 provides a simulated 3-dimensional view of the human body with a color profile that shows the MCNP dose for the beta radiation of Sr-90 absorbed by each organ. The color bar units to the right of the phantom are in MeV/organ weight in grams.

Y-90 organ dose profile

A Y-90 source located within the lung, stomach, liver, small intestine and colon would deliver a dose to the selected organs at T plus six hours after exposure that ranges from a high of 1.95×10^{-6} MeV/g for the trachea and a low of 9.04×10^{-11} MeV/g for the skin. This organ dose contribution is from a single beta emission with a maximum energy of 2.28 MeV. The beta emission is produced with a yield of about 100%. Table 18.5 provides the calculated dose conversions for each of the selected organs that will be considered in this problem.

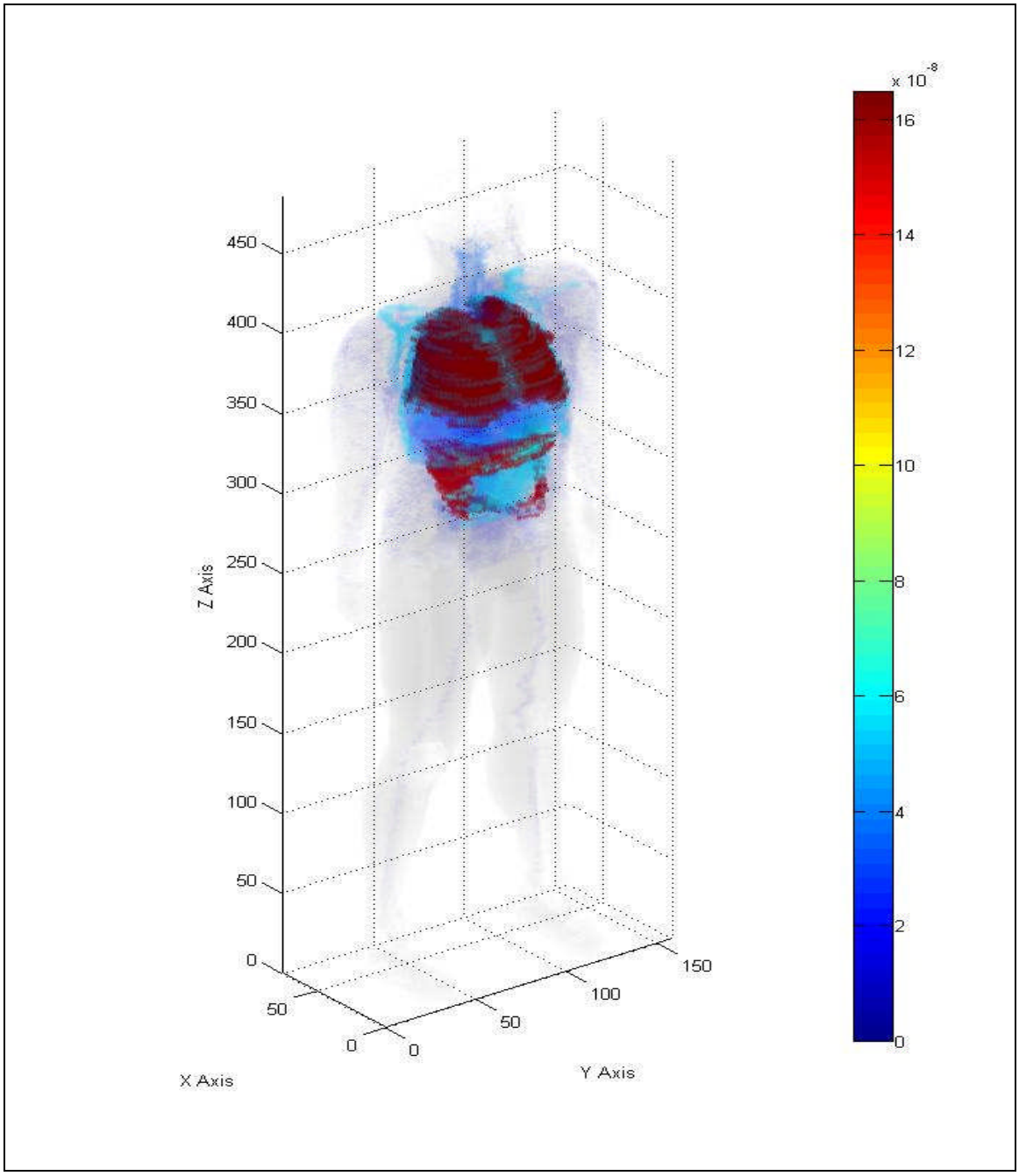

Fig. 18.5. Three-dimensional human dose profile from a Sr-90 beta source located within multiple organs after T plus six hours.

Table 18.5. Organ doses from a Y-90 volume source in multiple organs at time T plus six hours.

Organs	No. of Sources in Organ	Activity normalized to 1	MCNP Dose (MeV/g)/his	Std Deviation	Organ Dose (MeV/g)/his	Organ Dose (Gy)/his
Skin	0	0.00E+00	5.03E-06	7.78E-13	9.04E-11	1.45E-20
Rib Bone Group	0	0.00E+00	1.86E-02	3.22E-09	5.65E-07	9.05E-17
Small Int	3499	3.20E-02	1.15E-02	9.77E-09	8.65E-07	1.39E-16
Gonads	0	0.00E+00	5.07E-06	2.00E-09	6.63E-09	1.06E-18
Rectum	0	0.00E+00	5.94E-05	3.92E-09	4.62E-08	7.40E-18
Thyroid	0	0.00E+00	1.58E-04	2.44E-08	3.94E-07	6.32E-17
Lung	15000	1.92E-01	9.21E-02	5.48E-09	1.12E-06	1.79E-16
Eyes	0	0.00E+00	3.40E-06	4.80E-09	1.11E-08	1.78E-18
Trachea	0	0.00E+00	3.99E-04	7.23E-08	1.95E-06	3.13E-16
Colon	2124	8.36E-02	1.44E-02	1.51E-08	1.92E-06	3.07E-16
Stomach	1400	8.00E-04	2.58E-03	1.70E-08	8.42E-07	1.35E-16

As with Sr-90, the colon, trachea and lung received the highest dose from a highly-energetic beta radiation source located in multiple organs at time T plus six hours after exposure. Of the 26 percent of activity that remained in the lung at T plus one hour, the lung retained 19.2 percent at T plus six hours. The organ activity follows that of Sr-90. Compared to the Y-90 dose at T plus one hour which was 1.22×10^{-6} MeV/g, the lung dose at T plus six hours was 1.12×10^{-6} MeV/g. The colon dose from Y-90 at T plus one hour was 1.44×10^{-5} MeV/g and at the colon dose at T plus six hours was 1.92×10^{-6} MeV/g. This produced a decrease in the colon dose by roughly seven fold.

Statistical checks were performed on the Y-90 dose output file. The same warnings present with Co-60 were observed. The 10 statistical checks for tally-four fluence passed all checks except the pdf which was 0. The 10 statistical checks for tally-six dose passed. Of the 61 tally bins, no bin had a zero dose and 25 bins had relative errors exceeding 0.10 for the 2.28 MeV beta emission. Figure 18.6 provides a simulated 3-dimensional view of the human body with a color profile that shows the organ dose for the beta emission of Y-90. The color bar units to the right of the phantom are in MeV/organ weight in grams.

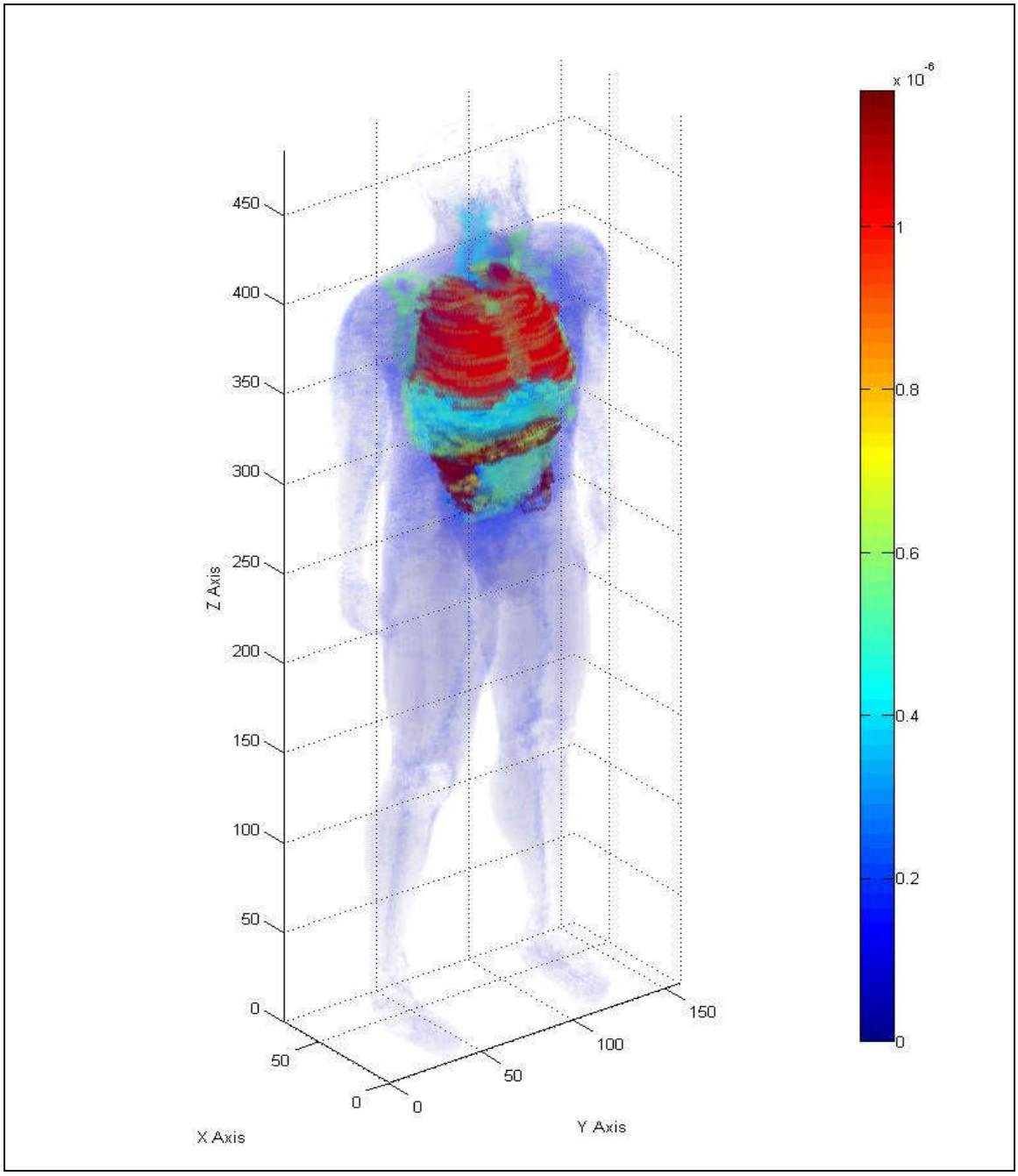

Fig. 18.6. Three-dimensional human dose profile from a Y-90 beta source located within multiple organs after T plus six hours.

Results from multi-organ lung, stomach, liver, small intestine and colon volume sources after six hours

Figure 18.7 provides a graph of all of the potential sources distributed in multiple organs after T plus 6 hours. Based upon the results of the observed programs, six hours after inhalation, Co-60 is the most limiting radionuclide with the exception of the colon. Ir-192 appears to provide a higher dose to the colon. Ir-192 and Co-60 appear to be within a margin of error for the small intestine and gonads. The trachea and stomach appear to be the most sensitive organs based upon a single emission from a source distribution described above. Even though the trachea shows the highest sensitivity, the dose is a little deceiving. The observed dose for the trachea is based on the number of voxels which include the air encircled by the trachea. The actual dose based on the weight of the organ is less than that for the lung, stomach and small intestine. The stomach, followed by the lung, appears to be the most sensitive organs at this time period.

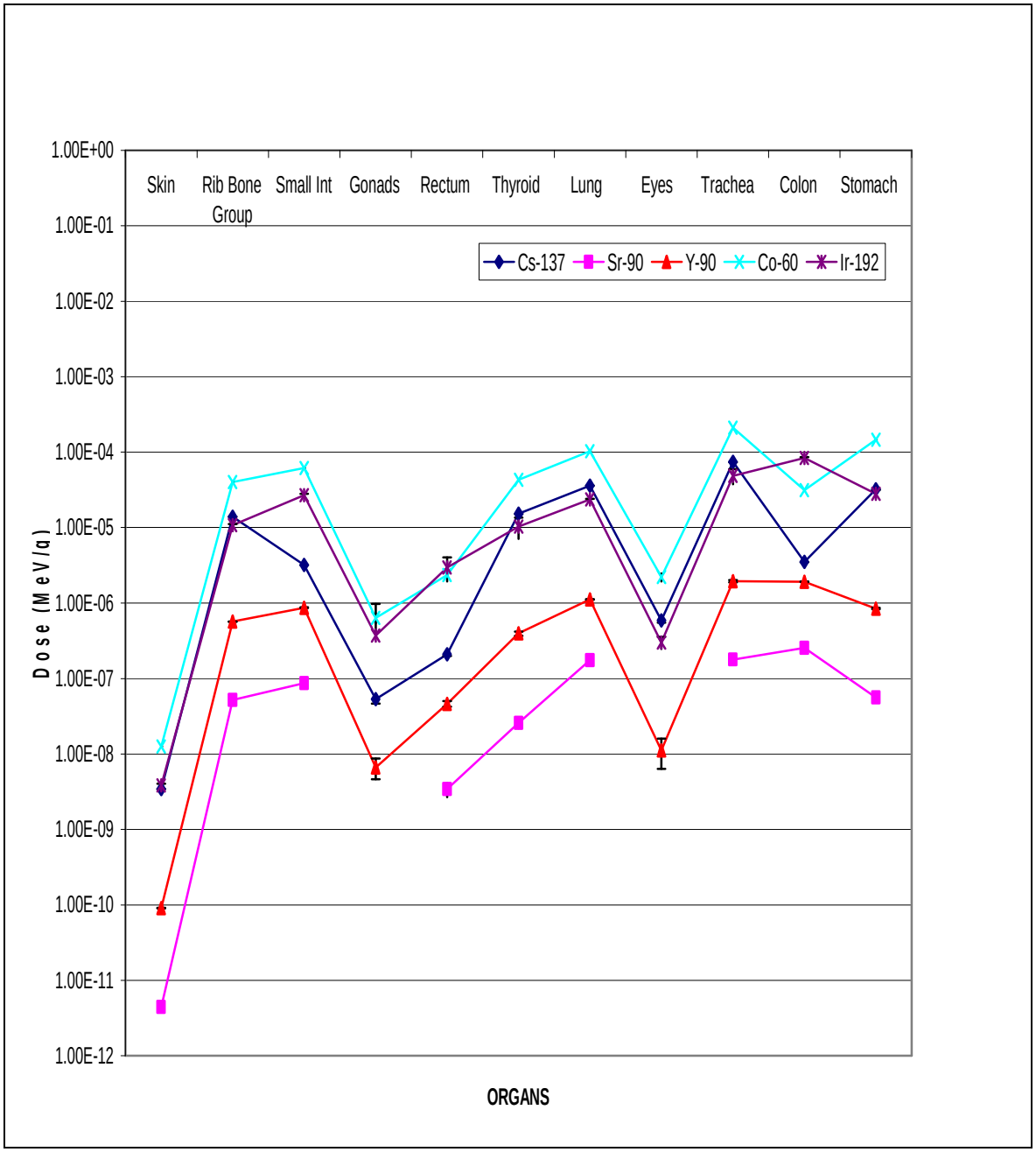

Fig. 18.7. Summary graph of organ doses for the five potential multi-organ sources located in multiple organs after time T plus six hours.

CHAPTER XIX

ESTIMATING ORGAN DOSE BASED ON VOLUME SOURCES IN THE LUNG, STOMACH, SMALL INTESTINE AND COLON TWELVE HOURS AFTER A LUNG INHALATION

Co-60 organ dose profile

A Co-60 source located within the lung, stomach, liver, small intestine and colon would deliver a dose to the selected organs that ranges from a high of 1.59×10^{-4} MeV/g for the trachea and a low of 1.24×10^{-8} MeV/g for the skin. This organ dose contribution is from the sum of two photon emissions that occur with a yield of about 100 percent. Table 19.1 provides the calculated dose conversions for each of the selected organs at time (T) plus twelve hours from exposure.

Table 19.1. Organ doses from a Co-60 volume source in multiple organs at time T plus 12 hours.

Organs	No. of Sources in Organ	Activity normalized to 1	MCNP Dose (MeV/g)/his	Std Deviation	Organ Dose (MeV/g)/his	Organ Dose (Gy)/his
Skin	0	0.00E+00	6.90E-04	2.98E-11	1.24E-08	1.98644E-18
Rib Bone Group	0	0.00E+00	1.06E+00	8.97E-08	3.20E-05	5.13E-15
Small Int	3499	6.50E-02	1.05E+00	4.43E-07	7.91E-05	1.26752E-14
Gonads	0	0.00E+00	9.79E-04	1.39E-07	1.28E-06	2.05191E-16
Rectum	0	0.00E+00	7.76E-03	2.38E-07	6.03E-06	9.67E-16
Thyroid	0	0.00E+00	1.36E-02	9.75E-07	3.41E-05	5.45892E-15
Lung	15000	3.74E-01	6.41E+00	1.87E-07	7.78E-05	1.24664E-14
Eyes	0	0.00E+00	5.23E-04	2.36E-07	1.71E-06	2.73499E-16
Trachea	0	0.00E+00	3.24E-02	3.23E-06	1.59E-04	2.54653E-14
Colon	2124	1.61E-01	1.11E+00	6.48E-07	1.47E-04	2.36076E-14
Stomach	1400	1.40E-02	3.50E-01	9.37E-07	1.14E-04	1.831E-14

As expected, the activity in the lung was reduced from 47 percent to 37 percent from time T plus six hours to time T plus 12 hours. Once again, the majority of the activity remains in the lung at time T plus 12 hours. As with time T plus six hours, the small intestine contains the second highest activity at T plus 12 hours. The activity of

the small intestine decreased from 41 percent to 6.5 percent. The activity in the stomach was further reduced from 2.2 percent to 1.4 percent. The activity in the colon increased from 6.1 percent to 16.1 percent. For Co-60, the most sensitive organs were the trachea followed closely by the colon, stomach and small intestine. Compared to the Co-60 dose at time T plus six hours, the lung dose was 1.03×10^{-4} MeV/g and the lung dose at time T plus 12 hours was 7.78×10^{-5} MeV/g. The stomach dose from Co-60 at T plus six hours was 1.46×10^{-4} MeV/g and the stomach dose at time T plus 12 hours was 1.14×10^{-4} MeV/g or approximately a 22 percent decrease in dose to the stomach.

Statistical analysis of output file

The tally-four fluence analysis for each detector provided a random behavior for the mean. The desired relative error should be less than 0.10 and the observed relative error was 0.03. The desired and observed relative errors decreased according to the inverse square root of the number of histories. The desired variance of the variance should be less than 0.10 and the observed VoV was 0.00. The figure of merit value was constant and the behavior was random. The probability density function (pdf) desired should be greater than three and the observed value was 10. The tally-four fluence passed all 10 statistical checks. Out of 10 tally-four bins, only one had a zero dose and no bins contained relative errors greater than 0.10. The second 1.33 MeV photon simulation provided similar results.

The tally-six dose analysis for each material provided a random behavior for the mean. The desired relative error should be less than 0.10 and the observed relative error was 0.00 for the 1.17 MeV photon and 0.00 for the 1.33 MeV photon. The desired and observed relative error decreased according to the inverse square root of the number of histories. The desired variance of the variance should be less than 0.10 and the observed VoV was 0.00. The figure of merit value was constant and the behavior was random. The desired probability density function (pdf) should be greater than 3.00 and the observed value was 10.0 for the 1.17 MeV photon and 6.77 for the 1.33 MeV photon.

The tally-six dose passed all 10 statistical checks. Out of 61 tally-six bins, no bin had a zero dose and only 5 bins contained relative errors greater than 0.10.

Figure 19.1 provides a simulated 3-dimensional view of the human body with a color profile that shows the MCNP dose for the 1.33 MeV photon of Co-60 absorbed by each organ. Each axis is represented in the figure along with a color bar that indicates the organ dose in MeV/organ in grams provided by the MCNPX output file. In the MCNPX output file, the trachea received a slightly lesser dose than the lung based upon the number of voxels versus the measured gram weight of the trachea. The phantom includes the airway as part of the trachea. The dose difference is not significant.

Cs-137 organ dose profile

A Cs-137 source located within the lung, stomach, liver, small intestine and colon would deliver a dose to the selected organs at T plus twelve hours that ranges from a high of 7.54×10^{-5} MeV/g for the trachea and a low of 3.41×10^{-9} MeV/g for the skin. This organ dose contribution is from a 0.66 MeV photon emitted from Cs-137 that occurs with a yield of about 86 percent. Table 19.2 provides the calculated dose conversions for the selected organs at time (T) plus twelve hours from detonation.

Table 19.2. Organ doses for a Cs-137 volume source in multiple organs at time T plus 12 hours.

Organs	No. of Sources in Organ	Activity normalized to 1	MCNP Dose (MeV/g)/his	Std Deviation	Organ Dose (MeV/g)/his	Organ Dose (Gy)/his
Skin	0	0.00E+00	1.90E-04	4.09E-12	3.41E-09	5.45694E-19
Rib Bone Group	0	0.00E+00	4.56E-01	1.52E-08	1.39E-05	2.22E-15
Small Int	3499	0.00E+00	4.15E-02	2.50E-08	3.12E-06	4.99783E-16
Gonads	0	0.00E+00	4.56E-05	7.80E-09	5.96E-08	9.54472E-18
Rectum	0	0.00E+00	2.74E-04	1.12E-08	2.13E-07	3.41E-17
Thyroid	0	0.00E+00	6.42E-03	1.76E-07	1.60E-05	2.56865E-15
Lung	15000	1.44E-01	2.96E+00	2.51E-08	3.59E-05	5.75445E-15
Eyes	0	0.00E+00	1.76E-04	3.69E-08	5.75E-07	9.21696E-17
Trachea	0	0.00E+00	1.54E-02	5.81E-07	7.54E-05	1.20779E-14
Colon	2124	0.00E+00	2.64E-02	2.84E-08	3.50E-06	5.61162E-16
Stomach	1400	1.20E-04	9.53E-02	1.31E-07	3.11E-05	4.98756E-15

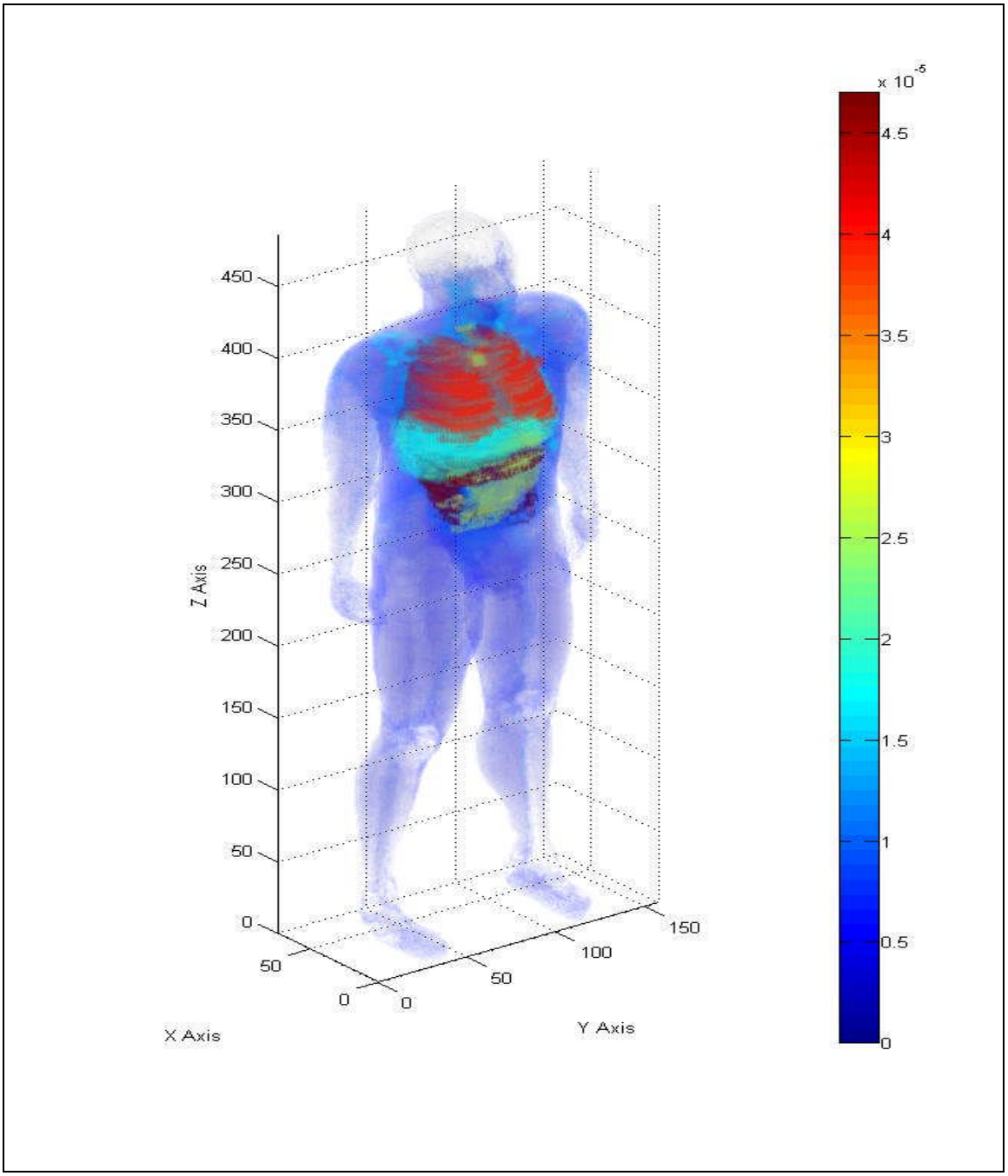

Fig. 19.1. Three-dimensional human dose profile from a 1.33 MeV photon source located within multiple organs after T plus 12 hours.

The activity in the lung was reduced from 19 percent to 14.4 percent from time T plus six hours to time T plus 12 hours. The majority of the activity was absorbed by the body. The activity in the stomach was reduced from 0.1 percent to less than 0.01 percent. For Cs-137, the most sensitive organs were the trachea followed by the lung, stomach and colon. Compared to the Co-60 dose at time T plus six hours, the lung dose was 4.91×10^{-5} MeV/g and the lung dose at T plus 12 hours was 3.59×10^{-5} MeV/g. The stomach dose from Co-60 at T plus six hours was 3.21×10^{-5} MeV/g and the stomach dose at time T plus 12 hours was 3.11×10^{-5} MeV/g or roughly a five percent decrease in dose to the stomach.

Statistical checks were performed on the Cs-137 dose output file. The same warnings present with Co-60 were observed. The 10 statistical checks for tally-four fluence passed and produced similar results. The same single bin detector contained a zero result. The 10 statistical checks for tally-six dose passed and produced similar results as with Co-60. Of the 61 tally bins, no bin had a zero dose and 8 bins had relative errors exceeding 0.10. Figure 19.2 provides a simulated 3-dimensional view of the human body with a color profile that shows the organ dose for the single photon of Cs-137. The color bar units to the right of the phantom are in MeV/organ weight in grams.

At T plus twelve hours, the most sensitive organ for a Co-60 and Cs-137 exposure was the trachea that received a dose of 1.59×10^{-4} MeV/g and 7.54×10^{-5} MeV/g, respectively. The change in activity is not enough to alter the most sensitive organ for either radionuclide. For Cs-137, 14.4 percent of the activity remained in the lung at T plus twelve hours while 19.2 percent of the activity remained in the lung at T plus 6 hours. The activity in the stomach dropped from 0.08 percent to 0.01 percent at T plus 12 hours. The relative majority of the residual activity remained in the lung.

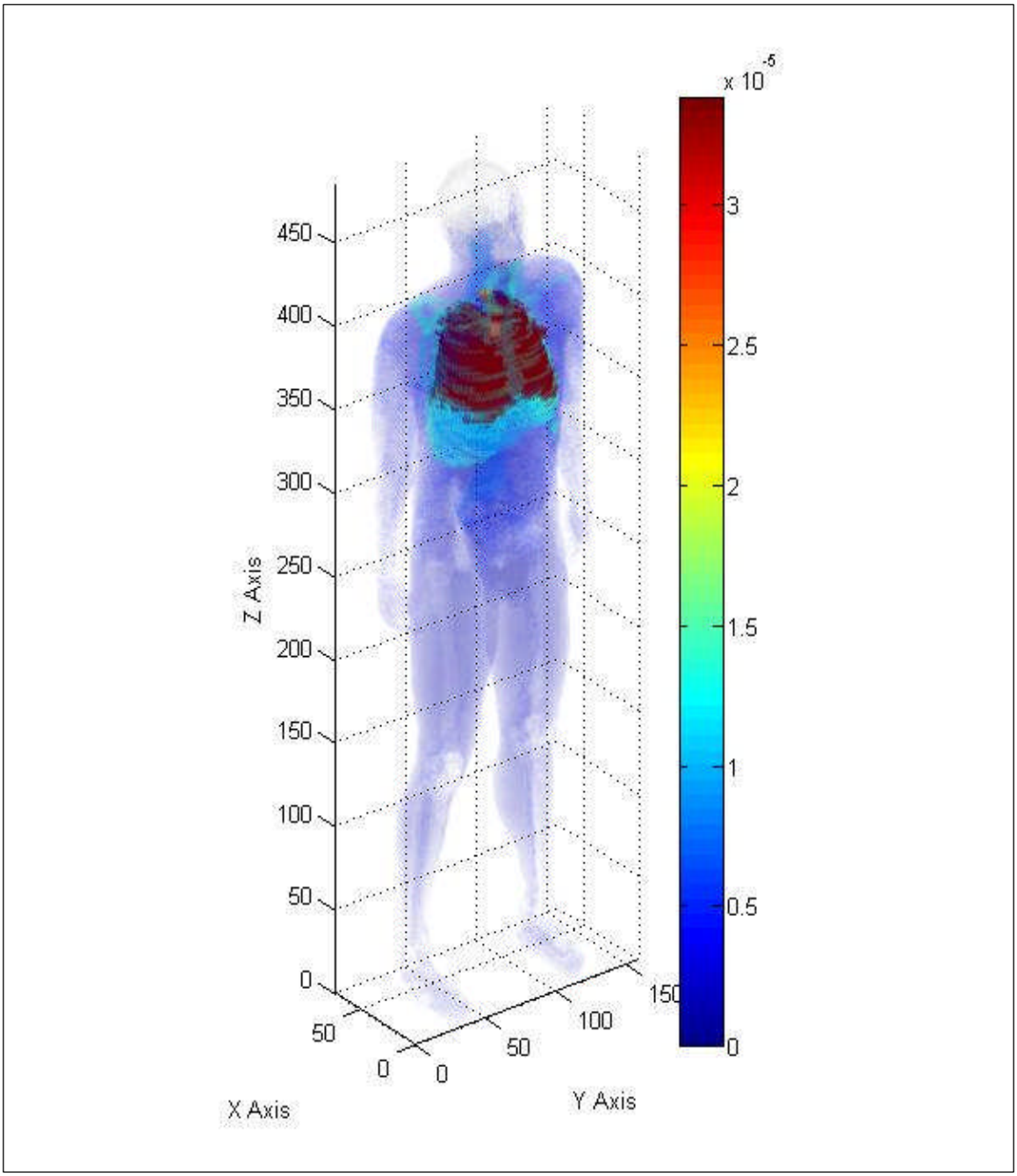

Fig. 19.2. Three-dimensional human dose profile from a Cs-137 source located within multiple organs after T plus 12 hours.

Ir-192 organ dose profile

An Ir-192 source located within the lung, stomach, liver, small intestine and colon would deliver a dose to the selected organs at T plus twelve hours from exposure that ranges from a high of 8.35 x 10^{-5} MeV/g for the colon and a low of 3.84 x 10^{-9} MeV/g for the skin. This organ dose contribution is from the sum of two photons with energies of 0.47 MeV and 0.32 MeV along with two electrons with maximum energies of 0.66 MeV and 0.54 MeV. All four emissions are produced with a yield of 26.2%, 22.4%, 10.1% and 6.7%, respectively. Table 19.3 provides the calculated dose conversions for each of the selected organs at time (T) plus twelve hours from detonation.

Table 19.3. Organ doses for an Ir-192 volume source in multiple organs at time T plus 12 hours.

Organs	No. of Sources in Organ	Activity normalized to 1	MCNP Dose (MeV/g)/his	Std Deviation	Organ Dose (MeV/g)/his	Organ Dose (Gy)/his
Skin	0	0.00E+00	2.13E-04	1.62E-10	3.83E-09	6.14052E-19
Rib Bone Group	0	0.00E+00	3.85E-01	4.03E-07	1.17E-05	1.87E-15
Small Int	3499	1.40E-02	4.59E-01	1.37E-06	3.45E-05	5.52347E-15
Gonads	0	0.00E+00	2.76E-04	6.43E-07	3.61E-07	5.78102E-17
Rectum	0	0.00E+00	3.15E-03	1.07E-06	2.45E-06	3.93E-16
Thyroid	0	0.00E+00	4.52E-03	3.44E-06	1.13E-05	1.81011E-15
Lung	15000	1.42E-01	2.16E+00	5.41E-07	2.63E-05	4.20752E-15
Eyes	0	0.00E+00	1.02E-04	7.20E-07	3.32E-07	5.3107E-17
Trachea	0	0.00E+00	1.10E-02	1.06E-05	5.38E-05	8.61934E-15
Colon	2124	1.30E-01	4.56E-01	1.80E-06	6.05E-05	9.69749E-15
Stomach	1400	0.00E+00	9.60E-02	3.14E-06	3.14E-05	5.0224E-15

As expected, like the Ir-192 multiple source organs at time T plus six hours, the majority of the activity remained in the lung but continues to pass through the stomach, small intestine and colon. Of the 19 percent of activity that remained in the lung at time T plus six hours, the lung retained 14.2 percent at time T plus 12 hours. The activity in the stomach was reduced from 0.1 percent to essentially zero and the activity in the small intestine was reduced from 4.9 percent to 4.6 percent. The most sensitive organ

for Ir-192 at time T plus 12 hours were the colon followed by the trachea, stomach and small intestine. The dose to the lung at time T plus six hours from Ir-192 was 3.59×10^{-5} MeV/g and the dose to the lung at time T plus 12 hours was 2.63×10^{-5} MeV/g. The colon dose at time T plus six hours from Ir-192 was 3.53×10^{-6} MeV/g and the colon dose at time T plus 12 hours was 6.05×10^{-5} MeV/g. This produced an increase in the colon dose by approximately two times.

Statistical checks were performed on the Ir-192 Dose output file. The same warnings present with Co-60 were observed. The 10 statistical checks for tally-four fluence photons passed and produced similar results. The 10 statistical checks for tally-six dose photons passed and produced similar results as with Co-60. Of the 61 tally bins, no bin had zero dose and 6 bins had relative errors exceeding 0.10 for the 0.47 MeV photon. The second 0.32 MeV photon produced similar results.

The tallies for the electron sources within the multiple organs had to be evaluated in a slightly different manner based on their inability to penetrate uniformly throughout the phantom. Secondary emissions, such as bremsstrahlung and characteristics x rays were the primary radiation source for organs outside of the source organs. Four of the 10 statistical checks did not pass. The relative error was 0.36, the VoV was 0.39 and the rate did not decrease according to the inverse of the number of histories, and the pdf value was 0. This reflects a large number of zero doses and slightly greater than zero doses based on the electron source.

Figures 19.3 and 19.4 provide a simulated 3-dimensional view of the human body with a color profile that shows the MCNP dose for the 0.47 MeV photon of Ir-192 and the 0.66 MeV electron of Ir-192 absorbed by each organ, respectively. The color bar units to the right of the phantom are in MeV/organ weight in grams.

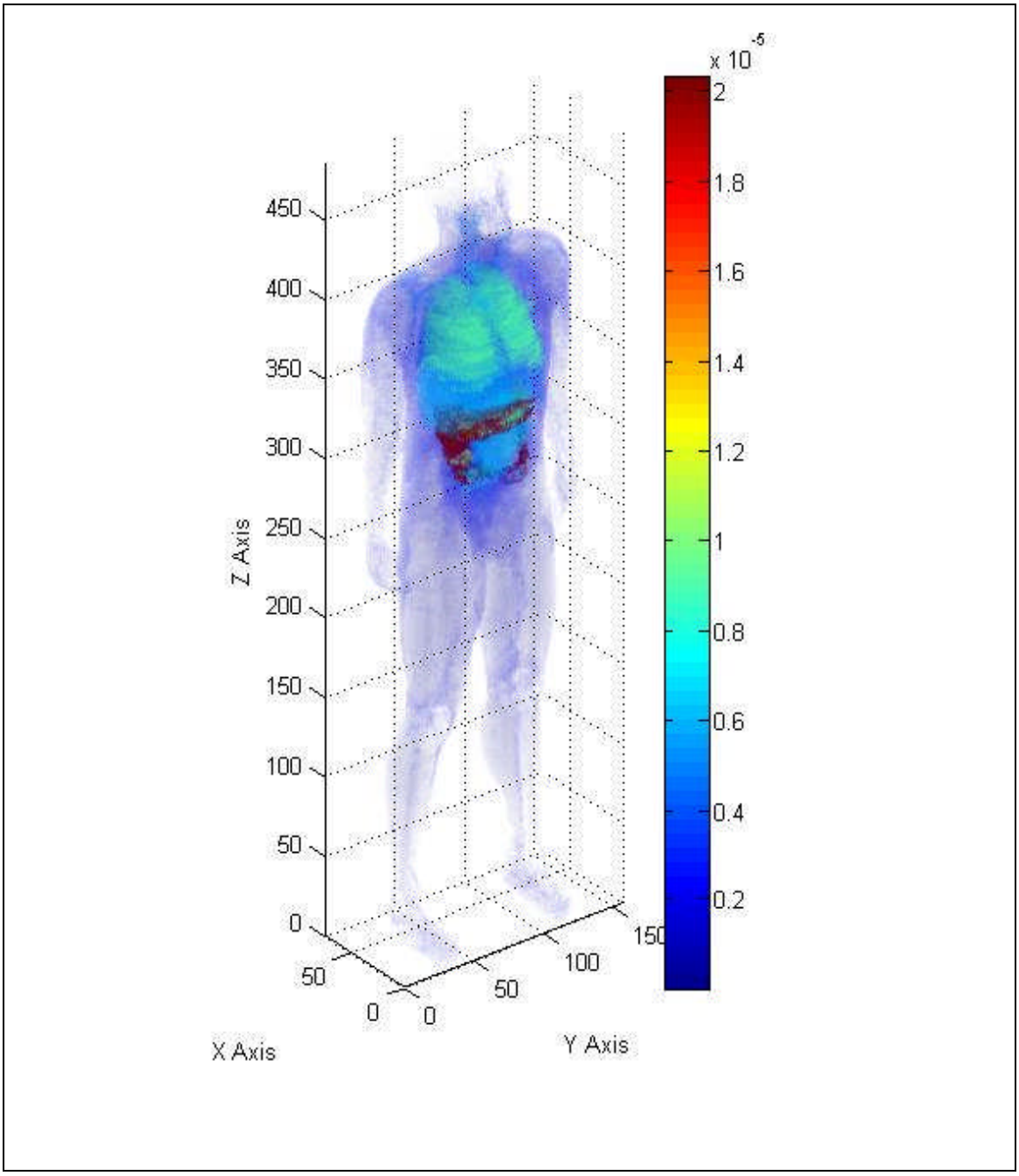

Fig. 19.3. Three-dimensional human dose profile from the 0.47 MeV Ir-192 photon source located within multiple organs after T plus 12 hours.

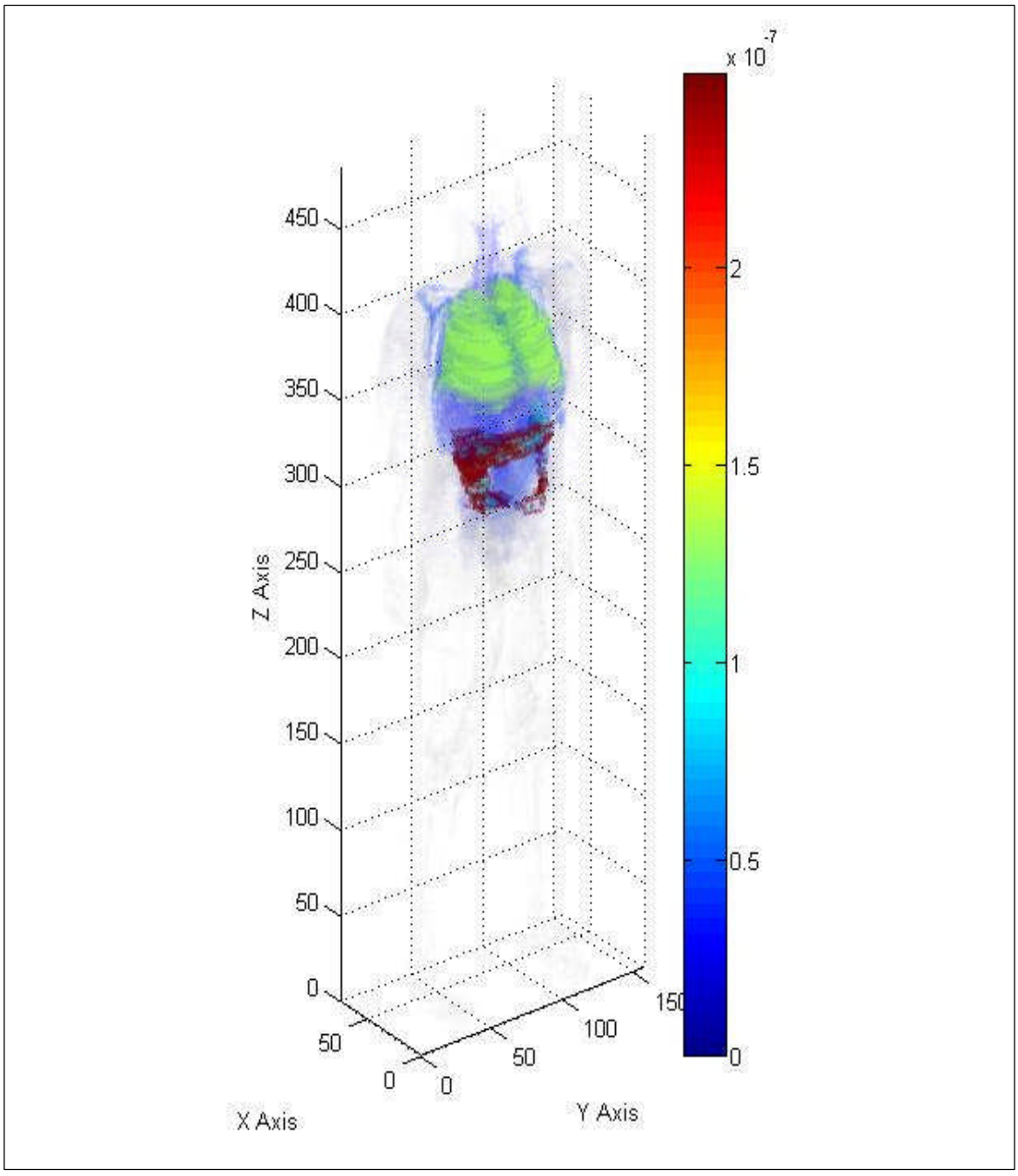

Fig. 19.4. Three-dimensional human dose profile from the 0.66 MeV Ir-192 electron source located within multiple organs after T plus 12 hours.

Sr-90 organ dose profile

A Sr-90 source located within the lung, stomach, liver, small intestine and colon would deliver a dose to the selected organs at T plus twelve hours that ranges from a high of 3.48 x 10^{-7} MeV/g for the colon and a low of 4.47 x 10^{-12} MeV/g for the skin. This organ dose contribution is from a single beta emission with a maximum energy of 0.55 MeV. The beta emission is produced with a yield of about 100%. Table 19.4 provides the calculated dose conversions for each of the selected organs that will be considered in this problem.

Table 19.4. Organ doses from a Sr-90 volume source in multiple organs at time T plus 12 hours.

Organs	No. of Sources in Organ	Activity normalized to 1	MCNP Dose (MeV/g)/his	Std Deviation	Organ Dose (MeV/g)/his	Organ Dose (Gy)/his
Skin	0	0.00E+00	2.49E-07	9.31E-14	4.47E-12	7.16824E-22
Rib Bone Group	0	0.00E+00	1.66E-03	8.31E-10	5.03E-08	8.07E-18
Small Int	3499	4.20E-03	5.90E-04	1.38E-09	4.43E-08	7.09273E-18
Gonads	0	0.00E+00	1.13E-07	1.48E-10	1.48E-10	2.3647E-20
Rectum	0	0.00E+00	5.88E-06	9.08E-10	4.57E-09	7.33E-19
Thyroid	0	0.00E+00	9.11E-06	3.02E-09	2.28E-08	3.64857E-18
Lung	15000	1.42E-01	1.36E-02	1.54E-09	1.65E-07	2.64667E-17
Eyes	0	0.00E+00	0.00E+00	0.00E+00	0.00E+00	0
Trachea	0	0.00E+00	3.42E-05	1.62E-08	1.67E-07	2.68191E-17
Colon	2124	9.38E-02	2.62E-03	4.14E-09	3.48E-07	5.57551E-17
Stomach	1400	0.00E+00	1.52E-04	2.85E-09	4.95E-08	7.93062E-18

The most sensitive organ for a Sr-90 electron source at time T plus 12 hours remained the colon. The trachea and lung follow the colon in sensitivity. The colon retained 8.4 percent of the activity at T plus six hours and 9.4 percent at T plus 12 hours. Of the 19.2 percent of activity that remained in the lung at T plus six hours, the lung retained 14.2 percent at T plus 12 hours. Compared to the Sr-90 lung dose at T plus six hours which was 1.75 x 10^{-7} MeV/g, the lung dose at T plus 12 hours was 1.65 x 10^{-7} MeV/g.

Statistical checks were performed on the Sr-90 Dose output file. The same warnings present with Co-60 were observed. The 10 statistical checks for tally-four fluence missed three of the 10 checks. The relative error was 0.38, VoV was 0.33 and the pdf was 0. The 10 statistical checks for tally-six dose passed. Of the 61 tally bins, 8 bins had a zero dose and 29 bins had relative errors exceeding 0.10 for the 0.55 MeV beta emission. Figure 19.5 provides a simulated 3-dimensional view of the human body with a color profile that shows the organ dose for the beta emission of Sr-90. The color bar units to the right of the phantom are in MeV/organ weight in grams.

Y-90 organ dose profile

A Y-90 source located within the lung, stomach, liver, small intestine and colon would deliver a dose to the selected organs at T plus twelve hours that ranges from a high of 2.55×10^{-6} MeV/g for the colon and a low of 8.94×10^{-11} MeV/g for the skin. This organ dose contribution is from a single beta emission with a maximum energy of 2.28 MeV. The beta emission is produced with a yield of about 100%. Table 19.5 provides the calculated dose conversions for each of the selected organs that will be considered in this problem.

Table 19.5. Organ doses from a Y-90 volume source in multiple organs at time T plus 12 hours.

Organs	No. of Sources in Organ	Activity normalized to 1	MCNP Dose (MeV/g)/his	Std Deviation	Organ Dose (MeV/g)/his	Organ Dose (Gy)/his
Skin	0	0.00E+00	4.97E-06	7.77E-13	8.94E-11	1.43148E-20
Rib Bone Group	0	0.00E+00	1.80E-02	3.18E-09	5.48E-07	8.78E-17
Small Int	3499	4.20E-03	7.62E-03	8.69E-09	5.72E-07	9.1634E-17
Gonads	0	0.00E+00	6.34E-06	3.17E-09	8.29E-09	1.32831E-18
Rectum	0	0.00E+00	8.05E-05	5.12E-09	6.26E-08	1.00E-17
Thyroid	0	0.00E+00	1.32E-04	1.89E-08	3.29E-07	5.27426E-17
Lung	15000	1.42E-01	8.72E-02	5.30E-09	1.06E-06	1.69655E-16
Eyes	0	0.00E+00	4.71E-06	7.64E-09	1.54E-08	2.46646E-18
Trachea	0	0.00E+00	3.73E-04	6.51E-08	1.83E-06	2.92813E-16
Colon	2124	9.38E-02	1.92E-02	1.78E-08	2.55E-06	4.08413E-16
Stomach	1400	0.00E+00	2.29E-03	1.68E-08	7.49E-07	1.19915E-16

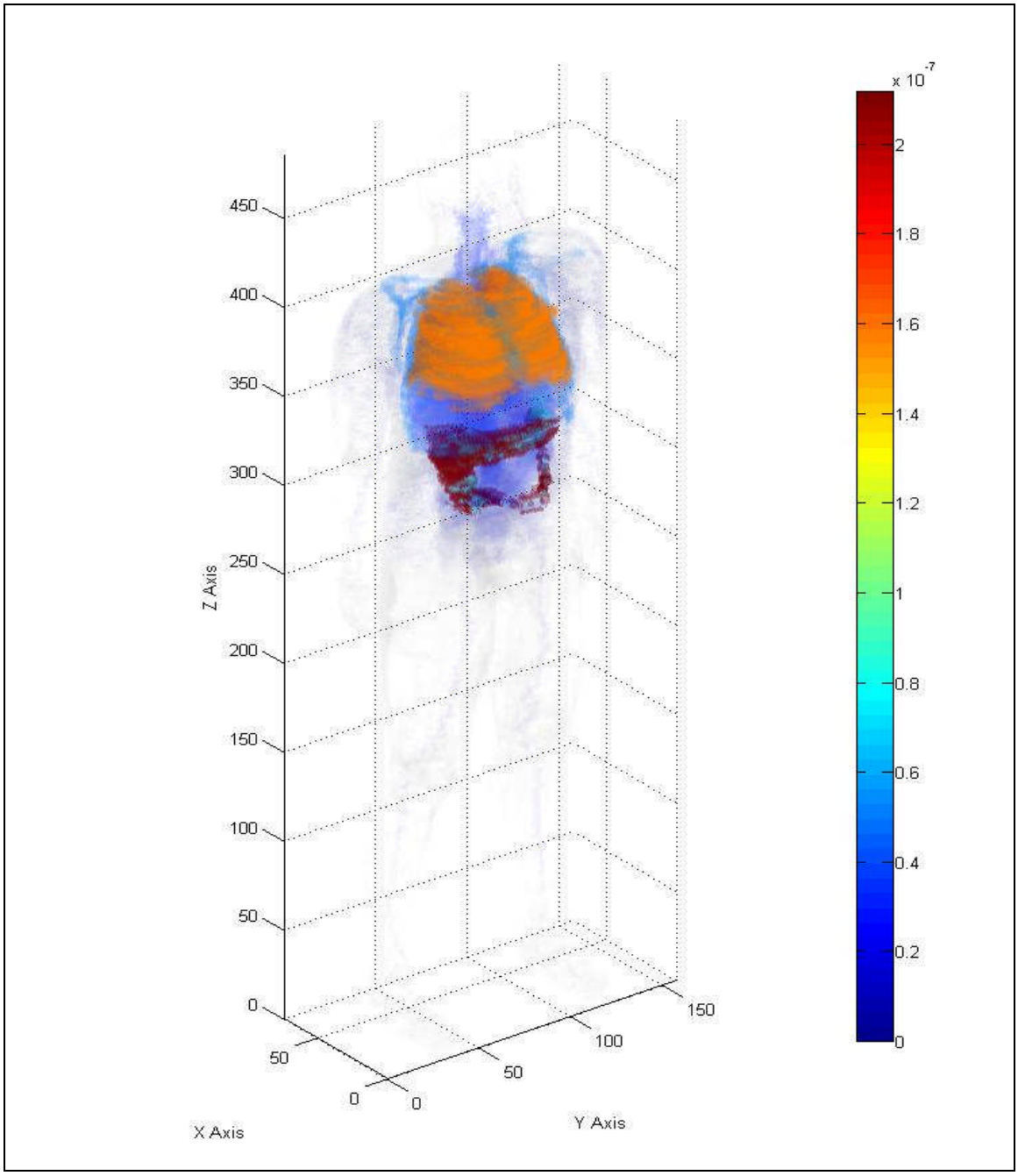

Fig. 19.5. Three-dimensional human dose profile from a Sr-90 beta source located within multiple organs after T plus 12 hours.

As with Sr-90, the colon, trachea and lung received the highest dose from a highly-energetic, beta radiation source located in multiple organs at time T plus 12 hours. Of the 19.2 percent of activity that remained in the lung at T plus six hours, the lung retains 14.2 percent at T plus 12 hours. The organ activity follows that of Sr-90. Compared to the Y-90 dose at T plus six hours which was 1.12×10^{-6} MeV/g, the lung dose at T plus 12 hours was 1.06×10^{-6} MeV/g. The colon dose from Y-90 at T plus six hours was 1.92×10^{-6} MeV/g and the colon dose at T plus 12 hours was 2.55×10^{-6} MeV/g. This produced an increase in the colon dose by roughly 30 percent.

Statistical checks were performed on the Y-90 Dose output file. The same warnings present with Co-60 were observed. The 10 statistical checks for tally-four fluence passed all but three checks. The VoV did not decrease according to the inverse of the number of histories and the pdf was 0. The 10 statistical checks for tally-six dose passed. Of the 61 tally bins, one bin had a zero dose and 24 bins had relative errors exceeding 0.10 for the 2.28 MeV beta emission. Figure 19.6 provides a simulated 3-dimensional view of the human body with a color profile that shows the organ dose for an Y-90 source in multiple organs. The color bar units to the right of the phantom are in MeV/organ weight in grams.

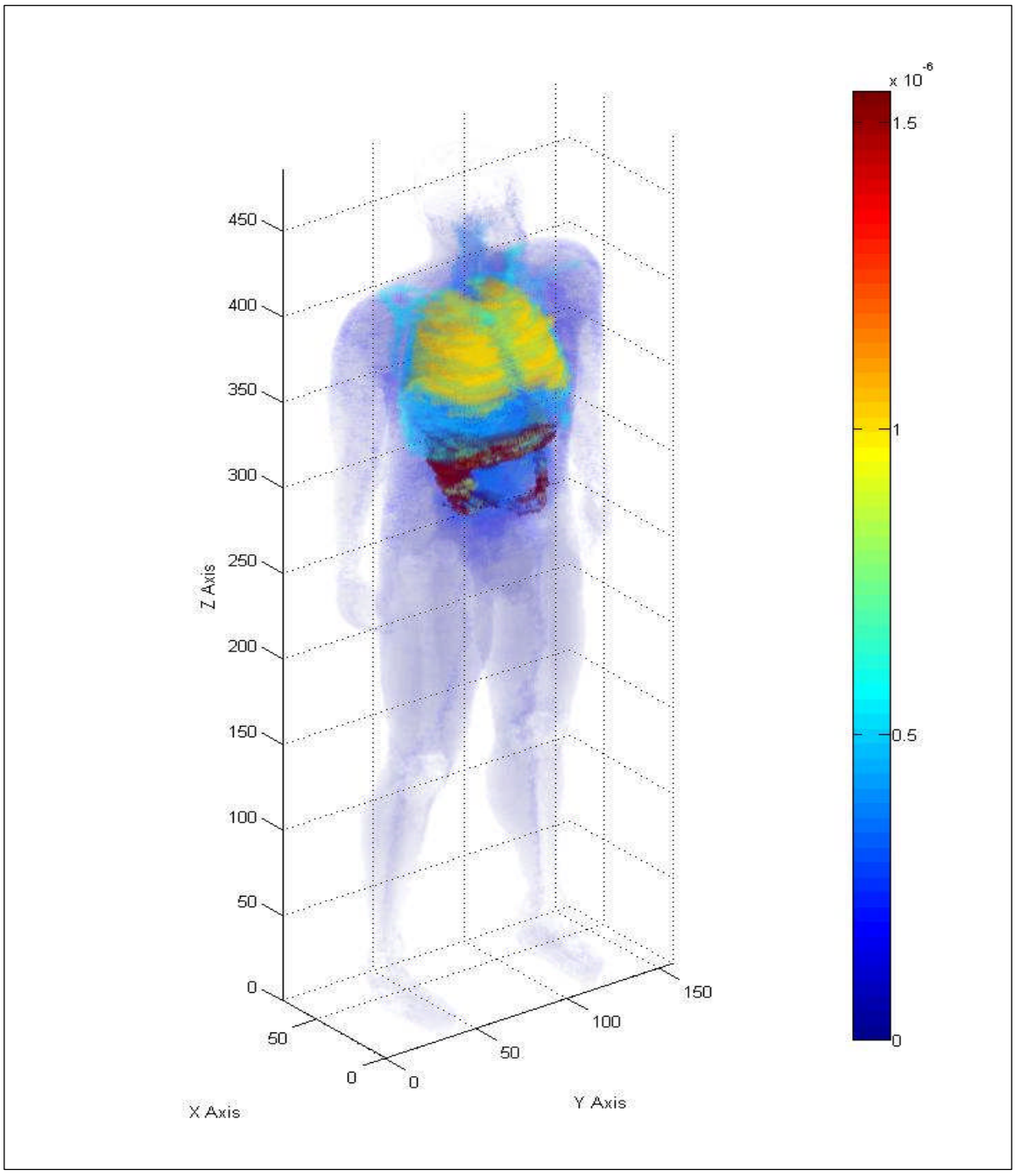

Fig. 19.6. Three-dimensional human dose from a Y-90 beta source located within multiple organs after T plus 12 hours.

Results from multi-organ lung, stomach, liver, small intestine and colon volume sources after twelve hours

Figure 19.7 provides a graph of all of the potential sources distributed in multiple organs after T plus 12 hours and their organ doses. Based upon the results of the observed programs, twelve hours after inhalation, Co-60 is the most limiting radionuclide. The trachea, colon and stomach appear to be the most sensitive organs based upon a single emission from a source distribution described above. Even though the trachea shows the highest sensitivity, the dose is a little deceiving. The observed dose for the trachea is based on the number of voxels which include the air encircled by the trachea. The actual dose, based on the weight of the organ, is less than that for the stomach and small intestine.

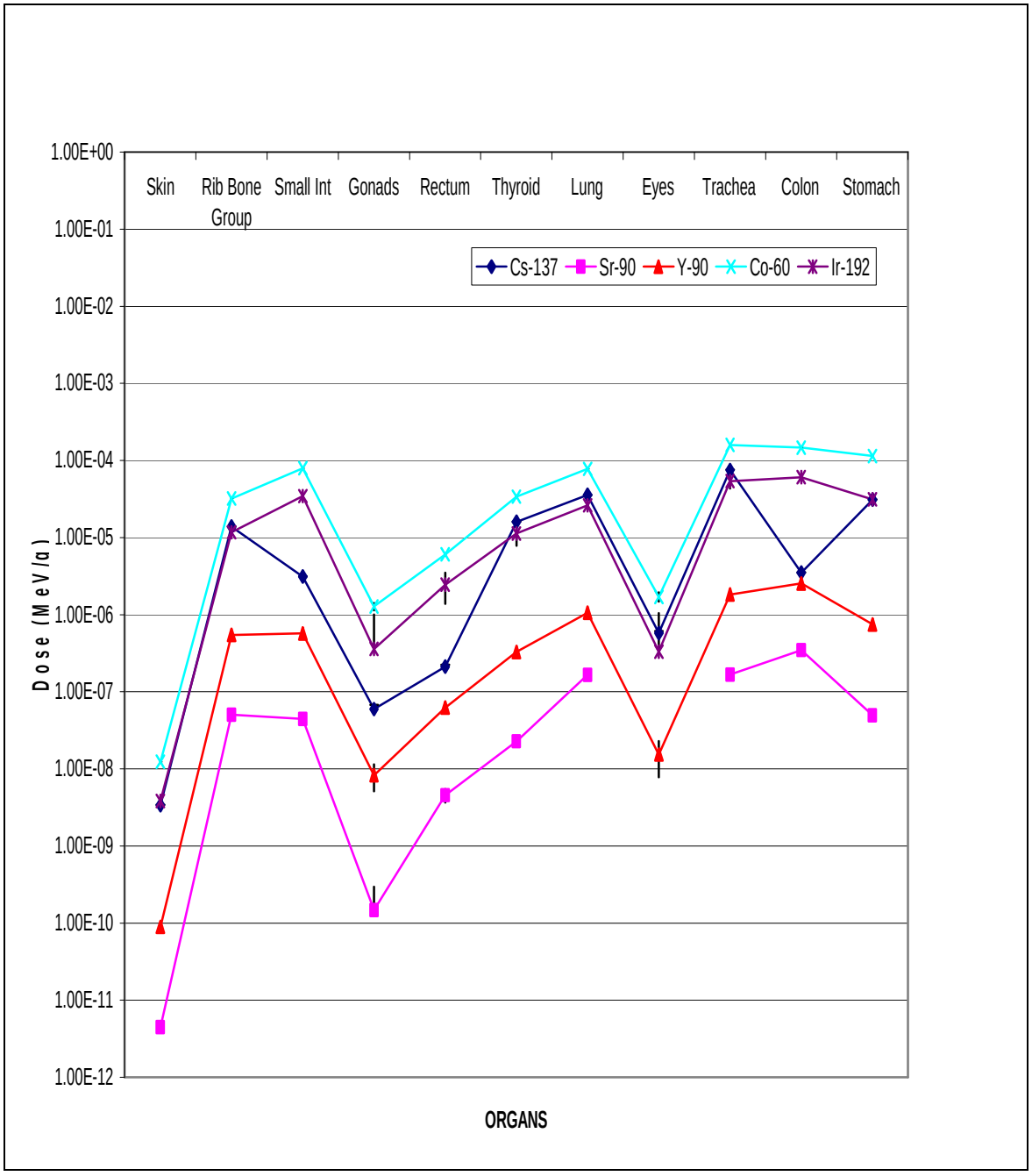

Fig. 19.7. Summary graph of organ doses for the five potential multi-organ sources after T plus 12 hours.

CHAPTER XX
ESTIMATING ORGAN DOSE BASED ON VOLUME SOURCES IN THE LUNG, STOMACH, SMALL INTESTINE AND COLON 18 HOURS AFTER A LUNG INHALATION

Co-60 organ dose profile

A Co-60 source located within the lung, stomach, liver, small intestine and colon would deliver a dose to the selected organs that ranges from a high of 2.00×10^{-4} MeV/g for the colon and a low of 1.23×10^{-8} MeV/g for the skin. This organ dose contribution is from the sum of two photon emissions that occur with a yield of about 100 percent. Table 20.1 provides the calculated dose conversions for each of the selected organs at time (T) plus 18 hours from detonation.

Table 20.1. Organ doses from a Co-60 volume source in multiple organs at time T plus 18 hours.

Organs	No. of Sources in Organ	Activity normalized to 1	MCNP Dose (MeV/g)/his	Std Deviation	Organ Dose (MeV/g)/his	Organ Dose (Gy)
Skin	0	0.00E+00	6.85E-04	2.96E-11	1.23E-08	1.97E-18
Rib Bone Group	0	0.00E+00	9.45E-01	8.61E-08	2.87E-05	4.60E-15
Small Int	3499	4.60E-02	1.04E+00	4.37E-07	7.80E-05	1.25E-14
Gonads	0	0.00E+00	1.15E-03	1.48E-07	1.51E-06	2.42E-16
Rectum	0	0.00E+00	1.18E-02	2.99E-07	9.18E-06	1.47E-15
Thyroid	0	0.00E+00	1.13E-02	8.68E-07	2.83E-05	4.53E-15
Lung	15000	3.10E-01	5.60E+00	1.77E-07	6.79E-05	1.09E-14
Eyes	0	0.00E+00	4.69E-04	2.27E-07	1.53E-06	2.45E-16
Trachea	0	0.00E+00	2.84E-02	3.04E-06	1.39E-04	2.23E-14
Colon	2124	2.27E-01	1.51E+00	7.22E-07	2.00E-04	3.21E-14
Stomach	1400	9.21E-03	3.04E-01	8.72E-07	9.91E-05	1.59E-14

The activity in the lung was reduced from 37 percent to 31 percent from time T plus six hours to time T plus 18 hours. As expected, the majority of the activity remains in the lung at time T plus 18 hours. As with time T plus six hours, the small intestine contains the second highest activity at T plus 18 hours. The activity of the small

intestine decreased from 6.5 percent to 4.6 percent. The activity in the stomach was further reduced from 1.4 percent to 0.9 percent. The activity in the colon increased from 16.1 percent to 22.7 percent. For Co-60, the most sensitive organ changed from the trachea to the colon followed closely by the stomach and small intestine. Compared to the Co-60 dose at time T plus 12 hours, the lung dose was 7.78×10^{-5} MeV/g and the lung dose at time T plus 18 hours was 6.79×10^{-5} MeV/g. The stomach dose from Co-60 at T plus 12 hours was 1.14×10^{-4} MeV/g and the stomach dose at time T plus 18 hours was 9.91×10^{-5} MeV/g or roughly a 10 percent decrease in dose to the stomach.

Statistical analysis of output file

The tally-four fluence analysis for each detector, setup as described in chapter VII, provided a random behavior for the mean. The desired relative error should be less than 0.10 and the observed relative error was 0.03. The desired and observed relative errors decreased according to the inverse of the square root of the number of histories. The desired variance of the variance should be less than 0.10 and the observed VoV was 0.00. The figure of merit value was constant and the behavior was random. The probability density function (pdf) desired should be greater than three, the observed pdf value was 10. The tally-four fluence passed all 10 statistical checks. Out of 10 tally-four bins, only one had a zero dose and no bins contained relative errors greater than 0.10. The second 1.33 MeV photon simulation provided similar results.

The tally-six dose analysis for each material provided a random behavior for the mean. The desired relative error should be less than 0.10 and the observed relative error was 0.00 for the 1.17 MeV photon and 0.00 for the 1.33 MeV photon. The desired and observed relative errors decreased according to the inverse of the square root of the number of histories. The desired variance of the variance should be less than 0.10 and the observed VoV was 0.00. The figure of merit value was constant and the behavior was random. The desired probability density function (pdf) should be greater than 3.00 and the observed value was 10.0 for the 1.17 MeV photon and 9.79 for the 1.33 MeV

photon. The tally-six dose passed all 10 statistical checks. Out of 61 tally-six bins, no bin had a zero dose and only 5 bins contained relative errors greater than 0.10.

Figure 20.1 provides a simulated 3-dimensional view of the human body with a color profile that shows the organ dose for the 1.33 MeV photon of Co-60. Each axis is represented in the figure along with a color bar that indicates the organ dose in MeV/organ in grams provided by the MCNPX output file. In the MCNPX output file, the trachea receives a slightly lesser dose than the lung based upon the number of voxels versus the measured gram weight of the trachea. The phantom includes the airway as part of the trachea.

Cs-137 organ dose profile

A Cs-137 source located within the lung, stomach, liver, small intestine and colon would deliver a dose to the selected organs at T plus 18 hours from exposure that ranges from a high of 7.24×10^{-5} MeV/g for the trachea and a low of 3.41×10^{-9} MeV/g for the skin. This organ dose contribution is from a 0.66 MeV photon emitted from Cs-137 that occurs with a yield of about 86 percent. Table 20.2 provides the calculated dose conversions to the selected organs at time (T) plus 18 hours from detonation.

Table 20.2. Organ doses for a Cs-137 volume source in multiple organs at time T plus 18 hours.

Organs	No. of Sources in Organ	Activity normalized to 1	MCNP Dose (MeV/g)/his	Std Deviation	Organ Dose (MeV/g)/his	Organ Dose (Gy)
Skin	0	0.00E+00	1.90E-04	4.10E-12	3.41E-09	5.47E-19
Rib Bone Group	0	0.00E+00	4.59E-01	1.39E-08	1.39E-05	2.23E-15
Small Int	3499	0.00E+00	4.21E-02	2.53E-08	3.16E-06	5.06E-16
Gonads	0	0.00E+00	2.83E-05	5.67E-09	3.71E-08	5.94E-18
Rectum	0	0.00E+00	2.78E-04	1.13E-08	2.16E-07	3.47E-17
Thyroid	0	0.00E+00	6.12E-03	1.73E-07	1.53E-05	2.45E-15
Lung	15000	1.07E-01	2.96E+00	2.51E-08	3.59E-05	5.75E-15
Eyes	0	0.00E+00	1.66E-04	3.39E-08	5.42E-07	8.69E-17
Trachea	0	0.00E+00	1.48E-02	5.72E-07	7.24E-05	1.16E-14
Colon	2124	0.00E+00	2.70E-02	2.86E-08	3.58E-06	5.73E-16
Stomach	1400	5.00E-05	9.23E-02	1.27E-07	3.01E-05	4.83E-15

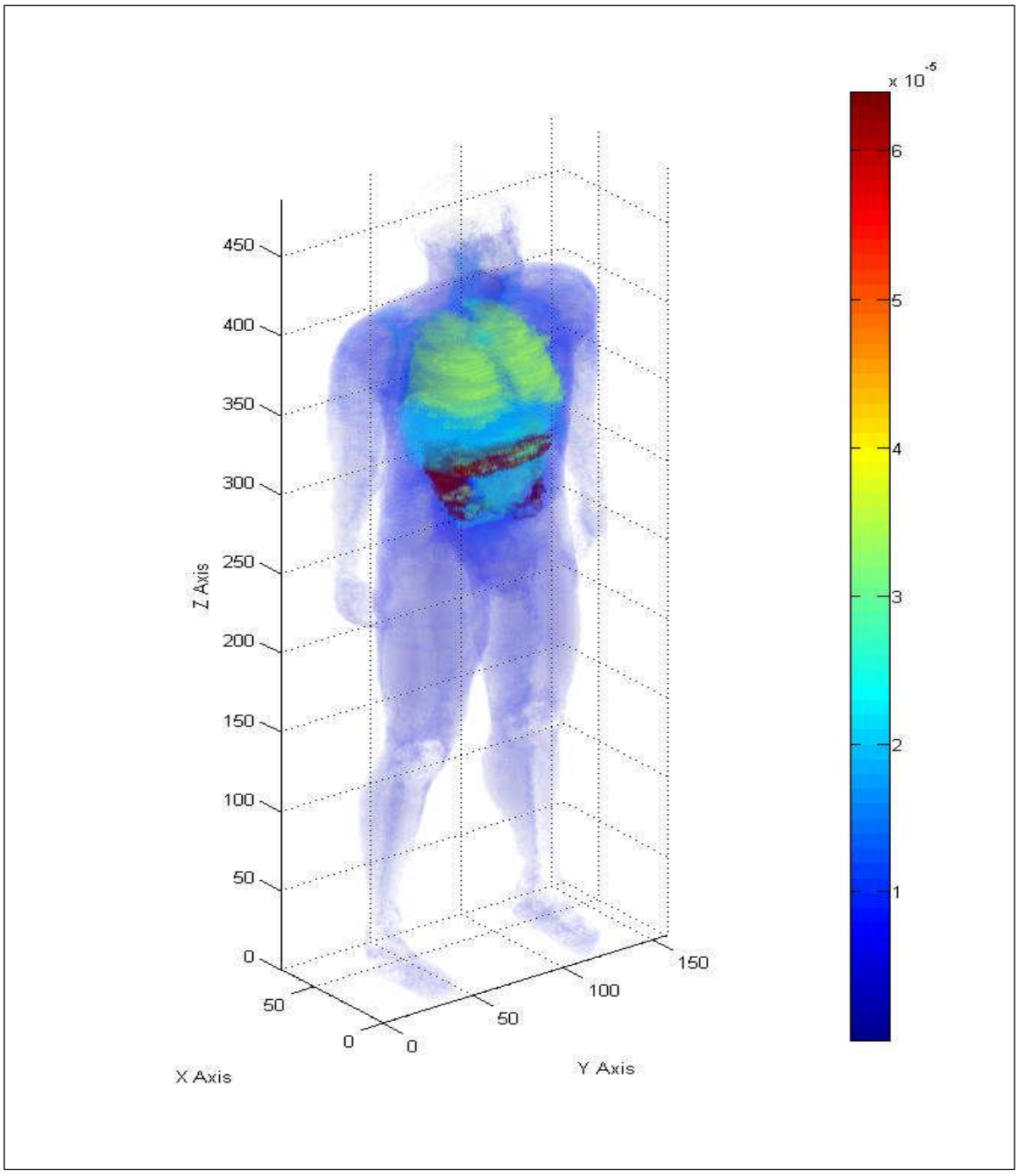

Fig. 20.1. Three-dimensional human dose profile from a 1.33 MeV photon source located within multiple organs after T plus 18 hours.

The activity in the lung was reduced from 14.4 percent to 10.7 percent from time T plus 12 hours to time T plus 18 hours. The majority of the activity is absorbed by the body. The activity in the stomach remains at less than 0.01 percent. For Cs-137, the most sensitive organs were the trachea followed by the lung, stomach and colon. Compared to the Cs-137 dose at time T plus 12 hours, the lung dose was 3.59×10^{-5} MeV/g and the dose remained the same at 3.59×10^{-5} MeV/g for T plus 18 hours. The stomach dose from Co-60 at T plus 12 hours was 3.11×10^{-5} MeV/g and at time T plus 18 hours the stomach dose was 3.01×10^{-5} MeV/g or roughly a ten percent decrease in dose to the stomach.

Statistical checks were performed on the Cs-137 dose output file. The same warnings present with Co-60 were observed. The 10 statistical checks for tally-four fluence passed and produced similar results. The 10 statistical checks for tally-six dose passed and produced similar results as with Co-60. Of the 61 tally bins, no bin had a zero dose and 8 bins had relative errors exceeding 0.10. Figure 20.2 provides a simulated 3-dimensional view of the human body with a color profile that shows the organ dose for the single photon of Cs-137. The color bar units to the right of the phantom are in MeV/organ weight in grams.

At T plus 18 hours, the most sensitive organ for a Co-60 shifted from the trachea to the colon. For Cs-137 the most sensitive organ was the trachea. The colon received a dose of 2.00×10^{-4} MeV/g from Co-60 and the trachea received a dose of 7.24×10^{-4} MeV/g from Cs-137. The change in Co-60 activity from T plus 12 hours to T plus 18 hours was enough to alter the most sensitive organ. There was not enough change in Cs-137 activity to alter the most sensitive organ. For Cs-137, 10.7 percent of the activity remains in the lung at T plus 18 hours while 14.4 percent of the activity remains in the lung at T plus 12 hours. The activity in the stomach dropped from 0.012 percent to 0.005 percent at T plus 18 hours. The key difference is the change in activity present in the colon. The relative majority of activity remains in the lung.

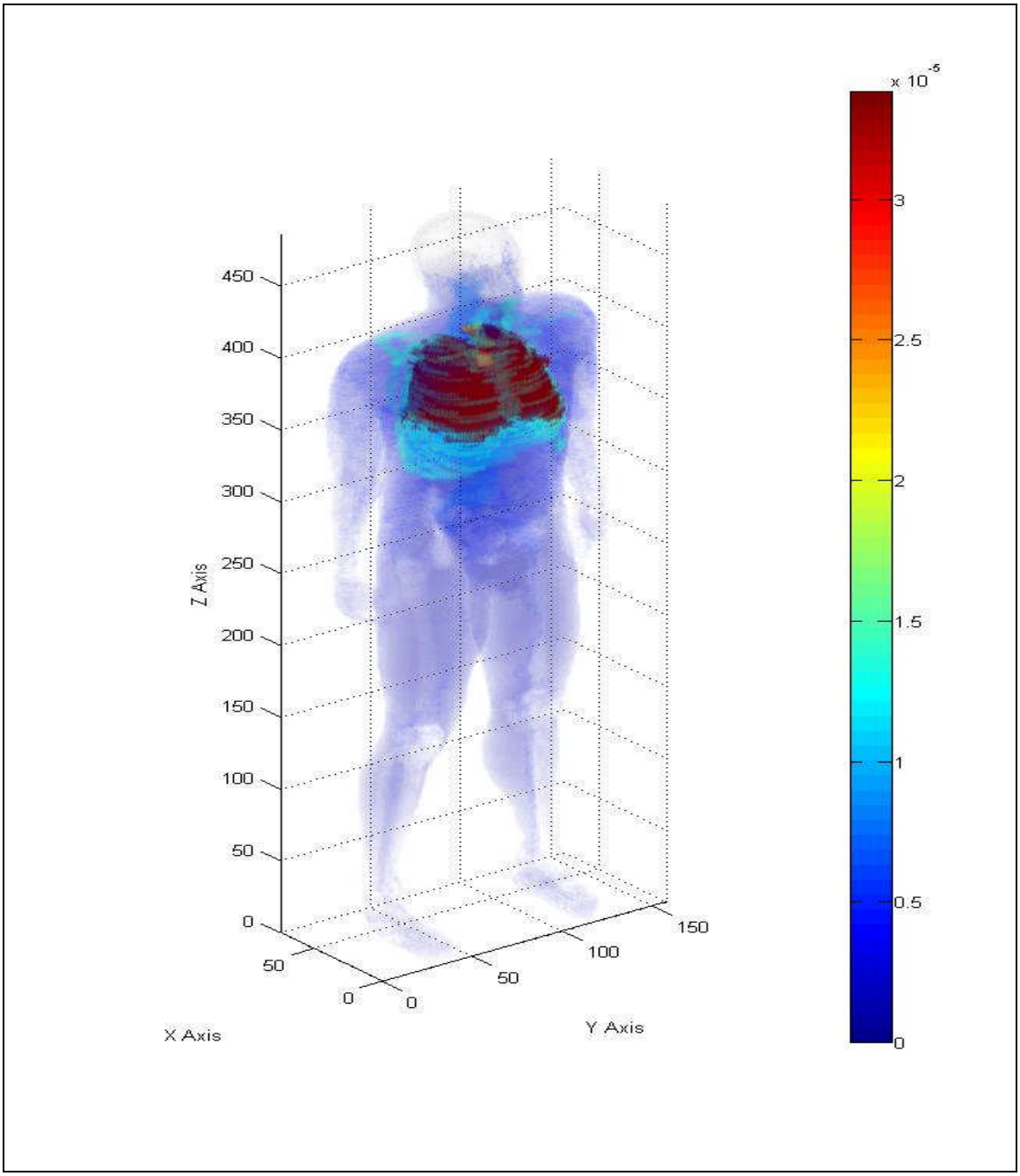

Fig. 20.2. Three-dimensional human dose profile from a Cs-137 photon source located within multiple organs after T plus 18 hours.

Ir-192 organ dose profile

An Ir-192 source located within the lung, stomach, liver, small intestine and colon would deliver a dose to the selected organs at T plus 18 hours from exposure that ranges from a high of 9.67 x 10^{-5} MeV/g for the colon and a low of 3.84 x 10^{-9} MeV/g for the skin. This organ dose contribution is from the sum of two photons with energies of 0.47 MeV and 0.32 MeV along with two electrons with maximum energies of 0.66 MeV and 0.54 MeV. All four emissions are produced with a yield of 26.2%, 22.4%, 10.1% and 6.7%, respectively. Table 20.3 provides the calculated dose conversions for each of the selected organs at time (T) plus 18 hours from detonation.

Table 20.3. Organ doses for an Ir-192 volume source in multiple organs at time T plus 18 hours.

Organs	No. of Sources in Organ	Activity normalized to 1	MCNP Dose (MeV/g)/his	Std Deviation	Organ Dose (MeV/g)/his	Organ Dose (Gy)
Skin	0	0.00E+00	2.13E-04	1.62E-10	3.83E-09	6.14E-19
Rib Bone Group	0	0.00E+00	3.39E-01	3.85E-07	1.03E-05	1.65E-15
Small Int	3499	2.55E-03	3.22E-01	1.49E-06	2.42E-05	3.88E-15
Gonads	0	0.00E+00	3.07E-04	7.84E-07	4.01E-07	6.43E-17
Rectum	0	0.00E+00	4.21E-03	1.28E-06	3.28E-06	5.25E-16
Thyroid	0	0.00E+00	3.94E-03	3.05E-06	9.84E-06	1.58E-15
Lung	15000	1.07E-01	1.81E+00	5.05E-07	2.20E-05	3.53E-15
Eyes	0	0.00E+00	9.70E-05	3.66E-07	3.17E-07	5.07E-17
Trachea	0	0.00E+00	9.36E-03	1.03E-05	4.59E-05	7.35E-15
Colon	2124	1.24E-01	7.28E-01	2.50E-06	9.67E-05	1.55E-14
Stomach	1400	0.00E+00	8.30E-02	3.23E-06	2.71E-05	4.34E-15

As expected, like the Ir-192 multiple source organs at time T plus 12 hours, the majority of the activity remains in the lung but continues to pass through the stomach, small intestine and colon. Of the 14.2 percent of activity that remained in the lung at time T plus 12 hours, the lung retained 10.7 percent at time T plus 18 hours. The activity in the stomach remained at essentially zero and the activity in the small intestine was reduced from 4.6 percent to 0.3 percent. The most sensitive organs for Ir-192 at time T plus 18 hours remained the colon followed by the trachea, stomach and small intestine. The dose to the lung at time T plus 12 hours from Ir-192 was 2.63 x 10^{-5}

MeV/g and the lung dose at time T plus 18 hours was 2.20 x 10^{-5} MeV/g. The colon dose at time T plus 12 hours from Ir-192 was 6.05 x 10^{-5} MeV/g and the colon dose at time T plus 18 hours was 9.67 x 10^{-5} MeV/g. This produced an increase in the colon dose by roughly 30 percent.

Statistical checks were performed on the Ir-192 dose output file. The same warnings present with Co-60 were observed. The 10 statistical checks for tally-four fluence photons passed and produced similar results. The 10 statistical checks for tally-six dose photons passed and produced similar results as with Co-60. Of the 61 tally bins, no bins had a zero dose and 6 bins had relative errors exceeding 0.10 for the 0.47 MeV photon. The second 0.32 MeV photon produced similar results

The tallies for the electron sources within the lung had to be evaluated in a slightly different manner based on their inability to penetrate uniformly throughout the phantom. Secondary emissions, such as bremsstrahlung and characteristics x rays were the primary radiation source for organs outside of the lung. Three of the 10 statistical checks did not pass. The relative error was 0.24, the VoV did not decrease at a rate according to the inverse of the number of histories, and the pdf value was 0. This reflects a large number of zero doses and slightly greater than zero doses based on the electron source. Figures 20.3 and 20.4 provide a simulated 3-dimensional view of the human body with a color profile that shows the organ dose for the 0.47 MeV photon of Ir-192 and the 0.66 MeV electron of Ir-192, respectively. The color bar units to the right of the phantom are in MeV/organ weight in grams.

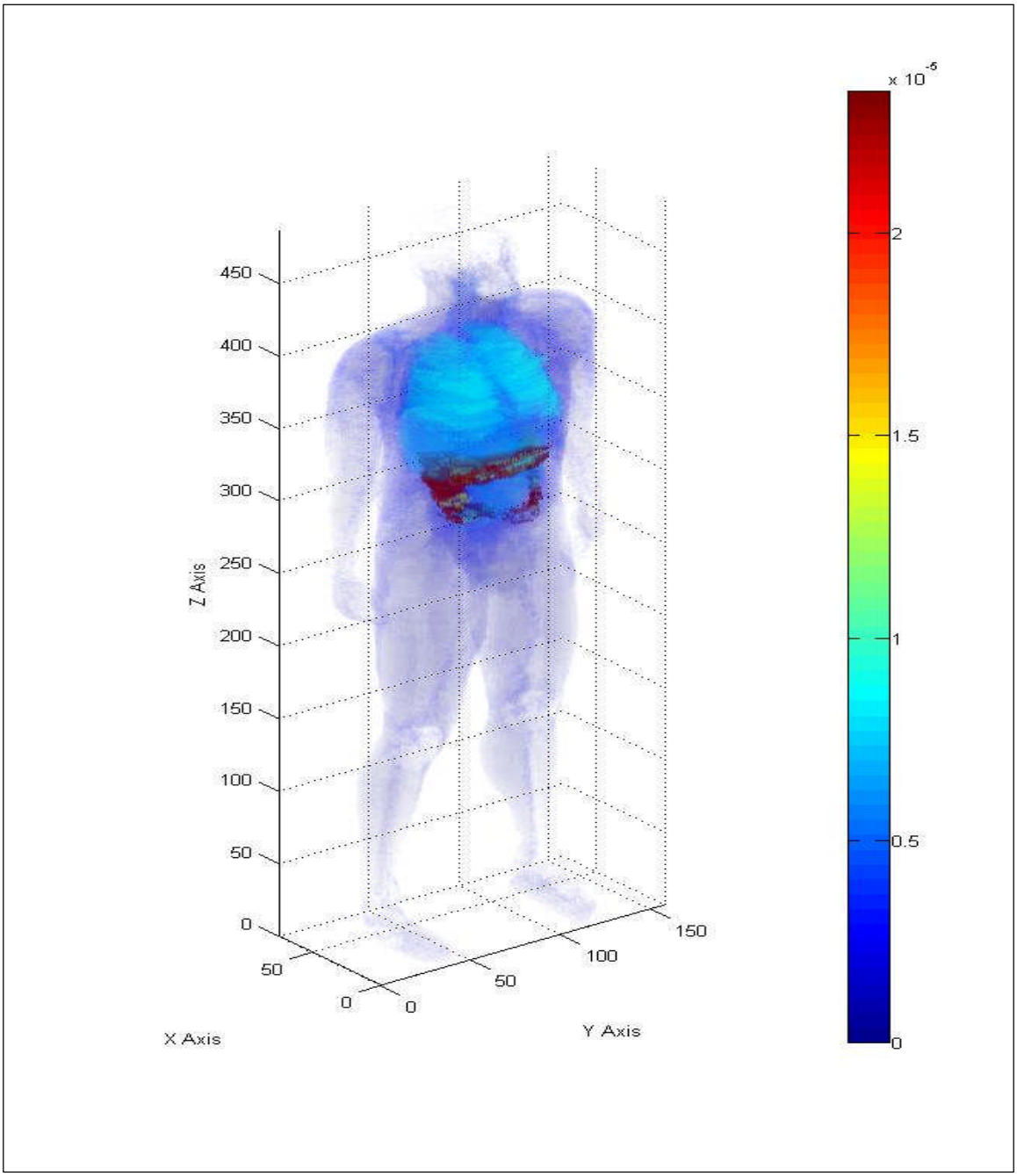

Fig. 20.3. Three-dimensional human dose profile from the 0.47 MeV Ir-192 photon source located within multiple organs after T plus 18 hours.

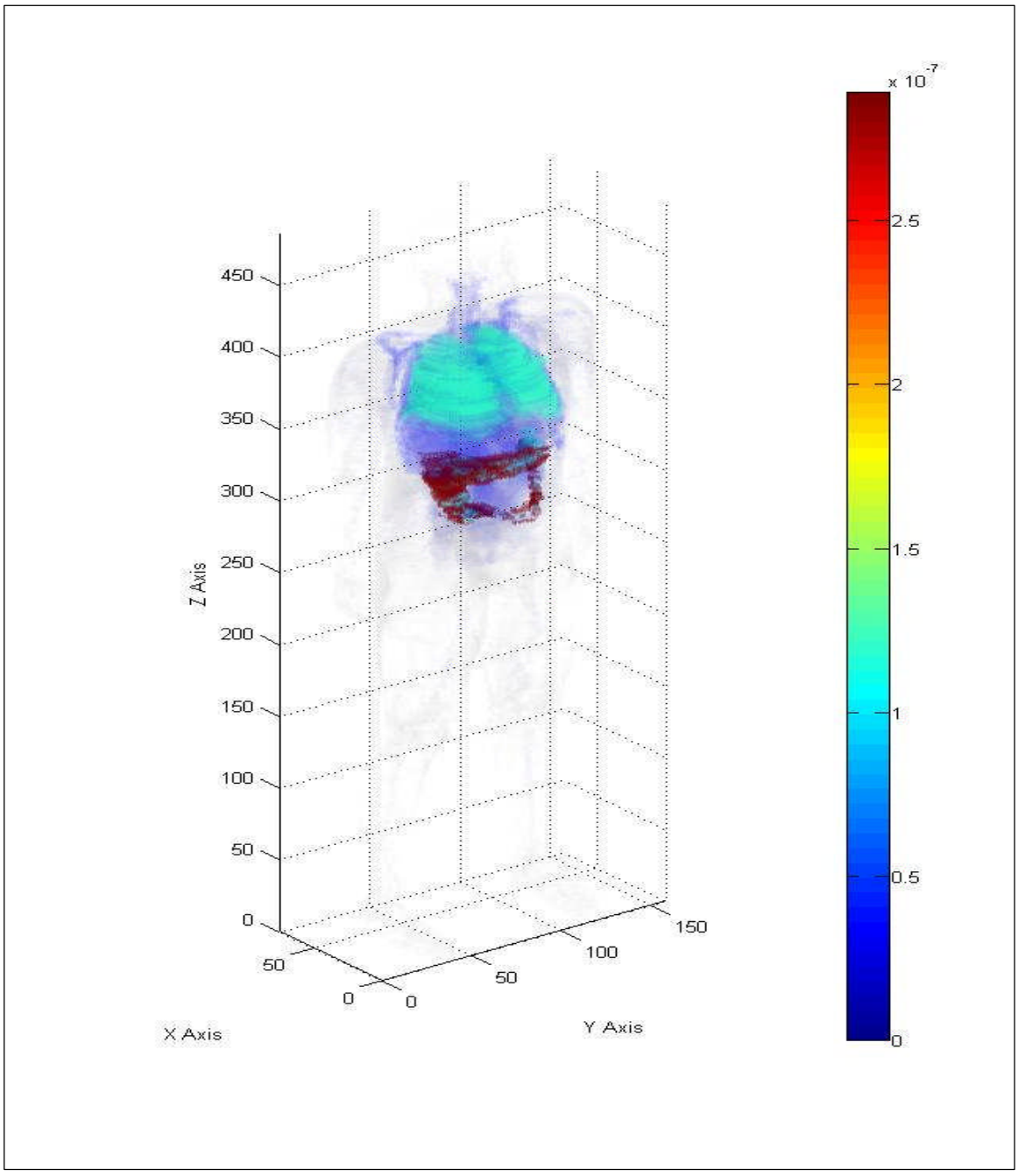

Fig. 20.4. Three-dimensional human dose profile from a 0.66 MeV Ir-192 beta source located within multiple organs after T plus 18 hours.

Sr-90 organ dose profile

A Sr-90 source located within the lung, stomach, liver, small intestine and colon would deliver a dose to the selected organs at T plus 18 hours that ranges from a high of 3.91 x 10^{-7} MeV/g for the colon and a low of 4.50 x 10^{-12} MeV/g for the skin. This organ dose contribution is from a single beta emission with a maximum energy of 0.55 MeV. The beta emission is produced with a yield of about 100%. Table 20.4 provides the calculated dose conversions for each of the selected organs that will be considered in this problem.

Table 20.4. Organ doses from a Sr-90 volume source in multiple organs at time T plus 18 hours.

Organs	No. of Sources in Organ	Activity normalized to 1	MCNP Dose (MeV/g)/his	Std Deviation	Organ Dose (MeV/g)/his	Organ Dose (Gy)
Skin	0	0.00E+00	2.50E-07	1.00E-13	4.50E-12	7.21E-22
Rib Bone Group	0	0.00E+00	1.55E-03	8.12E-10	4.72E-08	7.56E-18
Small Int	3499	7.00E-04	5.05E-04	1.34E-09	3.79E-08	6.08E-18
Gonads	0	0.00E+00	1.16E-07	1.00E-10	1.52E-10	2.44E-20
Rectum	0	0.00E+00	6.19E-06	8.83E-10	4.81E-09	7.71E-19
Thyroid	0	0.00E+00	9.62E-06	3.63E-09	2.40E-08	3.85E-18
Lung	15000	1.08E-01	1.27E-02	1.48E-09	1.54E-07	2.47E-17
Eyes	0	0.00E+00	0.00E+00	0.00E+00	0.00E+00	0
Trachea	0	0.00E+00	2.50E-05	1.31E-08	1.22E-07	1.96E-17
Colon	2124	8.48E-02	2.94E-03	4.42E-09	3.91E-07	6.26E-17
Stomach	1400	0.00E+00	1.50E-04	2.71E-09	4.89E-08	7.83E-18

The most sensitive organ for a Sr-90 beta source at time T plus 18 hours remained the colon. The trachea and lung followed the colon in sensitivity. The colon retained 9.4 percent of the activity at T plus 12 hours and 8.5 percent at T plus 18 hours. Of the 14.2 percent of activity that remained in the lung at T plus 12 hours, the lung retained 10.8 percent at T plus 18 hours. Compared to the lung dose from Sr-90 at T plus 12 hours which was 1.65 x 10^{-7} MeV/g, the lung dose at T plus 18 hours was 1.54 x 10^{-7} MeV/g.

Statistical checks were performed on the Sr-90 dose output file. The same warnings present with Co-60 were observed. The 10 statistical checks for tally-four fluence missed six of the 10 checks. The relative error was 0.42, the VoV was 0.64 and the rate did not decrease according to the inverse of the number of histories, the figure of merit was not constant and the pdf value was 0. The 10 statistical checks for tally-six dose passed. Of the 61 tally bins, 8 bins had a zero dose and 30 bins had relative errors exceeding 0.10 for the 0.55 MeV beta emission. Figure 20.5 provides a simulated 3-dimensional view of the human body with a color profile that shows the organ dose for the beta emission of Sr-90. The color bar units to the right of the phantom are in MeV/organ weight in grams.

Y-90 organ dose profile

A Y-90 source located within the lung, stomach, liver, small intestine and colon would deliver a dose to the selected organs at T plus 18 hours that ranges from a high of 2.81×10^{-6} MeV/g for the colon and a low of 8.86×10^{-11} MeV/g for the skin. This organ dose contribution is from a single beta emission with a maximum energy of 2.28 MeV. The beta emission is produced with a yield of about 100%. Table 20.5 provides the calculated dose conversions for each of the selected organs.

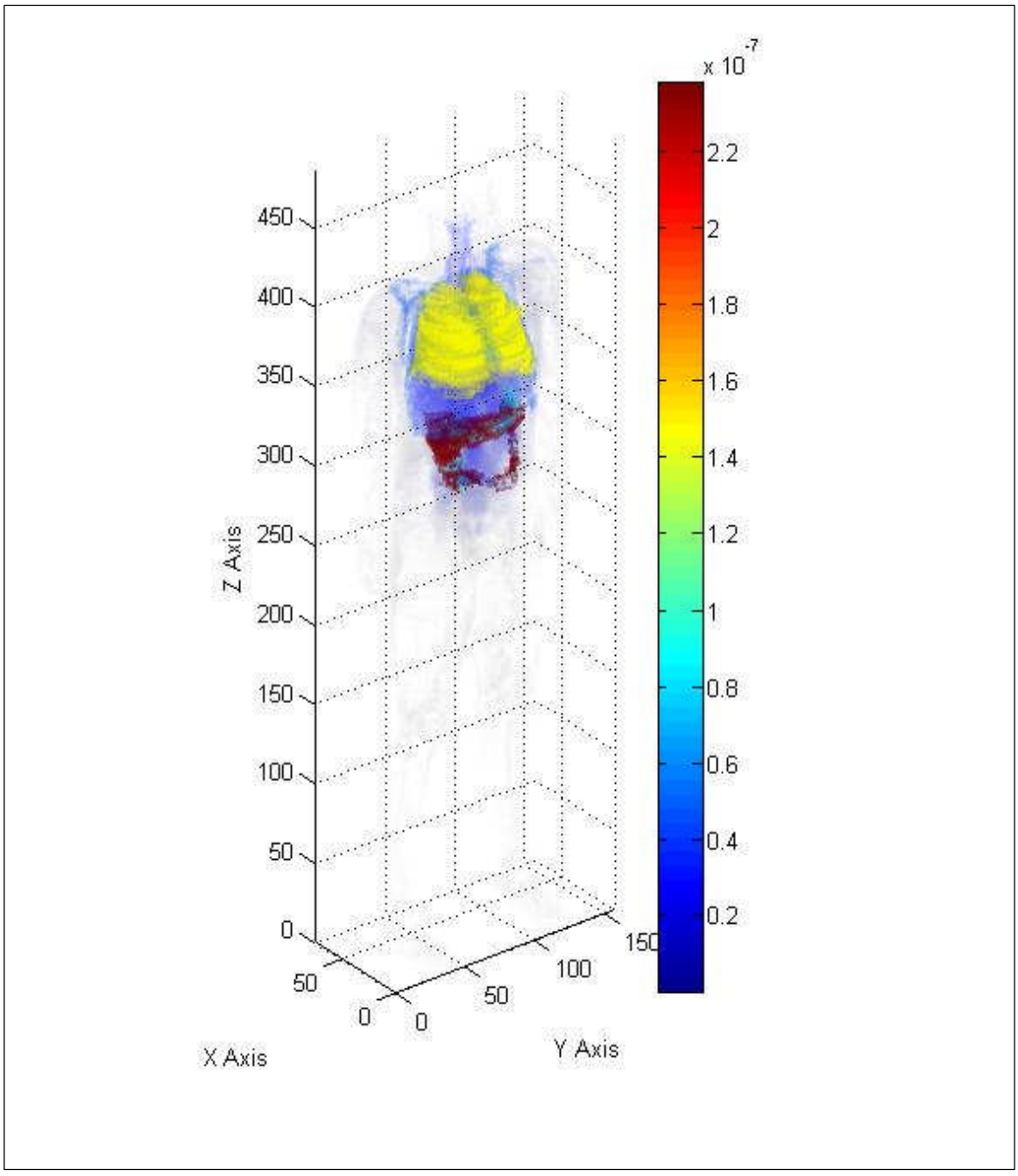

Fig. 20.5. Three-dimensional human dose profile from a Sr-90 beta source located within multiple organs after T plus 18 hours.

Table 20.5. Organ doses from a Y-90 volume source in multiple organs at time T plus 18 hours.

Organs	No. of Sources in Organ	Activity normalized to 1	MCNP Dose (MeV/g)/his	Std Deviation	Organ Dose (MeV/g)/his	Organ Dose (Gy)
Skin	0	0.00E+00	4.93E-06	7.44E-13	8.86E-11	1.42E-20
Rib Bone Group	0	0.00E+00	1.72E-02	3.14E-09	5.23E-07	8.37E-17
Small Int	3499	7.00E-04	7.29E-03	8.54E-09	5.47E-07	8.77E-17
Gonads	0	0.00E+00	3.36E-06	1.25E-09	4.40E-09	7.05E-19
Rectum	0	0.00E+00	1.04E-04	6.87E-09	8.09E-08	1.30E-17
Thyroid	0	0.00E+00	1.21E-04	1.80E-08	3.02E-07	4.84E-17
Lung	15000	1.08E-01	8.18E-02	5.16E-09	9.93E-07	1.59E-16
Eyes	0	0.00E+00	2.01E-06	2.87E-09	6.57E-09	1.05E-18
Trachea	0	0.00E+00	3.79E-04	7.01E-08	1.86E-06	2.97E-16
Colon	2124	8.48E-02	2.12E-02	1.88E-08	2.81E-06	4.5E-16
Stomach	1400	0.00E+00	2.26E-03	1.65E-08	7.38E-07	1.18E-16

As with Sr-90, the colon, trachea and lung received the highest dose from a highly-energetic beta radiation source located in multiple organs at time T plus 18 hours. Of the 14.2 percent of the activity that remained in the lung at T plus 12 hours, the lung retained 10.8 percent at T plus 18 hours. The organ activity follows that of Sr-90. Compared to the lung dose from Y-90 at T plus 12 hours which was 1.06×10^{-6} MeV/g, the lung dose at T plus 18 hours was 9.93×10^{-7} MeV/g. The colon dose from Y-90 at T plus 12 hours was 2.55×10^{-6} MeV/g and at the colon dose at T plus 18 hours was 2.81×10^{-6} MeV/g. This produced an increase in the colon dose by roughly 10 percent.

Statistical checks on the Y-90 dose output file were performed. The same warnings present with Co-60 were observed. The 10 statistical checks for tally-four fluence passed all but one check. The pdf was 0. The 10 statistical checks for tally-six dose passed. Of the 61 tally bins, one bin had a zero dose and 24 bins had relative errors exceeding 0.10 for the 2.28 MeV beta radiation. Figure 20.6 provides a simulated 3-dimensional view of the human body with a color profile that shows the organ dose for the beta radiation of Y-90. The color bar units to the right of the phantom are in MeV/organ weight in grams.

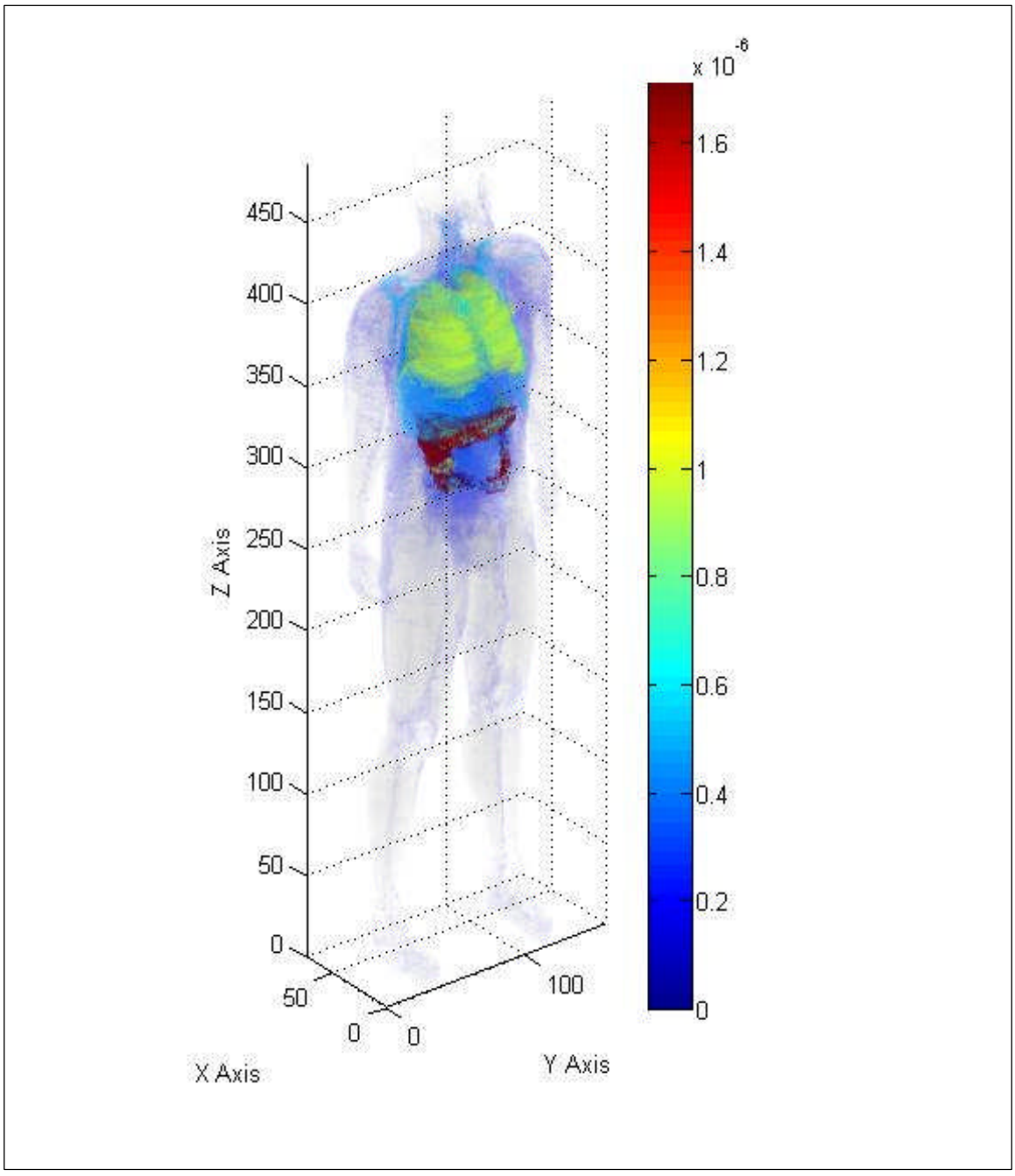

Fig. 20.6. Three-dimensional human dose profile from a Y-90 beta source located within multiple organs after T plus 18 hours.

Results from multi-organ lung, stomach, liver, small intestine and colon volume sources after 18 hours

Figure 20.7 provides a graph of all of the potential sources distributed in multiple organs after T plus 18 hours from exposure. Based upon the results of the observed programs, 18 hours after inhalation, Co-60 remained the most limiting radionuclide. The trachea, colon and stomach appeared to be the most sensitive organs based upon a single radiation from a source distribution described above. Even though the trachea shows the highest sensitivity, the dose is a little deceiving. The observed dose for the trachea is based on the number of voxels which include the air encircled by the trachea. The actual dose based on the weight of the organ is less than that for the stomach and small intestine.

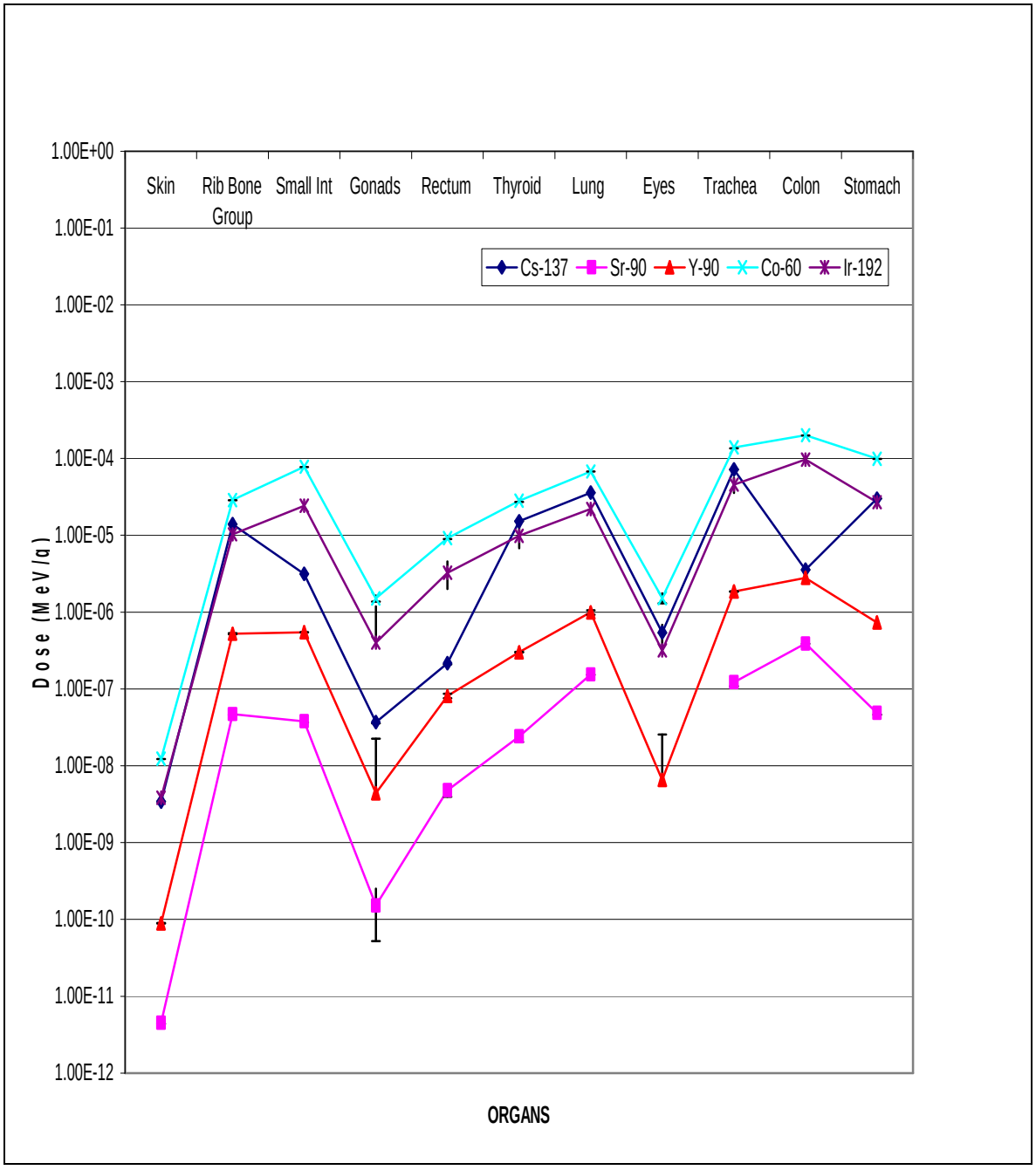

Fig. 20.7. Summary graph of organ doses for the five potential multi-organ sources after time T plus 18 hours.

CHAPTER XXI

ESTIMATING ORGAN DOSE BASED ON VOLUME SOURCES IN THE LUNG, STOMACH, SMALL INTESTINE AND COLON 24 HOURS AFTER A LUNG INHALATION

Co-60 organ dose profile

A Co-60 source located within the lung, stomach, liver, small intestine and colon would deliver a dose to the selected organs at time T plus 24 hours from exposure that ranges from a high of 2.40 x 10^{-4} MeV/g for the colon and a low of 1.23 x 10^{-8} MeV/g for the skin. This organ dose contribution is the sum of two photon emissions that occur with a yield of about 100 percent. Table 21.1 provides the calculated dose conversions for each of the selected organs at time (T) plus 24 hours from exposure.

Table 21.1. Organ doses a Co-60 volume source in multiple organs at time T plus 24 hours.

Organs	No. of Sources in organ	Activity normalized to 1	MCNP Dose (MeV/g)	Std Deviation	Organ Dose (MeV/g)	Organ Dose (Gy)
Skin	0	0.00E+00	6.87E-04	2.96E-11	1.23E-08	1.98E-18
Rib Bone Group	0	0.00E+00	9.17E-01	8.62E-08	2.78E-05	4.46E-15
Small Int	3499	3.10E-02	7.86E-01	4.01E-07	5.90E-05	9.45E-15
Gonads	0	0.00E+00	1.29E-03	1.56E-07	1.69E-06	2.7E-16
Rectum	0	0.00E+00	1.26E-02	3.14E-07	9.80E-06	1.57E-15
Thyroid	0	0.00E+00	1.11E-02	8.72E-07	2.77E-05	4.43E-15
Lung	15000	2.68E-01	5.33E+00	1.68E-07	6.47E-05	1.04E-14
Eyes	0	0.00E+00	4.21E-04	2.09E-07	1.38E-06	2.2E-16
Trachea	0	0.00E+00	2.73E-02	2.98E-06	1.34E-04	2.14E-14
Colon	2124	2.60E-01	1.81E+00	7.71E-07	2.41E-04	3.86E-14
Stomach	1400	6.24E-03	2.74E-01	8.41E-07	8.95E-05	1.43E-14

As expected the activity in the lung was reduced from 31 percent to 26.8 percent from time T plus 18 hours to time T plus 24 hours. Once again, the majority of the activity remained in the lung at time T plus 24 hours. As with time T plus 18 hours, the colon contained the second highest activity at T plus 24 hours. The activity in the colon

increased from 22.7 percent to 26.0 percent. The activity of the small intestine decreased from 4.6 percent to 3.1 percent. The activity in the stomach was further reduced from 0.9 percent to 0.6 percent. For Co-60, the most sensitive organs remained the colon followed closely by the trachea, stomach and lung. Compared to the lung dose from Co-60 at time T plus 18 hours which was 6.79×10^{-5} MeV/g and the lung dose at time T plus 18 hours was 6.47×10^{-5} MeV/g. The colon dose from Co-60 at T plus 18 hours was 9.53×10^{-5} MeV/g and at time T plus 24 hours the colon dose was 2.41×10^{-4} MeV/g or roughly a 20 percent increase in dose to the colon.

Statistical analysis of output file

The tally-four fluence analysis for each detector, setup as described in chapter VII, provided a random behavior for the mean. The desired relative error should be less than 0.10 and the observed relative error was 0.03. The desired and observed relative errors decreased according to the inverse of the square root of the number of histories. The desired variance of the variance should be less than 0.10 and the observed VoV was 0.00. The figure of merit value was constant and the behavior was random. The probability density function (pdf) desired should be greater than three, the observed pdf was 10. The tally-four fluence passed all 10 statistical checks. Out of 10 tally-four bins, only one had a zero dose and no bins contained relative errors greater than 0.10. The second 1.33 MeV photon simulation provided similar results.

The tally-six dose analysis for each material provided a random behavior for the mean. The desired relative error should be less than 0.10 and the observed relative error was 0.00 for the 1.17 MeV photon and 0.00 for the 1.33 MeV photon. The desired and observed relative errors decreased according to the inverse of the square root of the number of histories. The desired variance of the variance should be less than 0.10 and the observed VoV was 0.00. The figure of merit value was constant and the behavior was random. The desired probability density function (pdf) should be greater than 3.00 and the observed value was 10.0 for the 1.17 MeV photon and 8.10 for the 1.33 MeV

photon. The tally-six dose passed all 10 statistical checks. Out of 61 tally-six bins, no bin had a zero dose and only 5 bins contained relative errors greater than 0.10.

Figure 21.1 provides a simulated 3-dimensional view of the human body with a color profile that shows the organ dose for the 1.33 MeV photon of Co-60. Each axis is represented in the figure along with a color bar that indicates the organ dose in MeV/organ in grams provided by the MCNPX output file. In the MCNPX output file, the trachea received a slightly lesser dose than the lung based upon the number of voxels versus the measured gram weight of the trachea. The phantom includes the airway as part of the trachea.

Cs-137 organ dose profile

A Cs-137 source located within the lung, stomach, liver, small intestine and colon would deliver a dose to the selected organs at T plus 24 hours from exposure that ranges from a high of 7.37×10^{-5} MeV/g for the trachea and a low of 3.41×10^{-9} MeV/g for the skin. This organ dose contribution is from a 0.66 MeV photon emitted from Cs-137 that occurs with a yield of about 86 percent. Table 21.2 provides the calculated dose conversions to the selected organs at time (T) plus 24 hours from detonation.

Table 21.2. Organ doses for a Cs-137 volume source in multiple organs at time T plus 24 hours.

Organs	No. of Sources in organ	Activity normalized to 1	MCNP Dose (MeV/g)	Std Deviation	Organ Dose (MeV/g)	Organ Dose (Gy)
Skin	0	0.00E+00	1.90E-04	4.09E-12	3.41E-09	5.46E-19
Rib Bone Group	0	0.00E+00	4.59E-01	1.39E-08	1.39E-05	2.23E-15
Small Int	3499	0.00E+00	4.21E-02	2.53E-08	3.16E-06	5.07E-16
Gonads	0	0.00E+00	4.65E-05	7.57E-09	6.08E-08	9.74E-18
Rectum	0	0.00E+00	2.64E-04	1.07E-08	2.05E-07	3.29E-17
Thyroid	0	0.00E+00	6.06E-03	1.71E-07	1.52E-05	2.43E-15
Lung	15000	8.03E-02	2.96E+00	2.52E-08	3.60E-05	5.76E-15
Eyes	0	0.00E+00	1.72E-04	3.59E-08	5.63E-07	9.01E-17
Trachea	0	0.00E+00	1.51E-02	5.75E-07	7.37E-05	1.18E-14
Colon	2124	0.00E+00	2.69E-02	2.89E-08	3.57E-06	5.71E-16
Stomach	1400	0.00E+00	9.36E-02	1.28E-07	3.06E-05	4.9E-15

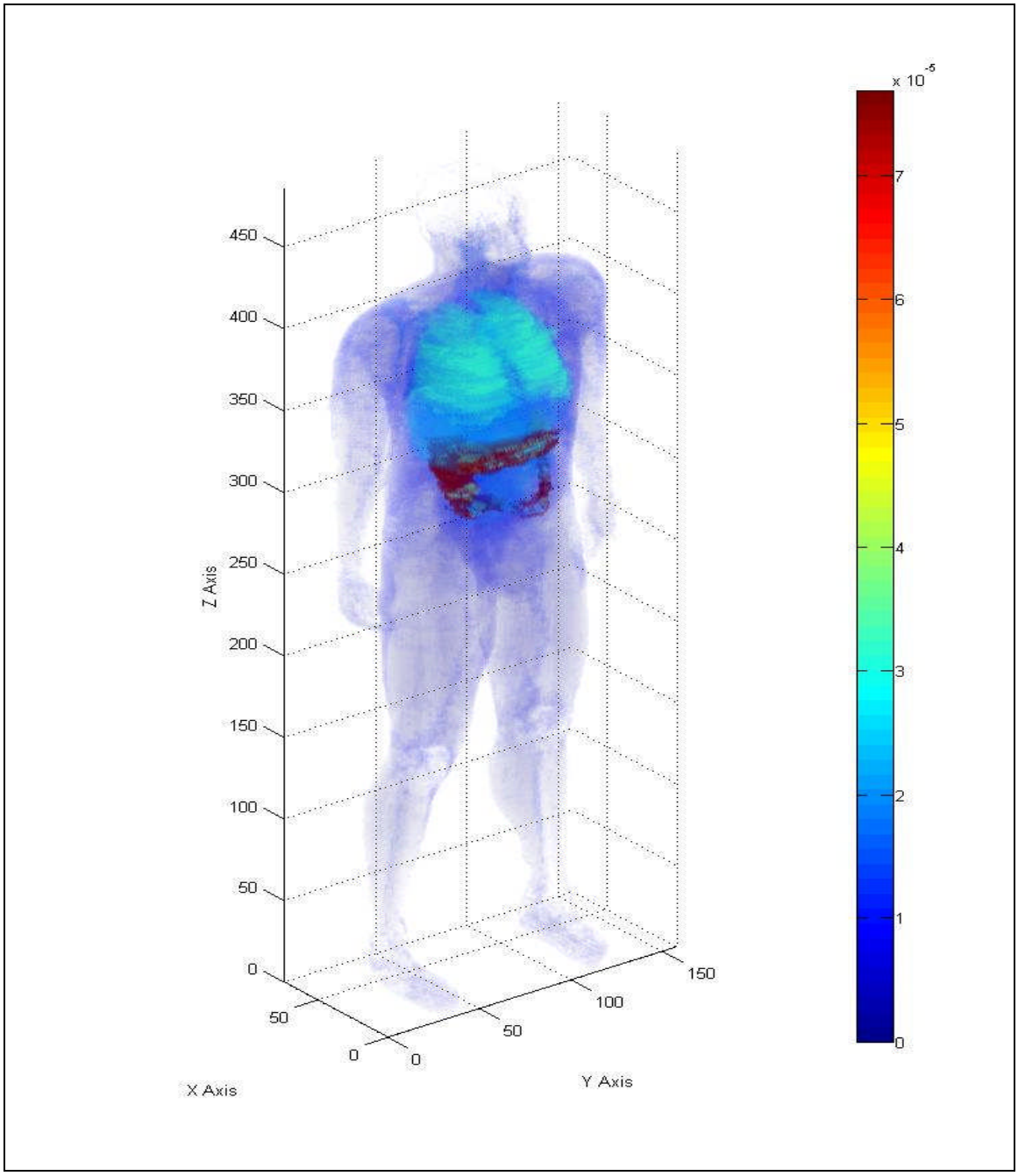

Fig. 21.1. Three-dimensional human dose profile from a 1.33 MeV photon source located within multiple organs at time T plus 24 hours.

As expected, the activity in the lung was reduced from 10.7 percent to 8.0 percent from time T plus 18 hours to time T plus 24 hours. The majority of the activity is absorbed by the body. The activity in the stomach remained at less than 0.01 percent. For Cs-137, the most sensitive organs were the trachea, followed by the lung and stomach. Compared to the lung dose from Cs-137 at time T plus 18 hours which was 3.59×10^{-5} MeV/g, the lung dose essentially remained the same at 3.60×10^{-5} MeV/g for T plus 24 hours. The stomach dose from Cs-137 at T plus 18 hours was 3.01×10^{-5} MeV/g and the stomach dose at time T plus 24 hours was 3.06×10^{-5} MeV/g or roughly a five percent increase in dose to the stomach. The increase is well within the margin or error for both the doses at T plus 18 and T plus 24 hours.

Statistical checks were performed on the Cs-137 dose output file. The same warnings present with Co-60 were observed. The 10 statistical checks for tally-four fluence passed and produced similar results. The 10 statistical checks for tally-six dose passed and produced similar results as with Co-60. Of the 61 tally bins, no bin had a zero dose and 8 bins had relative errors exceeding 0.10. Figure 21.2 provides a simulated 3-dimensional view of the human body with a color profile that shows the organ dose for the single photon of Cs-137. The color bar units to the right of the phantom are in MeV/organ weight in grams.

At T plus 24 hours, the most sensitive organ for a Co-60 remained the colon. For Cs-137 the most sensitive organ was the trachea. The Co-60 colon received a dose of 2.41×10^{-4} MeV/g and the Cs-137 trachea received a dose of 7.37×10^{-5} MeV/g. The change in activity for Co-60 and Cs-137 from T plus 18 hours to T plus 24 hours was not enough to alter the most sensitive organ. For Cs-137, 8.03 percent of the activity remained in the lung at T plus 24 hours while 10.7 percent of the activity remained in the lung at T plus 18 hours. The activity in the stomach dropped from 0.005 percent to 0.0 percent at T plus 24 hours. The relative majority of residual activity remained in the lung.

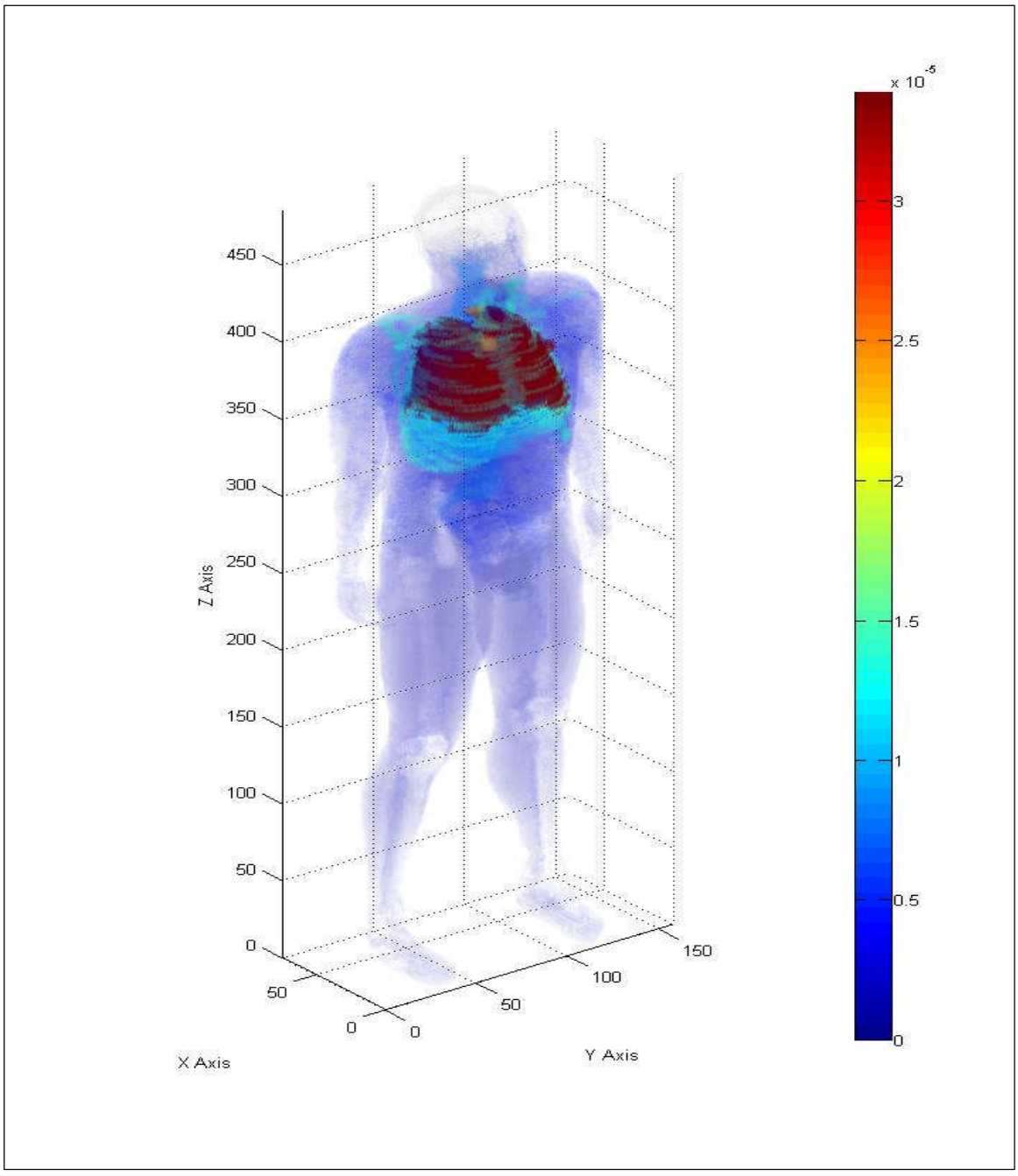

Fig. 21.2. Three-dimensional human dose profile from a Cs-137 photon source located within multiple organs at time T plus 24 hours.

Ir-192 organ dose profile

An Ir-192 source located within the lung, stomach, liver, small intestine and colon would deliver a dose to the selected organs at T plus 24 hours from exposure that ranges from a high of 1.03 x 10^{-4} MeV/g for the colon and a low of 3.82^{-9} MeV/g for the skin. This organ dose contribution is from the sum of two photons with energies of 0.47 MeV and 0.32 MeV along with two electrons with maximum energies of 0.66 MeV and 0.54 MeV. All four emissions are produced with a yield of 26.2%, 22.4%, 10.1% and 6.7%, respectively. Table 21.3 provides the calculated dose conversions for each of the selected organs at time (T) plus 24 hours from detonation.

Table 21.3. Organ doses for an Ir-192 volume source in multiple organs at time T plus 24 hours.

Organs	No. of Sources in organ	Activity normalized to 1	MCNP Dose (MeV/g)	Std Deviation	Organ Dose (MeV/g)	Organ Dose (Gy)
Skin	0	0.00E+00	2.12E-04	1.64E-10	3.82E-09	6.11E-19
Rib Bone Group	0	0.00E+00	3.19E-01	3.74E-07	9.67E-06	1.55E-15
Small Int	3499	7.50E-04	3.28E-01	1.55E-06	2.46E-05	3.95E-15
Gonads	0	0.00E+00	3.38E-04	8.81E-07	4.42E-07	7.08E-17
Rectum	0	0.00E+00	4.44E-03	1.39E-06	3.46E-06	5.54E-16
Thyroid	0	0.00E+00	3.56E-03	2.84E-06	8.89E-06	1.42E-15
Lung	15000	7.90E-02	1.68E+00	4.88E-07	2.04E-05	3.27E-15
Eyes	0	0.00E+00	9.77E-05	2.47E-07	3.19E-07	5.11E-17
Trachea	0	0.00E+00	8.40E-03	9.70E-06	4.12E-05	6.59E-15
Colon	2124	1.09E-01	7.75E-01	2.20E-06	1.03E-04	1.65E-14
Stomach	1400	0.00E+00	7.94E-02	3.04E-06	2.59E-05	4.15E-15

As expected, like the Ir-192 multiple source organ at time T plus 18 hours, the majority of the activity remained in the lung but continued to pass through the stomach, small intestine and colon. Of the 10.7 percent of activity that remained in the lung at time T plus 18 hours, the lung retained 7.9 percent at time T plus 24 hours. The activity in the stomach remained at essentially zero and the activity in the small intestine was reduced from 0.3 percent to 0.1 percent. The most sensitive organs for Ir-192 at time T

plus 24 hours remained the colon followed by the trachea, stomach and small intestine. The dose to the lung at time T plus 18 hours from Ir-192 was 2.20 x 10^{-5} MeV/g and the lung dose at time T plus 24 hours was 2.04 x 10^{-5} MeV/g. The colon dose at time T plus 18 hours from Ir-192 was 9.67 x 10^{-5} MeV/g and the colon dose at time T plus 24 hours was 1.03 x 10^{-4} MeV/g. This produced an increase in the colon dose by roughly 3 percent.

Statistical checks were performed on the Ir-192 dose output file. The same warnings present with Co-60 were observed. The 10 statistical checks for tally-four fluence photons passed and produced similar results. The 10 statistical checks for tally-six dose photons passed and produced similar results as with Co-60. Of the 61 tally bins, no bin had a zero dose and 5 bins had relative errors exceeding 0.10 for the 0.47 MeV photon. The second 0.32 MeV photon produced similar results.

The tallies for the electron sources within the lung had to be evaluated in a slightly different manner based on their inability to penetrate uniformly throughout the phantom. Secondary emissions, such as bremsstrahlung and characteristics x rays were the primary radiation source for organs outside of the lung. Three of the 10 statistical checks did not pass. The relative error was 0.31, the VoV was 0.28 and the pdf was 0. This reflects a large number of zero doses and slightly greater than zero doses based on the electron source. Figures 21.3 and 21.4 provide a simulated 3-dimensional view of the human body with a color profile that shows the organ dose for the 0.47 MeV photon of Ir-192 and the 0.66 MeV electron of Ir-192. The color bar units to the right of the phantom are in MeV/organ weight in grams.

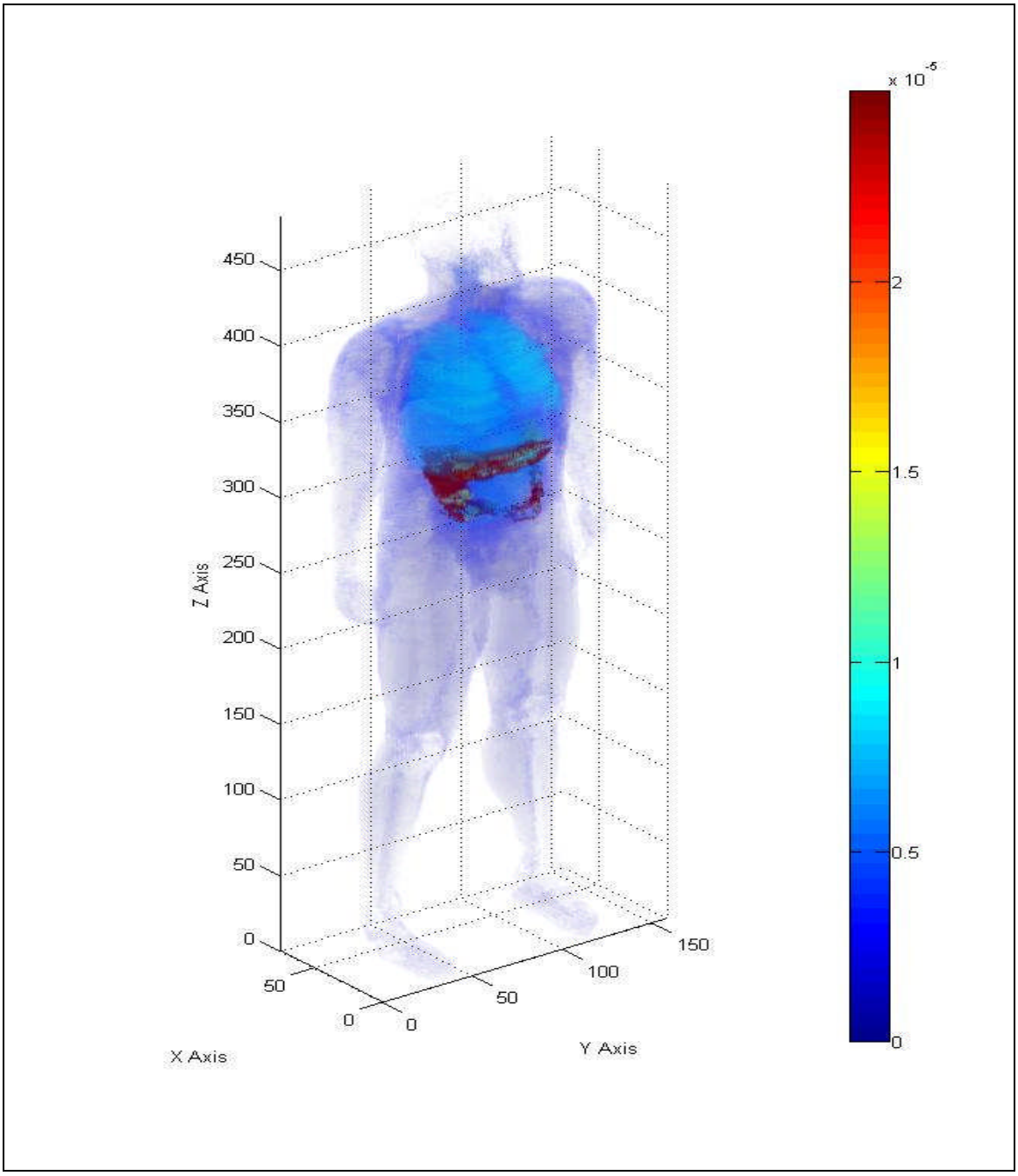

Fig. 21.3. Three-dimensional human dose profile from the 0.47 MeV Ir-192 photon source located within multiple organs at T plus24 hours.

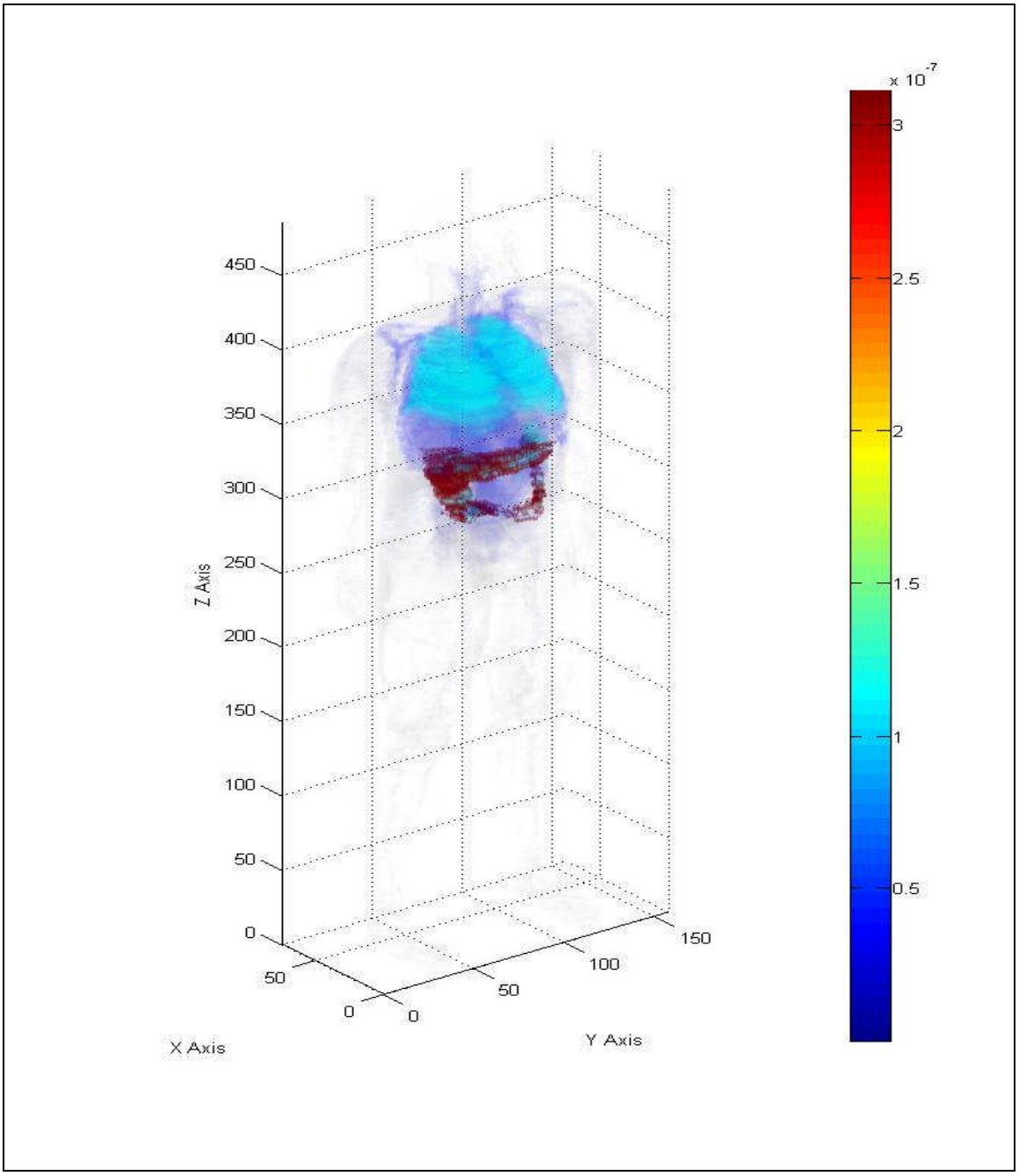

Fig. 21.4. Three-dimensional human dose profile from the 0.66 MeV Ir-192 electron source located within multiple organs at T plus 24 hours.

Sr-90 organ dose profile

A Sr-90 source located within the lung, stomach, liver, small intestine and colon would deliver a dose to the selected organs at T plus 24 hours from exposure that ranges from a high of 4.31 x 10^{-7} MeV/g for the colon and a low of 4.32 x 10^{-12} MeV/g for the skin. This organ dose contribution is from a single beta emission with a maximum energy of 0.55 MeV. The beta emission is produced with a yield of about 100%. Table 21.4 provides the calculated dose conversions for each of the selected organs that will be considered in this problem.

Table 21.4. Organ doses from a Sr-90 volume source in multiple organs at time T plus 24 hours.

Organs	No. of Sources in organ	Activity normalized to 1	MCNP Dose (MeV/g)	Std Deviation	Organ Dose (MeV/g)	Organ Dose (Gy)
Skin	0	0.00E+00	2.41E-07	8.99E-14	4.32E-12	6.93E-22
Rib Bone Group	0	0.00E+00	1.50E-03	8.15E-10	4.55E-08	7.29E-18
Small Int	3499	0.00E+00	5.10E-04	1.27E-09	3.83E-08	6.14E-18
Gonads	0	0.00E+00	4.13E-07	3.90E-10	5.41E-10	8.66E-20
Rectum	0	0.00E+00	6.80E-06	1.08E-09	5.29E-09	8.48E-19
Thyroid	0	0.00E+00	1.05E-05	4.06E-09	2.63E-08	4.21E-18
Lung	15000	8.00E-02	1.16E-02	1.41E-09	1.41E-07	2.25E-17
Eyes	0	0.00E+00	1.07E-07	3.51E-10	3.51E-10	5.62E-20
Trachea	0	0.00E+00	2.79E-05	1.47E-08	1.37E-07	2.19E-17
Colon	2124	7.64E-02	3.24E-03	4.65E-09	4.31E-07	6.9E-17
Stomach	1400	0.00E+00	1.58E-04	2.86E-09	5.16E-08	8.26E-18

As expected, the most sensitive organ for a Sr-90 electron source at time T plus 24 hours remained the colon. The trachea and lung follow the colon in sensitivity. The colon retained 8.5 percent of the activity at T plus 18 hours and 7.6 percent at T plus 24 hours. Of the 10.8 percent of activity that remained in the lung at T plus 18 hours, the lung retained 8.0 percent at T plus 24 hours. Compared to the lung dose from Sr-90 at T plus 18 hours which was 1.54 x 10^{-7} MeV/g, the lung dose at T plus 24 hours was 1.41 x 10^{-7} MeV/g.

Statistical checks were performed on the Sr-90 dose output file. The same warnings present with Co-60 were observed. The 10 statistical checks for tally-four fluence missed two of the 10 checks. The relative error was 0.29 and the pdf was 0. The 10 statistical checks for tally-six dose passed. Of the 61 tally bins, 8 bins had a zero dose and 31 bins had relative errors exceeding 0.10 for the 0.55 MeV beta emission. Figure 21.5 provides a simulated 3-dimensional view of the human body with a color profile that shows the organ dose for the beta radiation of Sr-90. The color bar units to the right of the phantom are in MeV/organ weight in grams.

Y-90 organ dose profile

A Y-90 source located within the lung, stomach, liver, small intestine and colon would deliver a dose to the selected organs at T plus 24 hours that ranges from a high of 3.13×10^{-6} MeV/g for the colon and a low of 8.8×10^{-11} MeV/g for the skin. This organ dose contribution is from a single beta emission with a maximum energy of 2.28 MeV. The beta emission is produced with a yield of about 100%. Table 21.5 provides the calculated dose conversions for each of the selected organs that will be considered in this problem.

Table 21.5. Organ doses from a Y-90 volume source in multiple organs at time T plus 24 hours.

Organs	No. of Sources in organ	Activity normalized to 1	MCNP Dose (MeV/g)	Std Deviation	Organ Dose (MeV/g)	Organ Dose (Gy)
Skin	0	0.00E+00	4.94E-06	7.54E-13	8.88E-11	1.42E-20
Rib Bone Group	0	0.00E+00	1.60E-02	3.01E-09	4.86E-07	7.78E-17
Small Int	3499	0.00E+00	7.57E-03	8.58E-09	5.68E-07	9.11E-17
Gonads	0	0.00E+00	4.55E-06	2.22E-09	5.95E-09	9.54E-19
Rectum	0	0.00E+00	1.06E-04	6.72E-09	8.26E-08	1.32E-17
Thyroid	0	0.00E+00	1.30E-04	1.98E-08	3.24E-07	5.2E-17
Lung	15000	8.00E-02	7.51E-02	4.92E-09	9.12E-07	1.46E-16
Eyes	0	0.00E+00	2.37E-06	3.97E-09	7.74E-09	1.24E-18
Trachea	0	0.00E+00	3.25E-04	6.27E-08	1.59E-06	2.55E-16
Colon	2124	7.64E-02	2.36E-02	1.97E-08	3.13E-06	5.02E-16
Stomach	1400	0.00E+00	2.21E-03	1.63E-08	7.21E-07	1.16E-16

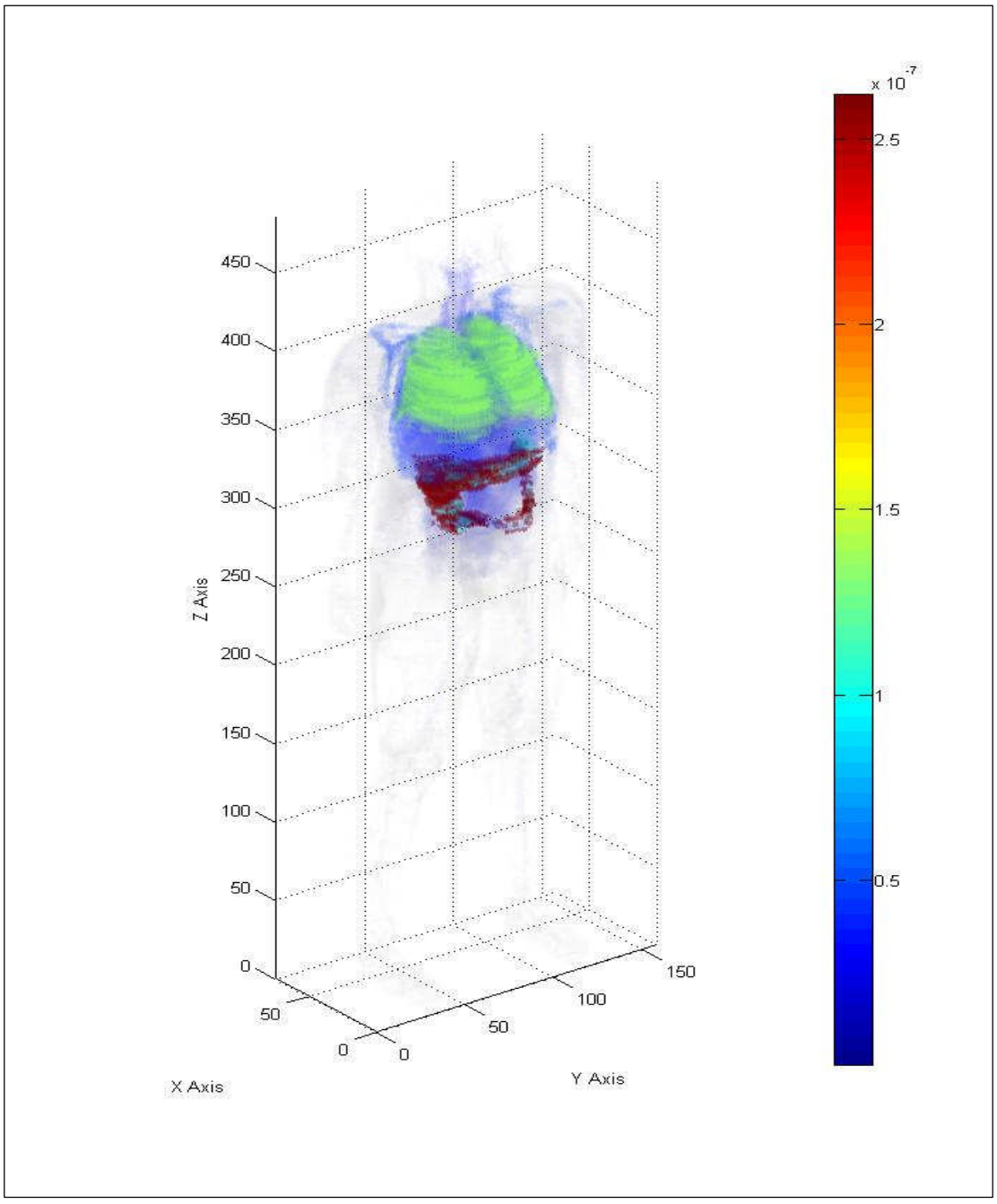

Fig. 21.5. Three-dimensional human dose profile from a Sr-90 beta source located within multiple source organs at T plus 24 hours.

As expected, following Sr-90, the colon, trachea and lung received the highest dose from a highly-energetic beta particle source located in multiple organs at time T plus 24 hours. Of the 10.8 percent of activity that remained in the lung at T plus 18 hours, the lung retained 8.0 percent of the activity at T plus 24 hours. The organ activity follows that of Sr-90. Compared to the lung dose from Y-90 at T plus 18 hours which was 9.93×10^{-7} MeV/g, the lung dose at T plus 24 hours was 9.12×10^{-7} MeV/g. The colon dose from Y-90 at T plus 18 hours was 2.81×10^{-6} MeV/g and the colon dose at T plus 24 hours was 3.13×10^{-6} MeV/g. This produced an increase in the colon dose by roughly 10 percent.

Statistical checks were performed on the Y-90 dose output file. The same warnings present with Co-60 were observed. The 10 statistical checks for tally-four fluence passed all but two checks. The relative error was 0.11 and the pdf was 0. The 10 statistical checks for tally-six dose passed. Of the 61 tally bins, two bins had a zero dose and 22 bins had relative errors exceeding 0.10 for the 2.28 MeV beta emission. Figure 21.6 provides a simulated 3-dimensional view of the human body with a color profile that shows the organ dose for the beta emission of Y-90. The color bar units to the right of the phantom are in MeV/organ weight in grams.

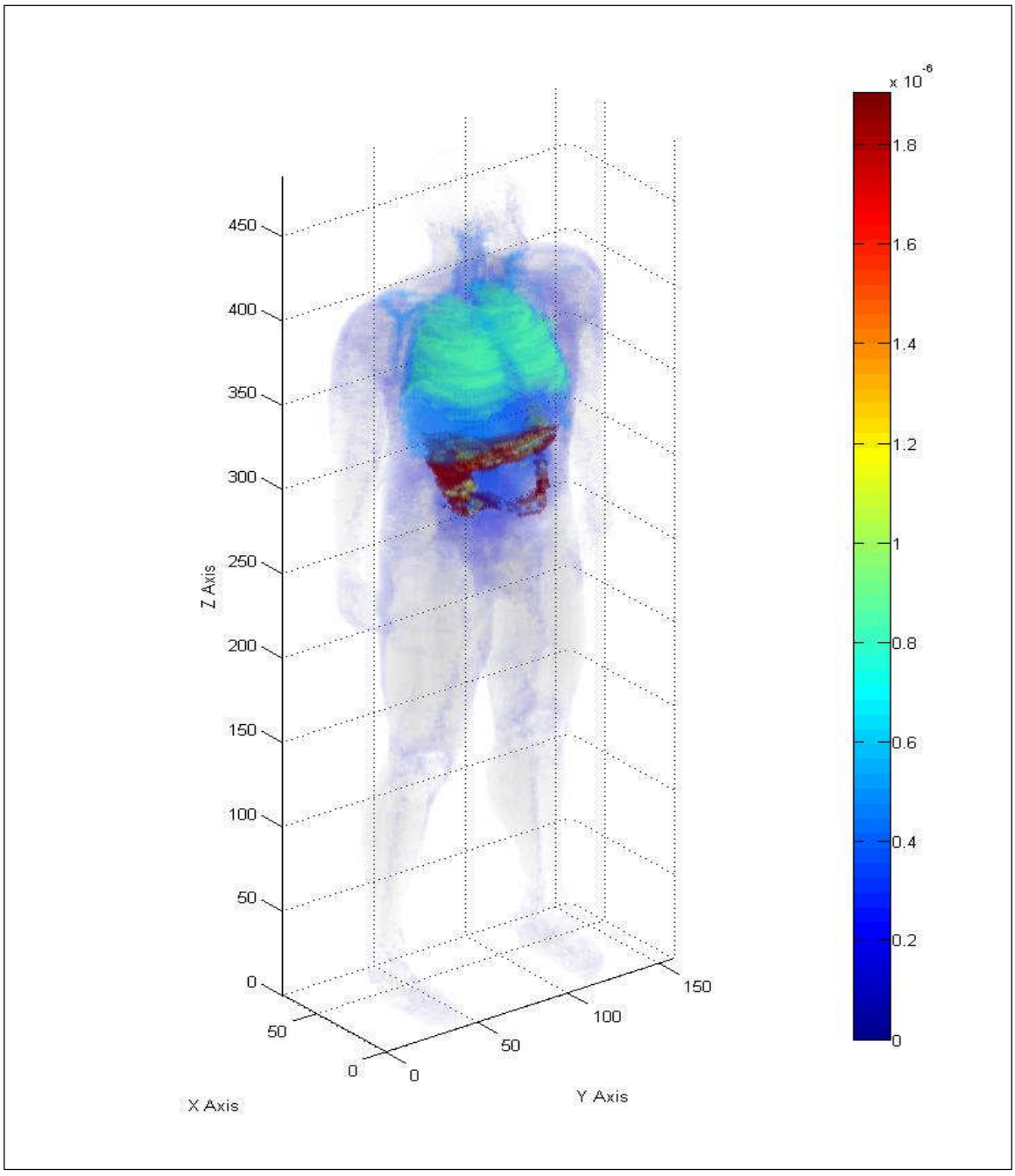

Fig. 21.6. Three-dimensional human dose profile from a Y-90 beta source located within multiple organs at time T plus 24 hours.

Results from multi-organ lung, stomach, liver, small intestine and colon volume sources after 24 hours

Figure 21.7 provides a graph of all of the potential sources distributed in multiple organs and their organ doses after T plus 24 hours. Based upon the results of the observed programs, 24 hours after inhalation, Co-60 remains the most limiting radionuclide. The trachea, colon and stomach appeared to remain the most sensitive organs based upon a single emission from a source distribution described above. Even though the trachea shows the highest sensitivity, the dose is a little deceiving. The observed dose for the trachea is based on the number of voxels which include the air encircled by the trachea. The actual dose based on the weight of the organ is less than that for the stomach and small intestine.

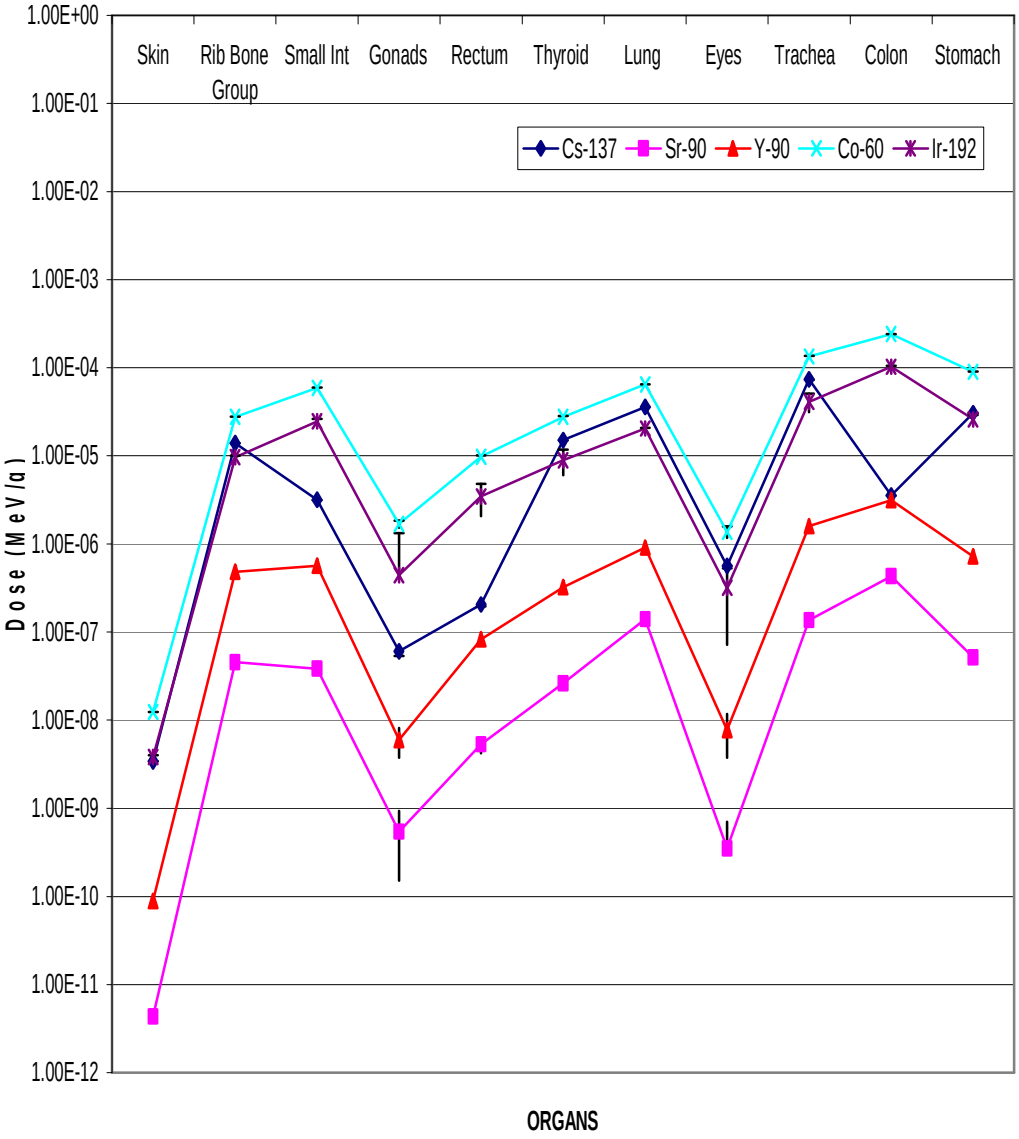

Fig. 21.7. Summary graph of organ doses for the five potential multi-organ sources after T plus 24 hours.

CHAPTER XXII
DOSE TO MODEL CONFIRMATION USING EXPERIMENTAL TESTING OF SCANDIUM-46 IN A RANDO MALE TORSO PHANTOM

Description of the RANDO phantom

The RAN100 phantom was selected as the experimental representation of the human torso. There is no head, arms or legs associated with the model that was used in this experiment. The phantom was constructed with a natural human skeleton cast inside soft tissue-simulating material. The shape of the lungs follows the natural contours of the rib cage. The material is removed representing the air space of the neck and stem bronchi. The phantom is horizontally sliced in 2.54 cm sections. 3 cm x 3 cm hole grid patterns are placed in each section to allow for a variety of TLD placements.

Experimental source and phantom arrangement

Based on the energy spectrum from the five radionuclides of concern, a radionuclide with an activity of around 60 to 120 days and one that emitted a photon energy of approximately 1 MeV was desired for testing the dose output from our computational phantom. Sc-46 has a half-life of 83.79 days and produces a beta and two gammas with a yield of approximately 100 percent. The average beta energy is 0.11 MeV and the two gamma energies are 1.12 MeV and 0.89 MeV respectively. Approximately 48.92 mg of scandium chloride salt was irradiated in the NSC Triga reactor for 2.15 hours at the A6 core position with an average thermal flux of 6.56×10^{12} neutrons/cm^2-s. The above set up produced an activity of 3.687 uCi of Sc-46 on 31JAN08 at 1415. The activity was confirmed through a measurement by the gamma spectrum analysis using a HPGe detector with the sample geometry of S48PS. The S48PS refers to a point source (PS) that is on a stand (S) that is 48 inches from the detector.

The source was encapsulated in a glass vial and placed in section 17 of the RANDO phantom. The source was centered approximately 15 cm from the chest wall at the midline between the phantoms nipples. An MCNPX file was created with a single Sc-46 source placement at position (16.44 29.70 136.98) which corresponds to the experimental phantom source position. The same number of histories was simulated for both photon energies as the other simulated sources. The dose and fluence were measured from the 10 lung detector placements. Table 22.1 provides the calculated dose conversions for each of the selected organs and the simulated detectors with point source of Sc-46.

Table 22.1. Organs and detector doses from a Sc-46 point source position in lung.

Organs	MCNP Dose (MeV/g-his)	Std Deviation	En Dep (MeV/his)	Organ Wt (g)	Organ Dose (MeV/g-his)	Organ Dose (Gy/his)
Skin	5.00E-04	2.16E-11	2.54E-05	2830	8.99E-09	1.44E-18
Rib Bone Group	1.14E+00	7.64E-08	7.53E-02	2167	3.47E-05	5.57E-15
Small Int	8.43E-02	1.25E-07	4.05E-03	640	6.33E-06	1.01E-15
Gonads	1.33E-04	4.48E-08	6.45E-06	37.1	1.74E-07	2.78E-17
Rectum	6.29E-04	5.88E-08	3.08E-05	63	4.89E-07	7.83E-17
Thyroid	2.15E-02	1.06E-06	1.05E-03	19.6	5.37E-05	8.60E-15
Lung	8.20E+00	1.39E-07	9.94E-02	999	9.95E-05	1.59E-14
Eyes	5.78E-04	2.27E-07	2.83E-05	15	1.89E-06	3.03E-16
Trachea	1.21E-01	6.94E-06	5.93E-03	10	5.93E-04	9.50E-14
Colon	5.05E-02	1.35E-07	2.47E-03	369	6.71E-06	1.07E-15
Stomach	1.40E-01	4.76E-07	6.86E-03	150	4.58E-05	7.33E-15
UpRtFt Det	2.03E-03	7.78E-07	1.23E-07	4.91E-03	2.51E-05	4.02E-15
UpLtFt Det	1.54E-03	7.05E-07	9.34E-08	4.91E-03	1.90E-05	3.04E-15
CeFt Det	1.03E-03	4.89E-07	6.28E-08	4.91E-03	1.28E-05	2.05E-15

There are many portable instruments available for use in the civilian sector. The Ludlum model 2350-1 Data Logger was chosen with a Model number 44-9 alpha, beta and gamma probe along with a 44-2 NaI probe to verify real time exposure data from the phantom. The detectors were calibrated using a Cs-137 check source. Lithium Iodide TLD chips were selected and placed in various locations throughout the phantom to test accumulated dose from the Sc-46 source over a period of one week.

For the purpose of this experiment, out of the 10 possible detector positions, the center chest position was chosen based on anatomical markers that are readily identifiable. On standard man, the center of the sternum is between the nipples and easily identifiable. However, care must be taken in recognizing that not everyone fits the mold of standard man. Different body shapes must be taken into account before emergency responders utilize a preset detector location. This may not be the best location for barrel-chested men or women with large mammary glands.

Addipose or breast tissue will add internal shielding as well as increase the distance from the lung source to the surface of the detector. This will reduce the dose rate by the simple one over r squared rule and reduce the number of primary photons reaching the detector. More importantly, this will provide a potential false negative reading based on the calibration of the detector at a given distance of 15 cm. The top or apex of the lung may prove to be a better location for performing lung surveys. The top of the lung does not change appreciably with a change in adipose tissue for most people. Mammary glands do not have a significant affect on this location for most people as well.

Depending upon the size or sex of the individuals, the emergency responders may choose the center back or apex of the back. This will significantly reduce the distance between the detector and the lung and may provide enough dose-rate above background to achieve good statistics. In either case, tables should be developed that provide emergency response personnel with dose rate limits based on detector location.

44-9 Alpha, beta and gamma probe measurements

The Ludlum model 44-9 Alpha, Beta, Gamma detector was a GM pancake detector that will detect alpha, beta and gamma radiation. The detector was energy dependent and operated between 850 – 1000 volts. It has a thin mica window that was protected by a stainless steel screen. The open area was 12 cm^2 and the operating voltage was 900 volts. The detector was calibrated with a 6 uCi Cs-137 source using a

2π geometry. Based on the known activity, the number of photons passing through the sensitive region of the detector would be approximately 1.11 x 10^5 photons/s. The measured count rate for the detector using the known Cs-137 source was 206.67 cps. Therefore, the overall efficiency of the detector for 0.66 MeV photons was 1.86 x 10^{-3}. The detector has an over-response to 1 MeV photons of approximately 1.3. Therefore, an energy correction factor of 1.3 must be applied, which reduces the overall efficiency to 1.43 x 10^{-3} if 1 MeV photons are measured.

The time adjusted activity of the Sc-46 source was 281.51 uCi based on the known activity of 368.7 uCi 35 days prior to the measurement. When the Sc-46 source was placed in section 17 of the RANDO phantom, the 44-9 detector probe measured 631.67 cps at 15 cm from the chest wall with the face of the probe perpendicular to the direction of the photons and centered between the nipples. The calculated measurement based on the MCNPX Sc-46 simulation, with the source in the above mentioned position, provided a photon fluence of 2.82 x 10^{-2} photons/cm^2 - decay. Since the sensitive volume of the detector is 12 cm^2, this would produce a fluence rate of 2.94 x 10^5 photons/s across the sensitive volume of the detector. Based on the calculated efficiency, the simulated detector should measure a count rate of 420.68 cps. Since Sc-46 emits 2 photons per decay, the actual measured count rate should be 841.36 cps. The error between the measured count rate and the simulated count rate was 33.2 percent which is within the acceptable error range of 25-50 percent.

44-2 NaI probe measurements

The Ludlum model 44-2 NaI gamma scintillator was capable of detecting low levels of gamma radiation in the range of 60 keV – 1.25 MeV. The probe contained a 2.54 cm diameter x 2.54 cm thick NaI crystal coupled to a photomultiplier tube. The detector was energy dependent and operated between 500 – 1200 volts. The operating voltage was 850 volts. The detector was calibrated with a 6uCi Cs-137 source using a 2π geometry. When the Sc-46 source was placed in section 17 of the RANDO phantom,

the 44-2 probe measured 8.0 mR/hr at 15 cm from the chest wall with the face of the probe perpendicular to the direction of the photons and centered between the nipples. Since the dose came from two photons averaging 1 MeV, an energy correction factor based on the calibration of Cs-137 which has a 0.66 MeV photon must be applied. The probe would under respond by 0.63 and therefore the actual dose to the detector volume would be approximately 11.4 mR/hr.

The calculated measurement based on the MCNPX Sc-46 simulation with the source in the above mentioned position provided a dose of 5.73×10^{-4} MeV/g from the 1.12 MeV and 4.62×10^{-4} MeV/g from the 0.89 MeV photon. The dose is in air was based on a detector volume of 4.67×10^{-2} cm^3 and a mass of 4.91×10^{-3} g. The density for air was 1.3×10^{-3} g/cm^3. The total dose to the air volume was 2.04×10^{-15} Gy. A quick conversion shows that the two Sc-46 photons would deliver a dose to the air volume of 2.04×10^{-15} rad/disintegration. The number of disintegrations for the given source was 1.36×10^{7} dps. Multiplying the disintegrations per second by the dose per disintegrations and converting the answer to mrad/hr provides a dose rate of 10 mrad/hr. The percent error between the measured dose rate and the simulated dose rate was approximately 12.3 percent. This is within the acceptable error range of 25 – 50 percent.

Lithium fluoride TLD dose confirmation

The phantom dose was independently confirmed by using 18 lithium fluoride TLD chips placed at defined locations on three different levels approximating the top, middle and lower portions of the lung. Table 22.2 provides the distance from the source and the dose rate of each TLD.

Table 22.2. Position and dose rate for 18 LiF TLDs inside the RANDO phantom with the Sc-46 source.

Phantom Position	Read. (μC)	Dose(R)	Disctance From Source (cm)	Standard Deviation	Time (hr)	Dose Rate (mR/hr)
A1	113.5	2.37	15.1	0.001	168.00	14.14
A2	116.3	2.43	15.1	0.001	168.00	14.48
A3	80.16	1.68	15.1	0.001	168.00	9.98
A4	102.6	2.15	15.1	0.001	168.00	12.78
A5	618.7	12.95	7.1	0.001	168.00	77.06
A6	590.4	12.35	7.1	0.001	168.00	73.53
A7	334.5	7.00	9	0.001	168.00	41.66
A8	358.8	7.51	9	0.001	168.00	44.69
A9	163.8	3.43	12	0.001	168.00	20.40
A10	88.11	1.84	17.7	0.001	168.00	10.97
B1	83.93	1.76	17.7	0.001	168.00	10.45
B2	95.5	2.00	17.7	0.001	168.00	11.89
B3	96.79	2.03	17.7	0.001	168.00	12.05
B4	78.39	1.64	18.8	0.001	168.00	9.76
B5	86.8	1.82	18.8	0.001	168.00	10.81
B6	67.01	1.40	19.4	0.001	168.00	8.35
B7	12.68	0.27	control	0.001	168.00	1.58
B8	9.77	0.20	control	0.001	168.00	1.22

The TLDs that were placed 15 cm from the source provided a dose rate that ranged from 9.98 mrad/hr to 14.48 mR/hr. After subtracting the background average from the controls, the dose rate ranged from 8.58 mrad/hr to 13.08 mrad/hr. The dose rate is consistent with the energy corrected dose rate from the NaI probe at 11.4 mR/hr as well as the simulated dose rate from the MCNPX program of 10.0mR/hr.

CHAPTER XXIII
EVALUATION OF EMERGENCY RESPONSE GUIDELINES APPLICABLE TO A RADIOLOGICAL DISPERSAL DEVICE

Particle dispersal in air

Sandia National Laboratories has run hundreds of explosive experiments with various materials and device geometries in order to understand the aerosol physics of a possible RDD (Harper 2006). Harper et al. related the aerosolization of the physical forms of radioactive material and how they would respond under different conditions. Table 2 of Harpers report provides the largest source that is potentially available for an RDD. A Co-60 metal irradiator source would provide 1.11 X 10^7 GBq. A Cs-137 CsCl salt irradiator source would provide 7.4 X 10^6 GBq. An Ir-192 metal irradiator source would provide 3.7 X 10^4 GBq and a Sr-90/Y-90 ceramic thermal generator source would provide 1.11 X 10^7 GBq (Harper 2006).

Table 3 of Harpers report provides a breakdown of selected dose limits, significance of each limit and realistic RDD hazards for varying devices. Intermediate and small sources provide no acute health effects. Doses of 1 Gy from 24 hours of exposure to ground shine only occur from very large sources at a distance of approximately 300 m from detonation. An inhalation dose of 2.7 Gy to the lung, based on the 30-day committed dose, can occur up to 2 km from the blast if sophisticated engineering is used with a very large source. The 50 year committed dose of 1 Sv from lung inhalation can occur up to 7 km from a very large source with sophisticated engineering (Harper 2006).

Dose comparison

In order to compare activity and dose based on one of the likely RDD events, a few assumptions were made. The first assumption is that a uniform dispersal would

occur. This is a worst case scenario that would require a sophisticated engineering device. The second assumption is that the entire radiation source would be reduced to a one μm AMAD. While this is unlikely without a sophisticated engineering device, it was considered to be a worst case scenario. The third assumption is that the radiation was considered airborne and easily re-suspended with the natural dust and debris that accompany an explosive device. While external exposure and internal exposure must be considered simultaneously when establishing control levels, the assumption that half of the dose will come from internal exposure was considered to be a conservative approach.

With the above assumptions, Table 23.1 provides an instantaneous activity for each isotope that would deliver an immediate dose that corresponds to a 0.01 Gy limit to the lung, stomach, small intestine and colon one hour after an inhalation exposure.

The activities can be adjusted based on the dose limit established. Dividing the dose limit by time would create dose rate limits that can be used to establish triage action levels as well as time limits for emergency response personnel. The dose rate can be directly measured using either the GM pancake probe or the NaI probe described in chapter XXI 21, with the appropriate correction factors applied.

Table 23.2 provides emergency responders with a Dose Rate for the GM pancake probe and the NaI probe located at the center of the sternum. The dose rates provided in Table 22.2 correspond to an activity from a source that would deliver a dose to the lung within 24 hours. The dose rates are based on the dose rate per activity derived from the experimental results from Sc-46. The ratio has been corrected for the gamma energy and yield for each isotope.

Table 23.1. Activities that correspond to preset organ dose limits for the five radionuclides considered in this problem.

Organ	Radionuclide	Acitivity (GBq)	Dose Limit (Gy)	Activity to reach Dose Limit in 1 hour (GBq)	Acitivity in mCi
Lung	Co-60	5.37E+02	0.01	1.49E-01	4.03E+00
Stomach	Co-60	4.40E+02	0.01	1.22E-01	3.30E+00
Small Intestine	Co-60	3.23E+03	0.01	8.98E-01	2.43E+01
Colon	Co-60	3.96E+03	0.01	1.10E+00	2.97E+01
Lung	Cs-137	2.02E+03	0.01	5.61E-01	1.52E+01
Stomach	Cs-137	5.79E+02	0.01	1.61E-01	4.35E+00
Small Intestine	Cs-137	1.20E+04	0.01	3.34E+00	9.03E+01
Colon	Cs-137	1.37E+04	0.01	3.81E+00	1.03E+02
Lung	Ir-192	1.94E+03	0.01	5.40E-01	1.46E+01
Stomach	Ir-192	5.43E+02	0.01	1.51E-01	4.07E+00
Small Intestine	Ir-192	2.18E+03	0.01	6.05E-01	1.63E+01
Colon	Ir-192	4.34E+03	0.01	1.21E+00	3.26E+01
Lung	Sr-90	3.33E+05	0.01	9.25E+01	2.50E+03
Stomach	Sr-90	1.41E+05	0.01	3.93E+01	1.06E+03
Small Intestine	Sr-90	6.22E+05	0.01	1.73E+02	4.67E+03
Colon	Sr-90	1.87E+06	0.01	5.20E+02	1.40E+04
Lung	Y-90	5.10E+04	0.01	1.42E+01	3.83E+02
Stomach	Y-90	1.67E+04	0.01	4.65E+00	1.26E+02
Small Intestine	Y-90	6.85E+04	0.01	1.90E+01	5.14E+02
Colon	Y-90	1.55E+05	0.01	4.31E+01	1.16E+03

In an emergency situation, there would be two preset levels for evaluating contaminated injured personnel, 0.01 Gy over a 24 hour period of time which provides a cut off for individuals who are either contaminated or non-contaminated and 1.0 Gy over a 24 hour period of time which corresponds to emergency medical treatment for the individual or no medical treatment based on the lung dose. The above two limits only apply to individuals who were present within the affected zone. Direct medical intervention should be reserved for any casualty that exceeds the 1.0 Gy exposure level. While the 50 year committed effective dose equivalent would be much higher, the aforementioned levels are for an acute dose scenario during an RDD emergency. Table 23.2 provides an accumulated activity for each of the five radionuclides considered in

this problem based on the one hour, six hour, 12 hour, 18 hour and 24 hour snap shots simulated in the multiple source organs.

Table 23.2. Lung activity limits to reach a dose limit of 0.01 Gy for the five radionuclides in this problem.

Organ	Radionuclide	Dose Limit(Gy)/ 24 hours	Activity Limit(GBq)/24 hours	Acitivity in mCi/24 hours
Lung	Co-60	0.01	2.30E-03	6.23E-02
	Cs-137	0.01	4.14E-03	1.12E-01
	Ir-192	0.01	5.80E-03	1.57E-01
	Sr-90	0.01	8.79E-01	2.38E+01
	Y-90	0.01	1.36E-01	3.68E+00

Using this table, emergency responders can establish action levels based on the two limits listed previously in this chapter by simply comparing the ratio of the dose limit/24 hours divided by the activity limit per 24 hours.

Table 23.3 provides a real time detector response based on the above limits. The dose rate is calculated using the calibration factor and probe setup based on the Sc-46 experimental data. Each probe was calibrated using Cs-137 and corrected for energy. The probe was positioned centered on the sternum.

Table 23.3. Dose rate limits for GM pancake and NaI probes based on five radionuclides within the Lung using a dose limit of 0.01 Gy.

Radionuclide	Acitivity in mCi/24 hrs	Dose Rate from GM Pancake Probe (cps)	Dose Rate from NaI Probe (mR/hr)
Co-60	6.23E-02	3.18E+03	4.57E-02
Cs-137	1.12E-01	7.70E+03	1.49E-01
Ir-192	1.57E-01	1.44E+04	1.05E+00
Sr-90	2.38E+01	N/A	1.01E-03
Y-90	3.68E+00	N/A	1.56E-04

Since Sr-90 and Y-90 are beta emitters, the dose rate for the GM pancake probe was not applicable. The GM detector can be utilized to differentiate between beta and gamma contamination on individuals using a combination of open and closed windows. Nasal and mouth swabs can be obtained to indirectly assess the internal contamination if a beta radionuclide has been identified. Once the radionuclide from the RDD has been identified, indirect calculations based on ICRP 30 methodology can be used to assess internal dose. The internal dose can then be indirectly measured using bioassay techniques.

Table 23.4 provides the dose rate limits for medical intervention based on an internal dose of 1 Gy delivered to the lungs over 24 hours. The dose rate limit is provided for each of the five radionuclides. The same assumptions were applied as with Table 23.3. The applied dose rates are above background rates and should be used with a 95 percent confidence interval.

Table 23.4. Dose rate limits for GM pancake and NaI probes based on five radionuclides within the lung using a dose limit of 1 Gy.

Radionuclide	Acitivity in mCi/24 hrs	Dose Rate from GM Pancake Probe (cps)	Dose Rate from NaI Probe (mR/hr)
Co-60	6.23E+00	3.18E+05	4.57E+00
Cs-137	1.12E+01	7.70E+05	1.49E+01
Ir-192	1.57E+01	1.44E+06	1.05E+02
Sr-90	2.38E+03	N/A	1.01E-01
Y-90	368.079	N/A	1.56E-02

Every model contains known and unknown errors. Individual quantity errors were provided in all of the computer simulation runs based on the MCNPX model. While errors propagate throughout each system, care has been taken to minimize and test the statistical reliability and predictability of the program. The most significant error is associated with atomic cross-sections. Cross-sections are used in every interaction calculation. This can easily lead to a 25 percent difference in organ or whole body dose

between the program prediction of dose and the experimental measurement of dose used to validate the program. Based on this reality, a safety margin should be built in to the dose rate limit in order to better protect an individual from deterministic effects of ionizing radiation associated with internal contamination. Emergency responders should reduce the dose rate limit for their instruments by at least 25 percent. While this may increase the number of individuals who are segregated into the categories of known internal contamination, it should not significantly affect the limited medical resources available for patient care. It will also ensure that someone who may be more susceptible to radiation sickness will not be overlooked based on having a dose that is just under the limits established by the emergency responders.

CHAPTER XXIV
CONCLUSIONS AND FUTURE WORK

The action levels provided in chapter XXIII 23 are for a radiological dispersal device and should not be used for other types of radiological events. Radiological events such as Chernobyl, 3-mile Island, or nuclear weapons testing are outside of the scope of this study. The organ and individual dose rate limits have been tailored specifically for an RDD event using computer simulation and verification through experimental testing. Based on the experimental testing and simulated modeling of the five radionuclides, real time lung measurements using the instruments mentioned in chapter XXI 21 or equivalent instrumentation, emergency responders can rapidly scan personnel and segregate them according to the two action levels provided for potentially contaminated individuals within the affected area. The initial segregation should be between injured and non-injured personnel. All personnel should be medically treated without regard for radioactive contamination. Once an individual is medically stable, care can be provided on monitoring and decontaminating the individual followed by reducing or treating internal radioactive contamination if necessary. All personnel who do not exhibit a medical injury, should be monitored and decontaminated as rapidly as possible. Only individuals who exceed action level two should receive medical care based on internal contamination. The acceptance of scientifically based dose limits would aid in the triage of injured personnel as well as possibly reassures the general public that they do not have to overload the medical community if and when an event may occur.

The MAX phantom coupled with the MATLAB programs and the MCNPX output code are flexible enough to accurately model acute organ doses resulting from a RDD event. It can be tailored to fit different scenarios. It is designed to provide a rapid estimate of organ dose based on the likely radioactive make-up of a RDD to assist emergency response personnel in performing triage of potentially contaminated injured people as well as establish scientifically based dose limits for emergency responders.

Further refinement of the dose distribution to the skin would provide more accurate dose modeling of the skin. Dr. Kemper and his group have just developed a new MAX model that reduces the voxel size from 0.36 cm^3 to 0.36 mm^3 this will greatly enhance the resolution between organ surfaces as well as assist in better defining vascular organs. The lung simulation would greatly benefit from a different approach that takes into consideration the truncated air passages and defines them separately from the lung tissue.

REFERENCES

Abraham S. The department of energy strategic plan protecting national, energy, and economic security with advanced science and technology and ensuring environmental cleanup. Washington DC: Department of Energy; DOE/ME-0030; 2003.

Adela S. Handbook for response to incidents involving radiological dispersion devices (RDD). Troy, NY: Conference of Radiation Control Program Directors HS-5 Task Force; 2006.

Alverez J. Radiological dispersal devices. Knoxville TN: Health Physics Society; https://hps.org/hsc/dispersive.html; 2007

Department of Energy, Nuclear Regulatory Commission. Radiological dispersal devices: an initial study to identify radioactive materials of greatest concern and approaches to their tracking, tagging, and disposition. Bethesda, MD: Nuclear Regulatory Commission;
2003.

Dimbylow W. The development of realistic voxel phantoms for electromagnetic field dosimetry, 6-7 July 1995. Chilton, UK: Nationial Radiological Protection Board; Process international workshop on voxel phantom development; 1995.

Gibbs SJ, Chen TS, Malcolm AW, James AE. Patient risk from interproximal radiography. New York: Oral surgery Oral medicine Oral pathology 58:347-354; 1984.

Harper FT, Musolino SV. Emergency response guidance for the first 48 hours after the outdoors detonation of an explosive dispersal device. Health
Physics 93:1-16; 2006.

International Commission on Radiological Protection. Report of the task group on reference man. New York: Elsevier Science; ICRP Publication 23; 1975.

International Commission on Radiological Protection. Limits for intakes of radionuclides by workers. New York: Elsevier Science; ICRP Publication 30; 1978.

International Commission on Radiological Protection. Recommendations of the international commission on radiological protection. New York: Elsevier Science; ICRP Publication 60; 1991.

International Commission on Radiological Protection. Basic anatomical and physiological data for use in radiological protection. New York: Elsevier Science; ICRP Publication 89; 2003.

International Commission on Radiological Units and Measurement. Tissue substitutes in radiation dosimetry and measurement. Bethesda: ICRU; ICRU Publication 44; 1989.

International Commission on Radiological Units and Measurement. Photon, electron, proton and neutron interaction data for body tissues. Bethesda: ICRU; ICRU Publication 46; 1990.

Knolls Atomic Power Laboratory. Nuclides and isotopes. New York: Lockheed Martin Distribution Services; 2002.

Kramer R, Vieira WV, Khoury HJ, Lima FR, Fuelle D. All about MAX: a male adult voxel phantom for Monte Carlo calculations in radiation protection dosimetry. London, UK. Physics in Medicine and Biology 48:1239-1262; 2003.

Kramer R, Vieira WV, Khoury HJ, Lima FR, Fuelle D, Hoff G. All about FAX: a female adult voxel phantom for Monte Carlo calculations in radiation protection dosimetry. London, UK. Physics in Medicine and Biology 48:1239-1262; 2003.

Los Alamos national Laboratory. MCNP – a general Monte Carlo N-particle transport code. Los Alamos, NM: Los Alamos National Laboratory; MCNP Version 5; 2003.

MathWorks Incorporated. MATLAB the language of technical computing. Natick, MA: MATLAB Incorporated, MATLAB 7.4.0.287; 2007.

O'Connell TF. Welcome to the health physics society homeland security committee. West Boylston, MA: Health Physics Society, http://hps.org/hsc/; 2007.

Phantom Laboratory. RANDO phantom. Salem, NY: Phantom Laboratory; http://www.phantomlab.com/rando.html; 2008.

Radiation Safety Information Computational Center. Monte Carlo N-particle transport code system for multiparticle and high energy applications. Oak Ridge, TN: Oak Ridge National Laboratory; RSICC computer code collection MCNPX 2.4.0; 2002.

Vieira JW. Scion Image Beta. Frederick, MD: Scion Corporation, Scion Image 4.0.3; 2005.

Williams G, Zankle M, Abmayr W, Veit R, Drexler G. The calculation of dose from external photon exposures using reference and realistic human phantoms and Monte Carlo methods. Physics in Medicine and Biology 31:347-354; 1986.

Zubal IG, Harrell CR, Smith EO, Smith AL Krischlunas P. High resolution, MRI-based, segmented, computerized head phantom, the Zubal phantom data, voxel-based anthropomorphic phantoms. Chilton, UK; http://noodle.med.yale.edu/phantom;

1994a.

Zubal IG, Harrell CR, Smith EO, Rattner Z, Gindi G, Hoffer PB. Computerized three-dimensional segmented human anatomy. Medical Physics 21:299-302; 1994b.

Zubal IG, Harrell CR, Smith EO, Smith AL. Two dedicated software, voxel-based, anthropomorphic (torso and head) phantoms. Chilton, UK: Process International workshop on Voxel Phantom Development 6-7 July; 1995

APPENDIX A

```
1tally   6       nps =  1000000
         tally type 6    track length estimate of heating.          units   mev/gram
         particle(s): photon

         masses
              cell:      1          2          3          5          6          7          8
                   5.08550E-02  4.69826E-02  6.06528E-05  4.84289E-02  6.57850E-02  6.01862E-02  4.89888E-02
              cell:      9         11         12         14         15         16         18
                   4.94554E-02  4.89888E-02  4.94554E-02  4.89888E-02  4.89888E-02  4.89888E-02  4.80557E-02
              cell:     22         24         25         26         27         31         32
                   4.43232E-02  6.06528E-05  4.66560E-02  4.99219E-02  4.89888E-02  4.94554E-02  4.80557E-02
              cell:     33         34         35         36         37         38         39
                   4.89888E-02  4.85222E-02  4.89888E-02  6.20525E-02  4.89888E-02  4.89888E-02  4.89888E-02
              cell:     40         41         42         43         44         45         46
                   4.85222E-02  6.81178E-02  6.81178E-02  6.81178E-02  6.81178E-02  6.20525E-02  6.20525E-02
              cell:     47         48         49         50         55         60         70
                   6.20525E-02  6.20525E-02  6.20525E-02  6.20525E-02  4.89888E-02  4.89888E-02  5.50541E-02
              cell:     71         76         77         79         81         90         95
                   7.83821E-02  7.51162E-02  4.85222E-02  4.85222E-02  7.83821E-02  1.21306E-02  4.89888E-02
              cell:     98         99         102        106        110        116        119
                   4.66560E-02  4.85222E-02  7.51162E-02  4.89888E-02  4.89888E-02  4.89888E-02  4.89888E-02
              cell:     121        125        140        150        160
                   4.94554E-02  7.83821E-02  4.89888E-02  4.89888E-02  4.89888E-02
```

Fig. A-1. MCNPX output file section on mass calculations for each material. Cell 90 corresponds to the lung with a value of 1.21 X 10^{-2}g per voxel.

Table A-1. Hand calculated volume of lung using a voxel size of 3.6mm x 3.6mm x 3.6mm.

ID MAX	Organ/Tissue	Nº of voxels	Vol (cm3)
0	Air	4127281	192562.4223
1	Skin	122984	5737.941504
6	Ribs+clavicles+sternum+scapulae	32948	1537.221888
12	Liver	36743	1714.281408
14	Kidneys	6328	295.239168
18	Small intestine	20413	952.388928
34	Testes	709	33.079104
35	Prostate	438	20.435328
45	Leg bone right (superior 1)	4976	232.160256
60	Thyroid	405	18.89568
90	Lungs	87506	4082.679936
119	Eyes	309	14.416704
140	Trachea	1182	55.147392
150	Colon	12391	578.114496
160	Stomach	8165	380.94624
	Voxel size: 3.6mm x 3.6mm x 3.6mm		

VITA

LCDR Shannon Prentice Voss was commissioned as a Medical Service Corps office in the United States Navy on September 10th 1993. He received his Bachelor of Science degree in radiation health physics from Oregon State University at Corvallis in 1991. He received his Master of Science degree in radiation health physics from San Diego State University in San Diego in 2000. He entered the Nuclear Engineering program at Texas A&M University in September 2005 to pursue a Doctorate of Philosophy degree in Nuclear Engineering. His research interests include radiation detection and measurement and acute biological response to ionizing radiation. He plans to publish a book on these topics.

LCDR Voss may be reached at Texas A&M University Nuclear Engineering Department, 3133 TAMU, College Station, TX, 77843. His email address is vosssp@tamu.edu.